Performance Enhancement of Photovoltaic Cell Using Phase Change Material

By

Ahmed Rakib Ahsan

ID No: 17MME004P

In partial fulfilment of the requirements for the degree of

MASTER OF SCIENCE IN MECHANICAL ENGINEERING

DEPARTMENT OF MECHANICAL ENGINEERING

CHITTAGONG UNIVERSITY OF ENGINEERING & TECHNOLOGY

December, 2024

Approval

The thesis titled **"Performance enhancement of photovoltaic cell using phase change material"** submitted by **Ahmed Rakib Ahsan, ID No. : 17MME004P, Session : 2017-2018,** has been accepted as satisfactory in partial fulfillment of the requirement for the Degree of Master of Science (M.Sc) in Mechanical Engineering.

BOARD OF EXAMINERS

____
Prof. Dr. Bodius Salam — Chairman
Department of Mechanical Engineering — (Supervisor)
Chittagong University of Engineering & Technology

____
Head
(Prof. Dr. Mohammad Mizanur Rahman) — Member
Department of Mechanical Engineering — (Ex-Officio)
Chittagong University of Engineering & Technology

____
Prof. Dr. Kazi Afzalur Rahman — Member
Department of Mechanical Engineering
Chittagong University of Engineering & Technology

____
Prof. Dr. Mohammad Mizanur Rahman — Member
Department of Mechanical Engineering
Chittagong University of Engineering & Technology

____
Prof. Dr. Md Rabiul Islam Sarker — Member
Department of Mechanical Engineering — (External)
Rajshahi University of Engineering & Technology

DECLARATION

I declared that thesis entitled **PERFORMANCE ENHANCEMENT OF PHOTOVOLTAIC CELL USING PHASE CHANGE MATERIAL** is the result of my own research except as cited in references. The thesis has not been accepted for any degree and is not concurrently submitted in candidature of any degree.

Name of candidate : AHMED RAKIB AHSAN

ID no : 17MME004P

To my parents

ACKNOWLEDGEMENT

First, I am grateful to Allah for giving me health and the ability to complete this thesis. I would like to express my gratitude to my supervisor Dr. Bodius Salam, who guided me at the study area during data collection and also during data analysis processes.

I would like to thank my parents, particularly my mother, Monoara Begum for her kindness and care since I was young. I would also like to thank my wife Sanjana Tasme for her patience and support during my studies.

I would like to express my appreciation to Anwar Hossain Mollah for his kind assistance during my studies.

ABSTRACT

One renewable energy source that can be used for a variety of purposes in the modern world is solar energy. A storage media that can help store extra energy and then release it when needed is necessary for the efficient utilization of solar energy. Phase change materials (PCMs) are an efficient way to store thermal energy from the sun. Because PCMs are isothermal, they can function in a range of temperature settings and provide better density energy storage. The use of PCMs for solar energy storage and utilization, including solar power generation, is thoroughly reviewed in this article. Further study on solar power generation, water heating systems, solar cookers, and solar dryers employing PCMs for commercial development would be aided by this paper.

সার-সংক্ষেপ

সৌর শক্তি একটি নবায়নযোগ্য শক্তি উৎস যা আজকের বিশ্বের বিভিন্ন অ্যাপ্লিকেশনের জন্য ব্যবহার করা যেতে পারে। সৌর শক্তির কার্যকর ব্যবহারের জন্য একটি স্টোরেজ মাধ্যম প্রয়োজন যা অতিরিক্ত শক্তি সঞ্চয় সহজতর করতে পারে এবং তারপর যখন প্রয়োজন হয় তখন এই সঞ্চিত শক্তি সরবরাহ করতে পারে। সৌর থেকে তাপ শক্তি সঞ্চয় করার একটি কার্যকর পদ্ধতি ফেজ পরিবর্তন উপকরণ (পিসিএম) ব্যবহারের মাধ্যমে। পিসিএমগুলি সমতাপক প্রকৃতির, এবং এইভাবে উচ্চতর ঘনত্বের শক্তি সঞ্চয় এবং তাপমাত্রার অবস্থার পরিবর্তনশীল পরিসরে কাজ করার ক্ষমতা সরবরাহ করে। এই নিবন্ধটি সৌর শক্তি ব্যবহার এবং স্টোরেজ যেমন সৌর বিদ্যুৎ উৎপাদনের জন্য পিসিএম প্রয়োগের একটি ব্যাপক পর্যালোচনা প্রদান করে। এই গবেষণাপত্রটি বাণিজ্যিক উন্নয়নের জন্য পিসিএম ব্যবহার করে সৌর বিদ্যুৎ উৎপাদন, ওয়াটার হিটিং সিস্টেম, সোলার কুকার এবং সৌর ড্রায়ার সম্পর্কে আরও গবেষণা পরিচালনায় গবেষককে উপকৃত করবে।

Table of Contents

LIST OF TABLES

LIST OF FIGURES

Figure **Title** **Pages**

NOMENCLATURE

T	Temperature [°C]
I	Current [A]
V	Voltage [V]
W	Power [W]
Subscripts	
amb	Ambient
sc	Short-circuit
oc	Open-circuit
Abbreviations	
BIPV	Building-integrated photovoltaic
FPV	Floating photovoltaic
HP	Heat pipe
HP-PV/TEG	Heat pipe-based photovoltaic thermoelectric generator
PCM	Phase change material
PHP	Pulsating heat pipe
PV	Photovoltaic
PVT	Photovoltaic thermal
PV-TGS	Photovoltaic-thermoelectric generation hybrid system
PV-TCS	Photovoltaic-thermoelectric cooling hybrid system
SBS	Spectral beam splitter
SCD	Simultaneous charging and discharging
STC	Standard test conditions
TEG	Thermoelectric generator
FF	Fill Factor

CHAPTER-I

INTRODUCTION

1.1 Introduction

The introduction of new technologies and the ever-increasing population have made energy one of the most important necessities. One of the most effective, widely used, and widely recognized renewable energy sources with limitless potential is solar energy, which is clean, accessible, simple to use, and sustainable [1]. One of the most well-known solar energy conversion technologies, photovoltaics transforms solar radiation directly into electrical power with limitless potential and silent operation [2].

Photovoltaic, or solar panel that produce electricity, are affected by their operating temperature, which is primarily a product of the ambient air temperature as well as the level of sunlight. The strength of the solar radiation flow, the quality of the semiconductor being used, and the semiconductor cell's operating temperature all affect how efficient photovoltaic cells are. It is impossible to regulate the fluctuation of sunlight radiation. Thus, current research is either focused on maintaining low operating temperatures or on new materials such as copper, indium di-selenium, cadmium, tellurium, and chalcopyrites. According to the industry standard STC (Standard Test Conditions), high operating temperatures for photovoltaic (PV) panels reduce their conversion rate by around 0.5% per degree Celsius over the nominal cell operating temperature of 25°C [3]. The normal summertime temperature range for panels is 40 to 70°C, which results in a 7.5–22.5% decrease in conversion rate. Similarly, as the operating temperature rises above ambient, radiation losses are the primary cause of a solar panel's decreased efficiency. But while the rest of the incident radiation is absorbed inside the PV cell, some of the radiation that falls on the cell's surface is converted into electricity [4]. Consequently, this raises its surface temperature, which lowers its electrical efficiency [5]. According to Skoplaki and Palyvos [6], when the PV operating temperature rose, the power production dropped because the voltage reduced while the current somewhat increased. This led to a reduction in electrical efficiency overall. Rahman et al. [7] found that under solar intensities of 1000, 800, 600, and 400 W/m2, a one-degree rise in the PV working temperature resulted in a 0.37, 0.33, 0.24, 0.17, and 0.06% drop in the power output and efficiency of the PV module, respectively. In order to increase the PV cell's electrical efficiency, the heat that has been absorbed inside it must be eliminated.

Through experimental observations, Amelia et al. [8] demonstrated that utilizing a DC fan to cool the PV cell increased power production by 12%. Increasing the number of fans to 2, 3, and 4 increased power by 37%, 41%, and 44%, respectively. In studies, Krauter [9] pumped water onto the PV cell's surface to cool it; the electrical efficiency increased by 9%, according to the data.

Together, the PV modules and thermal units in PV/T devices transform solar energy into both heat and electricity (simultaneously).There has been a great deal of effort done on these systems. When employing the PV/T system, Ozgoren et al. [10] found that the overall efficiency increased to 51% and the electrical efficiency increased from 11.5% to 13.6%. In an experiment using an air-based PV/T system, Teo et al. [11] reported effectively lowering the maximum PV temperature by 30 °C, leading to a 45% increase in electrical efficiency. In a different study, Wilson [12] conducted an experiment to cool the PV solar cell using water at the proper head. He found that the temperature of the PV solar cell decreased by 30°C and that the electrical performance of the PV solar cell increased by up to 12%. In order to cool the PV cell, Mehrotra et al. [13] dipped it in a water tank at a depth. The findings demonstrated that the temperature of the PV cell's surface decreased with increasing water depth, increasing cell efficiency by 4.76% at a depth of 1 cm. According to Bayrak et al. [14], cooling the PV cell with fins resulted in a maximum temperature differential between the cells of 3.39°C under radiation of 772 W/m2, and the electrical efficiency reached 11.55%.

Phase change materials have been widely used recently for PV solar cell thermal control because of their high energy storage capacity and ability to function at constant temperatures [15,16]. Numerous academics have looked into the integration of PCM with PV systems both experimentally and numerically. Due to its wide temperature range, high heat of fusion, and ability to freeze without supercooling, paraffin is a good candidate for use as a phase change material (PCM) [17]. Through experimental observations, Stropnik and Stritih [18] clarified how utilizing RT 28 HC affected PV panel performance. The results showed that the power output and electrical efficiency were improved by 4.3–8.7% and 0.5–1%, respectively, in comparison to the conventional PV module. The electrical efficiency of the PV + PCM and PV + combined PCM systems was improved by 3% and 5.6%, respectively, according to experiments conducted by Hachem et al. [19] to cool the PV solar cell using PCM and a combined PCM. Waqas and Ji [20] experimentally examined the effectiveness of using PCM inside rotatable shutters to enhance the performance of PV solar cells. PCM-filled shutters were closed during sunny hours, absorbing the excess heat produced by the photovoltaic panel. During the hours when there was no sunlight, the PCM-filled shutters were rotated to release the absorbed heat. According to the findings, summer was the ideal time of year to use PCM, and electrical efficiency increased at a rate of

9%. The electrical efficiency of the three PV cells was 11.35%, 12.4%, and 12.75% for PV, PV/T, and PV/T-PCM, respectively, based on theoretical and practical research on the performance of PV solar cells using thermal systems and thermal systems with PCM by Fayaz et al. [21]. According to the practical findings, the electrical efficiency of the three cells was 11.24% for PV, 12.37% for PV/T, and 12.6% for PVT/PCM. Additionally, it was stated that PV/T and PV/T-PCM achieved respective total efficiencies of 89.6% and 83.95%. The impact of adding organic PCM (OM37) on the PV/T system's energy and exergetic performance under various seasonal meteorological circumstances was theoretically examined by Gaur et al. [22]. The addition of PCM was shown to improve the system's overall performance, electrical, thermal, and exergy by 64.3%, 5.8%, 18.6%, and 42.3% respectively, when compared to the PV/T system without PCM, during the summer. In contrast, under winter conditions, the comparable improvement was 41.7%, 0.53%, 0.95%, and 19.9% respectively. In their tests, Hassan et al. [23] used PCM and a thermal system with PCM and nanofluid inside the water PVTn + PCM to cool the PV solar cell. According to the findings, the PVTn + PCM PV solar cell had the maximum electrical efficiency at 15.4%, while the conventional PV solar cell had the lowest electrical efficiency at 10.4%. In a different work, Hossain et al. [24] investigated the energetic performance of employing lauric acid as a storage material in a PV/T-PCM system with a double side serpentine flow. To achieve optimal performance, the system was tested across a broad range of flow rates (0.5–4 L/min). The maximum exergy efficiency of PV/T-PCM and PV-only systems was found to be 12.19% and 7.09%, respectively, at a flow rate of 0.5 L/m. Hasan et al. [25] conducted an experimental investigation to determine the efficacy of PCM (RT42) for thermal regulation of PV panels in the hot climate of the United Arab Emirates. According to the paper, the proposed solution reduced the PV temperature by a maximum of 12°C while increasing the yearly electricity generation by 5.9% when compared to uncooled PV panels. Wongwuttanasatian et al. [26] conducted an experimental investigation into the thermal regulation of an air-based PV/T collector that used palm wax as a storage material. A comparison of the performance of three different PCM container configurations—tubed, finned, and grooved—was carried out. Compared to the other container configurations, the finned container demonstrated superior cooling ability, lowering the temperature of the solar cells by about 6.1°C, achieving a 5.3% increment in electrical efficiency compared to uncooled PV module.

The PCMs have a high latent heat of fusion [27], however, the low thermal conductivity of the PCMs is considered a negative aspect in case of using it in cooling the PV solar cells [26, 27]. In order to increase the PCM's thermal conductivity and, thus, its efficiency in cooling PV solar cells, numerous studies have focused on adding external materials to the PCM [27, 28]. Huang et al. [29] used fins inside PCM to cool the PV solar. An aluminum plate with PCM was employed by

Rajvikram et al. [30] to improve heat conductivity. According to the findings, the PV solar cell's average electrical efficiency increased by 2%. In order to enhance the effectiveness of PCM in cooling the PV/T, Mousavi et al. [31] used numerical simulations with an absorbent material. The results indicated a 2% increase in electrical efficiency. Munem et al. [32] looked into how employing PCM with a copper foam matrix could improve the performance of the PV solar cell. The results showed that compared to the conventional PV system, the electrical efficiency of the PV + PCM with copper foam matrix increased by 5.68%, while the efficiency of the PV + PCM increased by 1.97%.

The efficiency of employing Al_2O_3 nanoparticles distributed with PCM as a heat-dissipating mechanism for cooling PV modules was investigated experimentally by Nada et al. [33]. The electrical performance was shown to be improved by 6.8% and 12.1%, respectively, when the suggested approach was used with and without distributing Al_2O_3 nanoparticles inside the PCM. Al-Waeli et al. [34] added nanofluid to water and nano SiC particles to PCM in their studies to improve the PV/T's performance. It was claimed that the thermal efficiency was 69% and the electrical efficiency had increased by 92%. In order to improve PCM's thermal performance, Siahkamari et al. [35] investigated the inclusion of CuO nanoparticles. Using the suggested cooling strategy was shown to increase power output by roughly 6.5%.

Incorporating PCM with metal foams for PV cell thermal control has not been extensively researched, and the majority of these studies were simulation-based. Furthermore, there were still no experimental investigations in the literature that looked at PV-PCM systems' performance in cold climates. Thus, the primary goal of those studies was to investigate experimentally how PV performance may be improved utilizing both organic and in-organic PCM in both the summer and winter. The output power produced, the open-circuit voltage, and the temperature distribution on the surface of the PV solar cell would all be shown in experiments with and without PCM.

1.2 Soler Energy

The radiation from the Sun that may produce heat, electricity, or chemical reactions is known as solar energy. The entire amount of solar energy that strikes Earth is far more than what is currently needed and will be needed in the future. This widely dispersed source might potentially provide all of the world's energy demands if properly utilized. In contrast to the limited supply of fossil fuels like coal, oil, and natural gas, solar energy is predicted to grow in popularity as a renewable energy source in the twenty-first century due to its limitless supply and non-polluting nature.

Although sunlight is by far the most abundant source of energy that the Earth receives, the Sun is a very strong energy source. However, the intensity of sunlight at the Earth's surface is really very modest. The main reason of this is the massive radial dispersion of radiation from the far-off Sun. The Earth's atmosphere and clouds, which absorb or scatter up to 54% of the incoming sunlight, are responsible for a very small extra loss. Of the sunlight that reaches the planet, about half is visible, while the other 45% is infrared. Tinier levels of ultraviolet and other electromagnetic radiation are also present.

Solar energy has enormous potential because Earth receives approximately 200,000 times the world's daily electric-generating capacity in the form of solar energy. Although solar energy is free in and of itself, its usage is regrettably limited in many places due to the high cost of collecting, processing, and storing it. Although the former is simpler to achieve, solar radiation can be transformed into electrical energy or thermal energy (heat) [36].

1.2.1 Electricity Generation

Solar cells (photovoltaic cells) can directly convert solar radiation into electrical power. When light hits the junction of two distinct semiconductors or the junction of a metal and a semiconductor (like silicon), a tiny electric voltage is produced in these cells. Figure 1.1 displays the photovoltaic cell configuration. Usually, a single photovoltaic cell can only produce two watts of power. However, a solar electric plant or a large household array can generate hundreds or even thousands of kilowatts of electricity by connecting a large number of individual cells together, as in solar-panel arrays. The majority of contemporary photovoltaic cells only have an energy efficiency of 15 to 20 percent since solar radiation is already low. Large and costly assemblies of these cells are required to produce even moderate quantities of electricity.

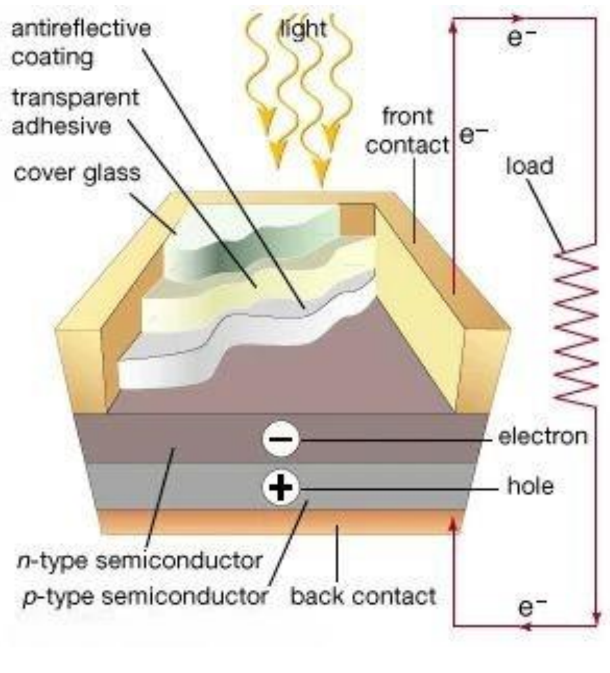

Fig. 1.1. Photovoltaic cell

Small photovoltaic cells that run on artificial or solar light have become very popular in low-power applications, such as powering watches and calculators. Water pumps, communications networks in distant areas, and weather and communications satellites have all been powered by larger units. Homeowners and businesses can replace or supplement the traditional electric supply by installing traditional crystalline silicon panels and cutting-edge technologies that use thin-film solar cells, such as building-integrated photovoltaics, on their rooftops.

In concentrated solar power plants, sunlight from a large area is concentrated onto a small blackened receiver using concentrating, or focusing, collectors. This significantly increases the intensity of the light, which generates high temperatures. A target can be heated to 2,000°C (3,600°F) or higher by focusing enough sunlight onto arrays of precisely positioned mirrors or lenses. This heat can then be used to run a boiler, which produces steam for an electric generator power plant that uses steam turbines. By focusing a lot of solar radiation on blackened pipes that circulate water and heat it, the movable mirrors can be used to directly produce steam [36].

1.3 Effect of Temperature

One of the main parameters that affect the photovoltaic cell performance is cell temperature; the solar cell output decreases with the increase of temperature. Photovoltaic cells are made of semiconductor materials, like the most used crystalline silicon. Semiconductors are sensitive to temperature changes. While lower temperatures raise the voltage of solar cells, higher temperatures reduce the open circuit voltage and power production of solar cells. The output of most solar panels is measured under Standard Test Conditions (STC) – this means a temperature of 25°C or 77°F. The average temperature during sun peak hours is represented by the test temperature. The top of the ideal temperature range for photovoltaic solar panels is 25°C, or 77°F. It is when solar photovoltaic cells are able to absorb sunlight with maximum efficiency and when it can be expected to be performed the best.

The solar photovoltaic cell output fluctuates in real life conditions. This is due to variations in solar panel temperature and sunshine intensity throughout the day.

Low energy states are where electrons are bound in a solar cell. In order to break the bond and move, these electrons must first enter a new state called the excited state after receiving additional energy. Conduction is possible when an electron is in its excited state. Heat or light, such as sunlight, can provide the additional energy that raises them to the excited state. How much energy (voltage) separates these two states determines how much power a solar cell can generate. The parameters of semiconductor materials are impacted by temperature increases because they raise the energy of bound electrons. As a result, the energy difference required to reach the exited state is smaller, lowering the solar cell's efficiency and power output.

The heat from the sun causes the temperature of solar cells to increase when they absorb it. Moreover, crystalline silicon, a common component of solar cells, does little to stop them from heating up. On hot, sunny days, silicon's exceptional ability to conduct heat actually accelerates the heat accumulation in solar cells.

As the temperature rises, the temperature coefficient shows how quickly solar panel efficiency will drop for each degree Celsius (1.8°F).

For example, when the temperature coefficient is minus 0.5 percent, efficiency decreases by 0.5 percent for every degree over 25°C (or every 1.8 degrees above 77°F).

The precise number of degrees that solar photovoltaic cells can reach is difficult to determine because it depends on a number of variables, including solar irradiance, ambient temperature, panel placement, and installation type.

1.3.1 The Effect of High Temperature

When solar panels reach high temperatures, their efficiency in producing energy decreases. In 2008, Nigeria discovered similar results: solar panel energy production steadily decreased once the panel temperature reached 44°C. A field experiment conducted in the United Kingdom showed that a home photovoltaic solar panel's peak output decreased by 1 to 1 percent for every degree Celsius that the panel's temperature rose. The temperatures of the solar panels tested were, on average, about 20°C higher than the ambient air temperature. Accordingly, the drop-off in efficiency begins at about 87 to 91°F temperatures frequently reached during summer daytime hours in temperate climates, and often exceeded in equatorial nations.

1.3.2 The Effect of Low Temperatures

The efficiency of photovoltaic solar panel power generation is optimized in cold temperatures, yet it is unfortunate that the regions nearest the poles, which are characterized by colder climates, experience weaker sunlight and shorter daylight hours. The insolation value, referred to as the strength of sunlight hitting the ground in a specific area, decreases as one approaches the poles due to the sun's lower angle. Moreover, irradiance, or the brightness of the sun, is reduced when the sun is at a lower angle. Solar tracker systems, designed to adjust the angle of the photovoltaic panel to maximize irradiance and insolation values, can potentially enhance the potential benefits of cold temperatures on solar panel efficiency.

1.3.3 The Effect of Snow and Clouds

Clouds and snow can reduce solar panel efficiency, negating the benefits of low temperatures on solar panel power generation in colder climates. Cloudy skies cannot be prevented, but there are a few things that can be done to lessen the amount of snow that accumulates on solar panels. Snow can be encouraged to slide off more quickly by tilting solar tracker units or remounting fixed ground array units at a steeper angle. Both ground-mounted and roof-mounted panels can be cleared of snow using a roof rake, which resembles a push broom and has a long, angled handle. Using a roof rake to remove snow can also stop accumulation from potentially tumbling off the slick panels.

1.4 Phase Change Materials (PCMs)

Recent years have seen an increase in research interest in and significance for the use of PCMs in energy efficiency. The literature has extensively examined the theories, design, and analysis of PCMs for latent heat storage [37–46]. PCMs can be divided into four categories based on how they change phase: solid-solid, solid-liquid, solid-gas, and liquid-gas. Solid-liquid PCMs are the best kind among these four for storing thermal energy, and they can be found as organic PCMs, inorganic PCMs and eutectics, as seen in Fig. 1.2.

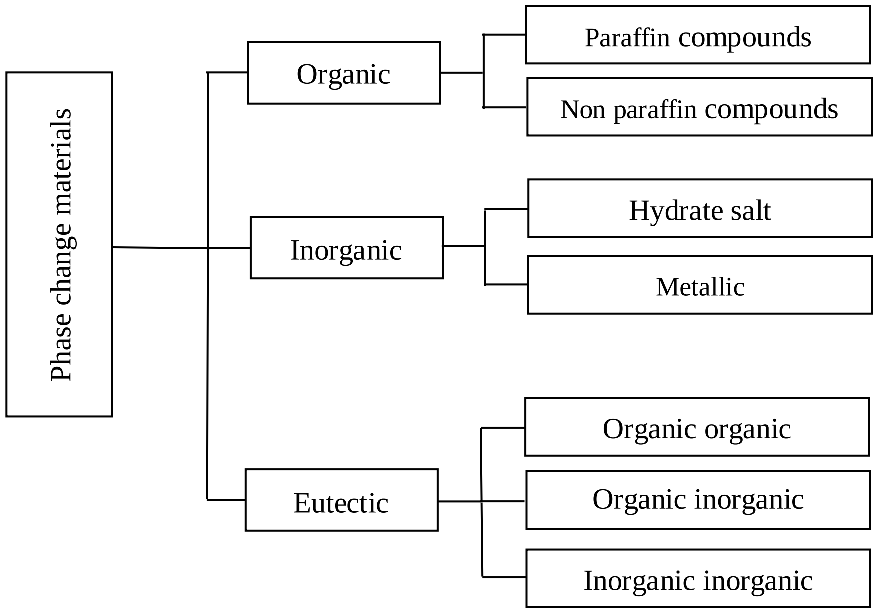

Fig. 1.2. Phase change material (PCM) [47, 48]

The fact that paraffin wax has a relatively high heat of fusion and can be employed at a variety of temperatures makes it a PCM. It is also possible for paraffin wax to freeze without supercooling. Technical grade paraffin wax is therefore the most practical, affordable, and extensively utilized PCM. Numerous research have been conducted on this subject, including those by the authors [49–52]. Compared to paraffin wax, fatty acids are organic molecules having a greater heat of fusion value. With little to no supercooling, fatty acids can replicate melting and freezing. The price of fatty acids, which can be 2.0 to 2.5 times more expensive than paraffin wax, is one factor that prevents their use [53, 54]. The chemical formula for salt hydrates is typically MnH_2O, where M is an inorganic molecule that plays a significant role in heat storage because of its high density of volumetric latent heat storage [49, 55]. Due to their weight, metals have not been a viable option for PCM. However, due to their high latent heat of fusion per unit volume and high thermal conductivities, metals are probably eligible when volume is considered [49, 56].

However, PCMs have a number of drawbacks. For instance, PCM systems need to last a long time to recoup their installation costs [57]; repairing a PCM system is impossible without damaging the system; and the supercooling effect lowers the PCM material's efficiency, which leads to inadequate heat rehabilitation. A number of studies have attempted to enhance PCMs by adding different agents, however this has led to a decline in performance [58,59]. PCM needs to be enhanced prior to installation [58] because of its extremely poor thermal conductivity, which decreases heat transmission during the solid-liquid phase transition [60]. Long-term stability may be hampered by phase segregation, which can happen when PCM has many components [61]. Building envelopes containing organic PCMs have a major impact on fire safety. When employing organic PCMs in building envelopes, researchers have proposed using fire retardants to increase fire safety [62, 63]. The advantages and disadvantages of both organic as well as the inorganic types of materials are listed in Table 1.1 [64, 65].

Table 1.1. Benefits and drawbacks of PCMs. [64, 65]

Types of Materials	**Benefits**	**Drawbacks**
Organic PCM	**1.** Accessible throughout a wide temperature range. **2.** No supercooling. **3.** Able to work with different materials. **4.** No separation. **5.** PCMs are chemically stable. **6.** These are safe to use. **7.** Non-reactive in nature. **8.** Can be recycled.	**1.** Low thermal conductivity. **2.** Significant variations in volume. **3.** Flammable. **4.** Expensive except technical grade paraffin wax.
Inorganics PCM	**1.** High volumetric latent heat. **2.** Less expensive. **3.** Easily available. **4.** Thermal conductivity is higher. **5.** These PCMs have a very high rate of thermal fusion. **6.** Lower volumetric variation. **7.** These PCMs are non-flammable.	**1.** The volume change is remarkably large. **2.** Supercooling **3.** Corrosiveness
Eutectics	**1.** These PCMs have a high melting point. **2.** High volumetric storage density.	**1.** There is less information on thermophysical proper ties.

Complete and thorough knowledge of the thermophysical characteristics of the materials in consideration is required. The melting temperature, heat of fusion, density, thermal conductivity, and stability of thermal characteristics in subsequent heating and cooling cycles are all included in this. While chlorides, carbonates, and fluorides require a high melting temperature, paraffin, wax, fatty acids, salt hydrates, and their eutectic combination have a low melting temperature. Depending on their melting temperature and material properties, these materials can be used in a variety of ways.

1.4.1 PCMs Solar Power Generation

In terms of yearly investment and rewards, solar energy is now the most widely used renewable power generation option for residential usage. Solar energy can be used in a variety of ways to generate electricity, including photovoltaics, solar thermal [66], solar organic Rankine cycle [67], and solar hybrids [68, 69]. Because solar thermal electricity generating systems (SEGS) can be employed with PCM to store energy, they have been examined in this study. As a result, they have a high potential for dispatch, which enables them to be utilized as needed, increasing their effectiveness and economy. Only a small number of power plants worldwide have been identified as testing high-temperature thermal energy storage (TES) systems, indicating that these systems have not been extensively tested [70,71]. Although more recent SEGS versions have increased working temperatures from 300°C to 400°C and employed costly synthetic oil as storage media, the technique is still not commercially viable [72]. Figure 1.3 shows an example of PCMs utilized as the heat storage medium for SEGS.

Due to its low thermal conductivity, which lengthens the charging and discharging time, PCM has not yet reached the anticipated commercial level or large-scale use, despite the fact that it has a significant possibility to help reduce the cost energy produced by SEGS. Using single-stage PCM storage, Hunold et al. [73–75] examined the heat transfer mechanism for single-stage PCMs of various PCM salts. The findings demonstrated that PCMs may theoretically achieve the intended outcomes and recommended a PCM storage design that uses a shell and tube heat exchanger oriented vertically.

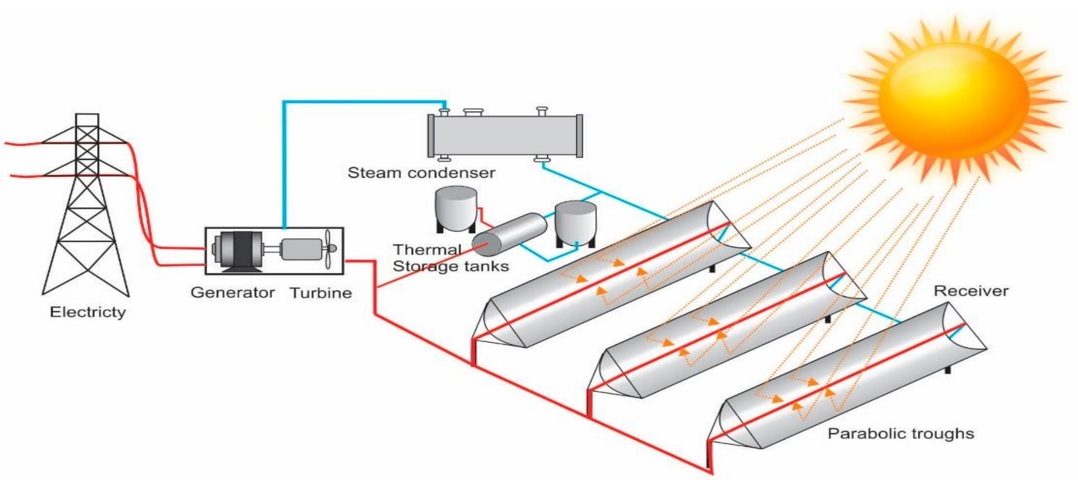

Fig. 1.3. Schematic diagram of a SEGS plant with TES (thermal energy storage)

The way in which PCMs and the heat transfer fluid interact during charging and discharging is an essential component of exploiting latent heat storage in a concentrated solar thermal (DSG) plant. A concentrated solar thermal plant's schematic diagram that uses a Rankine cycle and latent heat storage is shown in Fig. 1.4a. The concentrated solar thermal plant and latent heat storage can also be linked to a super-critical carbon cycle (s- CO_2), which can then be linked to a Brayton cycle for power generation, as illustrated in Fig. 1.4 (b) [76,77]. A heliostat field, power block, thermal energy storage system, and center tower (solar receiver) make up this procedure. Heliostat fields gather and focus sun energy on the solar receiver. The absorbed heat is then circulated through the system by the heat transfer fluid (such as molten salt) before being introduced to a power block (steam Rankine cycle or s- CO_2 Brayton cycle) to transform thermal energy into electrical energy.

Since research is still being conducted to find better methods for high-temperature PCM encapsulation and heat transfer enhancement, LHTES (latent heat thermal energy storage) employing high-temperature PCM is not yet common in commercialized CST plants [78,79]. However, the operational temperatures will be between 293°C and 393°C if PCM is used as the store medium in commercialized CST facilities. This is comparable to the storage temperature that is produced by the existing parabolic trough technology. It's also important to remember that in CST plants with higher operating temperatures (> 600°C), a PCM with a greater melting temperature is always preferred because it guarantees higher energy conversion efficiency.

Pirasaci and Goswami [80] conducted a numerical evaluation of PCM's potential for steam generation, preheating, and superheating through a direct steam generation (DSG) plant. The PCM-filled tanks are frequently linked in sequence to increase the temperature of the feedwater entering the TES [81]. As the feed water passes through N tubes, it can be heated, evaporated, and superheated. This system has been used to study the potential of the eutectic mixture (NaCl+MgCl2), which has a melting temperature of 550°C and a latent heat capacity of 317 kJ/kg. The system's water/steam can operate at temperatures between 300°C and 600°C, which is appropriate for a DSG plant. The findings demonstrated that the performance of the storage system was significantly impacted by several elements, including the water/steam flow rate and the design specifications (such as the tank's length and tube diameter) [80]. Therefore, more research was needed to demonstrate this system's dependability for a DSG plant.

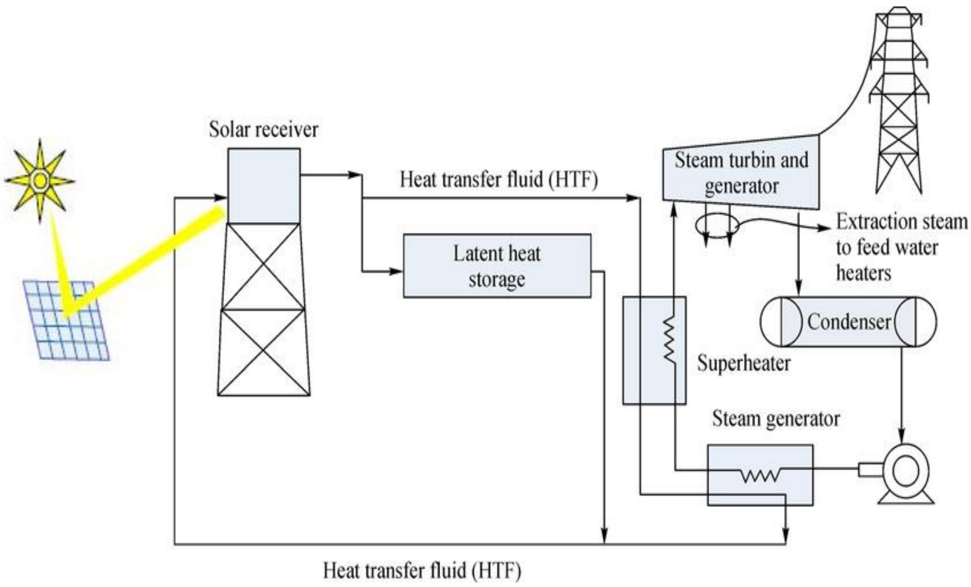

(a)

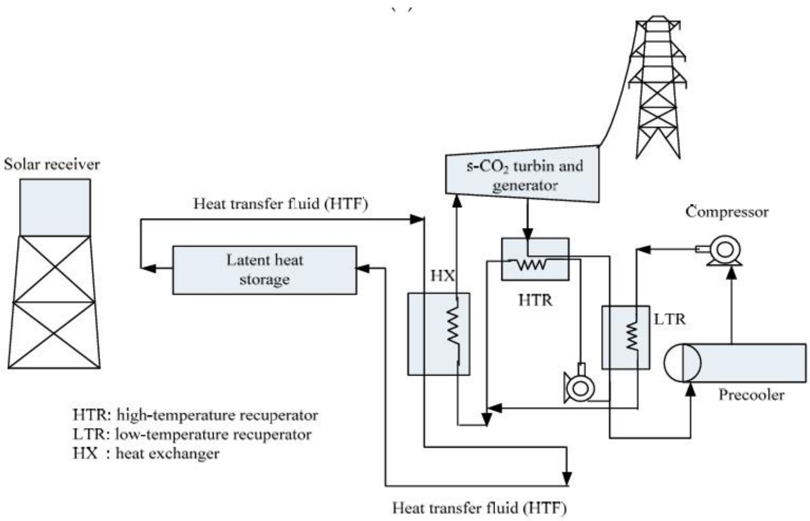

(b)

Fig. 1.4. Concentrated solar thermal power plant schematic diagram with (a) steam Rankine cycle, (b) s-CO_2 Brayton cycle

Michels and Pitz-Paal have developed the similar idea for cascaded latent thermal energy storage (CLHS) [72]. In the parabolic trough, where thermal oil is utilized as a heat transfer fluid, CLHS can serve as an alternate storage option, as seen in Fig. 1.5. Five distinct PCMs were employed in the temperature range of 300°C to 380°C, as this figure illustrates [82]. The findings demonstrated that, given the design and material characteristics, this system may be modified for the DS123G plant. However, the theoretical concepts had not been experimentally verified.

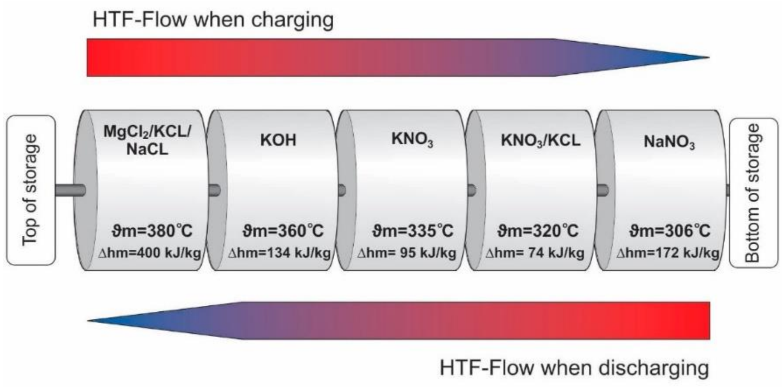

Fig. 1.5. The cascaded latent heat storage system

Michels and Pitz-Paal [72] applied the simulation using the Tech-thermos standard library "Dymola/Modelica" and a numerical model to run the simulation for various cascaded latent heat storage (CLHS) configurations. The PCM was thought to be a lumped mass with an evenly distributed temperature in order to simplify the model. For the simulation, natural convection was also taken to be the case. Their model was validated when the desired results were obtained from the experiment.

A rational next step in the development of PCM storage appears to be hybrid PCMs-sensible storage, which is still in its infancy but has been suggested as a storage system for solar plants [83,84]. Compared to PCM alone, the hybrid systems were able to lower costs and better use PCM store capacity. In comparison to sensible heat material systems, they can also improve the storage ratio [70, 85]. Azanganeg et al. evaluated the possibility of integrating sensible and latent heat using thermocline thermal energy storage [86]. They used sedimentary rock and encapsulated PCMs as sensible and latent storage materials. The findings demonstrated that a tiny quantity of PCM, or around 1.33% of the entire volume, may provide a consistent outflow temperature [86,87]. The system's operating temperature was around 575°C, which was appropriate for a DSG plant. Furthermore, by combining sensible and latent heat, the suggested system's thermal capacity might be increased. However, one of the primary disadvantages of the suggested method was thought to be the storage system's intricate architecture.

1.4.2 PCMs Solar Water Heating System

Water heating systems are one of the primary applications where solar energy has been fully utilized. The efficiency of solar thermal conversion was found to be around 70% higher than that of solar electrical direct conversion systems, which were shown to be 17% more efficient [88,89]. Hot water is required for industrial, commercial, and domestic use. Recently, solar water heaters have become more popular due to their low cost, ease of maintenance, and ease of fabrication. PCMs can be utilized as a thermal storage system to guarantee that hot water is supplied all day. A solar water heater and a PCM-contained heater storage unit are the two components that typically make up a standard solar water heating system, and they both function simultaneously. A water heater normally uses solar energy to heat the water throughout the day, but the PCM absorbs thermal energy and stores it inside the material. The PCM's thermal energy is used to heat the water at night when sunlight isn't accessible. The development of solar water heaters has drawn a lot of attention from researchers. For application and advancement in the solar water heater (LHTES), a variety of PCMs and thermal storage technologies are easily accessible [90–92]. Figure 1.6 shows the schematic diagram of an LHTES. Table 1.2 provides a summary of the substantial effort that has been made to enhance integrated solar water heater storage systems.

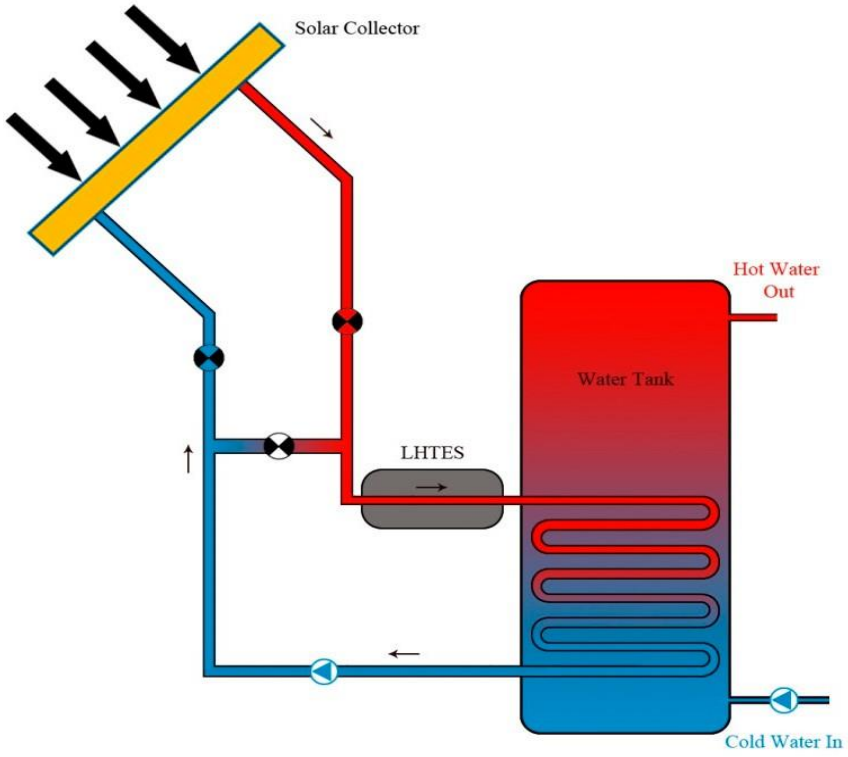

Fig. 1.6. Solar water heater system with LHTES (latent heat thermal energy storage)

Table 1.2. An overview of several integrated solar water heater storage system research.

Authors	Theoretical/Experimental Description	Results
Prakesh etal. [93]	Investigated a water heater with integrated storage that had a coating of PCM applied on its base.	As latent heat built up, the heat from the heated water was transmitted to the PCM beneath it, causing it to melt. In the absence of sunlight, cold water was used in place of the hot water, which absorbs thermal energy from the PCM and causes the

		liquid to phase into a solid. The method was less successful due to inefficient thermal energy transfer between PCM and the water.
Bansal andBudi [94]	Proposed a closed-loop cylindrical storage device with a flat plate collector for both charging and discharging. Stearic acid and paraffin wax (p-116) were the PCMs that were employed.	The fluid temperature and the moving boundary at its interface were calculated.
Porteiro and Míguez [95]	To check each PCM's thermal characteristics, a thermal study was conducted.	Thermal loss to the surrounding environment, PCM, and water temperature all contributed to the observed temperature recovery.
Benmoussa and Benzaoui [96]	A numerical analysis of two phase change material’s (PCM) thermal behavior in a shell and tube latent thermal energy storage (LTES) unit.	The melting rate of PCM and the intake temperature of all heat transfer fluids were changed. Additionally, the temperature evolution of PCMs was greatly impacted by changes in the HTF inlet temperature.
Kamiz Kayguz et al. [97]	Phase change energy storage materials' performance for the solar heating unit is investigated both theoretically and experimentally. The PCM used was $CaCl_2.6H_2O$.	The solar heating system with $Na_2SO_4.10H_2O$ has more F values compared to $CaCl_2.6H_2O$. The thermal properties of the PCM are not reduced during the operation.

Rabin et al. [98]	In addition, a comparison of the heat storage capacities of systems based on PCM, water, and rock was carried out. Investigated a solar thermal collector that uses salt hydrate as PCM for heating and thermal energy storage.	The study's findings demonstrate the relationship between the transition temperature, the salt hydrate PCM layer's thickness, and the impact on thermal performance during PCM charging.
Sharma et al. [99]	Utilized a box-type solar thermal collector to design, build, and assess the performance of a latent heat storage unit that may be used in the morning and evening when hot water is required. Paraffin wax was the PCM that was utilized.	It was discovered that the storage unit did a good job of maintaining the hot water at the appropriate temperature.
Mattewa and Assassa [100]	Investigated the thermal performance of a compact PCM solar collector that uses latent heat storage to store energy.	As natural convection becomes stronger during the charging process, the average heat transfer coefficient rises dramatically as the thickness of the molten layer increases. It was discovered that as the water mass flow rate increased during the discharge process, so did the useful heat gain.
Cabeza et al. [101]	Constructed a solar pilot plant at the University of Lleida to test PCM behavior in actual conditions. The solar pilot plant was built to run constantly using either an electrical	The PCM module geometry was chosen in order to use multiple cylinders at the top of the water tank.

	heater or a solar energy source.	
Kumar et al.[102]	Designed, created, and evaluated a latent heat storage device that uses a box-style solar collector to capture thermal energy and may be used whenever warm water is needed. Three finned heat exchangers made up the system, and the PCM stored heat using paraffin wax, which melts at 54 °C.	The findings demonstrated that the heat storage system's storage unit did a good job of maintaining the hot water's temperature within the intended range. Fifteen and twenty liters of water were used for the experiments.
Shukla [103]	Created two solar water heaters using paraffin as the heat storing substance. One system had tank-style storage, while the other system included reflector-equipped storage.	On a daily cycle, these systems could supply hot water both during the day and at night. The relative efficiency of these two systems was 45% and 60%.
Hasan et al.[104–106]	Fatty acids were used as PCM in the analysis of the home water heater.	According to the study, myristic acid, palmitic acid, and stearic acid are the best and most promising PCMs. They can all be used to heat water because their melting points range from 50 to 70 °C.
Tiwari et al.[107]	Analyzed how a solid-solid PCM interface, intended for use as a water heater, would be affected by flowing water flow within a parallel plate. The device was equipped with moveable insulation to lessen heat dissipation at night.	They discovered that elevating the melted PCM will lessen temperature swings and that hot water may be kept at a high temperature continuously.

Ling, Mo[108]	Investigated the system's thermal and energy efficiency, the solar portion, and the energy used for room heating.	The system's heating efficiency would be 31.7%, and its solar fraction would be 83.6%. The average temperature was 14.9 °C indoors and −1.5 °C outside.
Boy et al.[109]	Proposed an integrated collector storage system based on salt hydrate PCM to deliver immediate hot water.	Research has demonstrated that the system's efficiency might be significantly increased by adding a suitable PCM.
Tayeb [110]	Developed and analyzed a system for the home water heater using $Na_2SO_4.10H_2O$ as PCM.	However, because the salt hydrate PCM was housed in a specifically designed corrugated fin heat exchanger, the system was anticipated to be expensive. The simulation model, which gave the optimal intake water flow rate needed to maintain a constant water temperature at the output flow, was then compared to the findings.
Font et al.[111]	Conducted an initial investigation of solid-solid PCM in the construction of a household water heater. Utilizing a one-directional model, numerical simulation was employed to validate the experiment's results.	The model's ability to examine heat transport within PCMs and enhance the design of water heater devices was demonstrated by the consistency between simulation and experimental results.
Bhargava[112]	A solar-powered water heater using PCM was theoretically studied.	The findings demonstrated that raising the solid-solid PCM's thermal conductivity will also raise the system's efficiency in the evening and the temperature of the

		outflow water.
Canbazogluet al. [113]	Analyzed and compared PCM-powered solar water heating with traditional solar water heaters. About 180 kg of PCM was put into three rows of polyethylene bottles, which were then allowed to settle in the tank.	While the hot water did not fluctuate at all, the water's temperature remained steady at 46°C from night till morning.

To determine the ideal heating, solar water heating systems with various PCM kinds should be assessed [114]. Better heat exchange can be achieved by using a different heat transfer fluid instead of water. Additionally, the system performance may be examined using PCM augmented by nanoparticles.

1.4.3 PCMs Solar Cookers

Cooking is a major source of energy use in poor nations. Kerosene and liquid petroleum gas (LPG) are the energy sources for modern cooking methods in urban areas, whereas non-commercial fuels including firewood, cow dung, and agricultural waste are used in rural regions. Global problems with CO2 emissions and limited fuel sources could be resolved by solar cookers. Therefore, additional research projects are required to effectively market solar cookers as a competitive alternative to conventional cooking appliances. Utilizing solar cookers could benefit the environment by lowering CO2 emissions and assisting in the reduction of reliance on fossil fuels. In addition to the cost and performance constraints, some social prerequisites are necessary for full commercialization and widespread use [115–117]. Another drawback of using solar cookers is that they are only functional in bright, sunny weather; they cannot be used at night or on overcast days. To get over these restrictions and impracticities during the hours when the sun isn't shining, solar cookers need to be able to retain heat. For solar cookers to be practical and commercialized for future use, PCM research and marketing initiatives are required [118–120]. The schematic diagram of a concentrating type solar cooker using PCM A-164 is presented in Fig. 1.7.

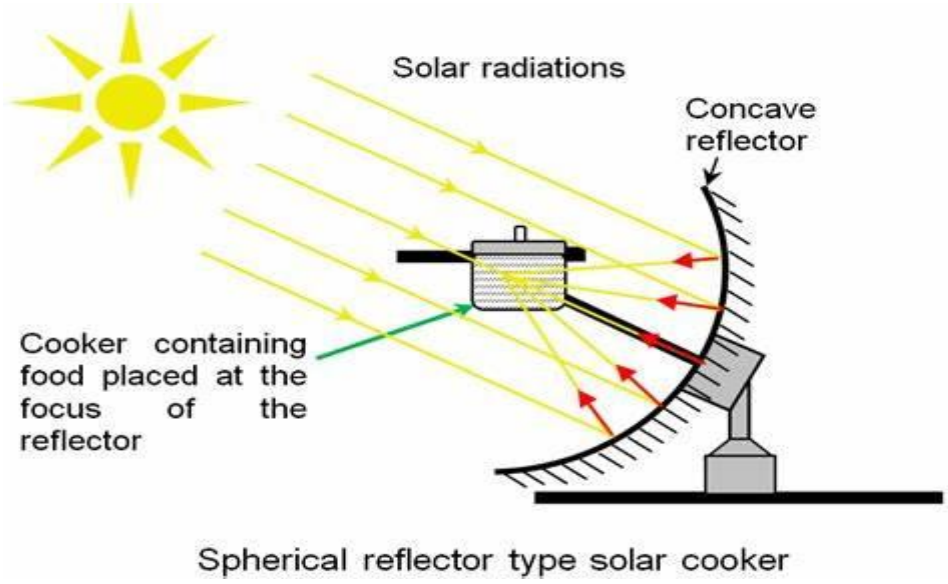

Fig. 1.7. Concentrating type solar cooker using PCM A-164

In order to cook food in the late evening, Buddhi and Sahoo [121] created and tested a solar-powered cooker that stores latent heat. Under the absorbing plate was a thermal energy storage substance composed of commercial grade stearic acid, which has a melting point of 55°C and a latent heat of fusion of 161 kJ/kg. Cooking food in the evening took longer due to the slow heat transfer rate during PCM discharge [122]. Using magnesium nitrate hexahydrate $Mg(NO_3)_2.6H_2O$ as the heat storage medium for a box-type solar cooker to be utilized during non-sunshine hours, Domanski et al. [123] investigated the application of PCMs. Sharma et al. [124] created a cylinder-shaped PCM storage unit for a hot box solar cooker that uses commercial-grade erythritol (Tm = 118°C) to prepare meals at night or in the evening. Their experiment's findings demonstrated that the solar cooker's daytime performance was unaffected by solar energy storage. For evening cooking, they recommended that the PCM melting temperature should be between 105 and 110°C [125].

A solar energy cooker based on an evacuated tube solar collector (ETSC) with PCM storage was also studied by Sharma et al. [125]. A PCM storage unit was connected to the solar energy collection and culinary components of the planned device. Commercial-grade erythritol was used to store the solar energy as latent heat, which was then released to be used for cooking at night. In addition to testing PCM storage procedures, cooking experiments were conducted throughout the day with varying loads and loading periods. It was discovered that cooking at noon and in the evening did not depend on one another, and that cooking in the evening with PCM heat storage took less time than cooking in the middle of the day without PCM.

Hussein et al. [115] designed a new indirect solar-powered cooker that consisted of a solar collector with a flat plate, outdoor elliptical cross-section wickless heat pipes, and an integrated PCM thermal storage which was placed indoors. While PCM composed of magnesium nitrate hexahydrate (the latent heat of fusion 134 kJ/kg, Tm=89°C) was utilized within the indoor cooking unit, two reflectors were used to direct the sun's rays onto the collector. When the reflector was oriented north and south, the arrangement demonstrated an average daily improvement of 24% in incident solar energy on the collector's surface. Different kinds of loads at various loading times, as well as other trials without the load, were also carried out. These were carried out in order to determine any advantages or consequences of using solar cookers to cook during the day and to keep meals warm at night and in the morning.

But according to the literature, the highest temperature that PCM could reach when used for solar cooking was about 120°C, according to the thermal stability test. When PCM was used as a heat storage material, it was discovered that indirect heating was the most effective method of heating. For this material, the temperature differential between the cooking container surface and the storage material would be roughly 10 to 15°C. Therefore, it could be concluded that the cooking vessel's surface could only reach a maximum temperature of 100°C, which was lower than the temperature required for frying and rapid cooking.

A solar cooking system with PCM A-164 as the store media was still being researched as a solution to that issue [126–128]. This system included an indoor cooking unit, a PCM-based thermal storage unit, and a solar collector with a concentrator [129]. In order to facilitate heat transfer between the collector and the cooking unit, the thermic fluid was selected as the heat transfer fluid. The thermal energy storage material PCM A-164 was utilized to store energy throughout the day and retrieve it during the hours when the sun isn't shining. Similar to electric cooking, the cooking unit used a flat surface hot area, and cooking oil circulation ensured flow beneath the finned hot plate, keeping the surface temperature at approximately 140 to 150°C. Cooking may be done all day long with this method. If the PCMs could be produced at a reduced cost, this system could be cost-effective for long-term use even though the initial capital and cost were high [130,131].

1.4.4 PCMs Solar Dryers

Foods and agricultural products can be stored using drying procedures, which reduce the moisture content of products [132]. Fruits and vegetables must be dried at an operating temperature between 40 and 60°C [133,134]. The humidity level and operation temperature can be used to regulate the items' moisture content and quality (such as their nutritional qualities). For many goods, these factors vary [135].

In the culinary and agricultural sectors, the solar drying technique has drawn a lot of interest because it facilitates the preservation process [135]. Additionally, it has substantial ecological advantages [136]. Devahastin et al. has evaluated paraffin wax's potential as a PCM in the solar dryer [137]. They found that PCMs could store surplus energy from the sun and discharge that energy when it was demanded. Various factors were examined during charging and discharging, including the effects of air velocity, intake and outlet temperatures, and heat transfer characteristics. The findings demonstrated that as the input velocity increased from 1 to 2 m/s, the extracted energy dropped from 1920 kJ.min/kg to 1386 kJ·min/kg [137]. Additionally, they discovered that with that inlet velocity, sweet potatoes may be dried up to 40%. The PCM is positioned in the latent heat storage tank in Fig. 1.8, which displays the schematic diagram illustrating the fundamental idea of that procedure.

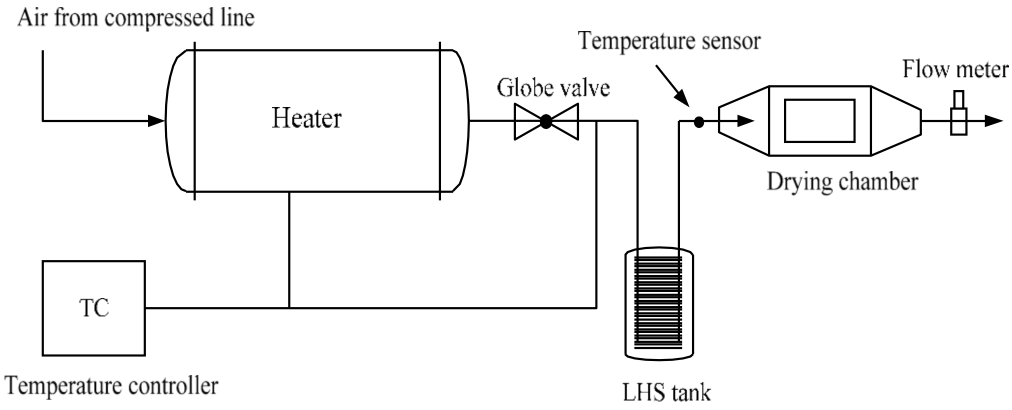

Fig. 1.8. Schematic diagram of the basic concept of the solar drying chamber

Using numerical simulation, Devahastin et al. [137] suggested latent heat storage from the expelled gas of a modified spouted bed grain drier. They asserted that combining these strategies might result in savings of up to 15%. Using paraffin wax as the PCM, Bal et al. [138] created and built a solar dryer with LHS to store excess solar energy throughout the day and release it when solar energy was insufficient or unavailable. The same authors described in fully a solar dryer with thermal energy storage devices used for drying agricultural food products in another work [138–140]. Shanmugam and Natarajan [141] evaluated the drying process of pineapple slices and green peas using a desiccant bed and indirect forced convection. Both sunny and overcast conditions were intended for that system's operation.

Shalaby et al. conducted another investigation that demonstrated how PCMs affected a solar dryer's performance [136]. The findings demonstrated that PCMs might raise the solar dryer's operating temperature by up to 6.5°C. The thermodynamics of this method for drying garlic cloves was investigated by Syringe et al. [142]. The findings showed that over the course of eight hours, a garlic clove's moisture content dropped from 55% to 6.5%. Additionally, the drying chamber with flowing air had an increase in energy and exergy efficiency of 14.9% and 88.2%, respectively [142]. Jain and Tewari created another solar dryer using PCM [145]. A flat plate collector, a pack bed for storage, a natural ventilation system, and a drying chamber made up that solar dryer. The findings demonstrated that the dryer's temperature was constant between 40 and 45°C, which aided in the drying process. Furthermore, that system's thermal efficiency increased to 28.2%. Sain et al. [144] had also evaluated the possibility of a natural convection type solar dryer under two distinct scenarios (load and unload). Over the course of the trial, the ginger's moisture content decreased from 74% to 3% by drying it under full load settings. The system's overall efficiency was 22.7%, despite the drying efficiency being calculated at 12.4%. Additionally, under no-load and full-load conditions, the efficiency of solar collectors rose by 96% and 55%, respectively [144]. Additionally, a sun dryer and desiccant thermal energy storage were used to dry the cocoa beans [145]. The findings showed that during sunny hours, the drying chamber's temperature ranged between 40°C and 54°C, which was greater than the surrounding air temperature. Additionally, they discovered that the product's specific energy consumption and drying time were enhanced when a solar dryer and thermal energy storage were combined.

Solar panels, a solar accumulator, an electrical heater, a drying chamber, and a centrifugal fan made up the solar hybrid dryer that Reyes et al. [146] suggested and designed. In that arrangement, paraffin wax served as a PCM. With that setup, an outlet air temperature of 60°C was attained, and the solar panel's temperature rose by up to 30°C above the surrounding air. According to the findings, the system's thermal efficiency ranged from 22% to 67%. The system's electricity consumption decreased as a result of the accumulator's value fluctuating between 10% and 21%. Additionally, they discovered that the system's thermal efficiency was greatly increased by using PCM.

PCMs with a high latent heat and a broad surface area for heat transfer are necessary to enhance the thermal performance of solar dryers. As a result, the system's energy efficiency is increased and heat loss and the gap between supply and demand are decreased [136]. However, PCM's low heat conductivity remained an issue, necessitating more study and advancement in this area.

1.5. Significance of the work in the perspective of Bangladesh

The energy demand from renewable energy sources has been proportionally increased due to population growth. In renewable energy production, not only energy production but also efficient use is crucial. One renewable energy source that can be used for a variety of purposes in the modern world is solar energy. A storage media that can help store extra energy and then release it when needed is necessary for the efficient utilization of solar energy.

Bangladesh receives a good amount of sun radiation every day because of its advantageous geographic location. The country's energy consumption might be significantly decreased with the right use of this solar energy. With a capacity development goal of 600 MW by the end of 2031, the government of Bangladesh has already created a master plan to use the plentiful solar energy in many ways. Up until 2018, 6.9 million solar home systems (SHSs) could be installed to reach a total capacity of 220 MW of solar power. Conversely, 3.07 MW and 5 MW of capacity were made possible by rooftop solar and solar mini-grid projects, respectively. Solar irrigation projects with over 1300 pumps might also reach a capacity of 32 MW to serve the nation's rural residents, and the telecom operators have been aided by the solar-diesel hybrid solution program (which involves the installation of 138 small power plants). In order to create a nation equipped with sustainable energy, the Infrastructure Development Company Limited (IDCOL) and the Bangladesh Power

Development Board (BPDB) have been pushing a number of research-development solar projects to numerous governments and private colleges.

The entire land area of Bangladesh, a South Asian nation, is 148,460 square kilometers (57,320 square miles). With a population of 162 million, the nation is ranked eighth among the world's most densely inhabited nations. Once more, the nation's natural resources are extremely scarce. Nevertheless, despite these constraints, the nation's economy continues to expand daily. But over the past ten years, Bangladesh's GDP has grown at a rate of 6.5%, making it a middle-income nation by the end of 2015 and rising to 8.15% in 2019. Furthermore, Bangladesh's GDP of 302.57 billion US dollars in 2019 indicates that it contributes 0.58% of the global GDP. This remarkable economic growth is mostly due to the expansion of industries, particularly those centered on exports, and the creation of new jobs. On the other hand, the nation's vast population and advancing economy are significantly raising the country's energy need. The country's current energy consumption per person is 344 kgoe (kilograms of oil equivalent), up 22% between 2013 and 2019. Bangladesh uses 33 kWh less electrical energy per person than any developed nation, including the United States. People who live in cities or other industrial locations frequently experience steady-state power outages. Even though the government is expanding its electrical projects with new innovations, the massive growth of industries and population growth made it impossible to distribute the electricity effectively. Consequently, there is a strong desire to raise the nation's per capita electricity generation [36].

This piece aims to illustrate Bangladesh's current situation with regard to using its renewable energy resources—particularly solar energy—as an environmentally friendly way to generate electricity. Through the use of solar home systems, rooftop solar projects, solar mini grids, solar irrigation programs, solar-diesel hybrid telecom solutions, etc., it is evident that the nation is approaching a significant milestone in the production of solar electricity.

1.6. Outline of methodology

An experimental setup is created and built at Academic Building 2's heat engine laboratory to examine the viability of the suggested thermal dissipation technology on the PV performance, the next subsections provide examples of experimental measurements and an explanation of the design of the components of the experimental setup. and Fig. 3.1.

Two distinct PV module combinations, each 20W, are planned and built in this system. Two configurations are conventional PV system and PV integrated with enhanced PCM.

The two configurations' electrical and thermal capabilities are concurrently tested in the same weather conditions. In this setup, paraffin and calcium chloride hexahydrate ($CaCl_2 \cdot 6H_2O$) are selected as organic and in-organic PCM. An aluminum container of 48 cm by 4 cm by 34 cm is integrated beneath the PV module in the PV-PCM system, where paraffin wax and calcium chloride hexahydrate ($CaCl_2 \cdot 6H_2O$) as organic and in-organic PCM are stored for passive cooling purposes. Melted wax is poured into the enclosure through two holes drilled at the top of the enclosure for the organic PCM experiment. These holes also act as a breather to prevent pressure buildup. Taking into account the possible volume growth during the phase transition process, about 4.56 kg of paraffin wax is needed to fill the enclosure. A rubber gasket with silicone sealant is positioned between the PV back and PCM enclosure, and it is compressed with the aid of screws to prevent liquid PCM from leaking. To get over PCM's drawback and improve heat transfer, a rectangular aluminum foam with 94% porosity and strong thermal conductivity the same size as a PCM container is embedded in paraffin wax. To receive maximum solar light, both panels are fixed on a stand at a south facing 22.4-degree inclination angle, according to the Chattogram latitude. The investigation in this setup is conducted using an RTD PT-100 temperature sensor. The average PV front surface temperature is determined using three RTD PT-100 temperature sensors. Additionally, the temperature of the PV modules' rear surface is measured using two additional RTD PT-100 temperature sensors. Additionally, two RTD PT-100 temperature sensors are employed to track the temporary temperature changes inside the PCM enclosure. These sensors are placed 1.5 cm and 3 cm below the container's top surface, and are designated PCM1 (upper point) and PCM2 (lower point), respectively. Even though two temperature sensors per container might not be enough to adequately depict the temperature distribution inside the PCM reservoir, the thermal behavior of PCM within the container might be better known. A solar radiation sensor and a wind speed sensor are used to measure the amount of solar radiation at the inclined surface, wind speed, and ambient temperature. Using an ammeter and a voltmeter, output current and output voltage are monitored at regular intervals and manually recorded for later use in computations. Every five minutes, all thermocouples and other sensors are immediately connected to a data logger so that data may be stored. The studies are carried out from 7 a.m. to 5 p.m. throughout the winter months of December, January, and February. Because the sky is clear and the weather is consistent, these days are chosen for better measurements.

1.7 Objectives with specific aims and possible outcome:

Observing and evaluating the impact of PCM on PV panel performance is the primary goal of this study. Additionally, it looks into how wind speed affects PV panel performance. This section lists the main objectives of this research project:

- To analyze the passive cooling of solar cell using Phase Change Material (PCM).
- To analyze the successful use of PCM in latent heat storage system.
- To analyze the performance of PV cell using inorganic PCM.

1.8. Scope and limitation of the research work:

The research is done by heading some scope and also some limitations.

1.8.1 Scope

1. Energy supply from many sustainable sources, such as solar thermal or wind, is intermittent in nature. Therefore efficient energy storage is critical for practical applications of these sustainable energies. PCMs have advantageous features such as nearly isothermal solid-liquid phase change and high energy storage capacity due to the high latent heat of fusion.
2. Stable super-cooling and insulated thermal mass are necessary for the PCM system to achieve seasonal heat storage. While insulated thermal mass is a feature shared by all heat storage media, PCM storage has the unique ability to super-cool. PCMs with stable supercooling easily supercool and can stay supercooled for extended periods of time at room temperature. Long-term storage without heat loss (i.e., no self-discharge) is made possible by this.

1.8.2 Limitations

1. The thermal conductivities of many organic and inorganic PCM materials are very low . As salts have low thermal conductivity, of nearly 1 W/mK. A significant amount of research is being done to increase the PCM's thermal conductivity.
2. Inorganic PCM materials are corrosive to most metals, which results in their short life span as well as the high cost in packing and maintenance.
3. Some problems occur when the salt hydrate is used as a phase change material. Salt hydrate's incongruent melting into a saturated aqueous phase and a solid phase is the primary problem. The process known as decomposition, which is typically irreversible, arises as a result of the variations in density. A nucleating agent can be used to improve the poor nucleating characteristics of salt hydrates, which is one of their additional problems. Furthermore, one of the main problems with employing salt hydrates is their toxicity, destructive character, and volume change.
4. Paraffin is a traditional phase change material and also bears some limitations. It is believed that pure paraffin compounds have extremely high latent temperatures. The excessive amount of carbon released by petroleum-based paraffin adds to the global warming catastrophe, which has geopolitical repercussions.

CHAPTER II

LITERATURE REVIEW

2.1 Introduction

Direct solar radiation is regarded as one of the most promising energy sources in many regions of the world. Globally, scientists are looking for innovative and sustainable energy sources. Creating energy storage devices is one alternative; these are just as crucial as creating new energy sources. One of the challenges facing technologists today is the storage of energy in forms that can be customarily transformed into the necessary form. Energy storage plays a significant role in energy conservation and enhances the performance and dependability of energy systems in addition to lowering the mismatch between supply and demand. It reduces energy waste and capital costs, which saves premium fuels and increases system cost-effectiveness. For instance, load leveling from storage would enhance a power plant's performance, and increased efficiency would result in lower generation costs and energy conservation. At the core of a PCM's function is the latent heat of fusion or the energy absorbed or released during a change in state, with no change in temperature. When a PCM absorbs heat from its surroundings, it changes from a solid to a liquid, effectively storing this thermal energy in the form of latent heat. Due to their large energy storage capacity and ability to function at a constant temperature, phase change materials have been widely used for thermal management of PV solar cells. Because PCM has a high heat of fusion and freezes without supercooling, several researchers have experimentally and numerically studied its inclusion with PV systems. Phase change materials present a fascinating and potent tool in the quest for efficient energy management. By harnessing the properties of these materials, scientists and engineers can significantly impact how thermal energy is utilized across various industries, potentially leading to more sustainable practices and innovations in temperature regulation technology. For this reason, experiments are carried out in this work to investigate how the addition of PCM to PV modules affects their performance.

2.2 Thermal energy storage

Thermal energy storage can be stored as a change in internal energy of a material as sensible heat and latent heat. Renewable energy systems require energy storage, and TES is used for heating and cooling applications. Unlike photovoltaic units, solar systems predominantly harness the Sun's thermal energy and have distinct efficiencies. However, they rely on a radiation source for thermal support. TES systems primarily store sensible and latent heat. Heating a solid or liquid to store thermal energy while taking specific heat and temperature changes during phase transition processes into account is known as sensible heat storage, or SHS. Because of its abundance and high specific heat, water is frequently used in SHS; at temperatures higher than 100°C, other materials such as oils, molten salts, and liquid metals are used. Phase change materials (PCMs), which absorb or release heat to maintain a constant temperature, are used in latent heat storage (LHS). These PCMs are quite good at storing heat. The families of energy storage materials and the classification of TES are shown in Fig. 2.1. There are three categories of PCMs: eutectic, inorganic, and organic. Organic PCMs include non-paraffin materials, which melt and freeze without phase separation, and paraffin wax, which releases a significant amount of latent heat during crystallization, making it perfect for heat fusion storage. Inorganic PCMs, including metallic materials and salt hydrates, replicate the melting and solidification thermodynamics and sustain constant fusion temperatures [61]. Eutectic materials melt and freeze at the same time, which reduces the possibility of component separation and segregation during phase transitions.

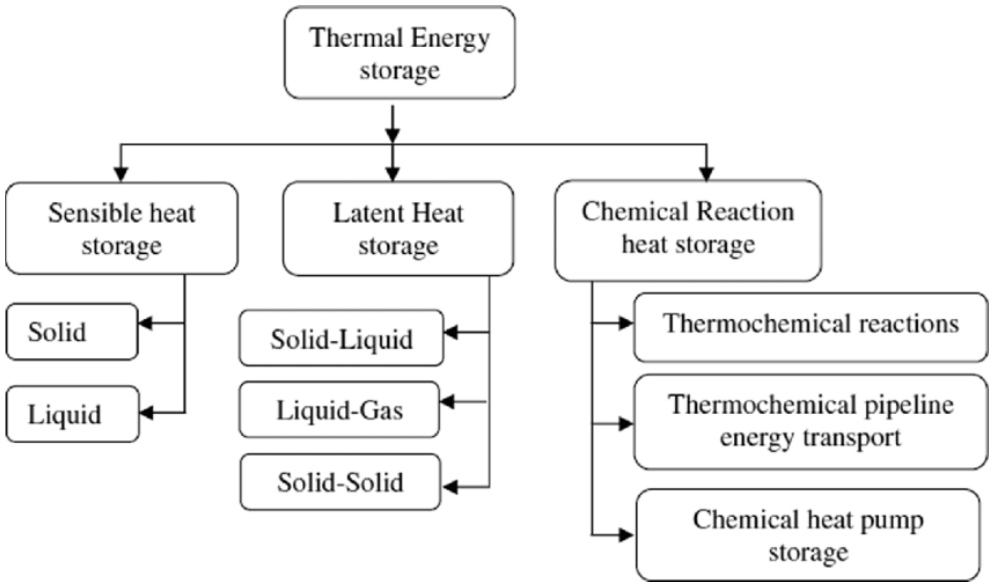

Fig. 2.1. Families of phase change heat storage materials

2.2.1 Sensible heat storage

Sensible heat storage (SHS) uses a solid or liquid's heat capacity to raise its temperature in order to store thermal energy. During the charging and discharging process, the SHS system makes use of the material's heat capacity and temperature change. Water is known as one of the best materials that can be used to store thermal energy in form of sensible heat because water is abundant, cheap, has a high specific heat, and has a high density. In addition; heat exchanger is avoided if water is used as the heat transfer fluid in the solar thermal system. Until now, commercial applications use water for thermal energy storage in liquid based systems. Table 2.1 shows selected materials use for sensible heat storage are:

Table 2.1 Materials for sensible heat storage

Phase	Medium	Temp. Range [°C]	Density Kg/m³	Specific Heat J/kg.K
Solid	Rock	7-27	2560	879
	Brick	17-37	1600	840
	Concrete	7-27	2100	880
	Sand	7-27	1550	800
	Soil	7-27	2040	1840
Liquid	Water	7-97	1000	4180
	Engine oil	Up to 157	888	1880
	Ethanol	Up to 77	790	2400
	CalorieaHT43	12-260	867	2200
	Butanol	Up to 118	809	2400
	Other organic	Up to 420	800	2300

2.2.2 Latent heat storage

Latent heat storage stores thermal energy by utilizing the material's latent heat. The quantity of heat that is absorbed or released when a substance transitions from one phase to another is known as latent heat. Latent heat of vaporization and latent heat of fusion are the two categories of latent heat that are recognized. The amount of thermal energy absorbed or released when a material transitions from the liquid phase to the vapour phase, or vice versa, is known as the latent heat of vaporization. The amount of heat absorbed or released when a material transitions from the solid phase to the liquid phase, or vice versa, is known as the latent heat of fusion. Indeed, due to the significant volume shift that occurs with this kind of phase change, latent heat of vaporization is rarely taken into consideration for latent thermal energy storage applications. The mass and latent heat value of the material being utilized determine how much thermal energy is stored as latent heat. Phase transition materials are those that can store thermal energy as latent heat.

2.2.3 Comparison between sensible and latent thermal energy storage

Latent heat storage is particularly attractive since it provides a high-energy storage density and has the capacity to store energy at a constant temperature or over a limited range of temperature variation which is the temperature that corresponds to the phase transition temperature of the material. Compared to sensible storage materials like rock, masonry, or water, they store 5–14 times as much heat per unit volume. However, there are still numerous issues with the materials used to carry out the storage process in latent thermal energy storage, including their high cost, poor thermal conductivity, and instability of thermophysical properties after numerous cycles.

2.2.4 Classification of latent heat storage materials

Phase change materials (PCMs) are another name for latent heat storage materials. Papers by Abhat [2], Lorsh et al. [3], Lane et al. [4], and Humpries and Griggs [5] provide lists of the majority of potential materials that could be utilized for latent heat storage. Classification of latent heat storage materials is shown in Fig. 2.2.

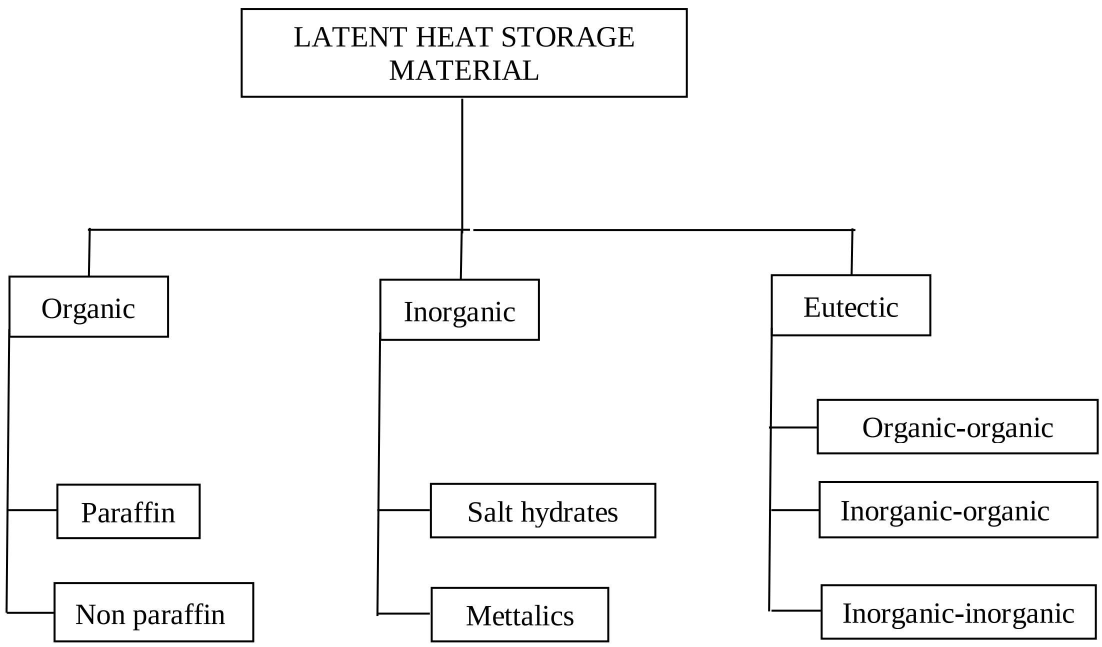

Fig 2.2. Classification of latent heat storage materials

2.3 Cooling Methods of PV System

The electrical efficiency of PV modules is sensitive to operational temperature, decreasing by 0.4% to 0.65% for every degree of temperature increase [158, 159]. Baghzouz et al. provide a clear explanation of the reasoning for this phenomenon [160]. For example, crystalline silicon cells exhibit a 0.37% and 0.5% decrease in VOC and maximum power attainable, respectively, with every degree of temperature increase. In contrast to the 0.05% increase in ISC per degree Celsius, this decline is more pronounced. It can be concluded that PV modules could operate with higher efficiency on cold than hot days. Since deserts are good places for solar farms to get operational, investigating their weather condition is essential. Taking the "Lut Desert" in Iran as an example, in the daytime in summer, the ambient temperature reaches up to 50ºC, and at night, it is dropped by about 10–20ºC. According to Helden et al. [161], PV modules may achieve temperatures of up to 35ºC above room temperature on bright days. This indicates that PV laminates are subjected to severe thermal loads both during the day and at night. Furthermore, solar cells will deteriorate over time if their temperature rises above a certain point [162]. These factors make it essential to build a cooling field for a photovoltaic module.

In general, there are three kinds of PV cooling methods:

1. Passive cooling, which doesn't require additional energy
2. Active cooling, which uses more energy
3. Active and passive cooling combined

Gharzi et al. [163] have investigated these techniques in detail. According to their findings, the best strategy for maintaining PV electrical efficiency and making use of thermal energy was to combine active and passive cooling. However, the active approach by itself or in combination with other techniques need additional equipment such [164]:

1. Piping (for cooling fluid circulation)
2. Pump (for the cooling fluid's drive)
3. Manometer (to gauge the pressure of the cooling fluid)
4. Flowmeter (to monitor the coolant fluid's mass/volume flow rate)
5. Sensors and controllers (to regulate the cooling fluid's flow rate at various periods)
6. The condenser is used to cool the working fluid.

These are but a handful of the crucial equipment needed to cool photovoltaic panels in a solar farm. The heat produced by the PV panels cannot be used if the solar farm is situated far from any residential, commercial, or industrial sectors, which is likely to occur because installing a solar farm requires a large amount of useless land. Consequently, the system's thermal efficiency would be zero. Another problem is the parasitic loss of PV panels used to circulate the working fluid that needs to be taken into consideration, in addition to all the additional expenses incurred by the supplemental devices. As a result, active cooling methods are very effective in locations that need hot water or air to activate photovoltaic thermal (PVT) systems [165]. In these situations, the cooling system produces thermal energy in addition to increasing electrical efficiency, resulting in an overall increase in efficiency [166].

Passive cooling is another effective way to cool the PV modules without consuming extra energy. With the least amount of negative environmental impact, this method uses radiation, natural convection, evaporation, and spectrum splitting to release the heat that a photovoltaic module has stored [167]. These passive methods would be practical and effective in cooling solar farm panels. Each technique has its attributes in terms of electricity improvement, initial investment, and maintenance costs. The comparison of attributes described above is mentioned in Ma et al. [168] (Table 2.2).

Table 2.2 Comparison of several methods for passive cooling. [168]

Empty Cell	Electricity improvement	Initial investment	Maintenance cost
Natural ventilation	✓	✓	✗
Liquid immersion	✓✓	✓✓	✗
Heat pipe	✓✓	✓✓	✗
Phase change material	✓✓✓	✓✓✓✓	✗

Notes: "✗" means no or very little, "✓" meaning the lowest, and "✓✓✓✓✓" representing the highest.

It is important to note that the contents of Table 2.2 only represent a small percentage of its primary reference, which covered both active and passive approaches.

There are several PV passive cooling techniques, including heat pipes, thermoelectric, phase change materials, natural ventilation, liquid immersion or floating, and spectrum beam splitters. State-of-the-art studies are presented for each passive approach, followed by additional recommendations. To make the comparison easier, all of the previously listed papers are compiled into a table. The summary table may make it easier to select the cooling technique for next work because it is based on the environmental factors and the amount of sunlight applied to the particular issue. Finally, the conclusion section is written, and each technique's future work development is highlighted.

2.3.1 Passive cooling methodologies

It is not secret to regulate the temperature of photovoltaic panels to guarantee their best performance and extended lifespan. Cooling solar farm panels that have been installed on a lot of bare ground would be difficult with active methods. The solution to the problem is in determining an appropriate passive cooling technique based on geographic location. Elbreki et al. [169] conducted a thorough analysis of active and passive cooling strategies for the thermal control of PV module temperature in 2016. But in the last five years, a lot of research has been done on PV modules and panels since water scarcity and global warming have emerged as two pressing issues that are endangering our future. As a result, there are now much more papers about "Photovoltaic" and "Passive Cooling." Since there hasn't been a review article on the passive cooling strategy of PV panels or modules in the last five years, it appears that the most recent published studies should be gathered in order to pave the way for the discovery of the best passive cooling methods to use with a solar farm.

2.3.1.1 Natural ventilation

The simplest and least expensive way to use PV cooling is by natural convection of water or air [170]. One way to convert traditional buildings to zero energy buildings is by the use of building-integrated photovoltaics, or BIPV [171]. By allowing air to naturally convect through a duct behind the PV panels, Brinkworth et al. [172] attempted to lower the temperature of the PV cladding. Their experimental and numerical study's schematic work is shown in Fig. 2.3. They were able to design several fundamental parameters, such the cooling duct's depth and height, based on their simulation. Furthermore, the temperature of the solar cells had dropped by roughly 15 to 20 K due to natural convection behind the PV panels. This was a major cut to increase the amount of power generated by PV cladding for building walls and rooftops. Since cooling solar panels for use in a solar farm was the primary goal of this work, Brinkworth et al. [172] provided only one illustration of how amazingly natural convection may lower the temperature of solar panels and increase their power production.

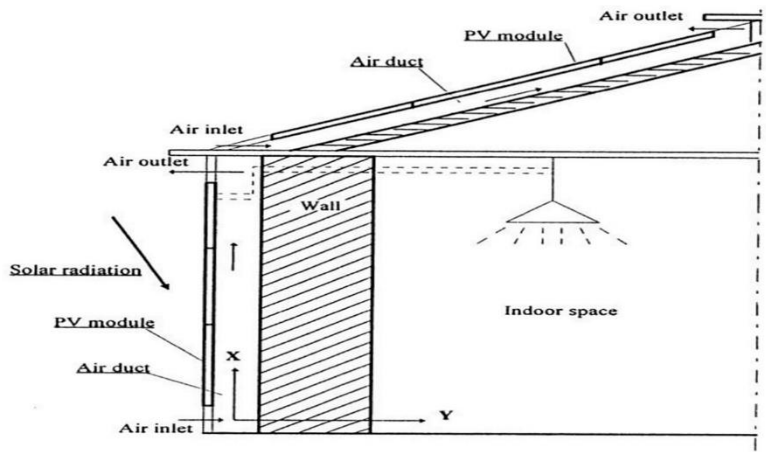

Fig. 2.3. Schematic illustration of PV cladding for building walls and roofs [172]

The cooling of a polycrystalline module with a 30 W capacity was experimentally investigated by Mays et al. [173] on a sunny day in Beqaa. The use of aluminum finned plates behind PV modules was found to improve power production by an average of 1.86 W and electrical efficiency by an average of 1.77%. Two configurations of L-profile aluminum fins were proposed by Grubisic-Cabo et al. [174]. In the first configuration, the fins were arranged in parallel, while in the second configuration, as shown in Fig. 2.4, the fins were arranged randomly. The ease of air circulation through randomly positioned perforated fins likely contributed to the second configuration's greater benefit in lowering the PV panel temperature. Further experiments were conducted for the second configuration for the city Split in Croatia. The results showed a 2% electrical efficiency improvement compared to the bare reference panel.

(a) (b)

Fig. 2.4. Two different L-profile fin configurations were used in the work of Grubisic-Cabo et al. [174]

Bayrak et al. [175] conducted another case study in the Turkish city of Elazig. From 9:00 a.m. to 4:00 p.m., ten examples, designated A1–A10, were examined in order to examine fin numbers and their configurations on a PV panel. The wind effect was also taken into account in Duffy and Beckman's research since they assumed that the heat transfer coefficient was a linear function of wind speed [176]. With 26 staggered-vertical fins, case A5 has the highest energy and exergy efficiencies, at 11.55% and 10.91%, respectively, making it stand out from the others. Interestingly, in both horizontal and vertical arrangements, the cases with 7 cm fin length fared better than those with 12 cm. The results of their experiments are shown in Fig. 2.5.

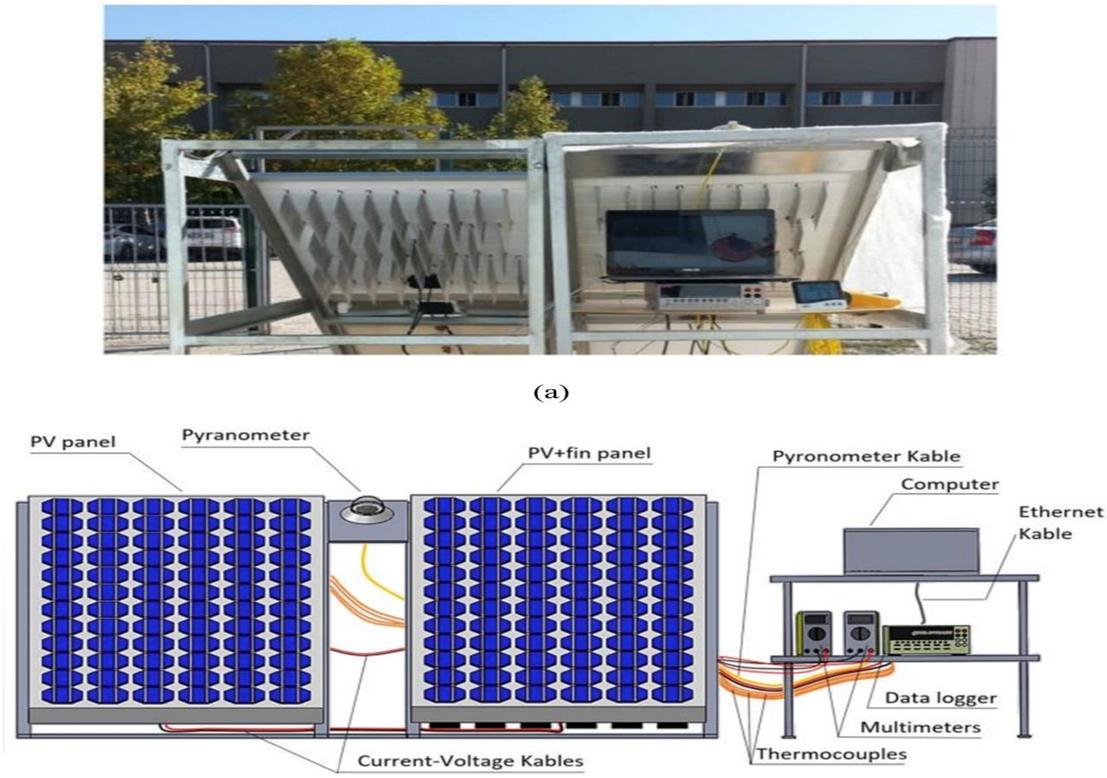

(b)

Fig. 2.5. Two views of the experimental setup: (a) real photograph, and (b) schematic view [175]

The cooling of a photovoltaic module with fins and a planar reflector was recently experimentally examined by Elbreki et al. [177] at the National University of Malaysia. For the passive cooling system, two distinct heat sink designs—longitudinal and lapping fins—were used. To determine each cooling system's shortest payback period in comparison to the reference module, economic analysis was also conducted. Using passive cooling with lapping fins under an average solar irradiance of 1000 W/m2 and an ambient temperature of 33ºC, the latter study produced the best performance, with mean PV module temperature, electrical efficiency, and power output of 24.6ºC, 10.68%, and 37.1W, respectively. According to the investigation, the payback periods for PV modules with longitudinal, lapping fins, and naked PV modules were 4.2, 5, and 8.4 years, respectively, from an economic perspective. Thus, to keep the PV module temperature at lower levels, a cooling system with lapping fins would be a viable choice. Their experimental work on the seventh floor of the National University of Malaysia's solar energy research institute is seen in Fig. 2.6. In a recent work, Ahmad et al. [178] quantitatively examined a truncated multi-level fin heat sink that is connected to the bottom of a PV module while taking the fin shape into account. Their results indicated that the truncated multi-level fin heat sink design offered an average temperature that was 6.13% lower than the conventional rectangular form. While previous work focused on fin shape, Marinic et al. [179] suggested changing the PV design by making a slit on a PV panel. Their simple yet effective modification has resulted in a 3°C decrease in the panel's temperature.

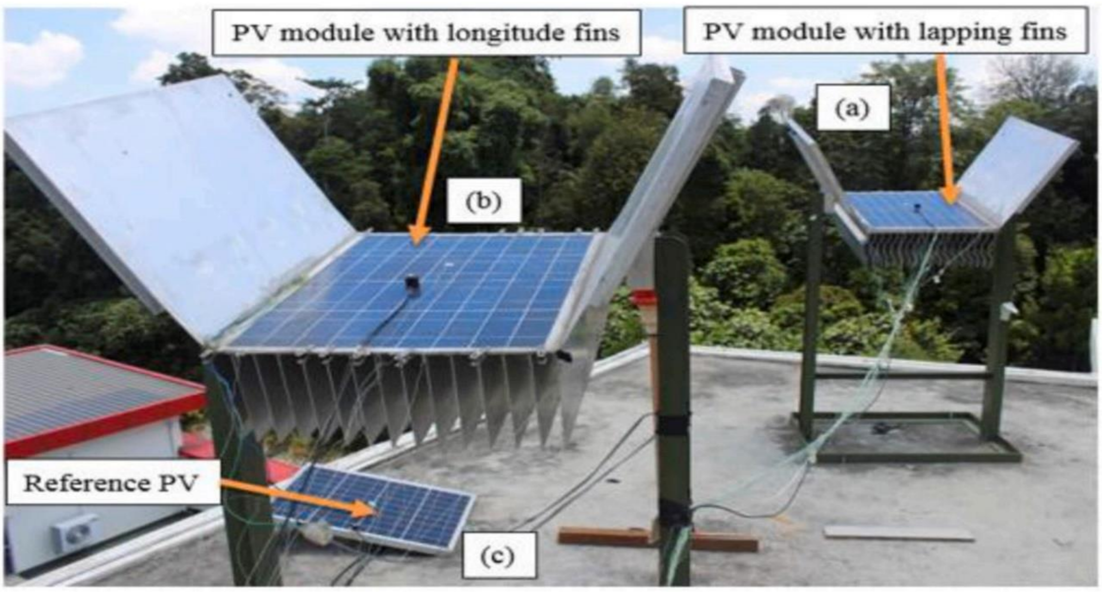

Fig. 2.6. Experimental setup [177]

A solar power plant known as a solar park or solar farm was designed by a large-scale grid-connected photovoltaic system whose power output is more than 1 MW. While most of the studies were focused on the PV panels' inclination angle to absorb the sunlight as much as possible, Glick et al. [180] investigated how the layout of PV panels affected the flow of incoming wind. Their experimental work's schematic diagram is displayed in Fig. 2.7. The PV panels' inclination angle was altered during their investigation, and the upper and lower surface heat transfer coefficients were computed. The greatest heat transmission on the lower surface was seen at an inclination angle of -30°, as illustrated in Fig. 2.7. To increase the lifespan and efficiency of PV panels, it was advised to improve the sub-panel flow by using deflectors or optimizing height. That investigation made it abundantly evident how the entering natural airflow might significantly extend the PV panels' lifespan and efficiency. The benefits of mounting PV panels on a solar updraft tower's collector have been well discussed in Eryener and Kuscu's study [181]. Eryener and Kuscu's experimental work is displayed in Fig. 2.8. [181]. They claimed that the hybrid system's integrated PV panels were more efficient than its standalone counterparts.

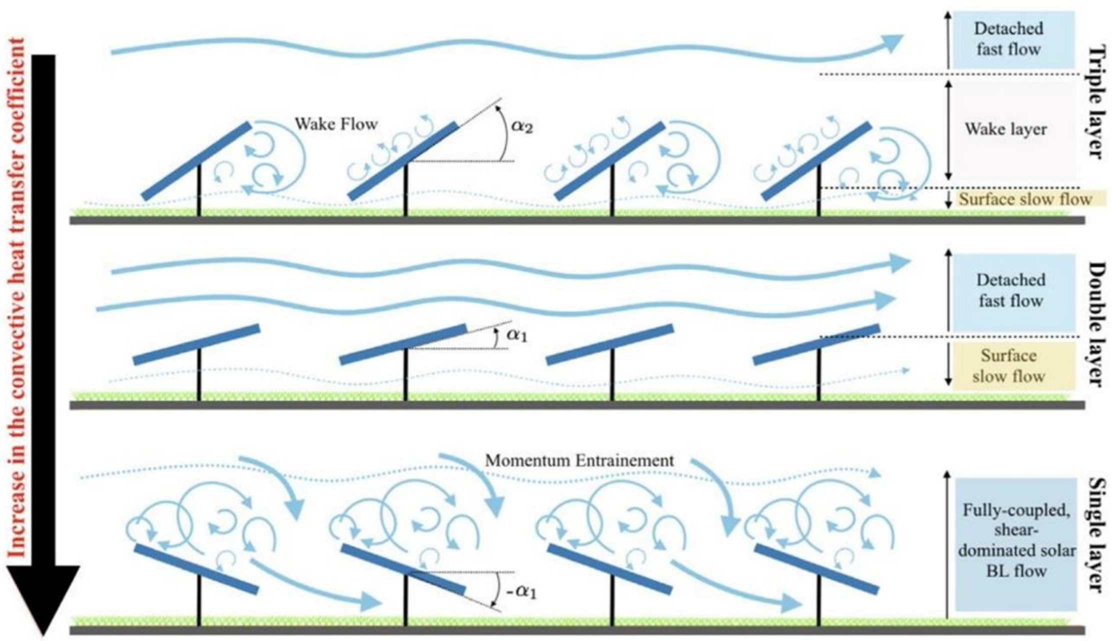

Fig. 2.7. Schematic diagram of different solar farm arrangements used in Glick et al. [180]

(a) Top view of hybrid solar updraft tower

(b) Close-up view of PV panels installed on the solar updraft tower's collector

Fig. 2.8. Experimental work of Eryener and Kuscu [181]

In Kirkuk, Iraq, Ahmed and Hussein [182] conducted an experimental investigation on the hybrid arrangement of PV panels and solar chimney. Two distinct configurations were analyzed and contrasted in their experimental work. Figure 2.9 displays those two configurations. The findings demonstrated that system (B) performed better overall than system (A), despite system (A) having a higher thermal gain. Because system (A) had the PV panel positioned underneath the chimney collector and system (B) had it on top, the greenhouse effect caused the temperature to rise and the electrical efficiency to decrease. They have reported that in system (A) the maximum temperature reached 90ºC while in system (B) it was below 67ºC.

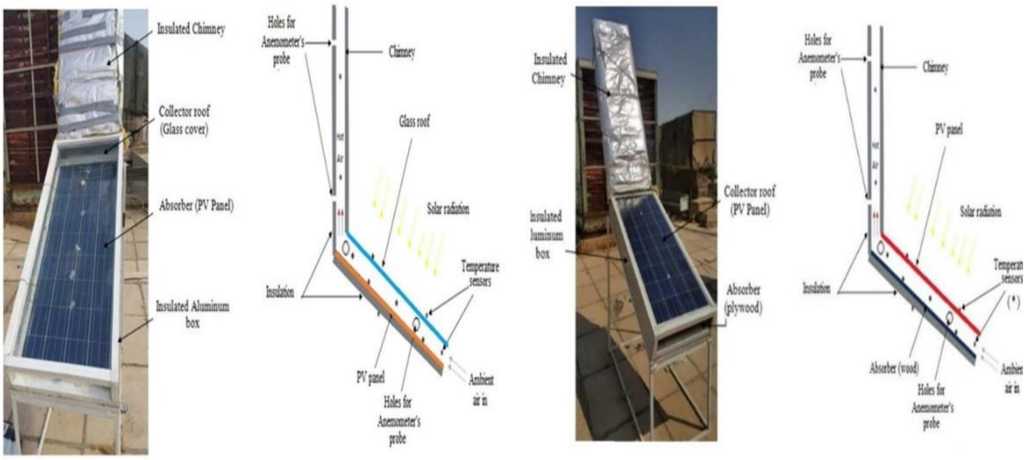

a) System A b) System B

Fig. 2.9. The same conditions were used to evaluate two distinct configurations [182]

We may be able to benefit from reduced land use for the same electricity output by combining PV panels and solar chimneys. However, the goal was significant. Engineers preferred the air flow rate through a solar chimney over the hybrid system's power production if the chimney was built for air purification. Huang et al. [186] investigated the behavior of such hybrid combinations experimentally and numerically for a number of goals. Their experimental setup is displayed in Fig. 2.10. They had stated that the volumetric flow rate would be at its highest and the electricity production would be at its lowest if the solar chimney was run solely. In order to produce more electricity, it was advised to combine PV panels with a solar chimney. In reference to the study of Ahmed and Hussein [182], the same findings have been drawn regarding the location of PV panels. The top and bottom PV panels were expected to have an average temperature of 50.01ºC and 67.32ºC, respectively. Combining the PV panels with a solar chimney decreased the thermal air flow rate, while using a suction fan boosted the overall airflow rate.

(a) The solar chimney system (b) The hybrid solar chimney and photovoltaic system

Fig. 2.10. Experimental setups of Huang et al. [186]

2.3.1.2 Liquid immersion or floating

One very effective passive cooling technique for PV panels is to submerge them in a liquid. Because there would be no heat resistance and the PV panel surface in contact with the coolant medium would be maximized in this scenario. [188] Wang et al. "This suggested solution is effective where both the ambient temperature and the level of irradiance, along the year, was fairly high," claim Tina et al. [189]. To investigate the optical characteristics of water and assess the power output and efficiency of the panel, they immersed crystalline silicon panels at several water depths. Their tests, which were set up in Catania and Pisa, Italy, are depicted in Fig. 2.11. According to their findings, the module's maximum power production would occur if the panel was immersed in water that was 5 cm deep. The power consumed by the panel would drop if the water depth was increased from 5 cm to 15 cm. This phenomena was caused by the fact that light absorption increases with depth in the water. Furthermore, Lanzafame et al. [190] observed that a water depth of 4 cm was appropriate, leading to a 15% increase in efficiency. The sun spectrum's fluctuation with respect to water depth was noted by Clot et al. [191] in Fig. 2.12. Water absorption on a logarithmic scale is represented by the black plot. Even though second-generation amorphous solar cells are less efficient than first-generation solar cells, their ability to withstand partial shading and convert light into electricity at a depth of up to 1.5 meters makes them a strong contender for use underwater, according to research by Clot et al. [191]. One of their executive initiatives that was operating is shown in Fig. 2.13.

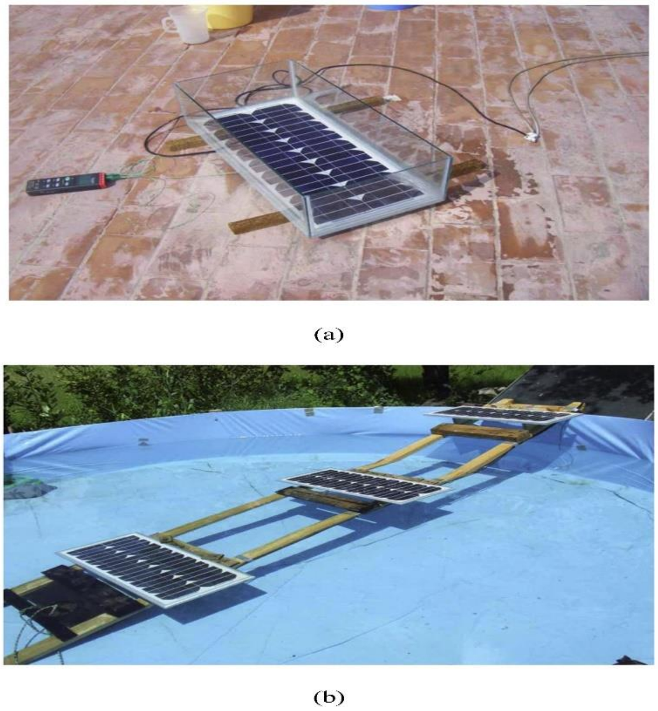

Fig. 2.11. Experimental apparatus in (a) Catania, and (b) Pisa [189]

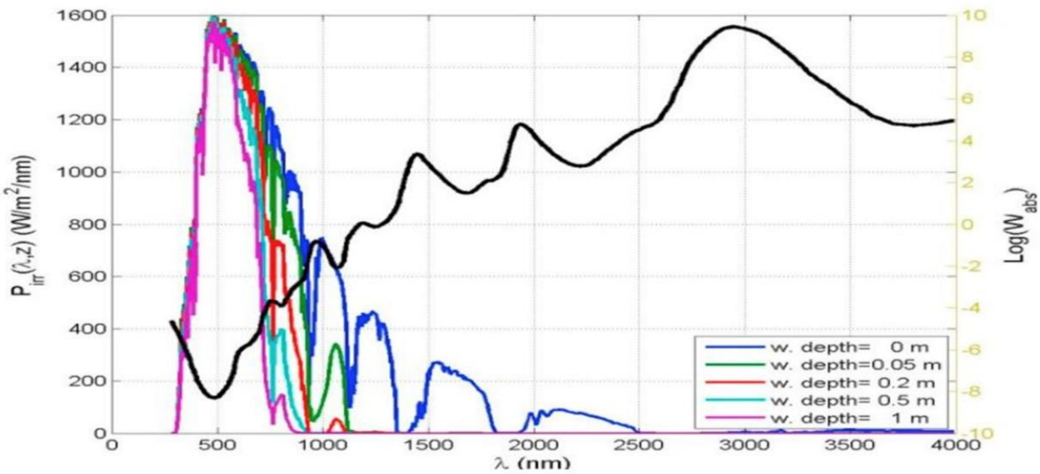

Fig. 2.12. Variation of the solar spectrum with water [191]

Fig. 2.13. PV panels installed at the bottom of a swimming pool [191]

The water immersion technique was also studied by Mehrotra et al. [192] as a passive method of cooling a 2W polycrystalline silicon solar panel. Their experimental work conducted from 10:00 a.m. to 5:00 p.m. on April 18–23, 2014, in Bhopal, India, is depicted in Fig. 2.14. They had stated that the highest electrical efficiency of 4.76% was obtained at a depth of 1 cm. In comparison to the system without cooling, this accomplishment represented a 17.8% increase. Water was the cooling medium in most study studies where solar panels were immersed, but it wasn't the only choice. Six liquids, including polar ethanol and glycerin, non-polar benzene and silicon oil, as well as inorganic distilled water and tap water, were studied by Wang et al. [188]. After being submerged in these solutions, the single crystalline solar cells were exposed to 1000 W/m2 of light. They concluded that silicone oil that was non-polar performed the best. Regarding different coolant liquids, Al-Amri et al. [193] have designed a cooling field for a polycrystalline silicon solar panel with a peak efficiency of 11% under Standard Test Conditions (STCs), with the combination of heat pipes and three different liquids such as engine oil, Ethylene glycol $(CH_2OH)_2$, and water. They had mentioned that owing to higher thermal conductivity and specific heat capacity, water was a better choice than other liquids. About 40 years ago, solar cells were submerged for a different reason and in a different situation. In order to determine whether solar cells could power maritime devices, Stachiw [194] investigated their performance in water ranging from 0.75 to 29 meters. According to their results, a solar cell immersed at a specific depth in their experiment would have an efficiency of 5–10% that of the identical solar cell in the atmosphere. They did note, however, that extremely effective silicon solar cells remained a viable option for maritime applications. The purpose of submerging PV cells was clarified by the previously cited citation. Once silicon cells were more than a few centimeters below the water, their efficiency significantly decreased because of the "shifting of the radiation towards the green and blue side of the spectrum underwater" [195]. Therefore, floating photovoltaic (FPV) panels on a water reservoir could be a good way to cool them down without having to worry about the liquid's optical qualities covering the panel's top surface.

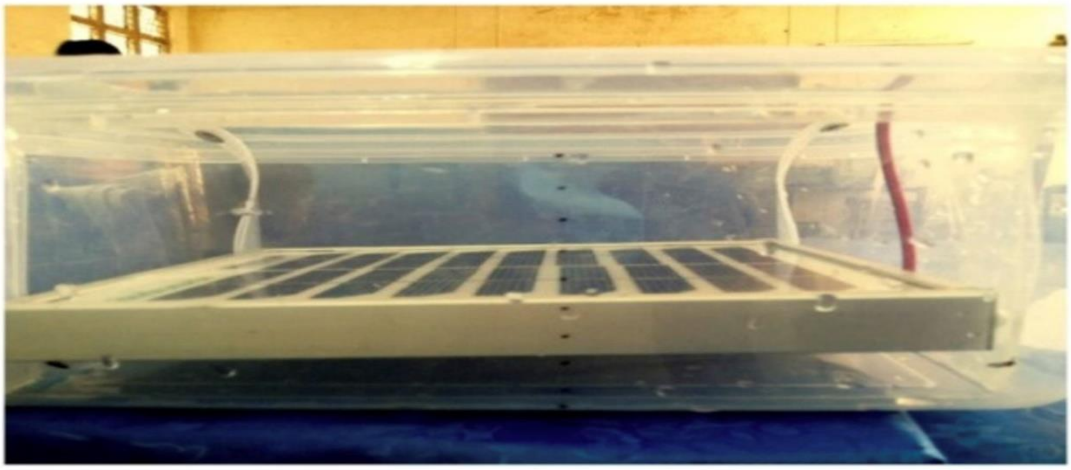

Fig. 2.14. Experimental work of Mehrotra et al. [192]

The efficiency improvement and environmental effects of floating solar panels as a workable way to cool a large solar farm are covered in this section. Compared to PV panels placed on land, floating PV panels demonstrated an efficiency of over 10%, according to a review paper by Sujay et al. [158]. We could benefit from photovoltaics in more ways besides this one. According to Barbuscia and Michele [197], installing PV panels on the water was approximately 15% more expensive than installing them on land; however, photovoltaics' operating and maintenance costs were frequently lower than those of PVs placed on the ground [198]. Regarding the effects on the environment, installing PV panels on water reservoirs such lakes, canals, dams, and ponds could cut evaporation by as much as 70% [199]. Furthermore, the shadowing effect would limit the growth of algae, reducing the level of contamination in the water [200]. For hybrid applications, floating PV panels could be combined with hydropower sites to increase the energy yield, and help manage periods of low water availability [201]. Other added values of the hybrid system could be found in the literature review of Lee. et al. [202]. Figure 2.15 depicts a schematic of a hybrid FPV-hydropower system.

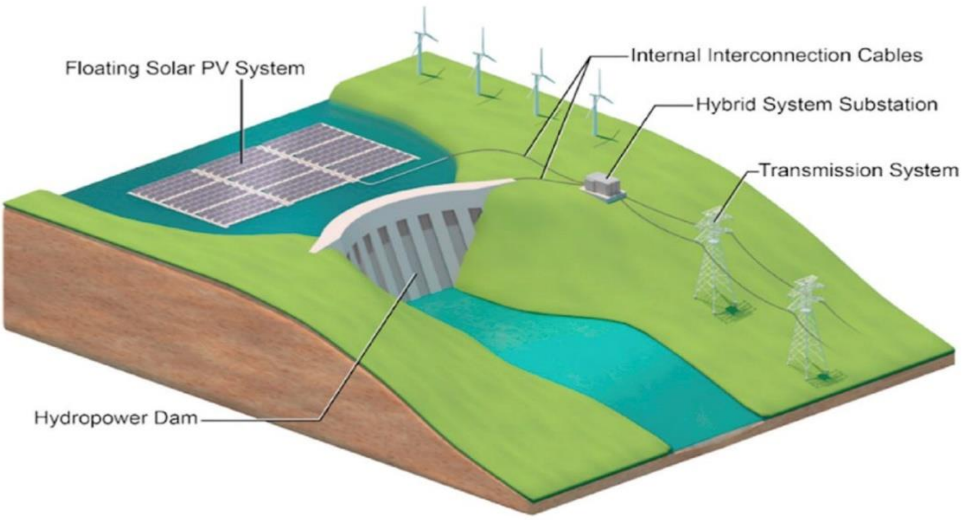

Fig. 2.15. Schematic of a hybrid FPV-hydropower system [202]

2.3.1.3 Heat pipe

Evaporation and condensation take place in a heat pipe (HP), a two-phase heat transfer device that enables substantial heat transfer [203]. One passive cooling method that is typically advised in high-latitude regions or during the winter months is the coupling of solar panels with heat pipes [209]. In order to increase the PV conversion efficiency, Han et al. [204] suggested a concentrating PVT system that integrated the benefits of HP cooling and nanofluid-based spectral beam splitter (SBS) technologies. At an eight-suns concentration ratio, the average electrical efficiency was 0.7% greater when a heat pipe was used than when one wasn't. The wickless heat pipe and the wire-meshed heat pipe PVT systems were the two distinct heat pipe PVT systems that Hu et al. [205] experimentally investigated. It had been studied how the inclination angle affected both systems. According to their report, the wickless heat pipe was more sensitive to the inclination angle than the wire-meshed heat pipe. At latitudes above 20° and below 20°, respectively, the wickless heat pipe PVT system and the wire-meshed heat pipe PVT system were advised. The geometrical features of the heat pipe system utilized in Zhang et al.'s [206] experimental and numerical studies are displayed in Fig. 2.16. In reference to the sort of operating fluid, they stated that R134a was advised for cold climates while water was appropriate for temperate climates. Another study had also confirmed that a combination of heat pipe with PV is suitable for freezing weather conditions [207]. However, using heat pipes in conjunction with a PV system wasn't just for the winter. In both spring and summer, Moradgholi et al. [208] examined the evaluation of heat pipes using PVT systems. The PVT system produced 5.67% more electrical power than the naked PV system in the spring when methanol was selected as the heat pipe's working fluid. Acetone was utilized as the thermosyphon's working fluid in the summer, and a 7.7% increase in power output was noted. They set up their experiment as shown in Fig. 2.17.

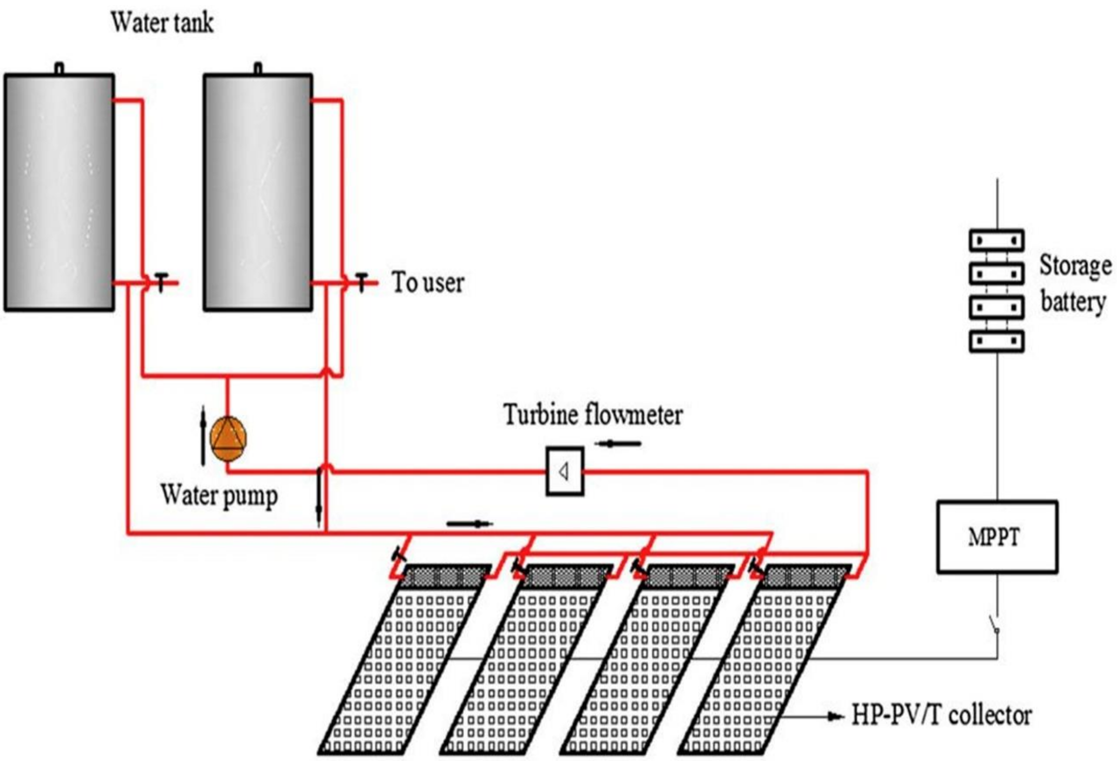

Fig. 2.16. Schematic diagram of Zhang et al. [206]

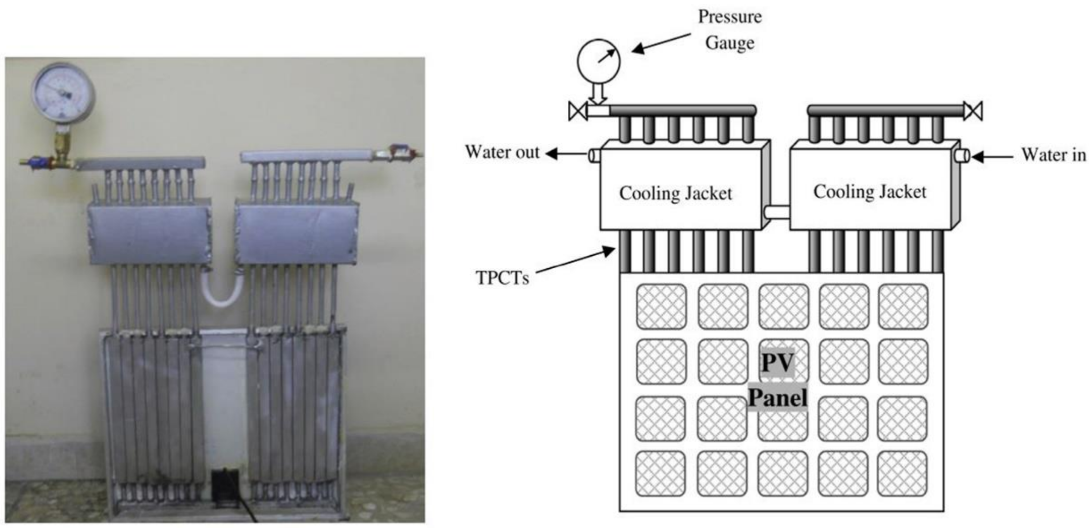

Fig. 2.17. Experimental setups and schematic diagram of Moradgholi et al. [208]

Heat pipe is consisted of an evaporation and condensation section. The excess heat of a PV panel could be absorbed from the evaporation section and released via the condensation section. In order to use the thermal energy of the system, the condensation part was coupled with tap water. As a result, HP-PVT systems were widely utilized in residential areas where simultaneous thermal and electrical energy requirements existed. The compound of HP-PVT was examined in all of the previously stated research. Studies on using heat pipes alone to cool PV modules or panels are quite rare. Koundinya et al. [209] investigated the cooling of PV panels using finned heat pipe technology both theoretically and empirically. The use of the technology resulted in a maximum decrease of

13.8K. Pulsating heat pipes (PHPs) were used by Alizadeh et al. [210] to cool photovoltaic systems. Their computer calculation revealed that the PV panel with PHP increased electrical power generation by about 18%. It was important to note that their simulation was run with an ambient temperature of 291K and a heat flow of 1000 W/m2. In conclusion, additional research is required to determine whether heat pipes alone are a viable cooling method for solar farms, based on the literature review.

2.3.1.4 Thermoelectric generator

The thermoelectric generator (TEG) system can either generate electricity if there is a temperature gradient at both legs (Seebeck effect) or operate as a cooling system when voltage is provided to the two p and n sides of the device (Peltier effect). When it comes to the Peltier effect, TEG can cool a PV module by using a portion of the PV power output, which is classified as active cooling. By absorbing the PV module's excess heat, the TEG could generate additional power in the event of the Seebeck effect. As a result, the PV module cools down and generates more power at the same time. It is possible to think of this as a hybrid technology that would benefit both systems.

Wu et al. [211] has examined these two-hybrid systems under various circumstances since the TEG system combination with PV cell has two distinct states with reference to Peltier or Seebeck effect. They found that while hybrid photovoltaic systems with thermoelectric cooling (PV-TCS) had lower cell temperatures than hybrid photovoltaic systems with thermoelectric generators (PV-TGS), they also had poorer output and efficiency. The effect of wind speed on standalone PV systems has drawn greater attention than that of hybrid systems. The performance of both hybrid systems was greatly enhanced by the cooling heat sink capacity. The heat sink was connected beneath the TEG systems, which was noteworthy. Babu and Ponnambalam [212] used mathematical modeling to investigate the PV-TEG system's performance. They concluded that the hybrid PV-TEG system may boost overall efficiency by 6% and generate an extra 5% of energy. Additionally, they reported that the hybrid PV-TEG system's power increased due to the rise in ambient temperature, but this had a negative impact on the standalone PV system.

The thermal impediments that exists between the interfaces as a result of the microscopic roughness of the PV and TEG surfaces is one of the primary difficulties in attaching TEG solid state devices to a PV module. The PV-TEG systems were evaluated by Kidegho et al. [213] using three distinct thermal interface materials: aluminum foil, heat spreader, and graphic sheet. They discovered that the thermal interface materials effectively reduced the difficulties associated with thermal coupling, which in turn enhanced their total power output.

A heat pipe-based PV-TEG (HP-PV/TEG) system could be created by combining the PV-TEG hybrid systems with heat pipes. In the Makki et al. [214] well, Figure 2.18 shows how to integrate such a hybrid HP-PV/TEG system. Makki et al.'s theoretical work [214] examined the hybrid system in a variety of operational conditions, including ambient temperature, wind speed, and irradiance. It was found that the hybrid system outperformed the PV-only system in every instance. The hybrid cooling method may be a viable solution for large-scale photovoltaic grid-connected systems because it was passive and performed better than a standalone PV system. However, further research was needed in that field before they could be completely marketed.

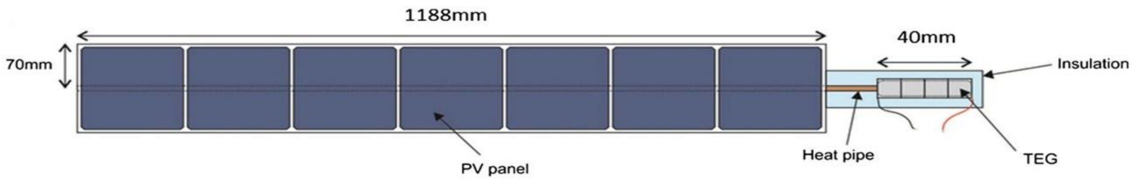

Fig. 2.18. Top view of heat-piped based PV-TEG system [214]

2.3.1.5 Phase change material

By altering the temperature within a limited range of operations, phase-changing materials (PCMs) offer a distinctive property [215]. They are able to retain as much thermal energy as possible because of their high latent heat of fusion during the melting range. Therefore, adding PCMs to PV modules or panels may be a passively practical solution. Furthermore, "PCM cooling is the most capable technique," per a recent state of the art study by Dwivedi et al. [216]. Because of the aforementioned advantages of PCMs, integrating them with solar modules or panels would prevent two major problems that could arise over a PV system's lifetime [217]:

1. Daytime and nighttime thermal stresses brought on by abrupt temperature fluctuations
2. Water vapor condensation at night causes a solid crust to form on a photovoltaic module.

Numerous published research studies have used PCMs with a solar module or panel because of the aforementioned benefits. They belong to an active classification when PVT and PCM are combined (PVT-PCM). Review studies by Mahian et al. [218], Ali [219], and Chandel and Agarwal [220] mention most of those papers. Nonetheless, the most recent research on PCMs with PV systems (PV-PCM) is described here, along with a discussion of the potential for using the concepts of improving PCMs' thermal conductivity for a solar farm application. This is a fresh perspective on the longevity and effectiveness of PV-PCM therapy.

The PV-PCM technique is credited to Huang's research team as its creator and forerunner. In order to increase the rate of heat transmission, Huang et al. [184] introduced the idea of PV-PCM technology in 2004. Both numerical and experimental methods were used in their investigation. While indoor experiments were conducted to verify the results report, the numerical investigation was conducted concurrently with the experimental study to examine the thermophysical performance of the PCM. Their results showed that the fin thickness had little bearing on the rate of heat transfer. Nonetheless, PCM thickness and ambient temperature did have a significant impact. In Huang et al. [183], the same research team conducted a 3D numerical investigation. They have contrasted their findings with those of their earlier research. Remarkably, the new 3D study, which is displayed in Fig. 2.19 [184], was in good agreement with the earlier 2D numerical simulated case. In a recent study, Huang et al. [185] investigated and experimentally evaluated three distinct PCMs, including waksol A, RT 27, and RT 35. They stated that during the PCM melting phase transition, extruded aluminum plates were able to keep the PV module at lower levels. Fins are crucial for dissipating excess heat, as all of the aforementioned research studies have shown. However, fin designs with PCM were shown to be effective at solar radiation intensities more than 500 W/m2 by Ezan et al. [221].

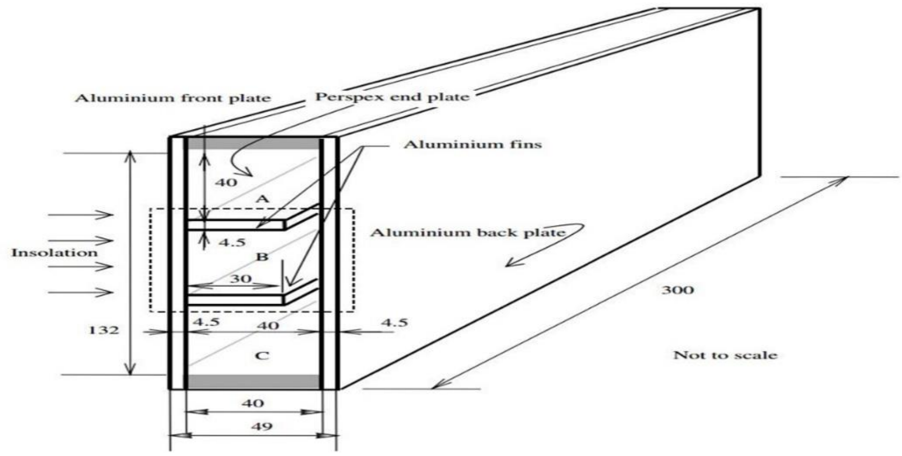

Fig. 2.19. Schematic diagram of the experimental PV-PCM system [184]

The use of PCM (paraffin wax) as a passive cooling method in a PV module with reflectors was experimentally investigated by Maiti et al. [222]. Both indoor and outdoor settings were used for the trials. The outdoor experiment setup for their work is shown in Fig. 2.20. To increase the rate of heat transfer, aluminum lathe turnings were used inside the PCM. The PV module temperature was successfully maintained at 65–68°C for three hours indoors with a PCM matrix that was 6 cm thick, according to the results. In contrast, the temperature increased to 90°C in 15 minutes without the PCM matrix. Chania, Greece. The results demonstrated that PCM could achieve temperature savings of 11ºC in comparison to the reference PV module. That was a significant accomplishment that supports PCM use. But in a different study conducted in Malaga and Utrecht by Hendricks and Sark [224], no obvious advantage of using a PCM-based cooling system was found. Geographical location was a determining factor in whether or not PCM was an acceptable cooling technology, according to Savvakis and Tsoutsos [223] and Hendricks and Van Sark [224].

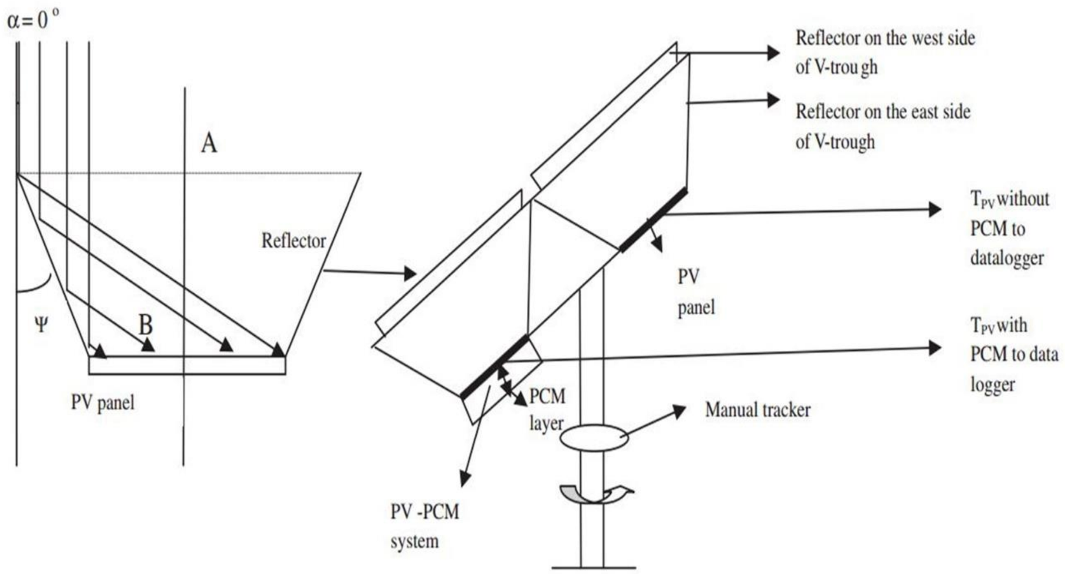

Fig. 2.20. Outdoor experimental setup of PV-PCM cooling system [222]

A numerical analysis of PV-PCM's performance with metallic fiber structure was conducted by Klemm et al. [217]. RT 44, RT 50, and RT 54 were the three PCMs they had taken into consideration. Their research states that during the PV module's daily life cycle, a 20 K temperature decline was noted in its peak temperature. Additionally, they had said that the latent heat of fusion was a determining factor in PCM selection, with higher latent heats of fusion indicating greater system performance. Additionally, there was little interest in improving heat transfer when the porosity was reduced from 90% to 80% or 70%. Khanna et al. [225] examined the geometrical optimization of fins and PCM thickness in a different numerical research. Their results showed that PCM thicknesses of 2.8 cm and 4.8 cm were suitable for daily average solar irradiation levels of 3 kWh/m2 and 5 kWh/m2, respectively. The fin that touched the bottom of the container had the best length, and the optimal thickness was 2 mm. The schematic domain of their numerical research, taking into account the boundary conditions, is shown in Fig. 2.21.

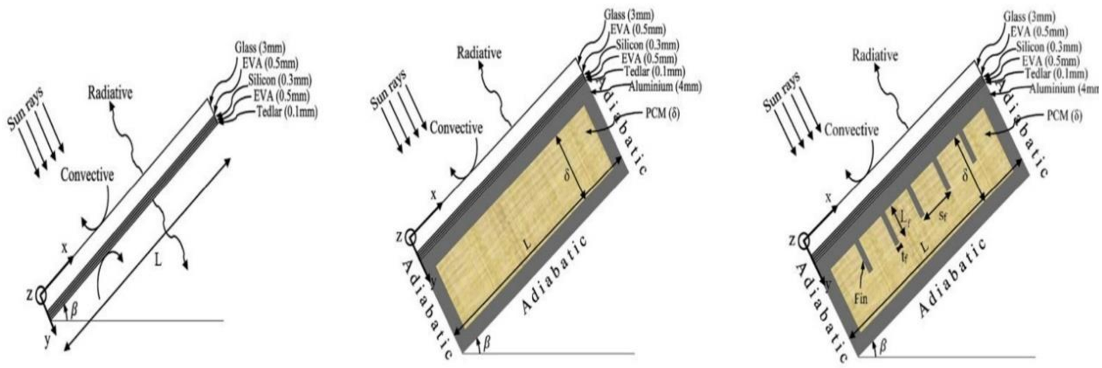

(a) (b) (c)

Fig. 2.21. Three different systems considered in the work of Khanna et al. [225]

Sun et al. [226] conducted a summers experimental and numerical study in Chiang Mai, Thailand. It should be mentioned that the PV module was installed with a 10° inclination, and Chiang Mai has a hot environment. Their objective was to determine the ideal thickness for the many types of PCMs they employed in their work, including RT 35, 42, 47, and 55. The aforementioned PCMs' ideal thicknesses, according to their findings, were 50, 40, 30, and 20 mm, respectively. In Chennai, India, Rajvikram et al. conducted an experimental investigation into the cooling of a PV-PCM system. An organic PCM, the OM 29 PCM, was chosen. According to their findings, the PV module with PCM and an aluminum sheet behind it had a conversion efficiency that was 24.4% higher than that of the reference module without a cooling system. They set up their experiment as shown in Fig. 2.22.

Fig. 2.22. Image of the experimental setup of Rajvikram et al. [227]

By including a TEG, Darkwa et al. [228] improved the PV-PCM system. Their unique compound system configuration is depicted in Fig. 2.23. The TEG was positioned between the monocrystalline PV module and PCM, as seen in the figure, and used the temperature differential between the two to produce power. To provide an insulated experiment and lessen the impact of any other uncontrollable factors, their indoor experimental setup was tested inside a chamber. They had created a numerical model for thermal simulations in addition to their experimental setup. The three systems, PV, PV-TEG, and PV-TEG-PCM, had their theoretical PV efficiencies and power output analyzed; the results are shown in Fig. 2.24. According to Fig. 2.23, the PV-TEG-PCM system produced more electricity on average than the other two. Even though the input variables for developing a PV-TEG-PCM cooling system had been thoroughly examined in that study, additional outdoor experimental research was still necessary to apply the findings to a real, functioning solar farm panel. Although Bayrak et al. [229] installed the TEGs behind the PCM, Darkwa et al. [228] used them between the PV module and PCM, and the compound system was less effective than the other cooling systems they evaluated. For instance, the PV-TEG system produced more power than the PV-PCM-TEG system. According to their reports, the PCM worked as insulation, which hampered the system's overall performance. As a result, choosing the right PCM type and combining it with TEG was just as crucial as arranging them in the assembly. More research was required in this area because there was still a significant gap.

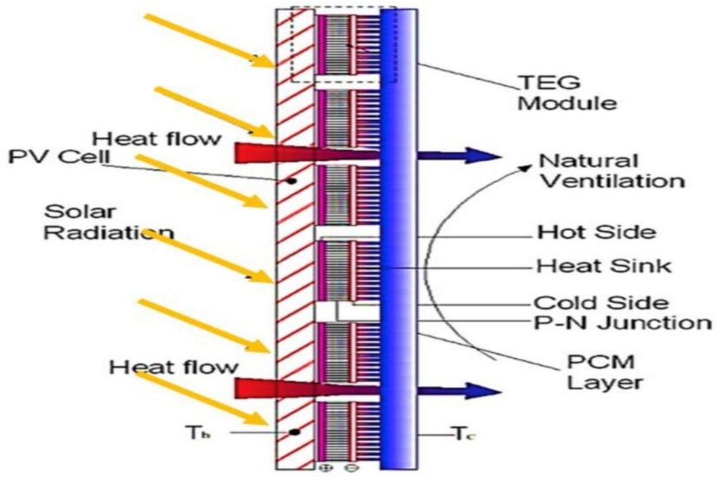

Fig. 2.23. The physical arrangement of the PV-TEG-PCM system [228]

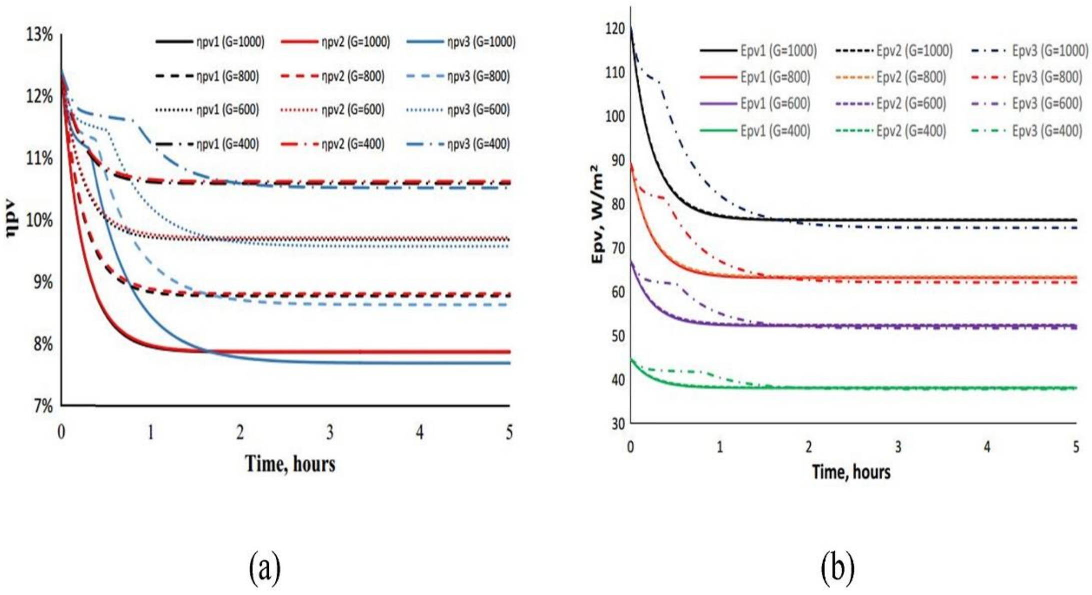

Fig. 2.24. (a) PV efficiency against solar radiation for the three systems, (b) PV power output for the three systems [228]

The geometry of the PCM container and its impact on the melting rate of RT 27 PCM were investigated statistically by Akshayveer et al. [230]. The reference rectangular container was used to compare the design of three distinct non-rectangular shapes. Each of those linear, parabolic, and cubic designs performed better at melting the PCM than traditional rectangular designs, lowering the PV temperature and boosting electrical efficiency. When the three PCM enclosures were compared to one another, the cubic one performed better. The PV-PCM system's schematic perspective is displayed in Fig. 2.25 (a) with a standard PCM enclosure and in Fig. 2.25 (b) with a modified PCM enclosure. There were still significant limitations in their research paper's ability to extrapolate its findings to a real-world scenario because it was a numerical simulation conducted vertically and under continuous sun radiation. Therefore, it was suggested that an experimental study be conducted outside in that location.

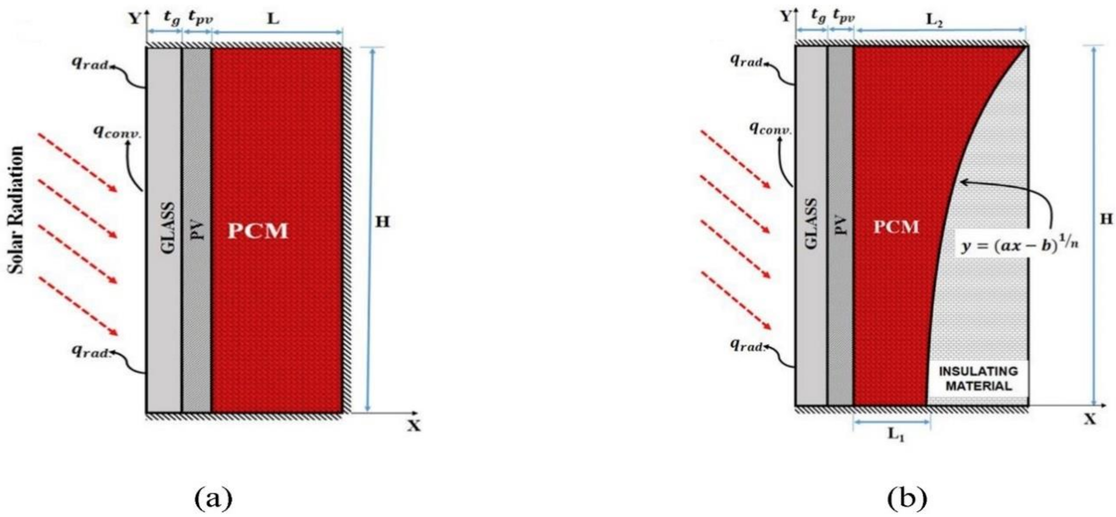

Fig. 2.25. Schematic diagram showing cross-section of PV-PCM system of (a) conventional container and (b) modified container [230]

Kumar et al. conducted an experimental case study of a cooling photovoltaic module for extremely hot temperatures [230]. The PV modules that were positioned horizontally were exposed to sunlight all the time. Every experiment was carried out in the Indian city of Jalandhar. In their investigation, they looked at three distinct systems: PV alone, PV-PCM, and PV-PCM with external fins and shown in fig. 2.26. Their passive cooling technique differed from the aforementioned experiments in a minor but noteworthy way. To help the system dissipate the heat trapped in the PCM more quickly, fins were placed outside the PCM container. The simultaneous charging and discharging (SCD) of PCM served as the justification for this engineering concept. Heat was taken up from the PV module and moved to the PCM on the front side, while the PCM was releasing heat into the surrounding air on the back side. The heat promoters in Mahdavi et al. [231] should be carefully selected because the PCM was under SCD conditions. According to Kumar et al.'s published findings [230], case 3 with external fins performed better overall. Additionally, they stated that "the PV module's temperature was reduced by approximately 22.3ºC for case 3 and 12ºC for case 2 in comparison to the case without cooling, respectively." when SCD circumstances are present. In order to boost the active surface area of heat transfer, Mahdi et al. [233] also used an external metal foam layer at the bottom of a PV-PCM system. Their computer simulation suggests that adding an outer layer of metal foam could increase the melting time by up to 32%. As a variable input, the tilt angle was also taken into consideration. The results showed that the melting time increased by almost 18% when the tilt angle was decreased from 90º to 30º.

Fig. 2.26. Experimental setup of Kumar et al. [232]

A unique heat sink for a concentrator photovoltaic system was created by Duan [234]. The cooling impact of a PCM-porous heat sink was noticeably better than that of a pure PCM heat sink since it has been observed that enclosing a metallic porous structure inside the PCM heat sink may greatly increase the heat transfer rate. The schematic diagram of their numerical work is shown in Fig. 2.27. In contrast to real-world applications where a PV module is positioned horizontally or at a specific tilted angle, the numerical simulation's PV-PCM-porous system was standing vertically, while the solar irradiance was perpendicular to the PV module, as shown in Fig. 2.27. Duan's work [234] was not the only instance in which the oversimplified assumption was made. As a result, it was strongly advised that future research take into account varying solar irradiance as a function of time in relation to a particular geographic location, with the PV module installed at an optimal angle where solar radiation is perpendicular to the plate. A one-dimensional mathematical model was created by Elsheniti et al. [237] in order to forecast the temperature of PV that came into contact with RT 27 PCM. In their numerical method, they applied a varying solar flux according to the location of Alexandria, Egypt, at various times, and they altered the tilt angle of the PV module from 0° to 90°. Their oversimplified mathematical model demonstrated a legitimate lack of agreement with published experimental results. As a result, they succeeded in cutting down on computation time. According to their findings, the ideal inclination angles for spring, summer, fall, and winter were 18°, 17°, 48°, and 41°, respectively. Additionally, during the high-incidence period, various PCM thicknesses of 10, 20, 30, and 40 mm were investigated. According to the results, PCM with a thickness of 30 mm produced the highest average efficiency, at 18%. Higher depths were unable to form during the day or night, whereas lower depths evaporated quickly.

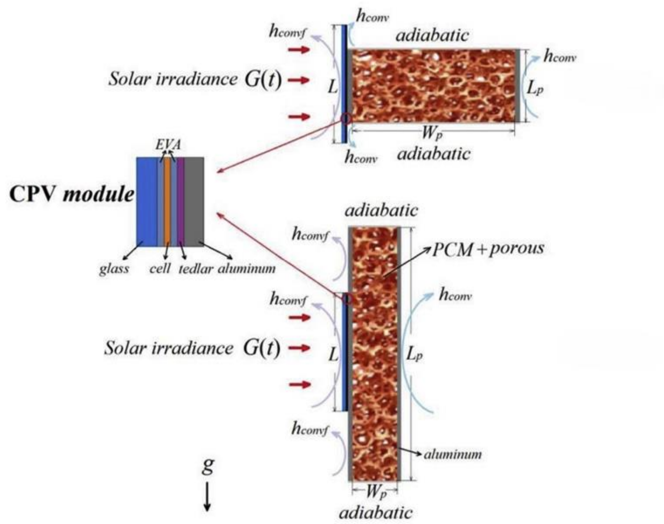

Fig. 2.27. The schematic diagram of the PV-PCM-porous system [234]

Under lab circumstances, Ahmadi et al. [238] conducted extensive research on various cooling techniques for a silicon solar cell. In their work, they took into account active, passive, and a combination of both. However, only passive approaches were covered there. The experimental setups for passive cooling techniques are displayed in Fig. 2.28. Figure 2.29 illustrates how embedding a carbon nanotube foam improved the low heat conductivity of paraffin, producing a PCM composite. The outcomes were contrasted with respect to the output voltage and glass temperature of the PV module. Utilizing PCM could keep the module cool under continuous irradiation for a long time, and utilizing PCM-composite would maintain the temperature lower for a longer period of time, according to Fig. 2.30. It was anticipated that lowering the temperature would prevent voltage drops, as seen in Fig. 2.30.

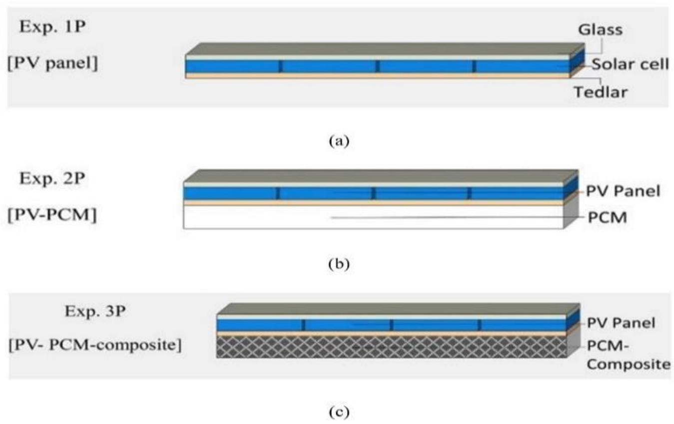

Fig. 2.28. Passive experimental configurations of Ahmadi et al. [238]

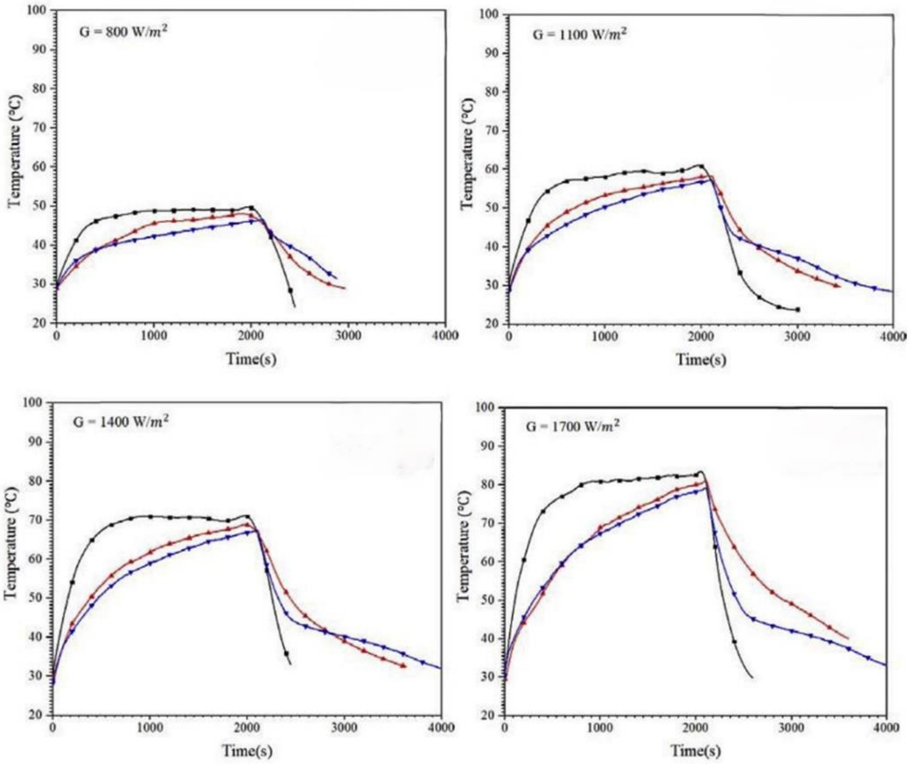

Fig. 2.29. PV module's glass temperature for passive experiments of Ahmadi et al. [238]

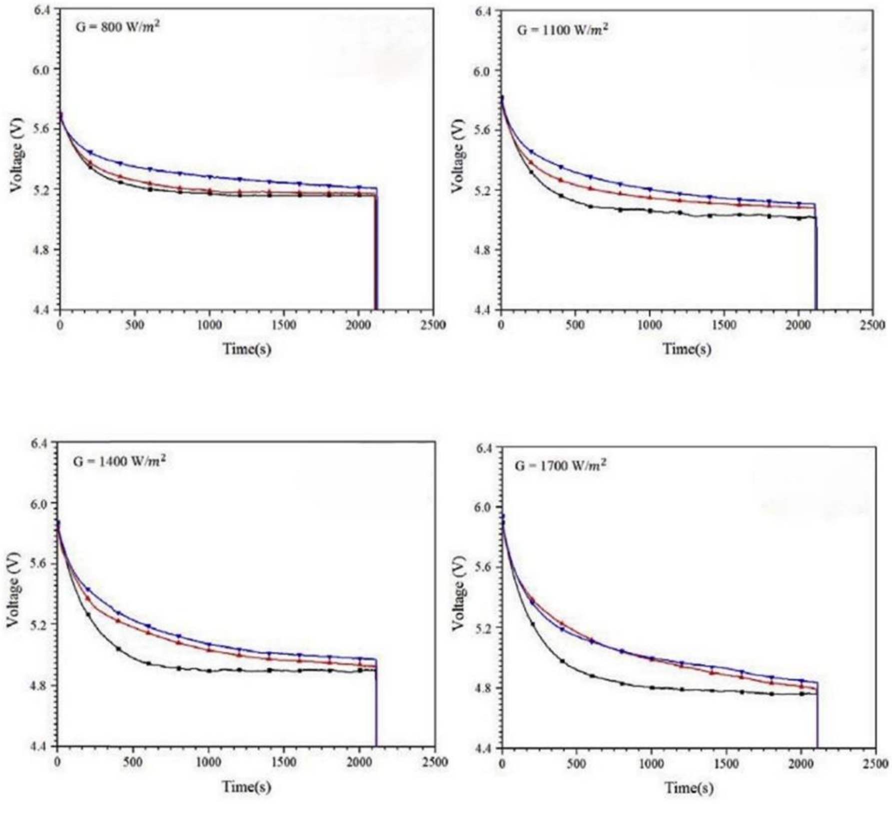

Fig. 2.30. Open-circuit voltage drop for passive experiments of Ahmadi et al. [238]

The notion of attaching separate PCM containers was proposed by Nizetic et al. [239], but nearly all of the articles have assumed a single solid container covering the entire PV module at the back side. Three distinct systems were compared with one another in their experimental investigation, which was carried out in Split, Croatia. The first was a reference PV panel, and the second and third were PCM-cooled PV panels with various setups. They set up their experiment as shown in Fig. 2.31.

Fig. 2.31. Photo of the experimental setup of Sandro et al. [239]

It's interesting to note that the PV panel performance was 10.7% better with the half PCM setup than with the reference scenario. On the other hand, the whole PCM arrangement saw a 2.5% improvement. Their innovative PCM container design was a crucial step in the commercialization of PCM-cooled PV panels because PCM materials are expensive. They claimed that their innovative design could save 36% aluminum and 47% PCM. Due to their great density, organic PCMs were able to drastically lower the cooling system's weight. All of these were seen as essential milestones in enabling PCMs to be used to control the temperature of PV panels.

The primary drawback of Zhang et al. [240] was their extremely poor thermal conductivity (≈0.1 Wm-1K-1), despite all the benefits that PCMs offered. According to Ostrý et al. [241], inorganic PCMs are more expensive than organic PCMs and have a higher thermal conductivity (about 0.5 Wm-1K-1). However, they would corrode when placed in metal containers. Therefore, an inorganic PCM's encapsulation type should be nonmetallic, which would limit its useful applications. But according to Ostrý et al. [241], organic PCMs demonstrated good compatibility with metals, making them a viable choice for PV panel cooling applications. As organic PCMs were more common in PV cooling applications, the following, research and methods which were vastly used to enhance their low thermal conductivity were illustrated.

These methods could be categorized into three groups:

1. Using nanoparticles
2. Using extended surfaces

3. Using metallic porous media

When compared to the usage of nanoparticles in Xiong et al. [242], the second and third techniques were more common in terms of heat transfer rate. All of the aforementioned techniques, however, have been used to increase a PCM's heat transfer rate when combined with PV modules. These techniques, which belonged to the active method category, were mostly employed for PVT-PCM cooling. However, the main reason for referencing those publications here was the notion of converting from active to passive ways by removing the heat collector component.

The performance of the PVT-PCM system was experimentally investigated by Siahkamari et al. [243] in a lab setting with continuous radiation = 1000 W/m² and Tamb = 23ºC. Figure 2.32 shows the schematic diagram of their experimental work. For their experiments, they employed two distinct PCMs: paraffin wax and sheep fat. The PV module may be cooled more efficiently with sheep fat than paraffin, according to the results. The PV module temperature could be further lowered by mixing CuO nanoparticles with sheep fat. That led to an increase in power output and output power characteristic curves of PV module at Q=6mL/s is depicted in Fig. 2.33.

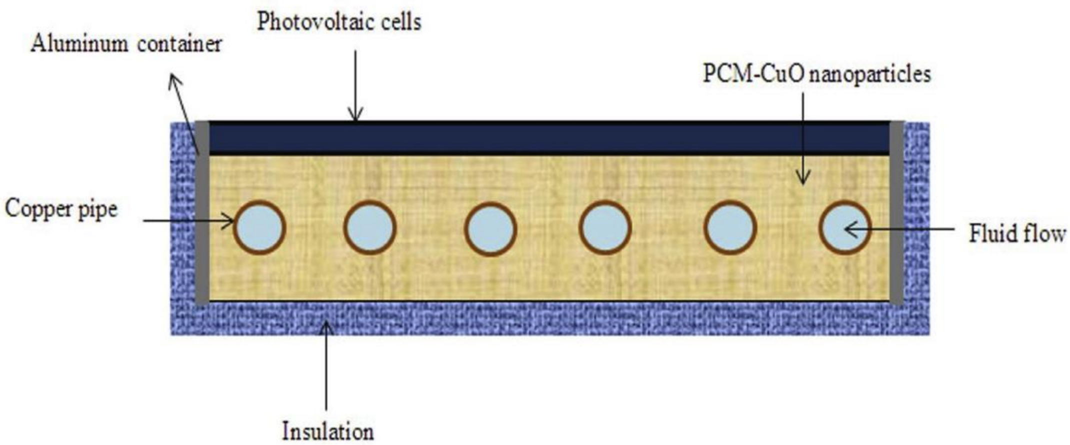

Fig. 2.32. Schematic diagram of experimental work [243]

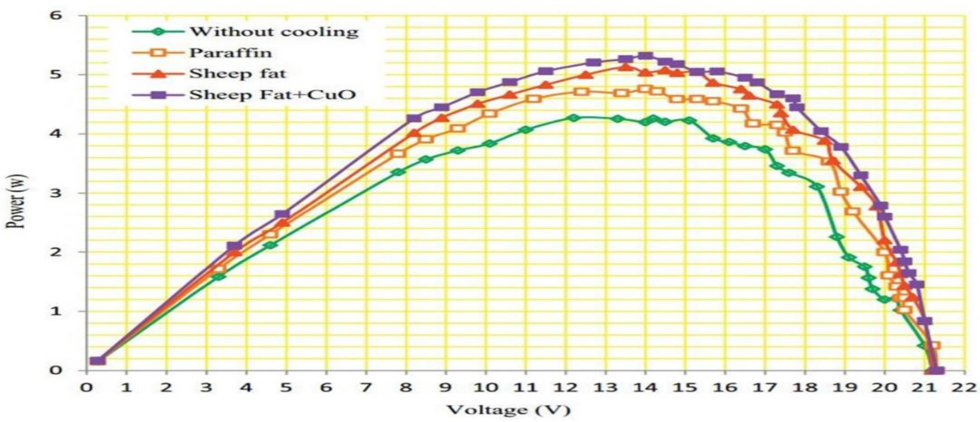

Fig. 2.33. Output power characteristic curves of PV module at Q=6mL/s [243]

The primary goal of Abdelrazik et al.'s work was to combine PVT with PCM and include nanoparticles into PCM [244]. They conducted their numerical study at the location of Dhahran, Saudi Arabia, on two separate days during the winter and summer. Their work's schematic diagram was shown in Fig. 2.34 (a), and the boundary conditions that were applied to the domain were shown in Fig. 2.34 (b). By using graphene nanoplatelets, they attempted to improve the paraffin wax's effective heat conductivity, which served as the PCM in their investigation. According to the results, compared to a standalone PV system, the electrical efficiency increased by 6.9% in the winter and 22% in the summer when 10% of nanoparticles were added to the paraffin.

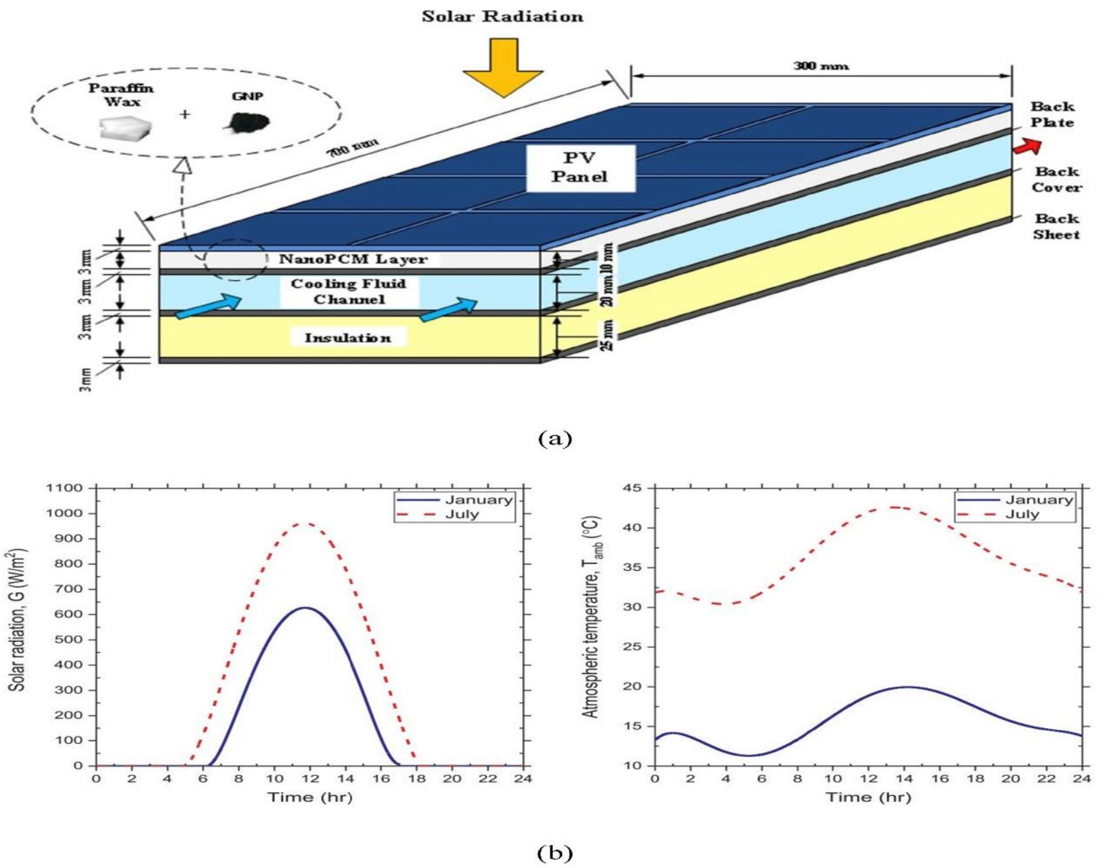

Fig. 2.34. (a) Schematic diagram of Abdelrazik et al. [244] (b) Boundary condition of work of Abdelrazik et al. [244]

Another numerical investigation including four distinct PCM types and different nanoparticles was conducted by the same research team [245]. Their works have the same boundary conditions and schematic diagram. The multi-walled carbon nanotube was the best of the nanoparticles, but the calcium chloride hexahydrate and paraffin wax RT 35 were the best of the four PCM kinds. The PVT-PCM system was experimentally investigated by Rad et al. [246] in Tehran, Iran, under outdoor settings. as seen in Fig. 2.35. the PV module was mounted at a tilt angle of 30°. The low thermal conductivity of salt hydrate PCM was improved by inserting aluminum shavings as a metallic porous media. That was a cheap technique to enhance a PCM's thermal conductivity and might be there was a possibility to apply it to solar farm panels without the active part. The PV module's power output during the warm and cold months was shown in Fig. 2.36 (a) and (b), respectively. It is possible to infer from Fig. 2.36 that using porous material with PCM will greatly increase the PV module power output. To improve the thermal conductivity of OM 47 PCM, Shastry and Arunachala [247] proposed incorporating an aluminum metal matrix honeycomb structure. Figure 2.37 depicted their outdoor experimental setup, which was carried out from 8:00 a.m. to 3:00 p.m. over the full month of M arch. Even though their findings demanded both active and passive reports, Figure 2.38 showed the passive segment where no water flowed through the twisted pipes. The addition of the metal matrix (shown by the green squares) further reduced the module temperature, as can be seen in Fig. 2.38. This graph confirmed that adding a metal matrix to a PCM was a smart way to increase the rate of heat dissipation. However, more research was needed to optimize its design for a passive alone system.

Fig. 2.35. A view of the experimental setup of Rad et al. [246].

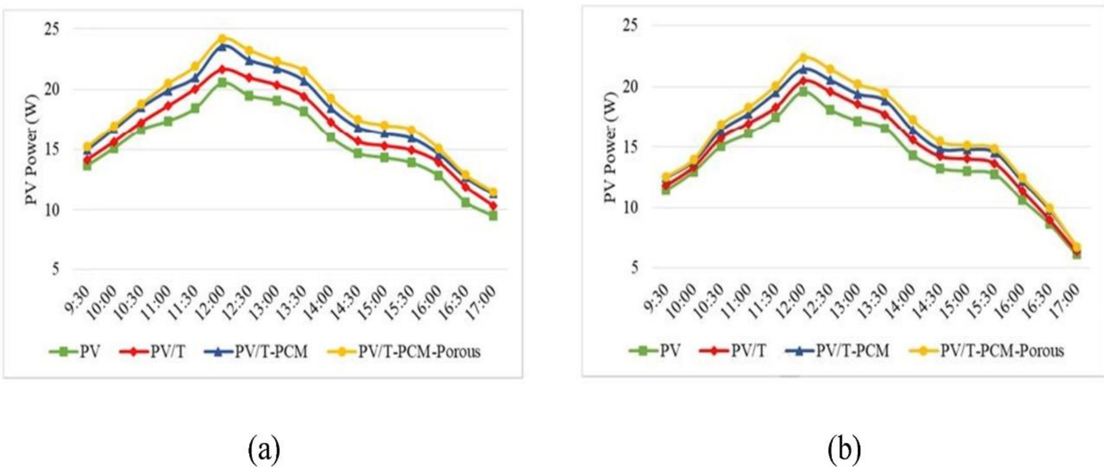

Fig. 2.36. PV power output in different systems during hours of the day: (a) warm month (b) cold month [246]

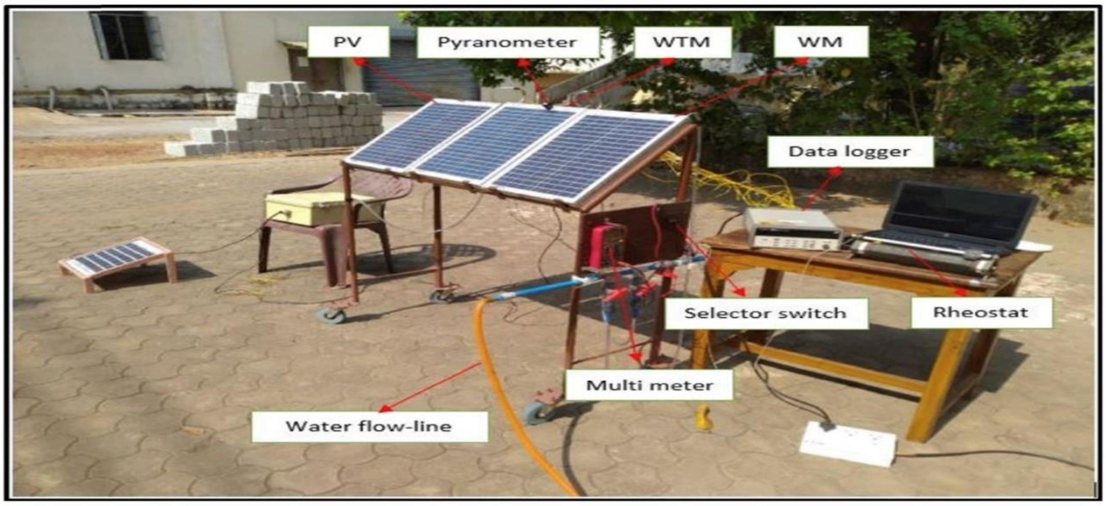

Fig. 2.37. A view of the experimental setup of Shastry and Arunachala [247]

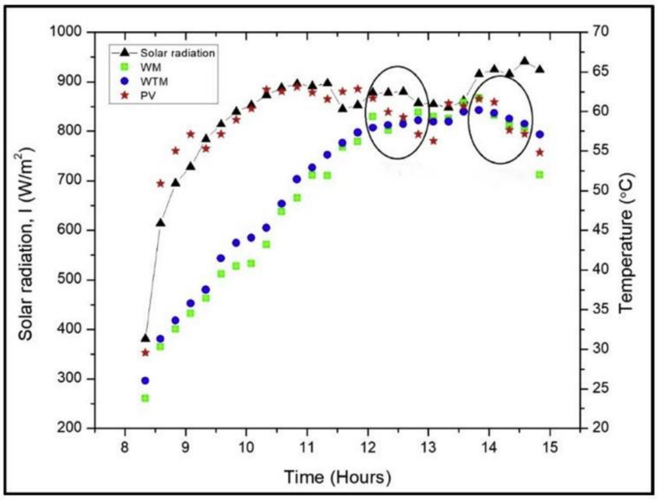

Fig. 2.38. PV module temperature profiles of different systems without water flow [247]

According to Chandel and Agarwal [248], the usefulness of a PCM for PV cooling was highly dependent on topographical and climatic factors; as a result, it was advised for locations with high insolations and hot ambient temperatures. For example, the review report by Kumar et al. [249] states that the PV-PCM system was not economically feasible in Dublin, Ireland. Nonetheless, these systems were cost-effective under such environmental circumstances because a PV-PCM system in Vehari, Pakistan, cost half as much.

2.3.1.6 Spectral beam splitter

A recent review report found that there were two efficient ways to get the most of the sun spectrum. [251]:

1) Using multi-junction cells, which transform a wide variety of photon energy into electrical energy. In order to completely use the spectrum of incoming sunlight, several semiconductors with varying bandgap energies were combined to make this possible. In a lab test, a 46% electrical efficiency was attained, surpassing the Shockley-Queisser limit, the maximum efficiency of conventional single p-n junction solar cells. Nevertheless, the cost of multi-junction photovoltaic cells prevented their widespread implementation [253].
2) Applying SBS technology to fully exploit sunlight across its full spectrum of wavelengths was an additional approach. The nature of single-junction solar cells was influenced by the development of that technology. Since single-junction solar cells could only use a limited portion of the incident sunlight spectrum, as seen in Fig. 2.39, the SBS technique would allow such devices to receive the beneficial portion of photon energy and route the destructive portion to a heat sink. Huang et al. [187] reported that SBS PVT collectors had a total efficiency limit that was over 20% greater than that of photothermal collectors and standalone PV modules. Generally speaking, there were three ways to get the most of the sun energy spectrum. This methods are graphically depicted in Fig. 2.40.

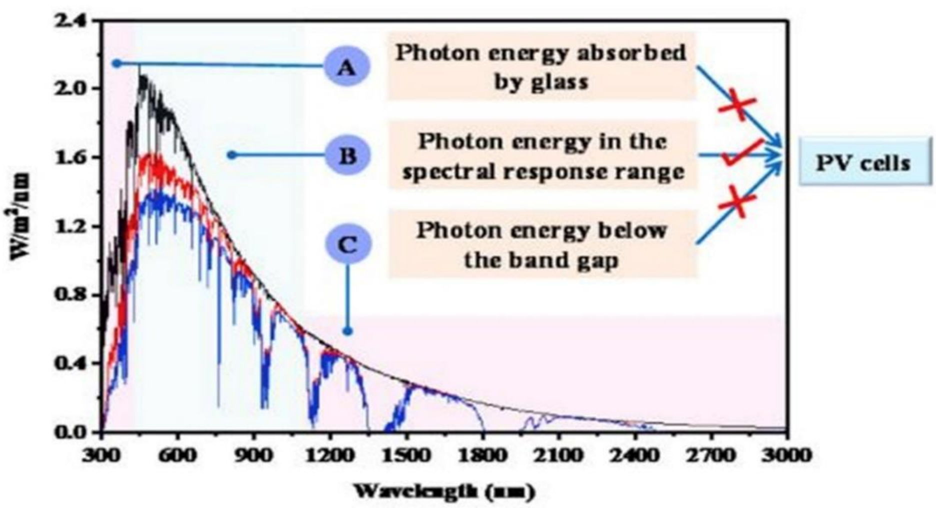

Fig. 2.39. Solar spectrum distribution diagram which could be converted to a useful form of energy by PV cells [251]

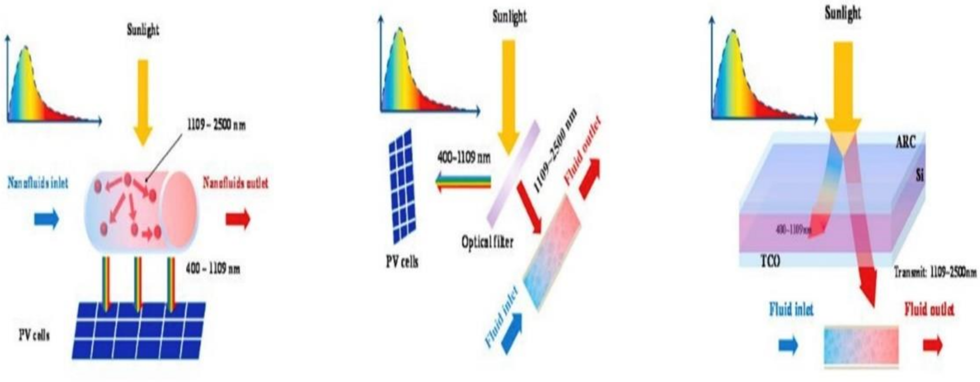

(a) (b) (c)

Fig. 2.40. Schematic diagrams of different SBS techniques of Liang et al. [251]

Numerous studies have been conducted on different SBS strategies in an effort to maximize the solar spectrum's cut-off wavelength and raise the system's overall efficiency. None of them have examined the suitability of SBS techniques for large-scale PV panels, though. For example, the precise optical path requirement, in addition to the cost of production and instability of nanofluids, limited the use of nanofluid-based SBS and nano-film-based SBS [250]. As a result, SBS based on semitransparent PV cells may be crucial to the passive cooling strategy. The technique's drawback was that it produced low-grade thermal energy because the transmitted long wavelength solar spectrum was not concentrated [254]. According to Fig. 2.41, a solar cell with a serrated groove structure at the bottom of a semitransparent cell could focus photons with wavelengths between 800 and 2500 nm on a small spot to provide high-temperature thermal energy (i.e. working fluid) and convert wavelengths between 400 and 800 nm to electrical energy [252]. As a result, a working fluid that could absorb heat above the PV panel's operating temperature was isolated from the panels. A thermal power plant could be erected in tandem with the solar farm panel since the heat engine's thermodynamic cycle's upper bound operation would not be constrained in that situation. Combining several power plants could effectively meet multiple objectives, including the production of fresh water, energy, and heat. In a recent study, Liew et al. [255] used wavelength selective filters to assess a PV/concentrated solar power hybrid plant once a year. The wavelength-selective filter was made to reflect all other spectra while transmitting solar irradiance between 700 and 1100 nm (400 nm bandpass width). Their results showed that due to the lower operating temperature of the PV station, the hybrid system out performed the contiguous hybrid plant of solar concentrated and PV systems. Therefore, the annual yield of their coupled system per unit area was 7% higher than the hybrid system which was operated non-compacted. That study ascertained the vital role of the SBS technique in hybrid PV solar power plants. Additionally, semitransparent PV cells can be integrated with solar distillation systems and solar updraft towers, among other plants. It might be feasible to generate more power from the large area of the collecting area covered with semitransparent solar cells rather than glass or other traditional glazing materials if combined with a solar updraft tower. Additionally, as semitransparent solar cells would create a greenhouse for plants, farming could continue beneath the collector area. Only a small number of experiments were documented in the literature, despite the previously described advantages of such integrated plants. The integrated solar updraft tower and semitransparent PV system was examined by Jamali et al. [256]. The temperature of the semitransparent PV panel was successfully lowered by up to 15°C thanks to the integrated technology. The schematic diagram of their numerical work is displayed in Fig. 2.42. In a different study [257], the impact of collector radius, chimney height, and solar cell packing factor was numerically examined while taking the combined system's power generation and economic performance into account. The ideal packing factor range was stated to be between 0.3 and 0.5, while the appropriate ranges for the collector radius and chimney height were rcollector>120 m and chimney<250 m, respectively. Despite being a successful passive method of cooling solar panels, SBS techniques were still in their infancy and far from being developed enough by researchers to be used on a large industrial basis [251].

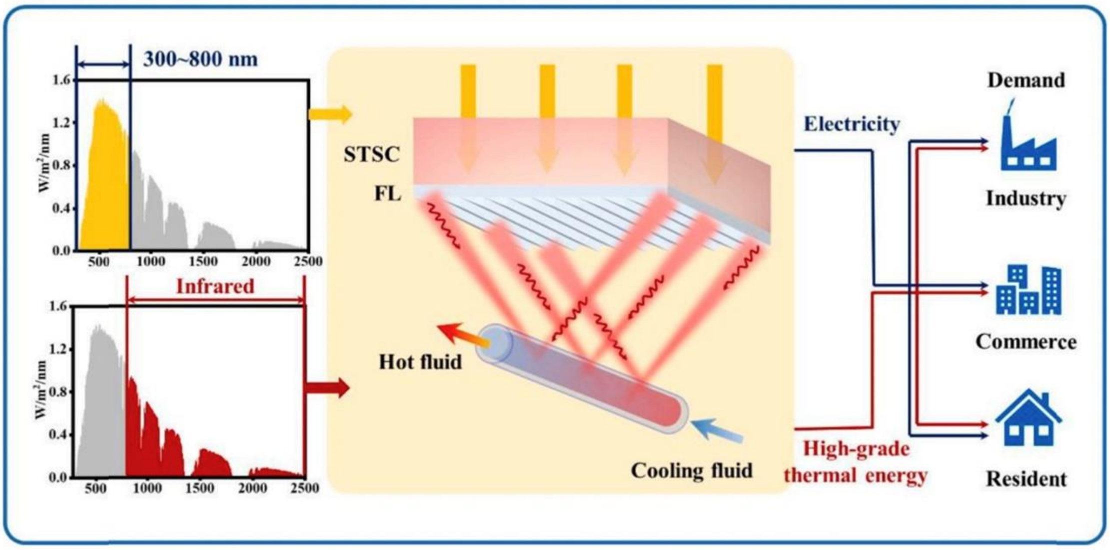

Fig. 2.41. Schematic and mechanism of novel semitransparent solar cell-based SBS system [252]

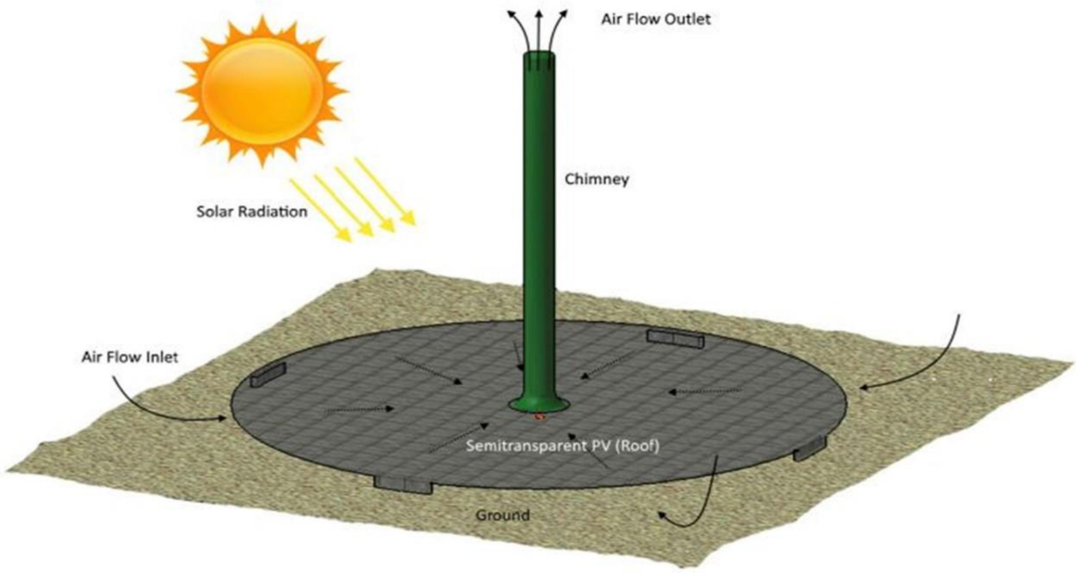

Fig. 2.42. Schematic diagram of the integrated system [256]

2.4 Conclusion

Active, passive, and a combination of the two are the three primary categories into which cooling PV panels can be divided. In household settings where hot water is needed and tap water is accessible, or where ventilation systems demand hot air, active cooling techniques work well. Compared to active systems, passive cooling techniques are more affordable and have the potential to be used on a wider scale. Natural air ventilation, liquid immersion, heat pipes, phase-changing materials, and spectrum beam splitters are a few examples of passive cooling techniques. There are no maintenance costs associated with any of these solutions. With a comparatively high initial investment cost, phase change material is the most efficient technique among them and has emerged as a standout choice for both cooling solar panels and thermal energy storage. Phase change materials are researched and used to solve a range of engineering problems.

CHAPTER-III

DESIGNING AND FABRICATION

3.1. Introduction

This chapter includes designing, fabrication and component details of the experiments of this research. An experimental setup is planned and built at the heat engine lab of Chittagong University of Engineering and Technology to examine the viability of the suggested thermal dissipating system on the PV performance.

Performance testing is currently one of the most crucial topics to ensure the security of photovoltaic instruments due to the rise in solar power usage. All materials and technologies utilized in the production of solar panels must undergo electrical and optical health testing in order for them to become efficient. Therefore, using solar simulators that provide numbers that are close to the actual sunshine spectrum is essential when thinking about future energy standards. Light sources are the most crucial parts of solar simulators used to test photovoltaic panels.

Solar radiation is directly converted into electrical energy using photovoltaic devices, which are non-linear energy sources with robust, low-maintenance designs. It is crucial to ascertain the characteristic values of photovoltaic devices under actual atmospheric circumstances, including the current-voltage (I-V) curve, short circuit current (ISC), open circuit voltage (VOC), and maximum power (PMAX) [258–261]. The so-called Standard Test Conditions (STC), which include an irradiation of 1000 W/m2, an AM (air mass) 1.5 spectrum, and a device temperature of 25°C, are used to grade photovoltaic devices in order to assess their performance [262]. I-V measurements are performed outdoors in the presence of natural sunshine or in a confined laboratory setting using a solar simulator [263]. The intensity and spectrum distribution of solar radiation, geographic location, time of day, year, climate, atmospheric composition, altitude change, and weather conditions are some of the elements that make the first alternative less desirable [264]. For reasons including simplicity, reproducibility, and dependability, the second alternative is favored [263]. Solar simulators are therefore a crucial component of current-voltage (I-V) characterization. This is due to the fact that in order to illuminate a solar panel, the I-V measurement needs a calibrated source that matches actual daylight and circumstances that may be altered on demand [265, 266]. Solar simulators are tools that provide spectral and optical composition similar to sunlight intensity. The fundamental aim of these tools is to test solar cells and photovoltaic panels under controlled laboratory conditions [267-271].

Light and power sources, an optical filter to modify beam characteristics to meet specifications, and control components to run the simulator are the three primary components of a solar simulator [258, 271].

In this researh work, 500 W linear tungsten halogen lamp has been used as solar simulator. Schematic Diagram and experimental setup are illustrated in Fig. 3.1 and Fig. 3.2.

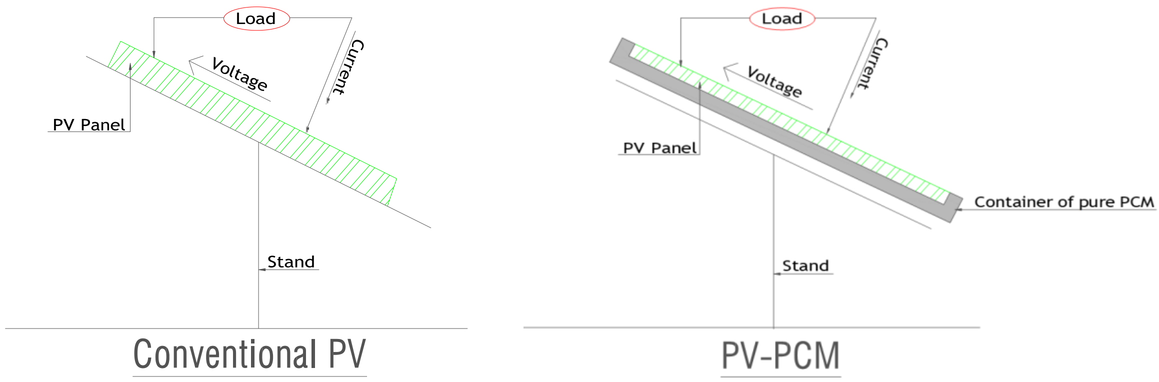

Fig. 3.1. Schematic diagram

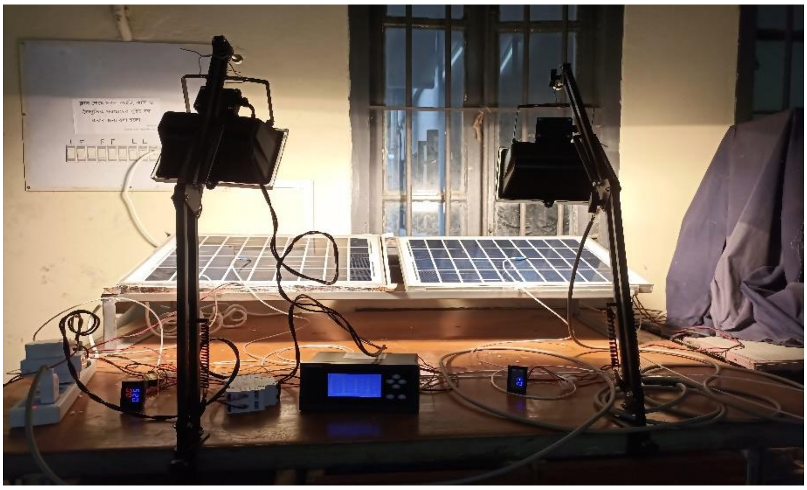

Fig. 3.2. Experimental setup

3.2. Materials

3.2.1. Paraffin

Paraffin is a pure PCM as shown in Fig.3.3, Large amounts of thermal energy are stored and released at a virtually constant temperature by this heat storage material using the processes of phase shift between solid and liquid (melting and congealing) [270].

Even in situations with restricted volumes and small operating temperature variations, phase change materials offer a very efficient way to store heat and cold. Table 3.1 shows properties of paraffin.

Fig. 3.3. Paraffin [270]

Table 3.1 Properties of Paraffin [270]

	Typical Values	
Melting area	38-43 main peak: 41	[°C]
Congealing area	43-37 main peak: 42	[°C]
Heat storage capacity ± 7.5% Combination of latent and sensible heat in a temperature range of 35°C to 50°C.	165 48	[kJ/kg]* [Wh/kg]*
Specific heat capacity	2	[$KJ \cdot kg^{-1} \cdot K^{-1}$]
Density solid at 15°C	0.88	[kg/l]
Density liquid at 80°C	0.76	[kg/l]
Heat conductivity (both phases)	0.2	[W/(m·K)]
Volume expansion	12.5	[%]
Flash point	186	[°C]
Max. operation temperature	72	[°C]

Because of its advantageous thermo-physical characteristics—such as its accessibility, affordability, and lack of corrosion—as well as its comparatively high enthalpy of fusion when compared to other PCM types, paraffin is chosen as an organic PCM.

3.2.2. Calcium chloride hexahydrate ($CaCl_2.6H_2O$)

Calcium chloride hexahydrate ($CaCl_2.6H_2O$) is a latent heat storage material as shown in Fig.3.4. It has several properties that make it suitable for this purpose [272]:

1. Latent heat of fusion: Calcium chloride hexahydrate has a high latent heat of fusion, which means it can absorb and release a significant amount of energy during phase transitions. Specifically, its latent heat of fusion is as high as 170-190 kJ/kg.
2. Melting temperature: The melting temperature of calcium chloride hexahydrate is around 29-30°C. This relatively low phase transition temperature makes it appropriate for applications involving low-temperature heat storage.
3. Non-toxic: Calcium chloride hexahydrate is a non-toxic salt hydrate, which is essential for safety considerations in various applications.
4. Volumetric energy storage density: It also exhibits a relatively large volumetric energy storage density of 289 MJ/m^3.

In practical applications, calcium chloride hexahydrate can play a crucial role in temperature regulation of buildings, storing and releasing latent heat efficiently. Table 3.2 shows the properties of calcium chloride hexahydrate ($CaCl_2.6H_2O$).

Fig. 3.4. Calcium chloride hexahydrate ($CaCl_2.6H_2O$) [272]

Table 3.2 Properties of Calcium chloride hexahydrate ($CaCl_2.6H_2O$) [273]

Hydrated inorganic salts	Melting point (°C)	Melting heat (kJ/kg)	Density kg/m^3		Specific heat capacity (J/(kg K))		Heat-storage density (MJ/m^3)
			Solid	Liquid	Solid	Liquid	
$CaCl_2.6H_2O$	29	190	1800	1560	1460	2130	283

3.3. Methods

3.3.1. Experimental setup

For the experiment, a set up was made by the following equipment.

i. PV modules each of 20W (2 Nos.)
ii. 500W linear tungstan lamp used as solar simulator (2 Nos.)
iii. Paraffin as organic PCM
iv. Calcium chloride hexahydrate ($CaCl_2.6H_2O$) as inorganic PCM
v. An aluminium container
vi. A rubber gasket with silicone sealant
vii. A stand
viii. RTD PT-100 temperature sensor
ix. Ammeter
x. Voltmeter
xi. Data logger
xii. Daystar solar meter
xiii. Anemometer

PV module 20W polycrystalline cell is used for this research purpose. This is lower temperature application. So RTD PT-100 temperature sensor is used in this research work.

3.3.2. Description of componants

3.3.2.1. PV modules of 20W

Through a mechanism known as the photovoltaic effect, a photovoltaic (PV) cell is an energy harvesting device that transforms solar radiation into usable power. PV cells come in a variety of forms, but they always work with semiconductors to convert incoming photons from the Sun into an electric current.

Each of the several layers of components that make up a photovoltaic cell has a distinct function. A solar cell's specifically prepared semiconductor layer is its most crucial layer. It has two separate layers (p-type and n-type) [284] is illutraed in Fig. 3.6, and is what really uses a mechanism known as the photovoltaic effect to transform solar energy into usable power. A layer of conducting material "collects" the generated electricity on each side of the semiconductor. It should be noted that while the front or lighted side of the cell must employ the conductors sparingly to prevent too much of the Sun's radiation from reaching the semiconductor, the backside or shaded side of the cell may afford to be fully covered with them. Figure 3.5 illustrates the anti-reflection coating, the last layer that is applied just to the side of the cell that is lighted. Due to the inherent reflective nature of all semiconductors, reflection loss can be substantial. To lessen the quantity of solar radiation reflected off the cell's surface, one or more layers of an anti-reflection coating might be applied.

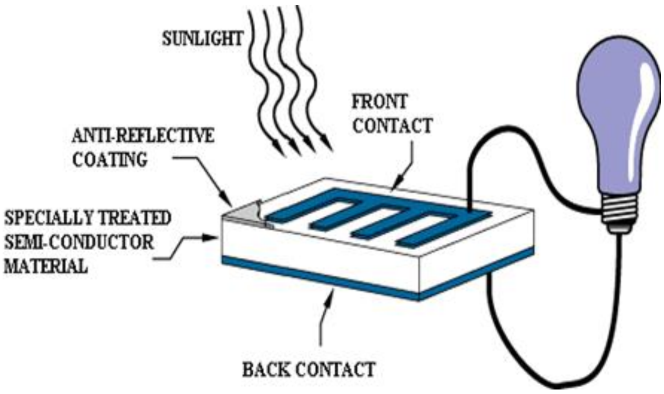

Fig. 3.5. The basic operation of a PV cell [282]

A mechanism known as the photovoltaic effect causes a photovoltaic cell exposed to sunlight to produce voltage or electric current. The two distinct semiconductor types that make up these solar cells the p-type and the n-type are connected to form a p-n junction. An electric field is produced in the junction area when these two semiconductor types are linked because electrons go to the positive p-side and holes to the negative n-side. Particles that are negatively charged go in one direction while those that are positively charged travel in the other way due to this field [285]. Photons, which are essentially tiny bundles of electromagnetic radiation or energy, make up light. These cells move to a higher energy state called the conduction band when light of the right wavelength strikes them. This is because the photon's energy is transferred to an electron in the semiconducting material. These electrons are free to travel through the material when they are stimulated in the conduction band, and it is this mobility that generates the electric current in the cell.

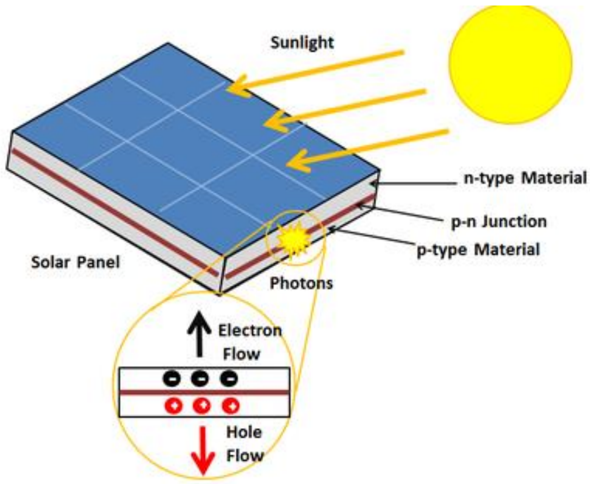

Fig. 3.6. Photovoltaic effect [285]

Since there are several elements that affect photovoltaic cells' efficiency, efficiency is a design problem. The primary reason is that a silicon semiconductor cannot transform one-fourth of the solar energy that reaches Earth into electrical power. The band-gap energy is the lowest photon energy required by semiconductor physics to extract an electron from a crystal structure. If a photon's energy is less than the band-gap, it is absorbed as thermal energy. The band-gap energy of silicon is 1.12 electron volts [285]. Some of the incoming energy from the Sun is insufficient to knock off an electron in a silicon photovoltaic cell because the energy of the photons from the Sun spans a wide range of energies. There is an issue even with the light that can be absorbed. Any energy above the band-gap energy is transformed into heat. This also cuts the efficiency because that heat energy is not being used for any useful task [285]. Of the electrons that are made available, not all of them actually make it to the metal contact and generate electricity. The voltage within the semiconductor does not accelerate all electrons to the point where they may exit the system. Together, these factors give silicon photovoltaic cells a potential efficiency of around 33% [285].

There are methods for increasing PV cell efficiency, however they are all more expensive. Increasing the semiconductor's purity, employing a more effective semiconducting material like gallium arsenide, including more layers or p-n junctions into the cell, or utilizing concentrated photovoltaics to focus the Sun's energy are a few of these techniques. However, a number of factors, including as weather cycles and UV exposure, will cause PV cells to deteriorate over time and produce less energy. The typical deterioration rate is 0.5% year, according to a thorough assessment by the National Renewable Energy Laboratory (NREL) [285].

Numerous techniques and materials may be used to create photovoltaic cells. Silicon (Si) is the most widely used material in the production of commercial solar cells, although alternative materials include copper indium gallium selenide (CIGS), gallium arsenide (GaAs), and cadmium telluride (CdTe). Flexible thin-film cells (Si, CdTe, CIGS) or brittle crystalline structures (Si, GaAs) can be used to create solar cells. As seen in Fig. 3.7, crystalline solar cells may be further divided into two groups: monocrystalline and polycrystalline. As the names imply, polycrystalline PV cells have a variety of crystal forms, while monocrystalline PV cells are made up of a homogeneous or single crystal lattice. Another way to categorize solar cells is by the number of p-n junctions or layers they include. Although multi-junction PV cells, which offer better efficiencies at a higher cost, have also been produced, the majority of commercial PV cells are simply single-junction.

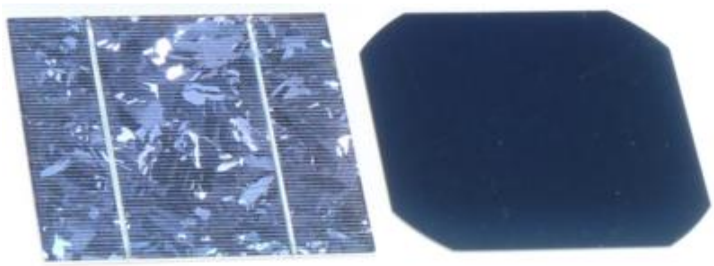

Fig. 3.7. An image comparing a polycrystalline silicon cell (left) and a monocrystalline silicon cell (right) [286]

A specific photovoltaic (PV) cell, module, or array's current and voltage (I-V) characteristics are displayed by the Solar Cell I-V Characteristic Curves. It provides a thorough explanation of its efficiency and capacity to convert solar energy. Determining the output performance and solar efficiency of a solar cell or panel requires an understanding of its electrical I-V properties, particularly its Pmax.

Photovoltaic solar cells directly generate energy from the sun's radiant radiation. Solar energy conversion is becoming more and more significant as a component of a mix of renewable energy sources due to the growing need for clean energy sources and the sun's potential as a free energy source. Because of this, there is a greater need than ever for effective solar cells that directly turn sunlight into power.

Nearly all of the semiconductor silicon used to make photovoltaic (PV) cells has been refined into an incredibly pure crystalline substance that absorbs photons from sunshine. When the photoconductive cell is coupled to an external load, the photons strike the silicon atoms, releasing electrons that cause an electric current to flow. Take a battery, for instance. The performance of the solar cell may be assessed using a number of different metrics, including its power production and photovoltaic efficiency.

The connection between the current and voltage generated on a typical solar cell I-V characteristics curve summarizes the primary electrical properties of a PV cell or module. The current (I) is determined by the intensity of the solar radiation (insolation) that strikes the cell, but the voltage (V) is decreased as the solar cell's temperature rises.

We can make solar cell I-V curves that show the current versus the voltage for a photovoltaic device because solar cells generate direct current (DC) electricity and current times voltage equals power. In essence, solar cell I-V characteristics curves provide a visual depiction of how a solar cell or module functions, summarizing the connection between current and voltage under the current temperature and irradiance circumstances. The data needed to set up a solar system to run as near to its optimal peak power point (MPP) as feasible is provided by I-V curves.

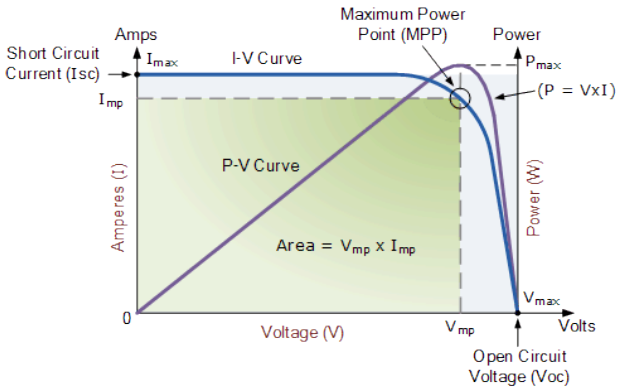

Fig. 3.8. Solar cell I-V characteristic curve

The current-voltage (I-V) characteristics of a typical silicon photovoltaic cell under normal operating conditions are displayed in Figure 3.8. The output current and voltage (I x V) of a single solar cell or panel determine how much power it can produce. When all voltages from short-circuit to open-circuit states are multiplied point by point, the power curve in Fig. 3.8 is produced for a specific radiation level.

When the solar cell is open-circuited—that is, not connected to any load—the voltage across the cell, sometimes referred to as the open circuit voltage, or Voc, is at its largest and the current is at its lowest (zero). At the opposite extreme, when the solar cell is short circuited, that is the positive and negative leads joined together, the voltage across the cell is at its minimum (zero) but the current flowing out of the cell reaches its highest, known as the solar cells short circuit current, or Isc.

From the short circuit current (Isc) at zero output voltages to zero current at the full open circuit voltage (Voc), the solar cell's I-V characteristics curve spans. To put it another way, a cell's maximum voltage is at open circuit and its maximum current is at closed circuit. There must be a point in between where the solar cell produces the most power, even yet neither of these two circumstances produces any electricity.

However, the power achieves its maximum value at Imp and Vmp for a specific combination of current and voltage. Stated differently, the upper right portion of the green rectangle represents the moment at which the cell produces its highest amount of electrical power. This is the MPP, or maximum power point. As a result, operating at the maximum power point is the best state for a photovoltaic cell (or panel).

A solar cell's maximum power point (MPP) is located close to the bend in the I-V characteristics curve. The open circuit voltage and short circuit current can be used to estimate the corresponding values of Vmp and Imp: Vmp ≅ (0.8–0.90)Voc and Imp ≅ (0.85–0.95)Isc. Temperature affects both the output voltage and current of solar cells, so variations in the surrounding temperature will affect the actual output power.

The relationship between the output current and voltage provides a summary of a photovoltaic array's electrical properties. The PV array's output voltage (V) is influenced by the solar cells' operating temperature, while the output current (I) is determined by the quantity and strength of solar insolation, or solar irradiance. Solar cell I-V characteristic curves that summarise the relationship between the current and voltage are generally provided by the panels manufacturer and are given as:

1. V_{OC} = open-circuit voltage – When there is no load on the PV's terminals (an open circuit condition), this is the highest voltage it can produce. Compared to Vmp, which is related to the PV's functioning and is determined by the load, this value is significantly larger. The number of PV panels linked in series determines this figure.
2. I_{SC} = short-circuit current – The maximum current provided by the PV when the output connectors are shorted together (a short circuit condition). This value is much higher than Imp which relates to the normal operating circuit current.
3. MPP = maximum power point – In the equation MPP = Imp x Vmp, this refers to the moment at which the power provided by the PV that is connected to the load (batteries, inverters) is at its maximum value. A solar cell's maximum power point is expressed in peak Watts (Wp) or Watts (W).
4. FF = fill factor – The link between the open-circuit voltage multiplied by the short-circuit current (VOC x ISC) and the maximum power that the PV can truly produce under typical operating conditions is known as the fill factor. A PV's quality can be gauged by its fill factor value; the closer the fill factor is to 1 (unity), the more power the PV can produce.

Values in the range of 0.7 and 0.8 are typical.

5. %eff = percent efficiency – The ratio of a photovoltaic cell's maximum electrical power output to the amount of solar radiation that strikes the array is known as the cell's efficiency. Depending on the kind of photovoltaic cell (monocrystalline, polycrystalline, amorphous, or thin film), the average solar panel's efficiency is often low, ranging from 10 to 12%.

Specifications of the PV module-

- Silicon solar PV module
- Polycrystalline
- P_m = 20W
- V_{mp} =18 V
- I_{mp} =1.11 A
- V_{oc} =21.2 V
- I_{sc} = 1.18 A
- Dimensions = 485x345x18 mm
- Max system Voltage = 1000 V
- Test conditions = AM 1.5 1000 W/m^2 25ºC

20 W solar cell used in this experiment is shown in Fig. 3.9.

Fig. 3.9. PV modules of 20 W

3.3.2.2. Solar Simulator

These solar spectrum standards are used in the construction of solar simulators used in both commercial and academic research. Depending on the type of solar simulator and its intended function, several light sources are chosen in order to meet these requirements generally is shown in Fig. 3.9.

According to ASTM E927 (Standard Specifications for Solar Simulation for Terrestrial Photovoltaic Testing) and IEC 60904-9, simulation performances of solar simulators are defined under three classes; Class A, Class B and Class C [276, 277]. This classification determines three main criteria; spectral match, spatial non-uniformity of irradiance and temporal instability [271, 276, 277].

Light source selection is the most important part of solar simulator design for the simulation of sunlight and its intensity, and spectral properties of light source, illumination pattern, collimation, light flow stability and light range should be taken into account for the selection [278]. In solar simulator applications, different light sources are used to simulate sunlight according to the ASTM standards.

The 500W linear tungsten lamp utilized as a solar simulator in this study is seen in Fig. 3.10.

Fig. 3.10. Solar simulator (500W Halogen Lamp) [278]

3.3.2.3. RTD PT-100 temperature sensor

Temperature sensors with a resistor that alters its resistance value in response to temperature changes are known as resistance temperature detectors, or RTDs. The PT-100 is the most often used RTD. They have established a reputation for precision, reproducibility, and stability during the many years that they have been used to monitor temperature in industrial and laboratory procedures.

The majority of RTD components are made up of a glass or ceramic core encircled by a length of finely coiled wire. Since the element is often rather delicate, it is frequently protected by being enclosed in a sheathed probe. The pure material used to make the RTD element has a recorded resistance at different temperatures. The resistance of the material changes predictably with temperature, and this change is what is utilized to measure temperature. Figure 3.11 displays the RTD PT-100 probe, one of the most precise temperature sensors. It offers outstanding stability and repeatability in addition to superb precision.

Fig. 3.11. RTD PT-100 temperature sensor

3.3.2.3. Data logger

KCM-LCD 16 series shown in Fig. 3.12 universal input temperature circuit measuring instrument, support thermal resistance, thermocouple signal input; Support 4-20mA analog signal. The instrument adopts LCD 256*128 liquid crystal, which can display the measured value of 16 channels at most, and supports RS485 communication compatible with Modbus-RTU protocol.

1. High accuracy：±0.5%F·S±1.0
2. Input Sensor Types A：K E J T Pt1000 Cu50
3. Input Sensor Types B: 4-20mA

The input type(Type A, Type B) is fixed ,cannot be switched

4. Temperature measurement range：

K（-30～1300℃）E（-30～800℃）J（-30～1000℃）T (-30.0～900.0℃)

RTD PT-100 (-200～600℃) Cu50(-100～150℃) 4-20mA（-1999～9999℃）

5. Input channels: 1-16 input channels optional
6. Relay contact：250 V AC, 3 A (Resistive load)
7. Dimensions: H×W×D (Unit: mm) 160×80×85 Panel cutout 152×76
8. Power supply: AC 220V±10% 50HZ Power, consumption less than 5W
9. Allowable range:

Allowable ambient temperature: 0 to 50°C

Allowable ambient humidity: 35 to 85 % RH.

Fig. 3.12. Data logger

3.3.2.4. Digital voltmeter ammeter

A device that detects the voltage or potential difference between two points in an electrical or electronic circuit is called a voltmeter, often referred to as a voltage meter. The voltmeter is often utilized in circuits that employ either direct current (DC) or alternating current (AC). As an alternative, specialized voltmeters may also detect radio frequency (RF) voltage.

Typically calibrated in volts, millivolts (0.001 volt), or kilovolts (1,000 volts), a voltmeter monitors voltages. A voltmeter is connected in parallel to a device to measure its voltage. Because parallel objects often experience the same potential difference, this configuration is crucial. For the primary reason that the same voltage drop happens across it, it is linked in parallel with the circuit. The internal resistance of a voltmeter is similarly high. This is done primarily for the purpose of measuring the potential difference between the circuit's two locations. As a result, the measuring device's current stays constant. Stated otherwise, the voltmeter's high resistance will prevent current from passing through it. This enables the instrument to obtain accurate voltage measurements.

The voltmeter is usually represented by the letter V, which is placed inside a circle adjoining two terminals and shown in Fig. 3.13.

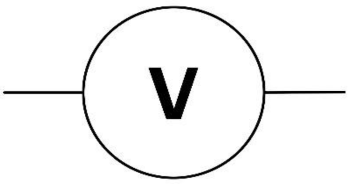

Fig. 3.13. Voltmeter symbol

Many voltmeters nowadays are digital, providing readings in the form of numerical displays. Analog versions of the voltmeter are also available, though, and these provide readings by moving a pointer in a certain way to show voltage on a scale. Because they often have a better level of accuracy than analogue voltmeters, digital voltmeters are recommended.

Ammeters were scientific devices that relied on the magnetic field of the earth to function. In the 19th century, the ammeter with the ability of accurate measurements, which could be mounted in any position was invented.

An ammeter is a device for measuring direct or alternating electricity. This instrument is called an ammeter because it measures the value in amperes.

The ammeter is often linked in series with the circuit to measure the current. A little amount of current, measured in the milliampere or microampere range, is the primary usage for this device. A milliammeter is a device that measures current in milliamperes, whereas a microammeter is a device that measures minuscule electric currents that are calibrated in microamperes. The letter "A" stands for the ammeter in a circuit.

An ideal ammeter has zero internal resistance and always provides low resistance.

In general, it has feeble internal resistance. Low resistance is offered by the ammeter because:

- Input current passes completely through the device.
- Low voltage drop takes place across the device.

The gadget is protected against excessive current by an integrated fuse. The fuse will blow if a significant amount of current passes through the ammeter. Until the replacement fuse is installed, the ammeter cannot detect the current.

It is divided into the following categories based on the present passed:

- AC ammeter
- DC ammeter

The ammeter is categorized according to its construction and design pattern as:

- Permanent moving coil ammeter
- Moving iron ammeter
- Electro-dynamometer ammeter
- Rectifier type ammeter

A permanent moving coil ammeter is also known as a D’Arsonval meter or galvanometer. It is possible to measure the current flowing through a coil by observing its angular deflection in a homogeneous magnetic field.

The coil in the moving iron ammeter freely travels between a permanent magnet's poles. Both alternating and direct current may be measured with this ammeter.
The Electro-dynamometer ammeter is very precise and may be used with both AC and DC supplies.

The ammeter is usually represented by the letter A, which is placed inside a circle adjoining two terminals and shown in Fig. 3.14.

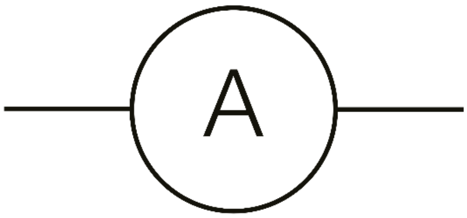

Fig. 3.14. Ammeter symbol

Digital voltmeter used in experiment is shown in Fig. 3.15 and specifications of digital voltmeter ammeter used in experiment are given below:

- Voltage measurement range:0.0V-100V
- Current test range:0-999mA, 0-10A, 0-50 A, 0-100 A
- Power supply range:DC4-30.0 V
- Voltage error:±0.1%
- Current error:±1%
- External shunt specifications:75 milliohms
- Working current< 20 mA
- Refresh rate:About 300 mS once
- Display method:Double three 0.28" LED digital tube
- Display color:Red + Blue
- Lead length:15cm
- Dimensions:48 x 29 x 22 mm
- Mounting holes:46 x 27 mm
- Operating temperature: -10°C~65°C

Fig. 3.15. Digital voltmeter ammeter

3.3.2.5. Anemometer

As shown in Fig. 3.16, an anemometer is a device that measures the velocity or speed of gases in either constrained flows, such as airflow in a duct, or unconfined flows, such as atmospheric wind. In order to determine velocity, an anemometer detects a fluid's change in physical properties or its effect on a mechanical instrument submerged in the flow.

Typically, an anemometer is used to monitor turbulent gas fluxes. While hot wire anemometers are frequently employed for measuring turbulence properties, such as transverse measurements in a cross-section, vane, thermal, and cup anemometers—which are typically found in weather stations—are primarily used to determine mean velocity. The term "thermal anemometer" is commonly used to describe any anemometer that uses the relationship between velocity and heat transfer to compute velocity.

Fig. 3.16. Digital anemometer

3.3.2.6. Daystar solar meter

The Daystar solar meter shown in Fig. 3.17 provides a quick and simply way to quickly measure global solar irradiance in W/m².

Fig.3.17. Daystar solar meter

3.3. Experimental procedure

In this work, experiments have been conducted in heat engine laboratory to examine the impact of PCM addition to PV modules on its performance. In this setup, two different configurations of PV modules each of 20W shown in Fig. 3.1 are designed and constructed conventional PV system and PV integrated with enhanced PCM. This setup is shown in the Fig. 3.2. and two 500 W halogen lamp have been used as solar simulator.

The two arrangements' electrical and thermal capabilities are concurrently compared. Because of their advantageous thermo-physical characteristics—such as their availability, affordability, durability, and non-corrosiveness—as well as their comparatively high enthalpy of fusion when compared to other types of PCM, paraffin and calcium chloride hexahydrate ($CaCl_2.6H_2O$) are chosen as the organic and inorganic PCM in the setup depicted in Fig. 3.2. An aluminum container measuring 48 cm by 4 cm by 34 cm has been integrated beneath the PV module in the PV-PCM system seen in Fig. 3.1, where PCM is kept for passive cooling. Paraffin wax is first allowed to gradually melt in a water bath set at 85°C. The melted wax is then poured into the enclosure through two holes drilled in the top, which also act as a breather to prevent pressure buildup. In the same way, experiment has been done for inorganic PCM by the same enclosure. A rubber gasket with silicone sealant is positioned between the PV back and PCM enclosure, and it is compressed with the aid of screws to prevent liquid PCM from leaking. In this setup, RTD PT-100 temperature sensors have been used during the experimentation. Three temperature sensors have been used in PV/PCM, two are used for measuring PV cell temperature and other has been used to completely express the temperature distribution inside the PCM reservoir, it might assist in understanding the thermal behavior of PCM inside the container. On the other hand two temperature sensors are used in conventional PV to measure only upper and lower surface temperature. Air flow with different velocity has been created inside laboratory by using mini table fan. The RTD PT-1OO, anemometer, and daystar solar meter are used to measure the ambient temperature, wind speed, and solar energy intensity at the inclined surface. Using an ammeter and a voltmeter, output current and output voltage are monitored at regular intervals and manually recorded for later use in computations. Every five minutes, all temperature sensors and other sensors are immediately connected to a data logger of the KCM-LCD 16 series to save data.

CHAPTER-IV

EXPERIMENTAL RESULTS AND ANALYSIS

4.1. Introduction

The performance of the photovoltaic module varies with respect to incident solar radiation and geographical climatic conditions. High solar intensity and ambient temperature and low wind speed lead to high surface temperature of the reference PV module and allow the possibility of PV temperature regulation by using PCM which leads to higher output power. So average monthly temperature, the variation of solar radiation during the days and average wind speed in bangladesh are shown in Fig. 4.1, Fig. 4.2 and Fig. 4.3.

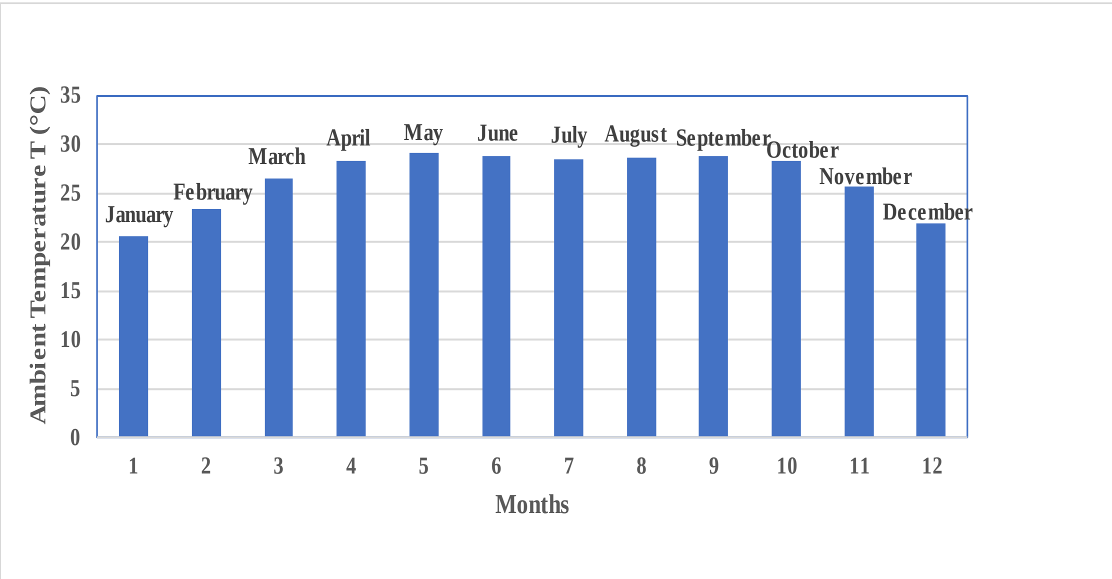

Fig. 4.1. Average monthly temperature in Bangladesh [287]

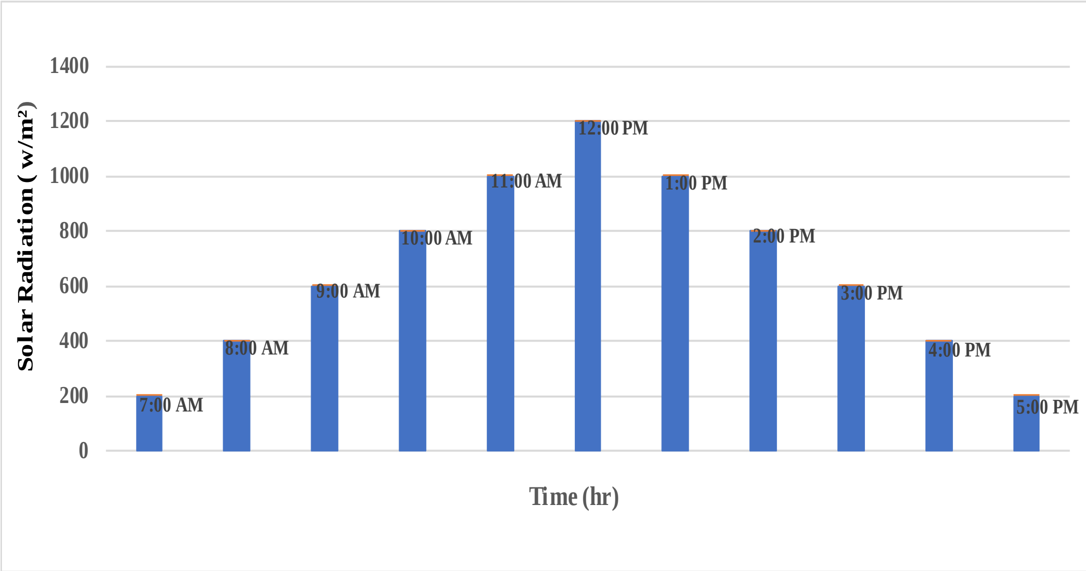

Fig. 4.2. The variation of solar radiation during the days in Bangladesh [288]

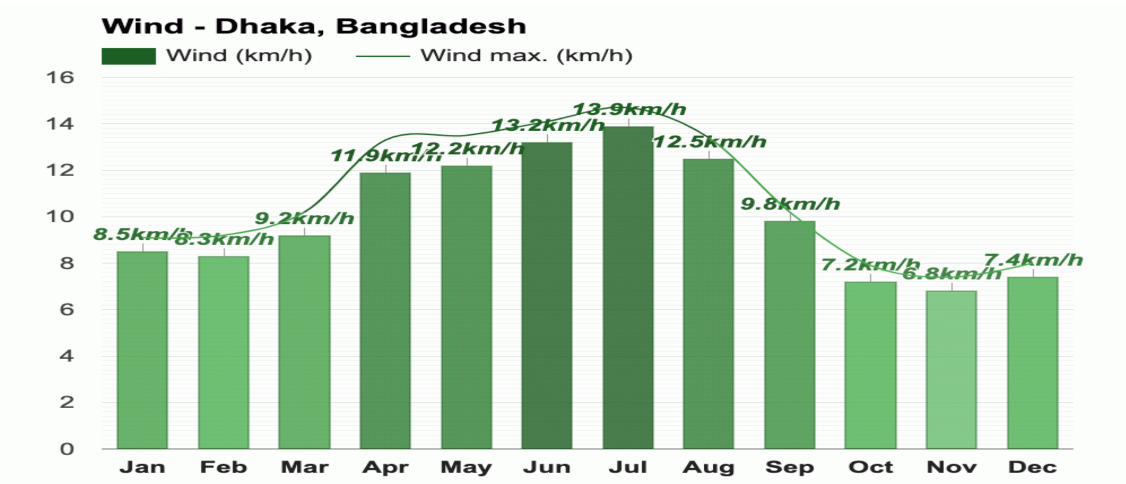

Fig. 4.3. Average wind speed of Bangladesh [289]

4.2. Thermal and electrical performance

One of the most promising solutions for meeting the electricity needs of many remote customers globally is the use of photovoltaic cells. Investigating the link between solar radiation, current, voltage, and efficiency of photovoltaic cells with and without PCM was the main goal of this experimental study. Digital equipment had been used to record data. Current, voltage, efficiency, and solar radiation have all been analyzed. According to the results, output current and efficiency were directly related to solar radiation. This implies that an increase in output current results from an increase in solar radiation, hence increasing the efficiency of a solar panel. Nevertheless, the temperature of the photovoltaic cell rose in tandem with the rise in solar radiation. However, solar systems—especially photovoltaic panels—generally have low efficiency. The solar module's output is negatively impacted by the surface temperature increase. The absorbed sunlight that is transformed into heat is the cause of this rise, which lowers the panel's power output, energy efficiency, performance, and lifespan. One possible way to prevent solar panels from overheating and to lower cell temperature is to employ cooling systems. Therefore, in this study, we have examined the use of PCM for passive cooling in order to improve photovoltaic cell performance.

4.2.1 Effect of solar radiation intensity on the enhancement of thermal and electrical performance of PV module by using organic PCM

4.2.1.1 Effect of solar radiation intensity on PV cell temperature

For wind speed = 5.5 m/s, the evolutions of solar cell temperatures for PV and PV-PCM configurations are depicted in Fig. 4.4. The surface temperature of the PV-PCM system remained less than that of the conventional PV due to the effect of PCM as a thermal dissipating system and this trend has been continued for each value of solar irradiance. The PV panel without PCM has a maximum operating temperature of 34.5°C and a minimum operating temperature of 28.4°C. In addition, the PV panel without PCM operates at an average temperature of 31.5°C. However, the PV panel with PCM appears to have a maximum operating temperature of 30.4°C and a minimum operating temperature of 23.5°C. Furthermore, a PV panel with PCM operates at an average temperature of 27.16°C. The PV panel with PCM can lower its temperature by 4.34°C compared to the PV panel without PCM. It has been demonstrated that the performance of PV panels can be impacted by the use of PCM.

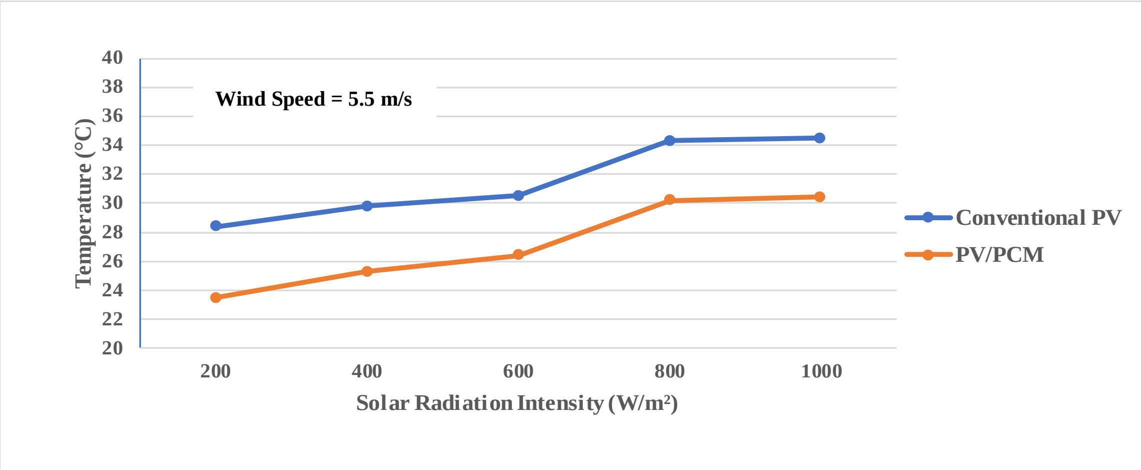

Fig. 4.4. Solar irradiance versus operating temperature for PV panels without and with organic PCM (Wind speed = 5.5 m/s)

For wind speed = 4.5 m/s, the evolutions of solar cell temperatures for PV and PV-PCM configurations are depicted in Fig. 4.5. The surface temperature of the PV-PCM system remained less than that of the conventional PV due to the effect of PCM as a thermal dissipating system and this trend has been continued for each value of solar irradiance. The PV panel without PCM has a maximum operating temperature of 36.6°C and a minimum operating temperature of 30.6°C. In addition, the PV panel without PCM operates at an average temperature of 33.66°C. On the other hand, the highest operating temperature of PV panel with PCM seems to be reached 32.6°C and its lowest operating temperature is 26.4°C. In addition, the average operating temperature of PV panel with PCM is 29.56°C. In the comparison of both PV panels, the PV panel with PCM can be reduced 4.1°C than PV panel without PCM. It can be proved that the effect of using PCM with PV panel can affect the performance of the PV panel.

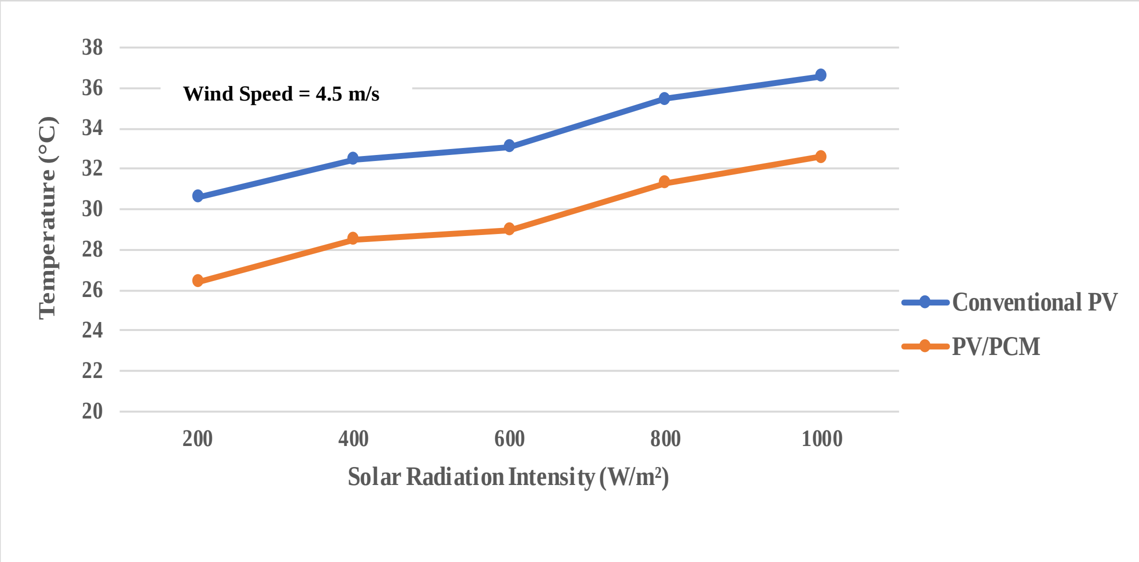

Fig. 4.5. Solar irradiance versus operating temperature for PV panels without and with organic PCM (Wind speed = 4.5 m/s)

For wind speed = 3.5 m/s, the evolutions of solar cell temperatures for PV and PV-PCM configurations are depicted in Fig. 4.6. The surface temperature of the PV-PCM system remained less than that of the conventional PV due to the effect of PCM as a thermal dissipating system and this trend has been continued for each value of solar irradiance. The PV panel without PCM has a maximum operating temperature of 39°C and a minimum operating temperature of 31.2°C. In addition, the PV panel without PCM operates at an average temperature of 34.88°C. However, the PV panel with PCM appears to have a maximum operating temperature of 36.2°C and a minimum operating temperature of 28.2°C. Furthermore, PV panels with PCM have an average operating temperature of 31.84°C. The PV panel with PCM can be 3.04°C cooler than the PV panel without PCM when the two panels are compared. It has been demonstrated that the performance of PV panels can be impacted by the use of PCM.

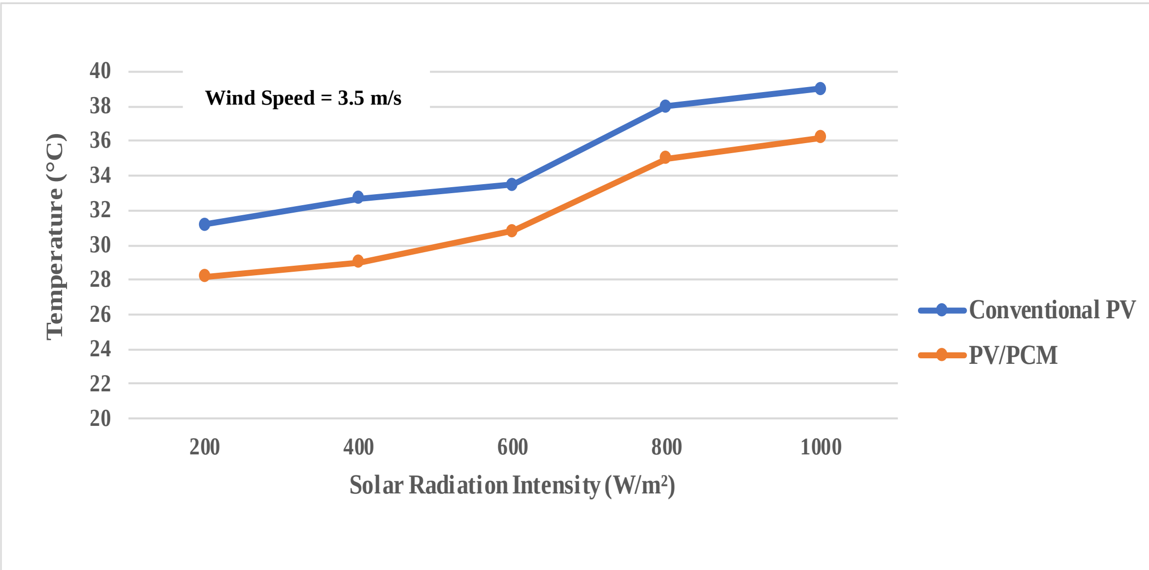

Fig. 4.6. Solar irradiance versus operating temperature for PV panels without and with organic PCM (Wind speed = 3.5 m/s)

For wind speed = 2.5 m/s, the evolutions of solar cell temperatures for PV and PV-PCM configurations are depicted in Fig. 4.7. The surface temperature of the PV-PCM system remained less than that of the conventional PV due to the effect of PCM as a thermal dissipating system and this trend has been continued for each value of solar irradiance. The PV panel without PCM has a maximum operating temperature of 53.2°C and a minimum operating temperature of 40.4°C. In addition, the PV panel without PCM operates at an average temperature of 44.36°C. However, the PV panel with PCM appears to have a maximum operating temperature of 50°C and a minimum operating temperature of 37°C. Furthermore, PV panels with PCM have an average operating temperature of 41.38°C. The PV panel with PCM can be 2.98°C cooler than the PV panel without PCM when the two panels are compared. It has been demonstrated that the performance of PV panels can be impacted by the use of PCM.

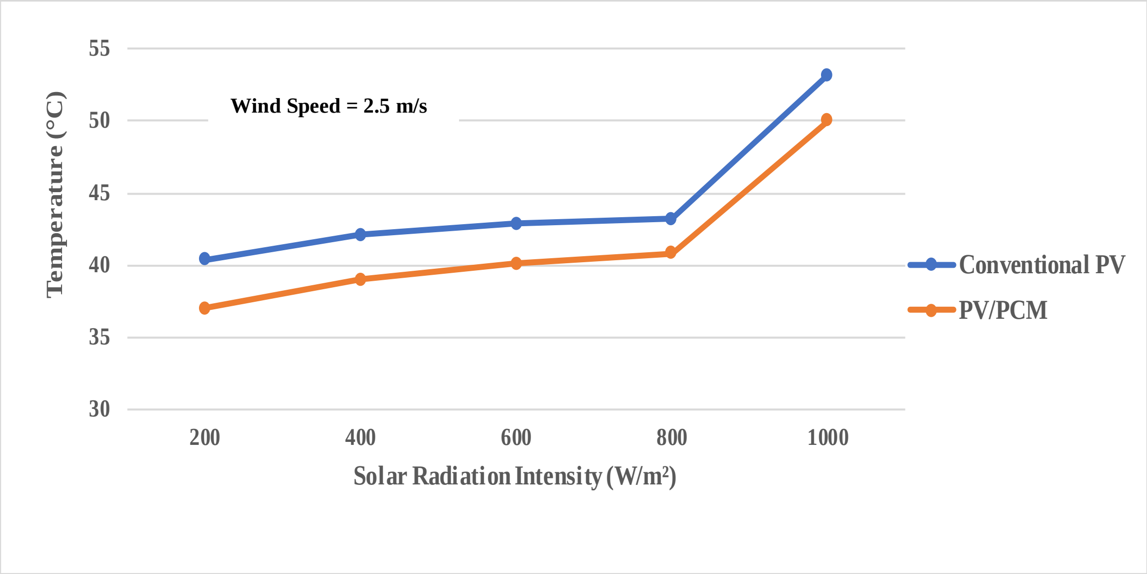

Fig. 4.7. Solar irradiance versus operating temperature for PV panels without and with organic PCM (Wind speed = 2.5 m/s)

For wind speed = 1.5 m/s, the evolutions of solar cell temperatures for PV and PV-PCM configurations are depicted in Fig. 4.8. The surface temperature of the PV-PCM system remained less than that of the conventional PV due to the effect of PCM as a thermal dissipating system and this trend has been continued for each value of solar irradiance. The PV panel without PCM has a maximum operating temperature of 61.7°C and a minimum operating temperature of 42.1°C. In addition, the PV panel without PCM operates at an average temperature of 48.32°C. However, the PV panel with PCM appears to have a maximum operating temperature of 59.7°C and a minimum operating temperature of 40°C. Furthermore, a PV panel with PCM operates at an average temperature of 46.12°C. In the comparison of both PV panels, the PV panel with PCM can be reduced 2.2°C than PV panel without PCM. It can be proved that the effect of using PCM with PV panel can affect the performance of the PV panel.

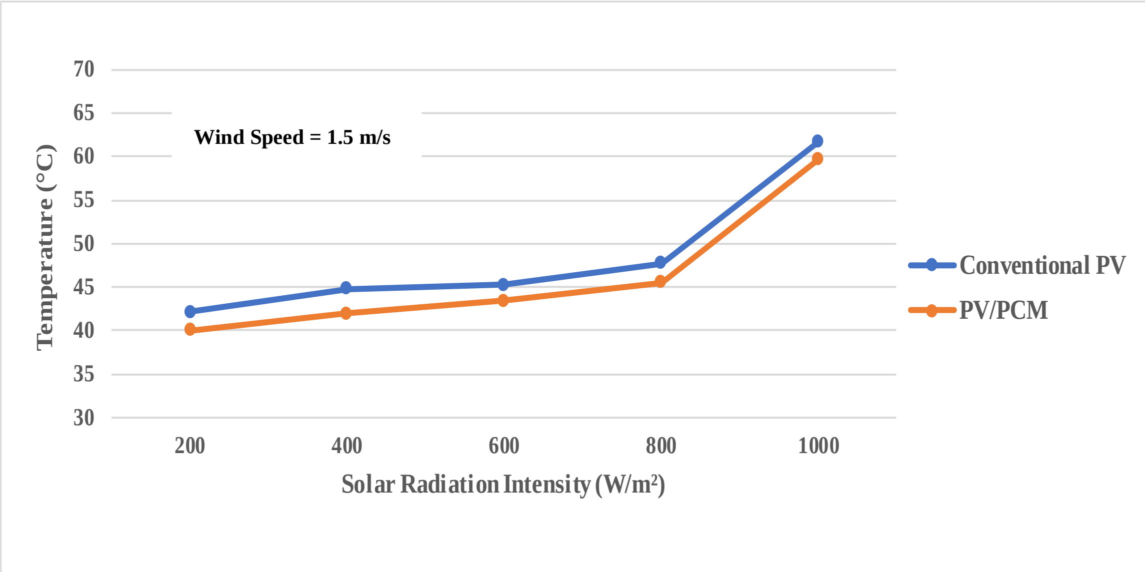

Fig. 4.8. Solar irradiance versus operating temperature for PV panels without and with organic PCM (Wind speed = 1.5 m/s)

For wind speed = 0.5 m/s, the evolutions of solar cell temperatures for PV and PV-PCM configurations are depicted in Fig. 4.9. The surface temperature of the PV-PCM system remained less than that of the conventional PV due to the effect of PCM as a thermal dissipating system and this trend has been continued for each value of solar irradiance. The PV panel without PCM has a maximum operating temperature of 65°C and a minimum operating temperature of 45.3°C. In addition, the PV panel without PCM operates at an average temperature of 51.8°C. However, the PV panel with PCM appears to have a maximum operating temperature of 63°C and a minimum operating temperature of 43.2°C. Furthermore, a PV panel with PCM operates at an average temperature of 49.64°C. The PV panel with PCM can be 2.16°C cooler than the PV panel without PCM when the two panels are compared. It has been demonstrated that the performance of PV panels can be impacted by the use of PCM.

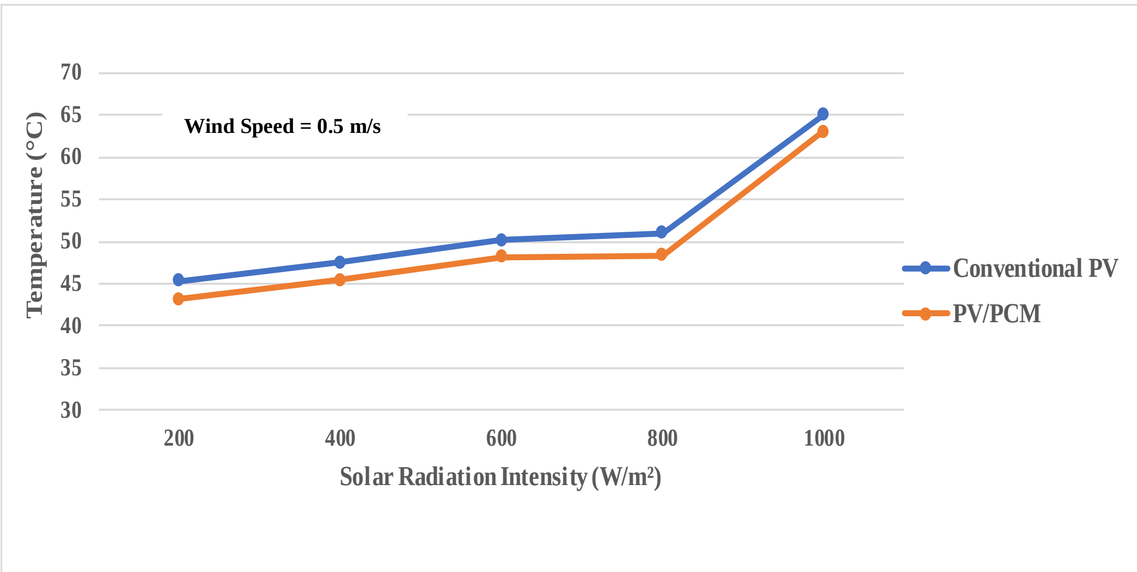

Fig. 4.9. Solar irradiance versus operating temperature for PV panels without and with organic PCM (Wind speed = 0.5 m/s)

4.2.1.2 Effect of solar radiation intensity on output current

Figure 4.10 shows the output current comparison between PV panels with and without PCM for wind speed = 5.5 m/s. When compared to a PV panel without PCM, the PV panel with PCM may deliver the maximum output current. The PV panel without PCM has a minimum output current of 0.12 A and a maximum output current of 0.18 A. Furthermore, the average output current of the PV panel without PCM was 0.16 A. At the same time, the PV panel with PCM produces an average output current of 0.2 A, with maximum and minimum output currents of 0.22 A and 0.16 A, respectively. The PV panel with PCM has a 20% higher output current than the PV panel without PCM when compared to these two PV panels.

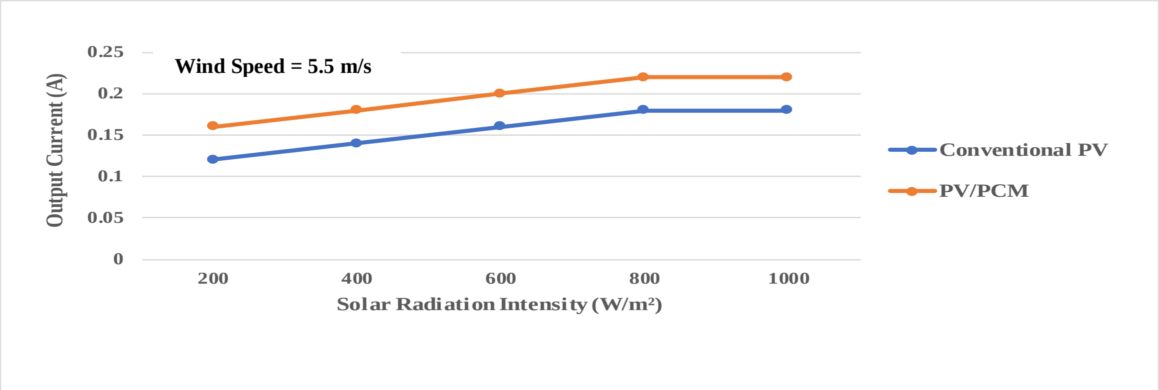

Fig. 4.10. Solar irradiance versus output current for PV panels without and with organic PCM (Wind speed = 5.5 m/s)

Figure 4.11 shows the output current comparison between PV panels with and without PCM for wind speed = 4.5 m/s. When compared to a PV panel without PCM, the PV panel with PCM may deliver the maximum output current. The PV panel without PCM has a minimum output current of 0.12 A and a maximum output current of 0.18 A. Furthermore, the average output current of the PV panel without PCM was 0.16 A. At the same time, the PV panel with PCM produces an average output current of 0.2 A, with maximum and minimum output currents of 0.22 A and 0.16 A, respectively. The PV panel with PCM has a 20% higher output current than the PV panel without PCM when compared to these two PV panels.

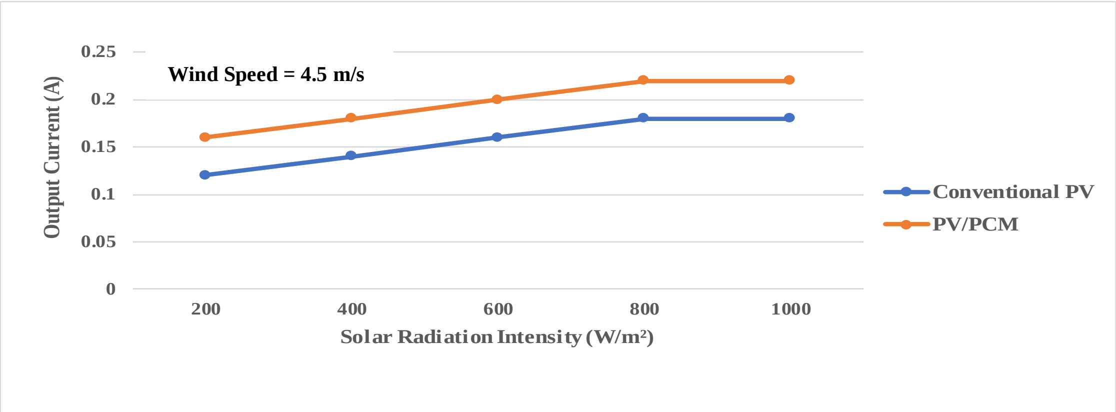

Fig. 4.11. Solar irradiance versus output current for PV panels without and with organic PCM (Wind speed = 4.5 m/s)

Figure 4.12 shows the output current comparison between PV panels with and without PCM for wind speed = 3.5 m/s. When compared to a PV panel without PCM, the PV panel with PCM may deliver the maximum output current. The PV panel without PCM has a minimum output current of 0.12 A and a maximum output current of 0.18 A. Furthermore, the average output current of the PV panel without PCM was 0.15 A. At the same time, the PV panel with PCM produces an average output current of 0.18 A, with maximum and minimum output currents of 0.21 A and 0.15 A, respectively. The output current of the PV panel with PCM is 16.7% higher than that of the PV panel without PCM when compared to these two PV panels.

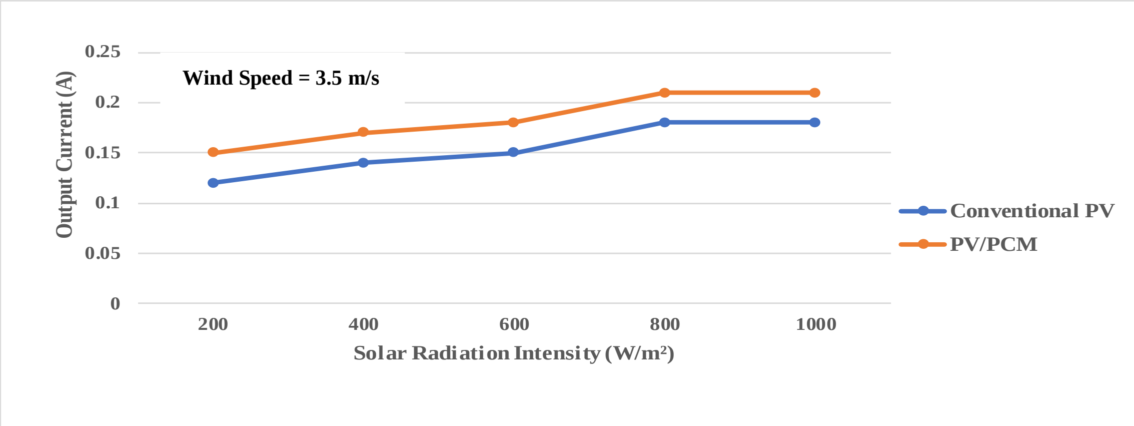

Fig. 4.12. Solar irradiance versus output current for PV panels without and with organic PCM (Wind speed = 3.5 m/s)

Figure 4.13 shows the output current comparison between PV panels with and without PCM for wind speed = 2.5 m/s. When compared to a PV panel without PCM, the PV panel with PCM may deliver the maximum output current. The PV panel without PCM has a minimum output current of 0.12 A and a maximum output current of 0.17 A. Furthermore, the average output current of the PV panel without PCM was 0.15 A. At the same time, the PV panel with PCM produces an average output current of 0.18 A, with maximum and minimum output currents of 0.20 A and 0.15 A, respectively. The output current of the PV panel with PCM is 16.7% higher than that of the PV panel without PCM when compared to these two PV panels.

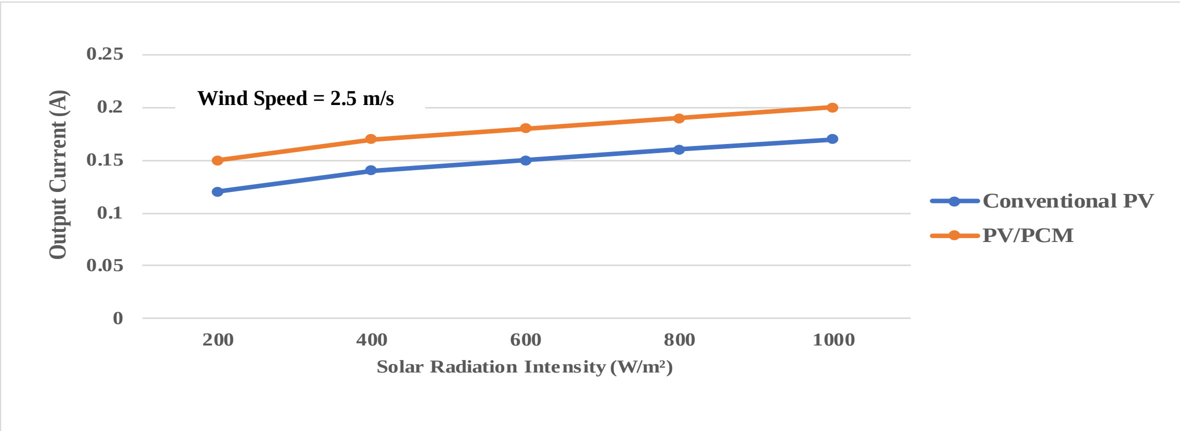

Fig. 4.13. Solar irradiance versus output current for PV panels without and with organic PCM (Wind speed = 2.5 m/s)

Figure 4.14 shows the output current comparison between PV panels with and without PCM for wind speed = 1.5 m/s. When compared to a PV panel without PCM, the PV panel with PCM may deliver the maximum output current. The PV panel without PCM has a minimum output current of 0.12 A and a maximum output current of 0.17 A. Furthermore, the average output current of the PV panel without PCM was 0.14 A. At the same time, the PV panel with PCM produces an average output current of 0.16 A, with maximum and minimum output currents of 0.19 A and 0.14 A, respectively. The PV panel with PCM has a 12.5% higher output current than the PV panel without PCM when compared to these two PV panels.

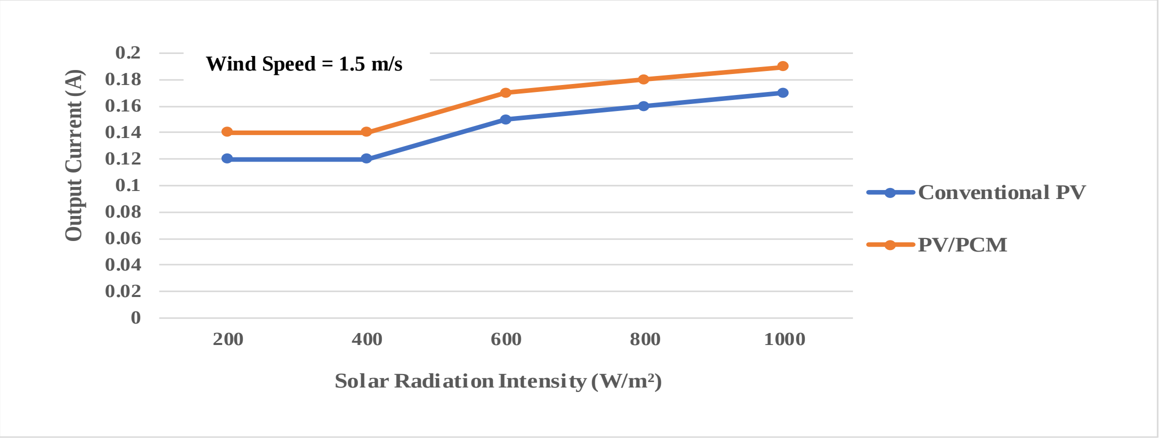

Fig. 4.14. Solar irradiance versus output current for PV panels without and with organic PCM (Wind speed = 1.5 m/s)

Figure 4.15 shows the output current comparison between PV panels with and without PCM for wind speed = 0.5 m/s. When compared to a PV panel without PCM, the PV panel with PCM may deliver the maximum output current. The PV panel without PCM has a minimum output current of 0.12 A and a maximum output current of 0.16 A. Furthermore, the average output current of the PV panel without PCM was 0.14 A. At the same time, the PV panel with PCM produces an average output current of 0.16 A, with maximum and minimum output currents of 0.18 A and 0.14 A, respectively. The PV panel with PCM has a 12.5% higher output current than the PV panel without PCM when compared to these two PV panels.

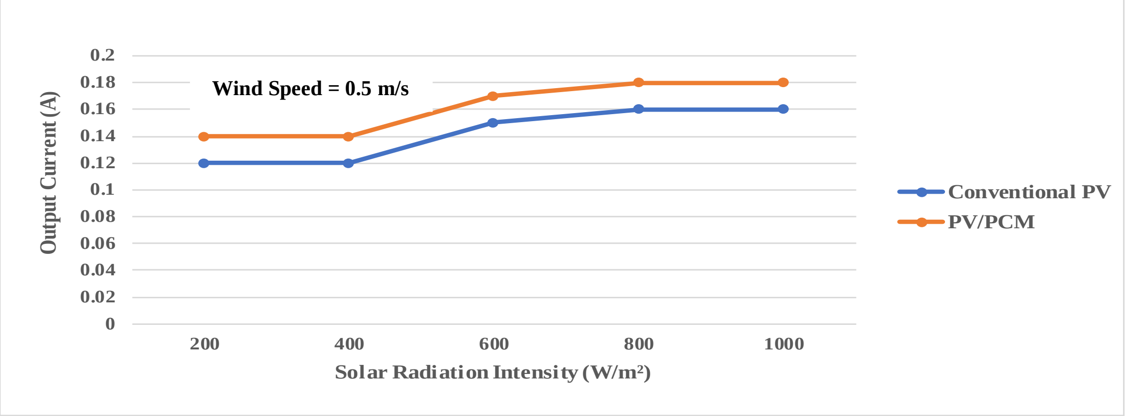

Fig. 4.15. Solar irradiance versus output current for PV panels without and with organic PCM (Wind speed = 0.5 m/s)

4.2.1.3 Effect of solar radiation intensity on voltage

The output voltage fluctuation produced by PV panels with and without PCM when the wind speed reaches 5.5 m/s is depicted in Fig. 4.16. It is evident that compared to a PV panel without PCM, one with PCM can yield a higher output voltage. PV panels without PCM have a maximum output voltage of 7.8 V and a minimum output voltage of 7.2 V. Meanwhile, a PV panel without PCM achieves an average output voltage of 7.5 V. Conversely, a PV panel with PCM can generate a minimum output voltage of 8 V and a maximum output voltage of 8.6 V. Additionally, the average output voltage of the PV panel with PCM is 8.3 V. The PV panel with PCM can create 9.6% more output voltage than the PV panel without PCM when these two panels are compared. It is evident that a PV panel with a low operating temperature can produce a higher output voltage.

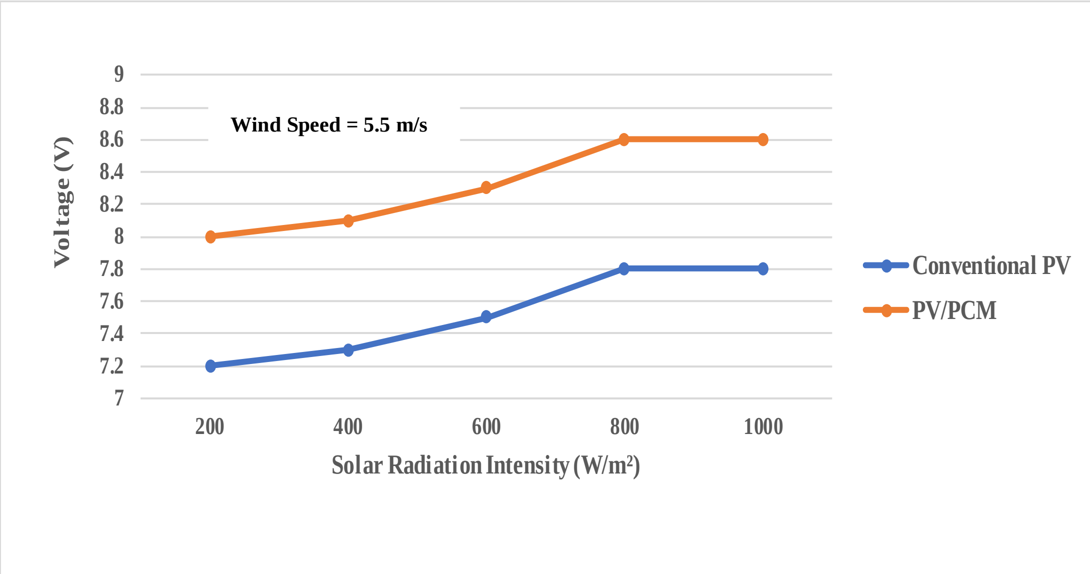

Fig. 4.16. Solar irradiance versus output voltage for PV panels without and with organic PCM (Wind speed = 5.5 m/s)

The output voltage fluctuation produced by PV panels with and without PCM when the wind speed reaches 4.5 m/s is depicted in Fig. 4.17. The ability of the PV panel with PCM to provide higher output voltage than the PV panel without PCM is evident. PV panels without PCM have a maximum output voltage of 7.8 V and a minimum output voltage of 7.2 V. Meanwhile, a PV panel without PCM achieves an average output voltage of 7.4 V. Conversely, a PV panel with PCM can provide a maximum output voltage of 8.6 V and a minimum output voltage of 7.5 V. The PV panel with PCM can create 5.13% more output voltage than the PV panel without PCM when these two panels are compared. It is evident that a PV panel with a low operating temperature can produce a higher output voltage.

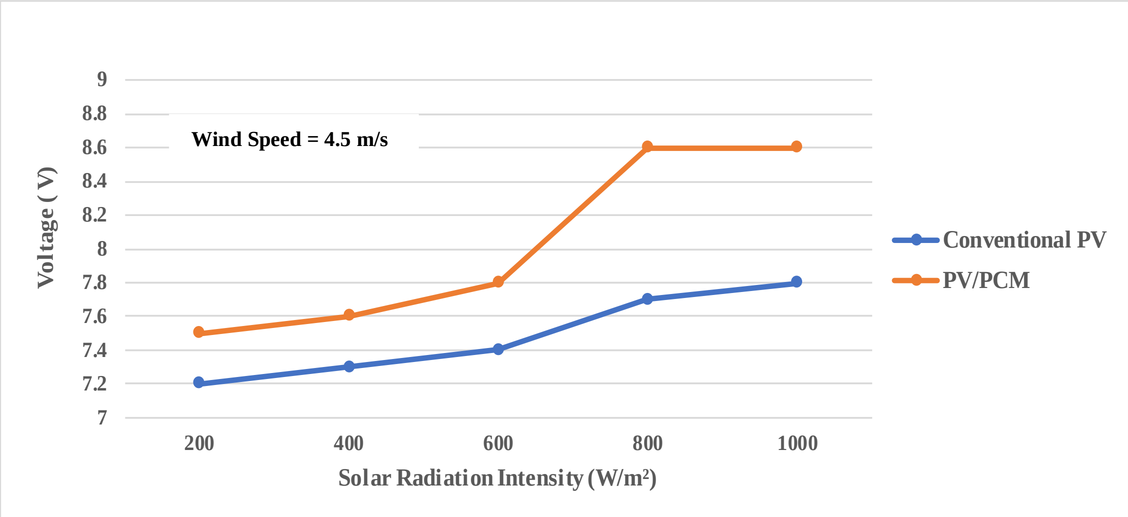

Fig. 4.17. Solar irradiance versus output voltage for PV panels without and with organic PCM (Wind speed = 4.5 m/s)

When the wind speed reaches 3.5 m/s, Figure 4.18 illustrates the difference in output voltage produced by PV panels with and without PCM. It is evident that compared to a PV panel without PCM, one with PCM can yield a higher output voltage. PV panels without PCM have a maximum output voltage of 7.7 V and a minimum output voltage of 7.2 V. Meanwhile, a PV panel without PCM achieves an average output voltage of 7.4 V. However, a PV panel with PCM can provide a minimum output voltage of 7.5 V and a maximum output voltage of 8.5 V. Additionally, the average output voltage of the PV panel with PCM is 7.7 V. The PV panel with PCM may create 3.9% more output voltage than the PV panel without PCM when these two panels are compared. It is evident that a PV panel with a low operating temperature can produce a higher output voltage.

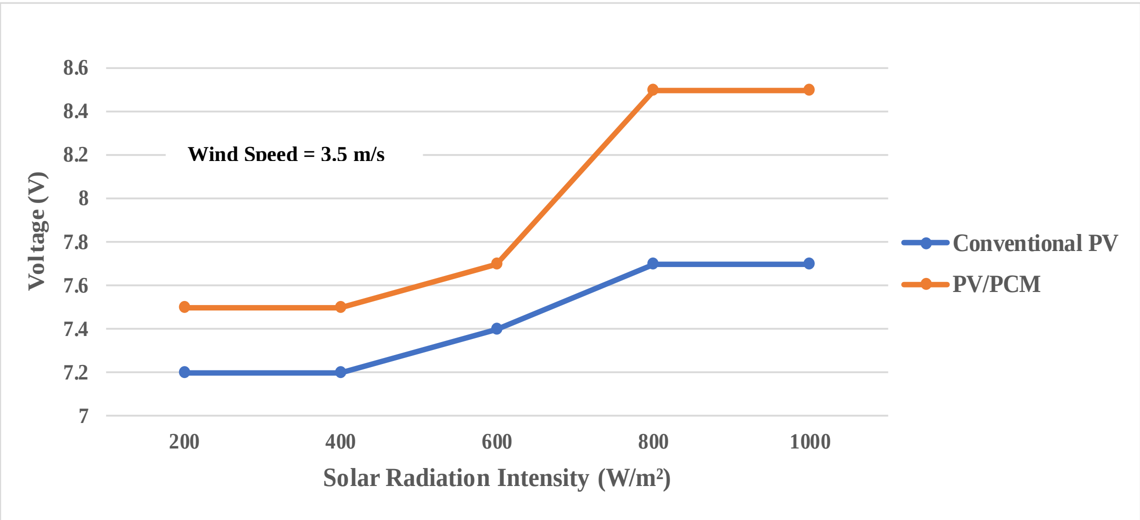

Fig. 4.18. Solar irradiance versus output voltage for PV panels without and with organic PCM (Wind speed = 3.5 m/s)

The output voltage fluctuation produced by PV panels with and without PCM when the wind speed reaches 2.5 m/s is depicted in Fig. 4.19. It is evident that compared to a PV panel without PCM, one with PCM can yield a higher output voltage. PV panels without PCM have a maximum output voltage of 7.7 V and a minimum output voltage of 7.2 V. Meanwhile, a PV panel without PCM achieves an average output voltage of 7.4 V. However, a PV panel with PCM can provide a minimum output voltage of 7.5 V and a maximum output voltage of 8.5 V. Additionally, the average output voltage of the PV panel with PCM is 7.7 V. The PV panel with PCM may create 3.9% more output voltage than the PV panel without PCM when these two panels are compared. It is evident that a PV panel with a low operating temperature can produce a higher output voltage.

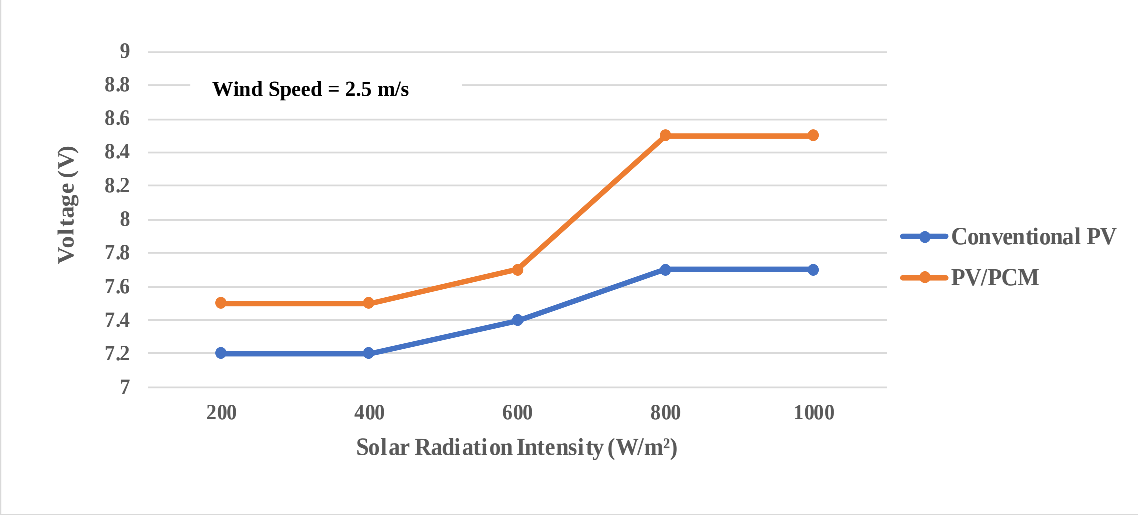

Fig. 4.19. Solar irradiance versus output voltage for PV panels without and with organic PCM (Wind speed = 2.5 m/s)

The output voltage fluctuation produced by PV panels with and without PCM when the wind speed reaches 1.5 m/s is depicted in Fig. 4.20. It is evident that compared to a PV panel without PCM, one with PCM can yield a higher output voltage. PV panels without PCM have a maximum output voltage of 7.6 V and a minimum output voltage of 7.2 V. Meanwhile, a PV panel without PCM achieves an average output voltage of 7.4 V. However, a PV panel with PCM can provide a minimum output voltage of 7.5 V and a maximum output voltage of 8.5 V. Additionally, the average output voltage of the PV panel with PCM is 7.7 V. The PV panel with PCM may create 3.9% more output voltage than the PV panel without PCM when these two panels are compared. It is evident that a PV panel with a low operating temperature can produce a higher output voltage.

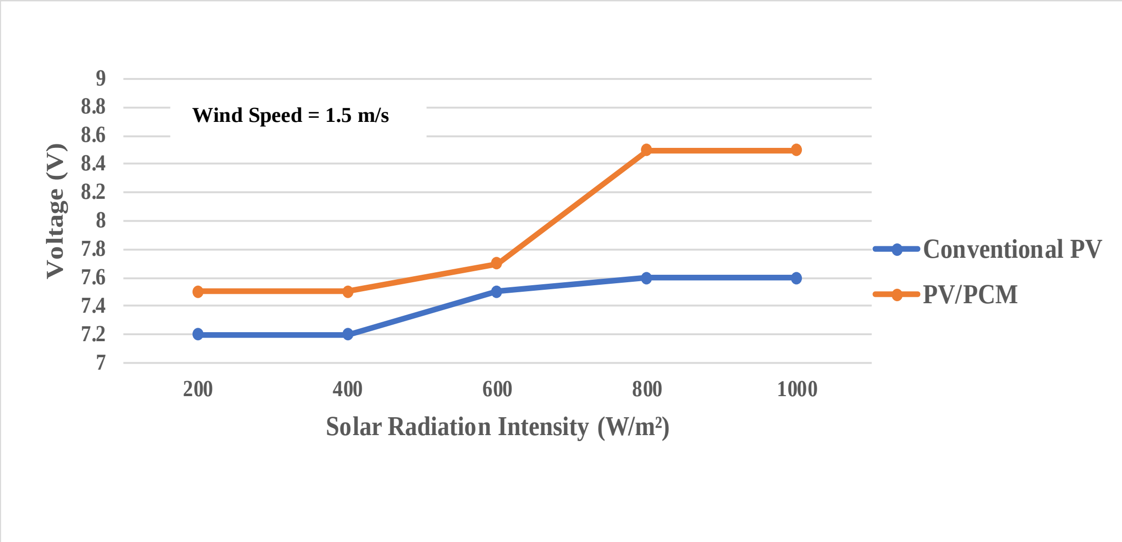

Fig. 4.20. Solar irradiance versus output voltage for PV panels without and with organic PCM (Wind speed = 1.5 m/s)

When the wind speed reaches 0.5 m/s, Figure 4.21 illustrates the difference in output voltage produced by PV panels with and without PCM. The ability of the PV panel with PCM to provide higher output voltage than the PV panel without PCM is evident. PV panels without PCM have a maximum output voltage of 6.8 V and a minimum output voltage of 6.5 V. Meanwhile, 6.6 V is the average output voltage of a PV panel without PCM. However, a PV panel with PCM can produce a minimum output voltage of 6.6 V and a maximum output voltage of 7 V. Additionally, the average output voltage of the PV panel with PCM is 6.7 V. The PV panel with PCM may create 1.49% more output voltage than the PV panel without PCM when these two panels are compared. It is evident that a PV panel with a low operating temperature can produce a higher output voltage.

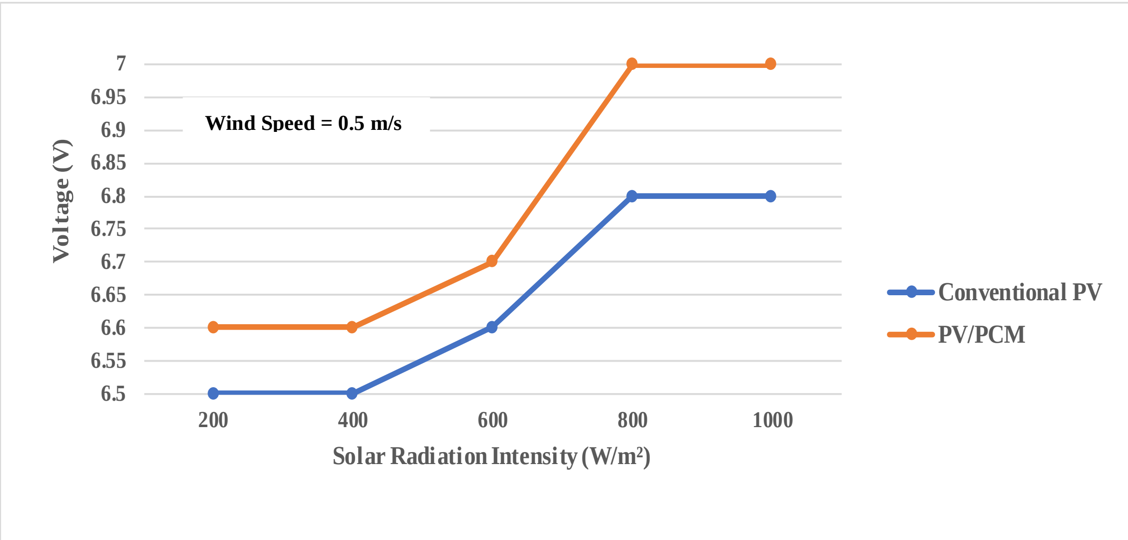

Fig. 4.21. Solar irradiance versus output voltage for PV panels without and with organic PCM (Wind speed =0.5 m/s)

4.2.1.4 Effect of solar radiation intensity on power

The output power produced by the two PV panels is compared in Fig. 4.22 when the wind speed reaches 5.5 m/s. The greatest output power of a PV panel without PCM is 1.404 W, and the lowest output power is 0.864 W. However, the PV panel with PCM has a minimum output power of 1.064 W and a maximum output power of 2.064 W. PV panels with PCM and those without PCM have respective average output powers of 1.56 W and 1.18 W. It is obvious that PV panel with PCM can produce higher output power than the PV panel without PCM. Using a PV panel with PCM results in a 24.36% increase in output power per unit of electricity.

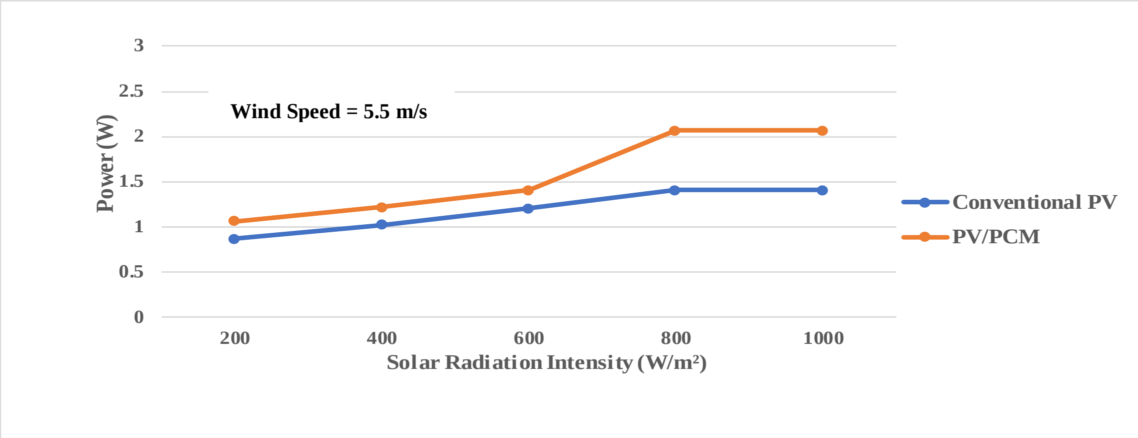

Fig. 4.22. Solar irradiance versus output power for PV panels without and with organic PCM (Wind speed =5.5 m/s)

The output power produced by the two PV panels is compared in Fig. 4.23 when the wind speed reaches 4.5 m/s. The greatest output power of a PV panel without PCM is 1.404 W, and the lowest output power is 0.864 W. However, the PV panel with PCM has a minimum output power of 1.064 W and a maximum output power of 2.064 W. PV panels with PCM and those without PCM have respective average output powers of 1.56 W and 1.18 W. It is obvious that PV panel with PCM can produce higher output power than the PV panel without PCM. Using a PV panel with PCM results in a 24.36% increase in output power per unit of electricity.

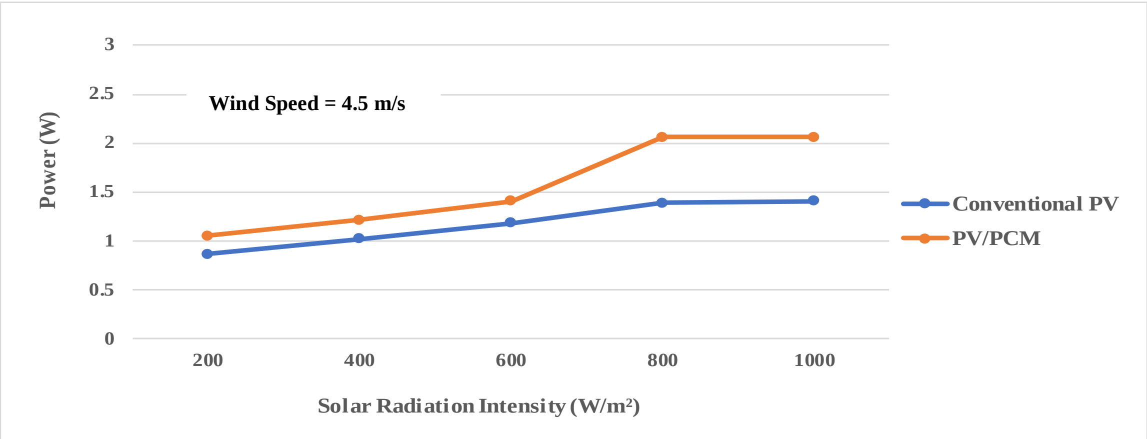

Fig. 4.23. Solar irradiance versus output power for PV panels without and with organic PCM (Wind speed = 4.5 m/s)

The output power produced by the two PV panels is compared in Fig. 4.24 when the wind speed reaches 3.5 m/s. The maximum output power of a PV panel without PCM is 1.386 W. whereas 0.864 W is the minimum output power. However, the PV panel with PCM has a minimum output power of 1.05 W and a maximum output power of 2.04 W. PV panels with PCM and those without PCM have respective average output powers of 1.49 W and 1.15 W. It is obvious that PV panel with PCM can produce higher output power than the PV panel without PCM. Using a PV panel with PCM results in a 22.8% increase in output power per unit of electricity.

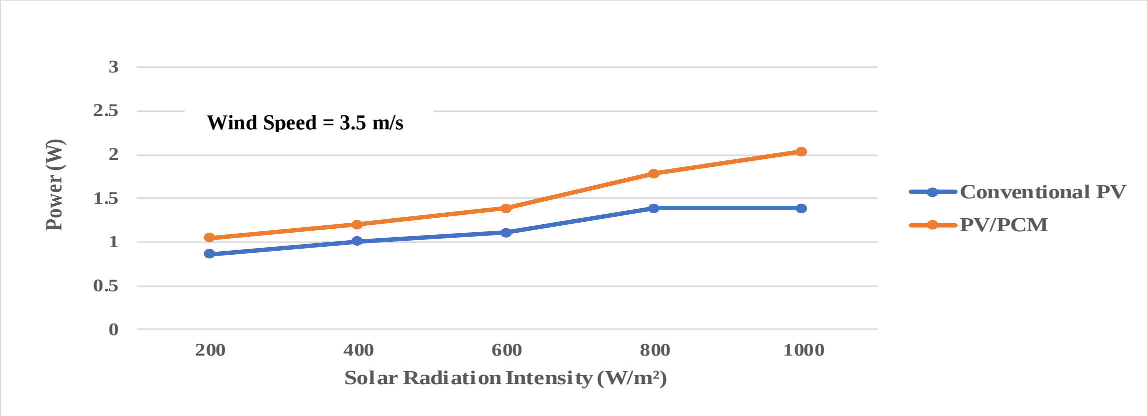

Fig. 4.24. Solar irradiance versus output power for PV panels without and with organic PCM(Wind speed = 3.5 m/s)

The output power produced by the two PV panels is compared in Fig. 4.25 when the wind speed reaches 2.5 m/s. PV panels without PCM have a minimum output power of 0.864 W and a maximum output power of 1.309 W. However, the PV panel with PCM has a minimum output power of 0.975 W and a maximum output power of 2.04 W. PV panels with PCM and those without PCM have respective average output powers of 1.43 W and 1.11 W. It is obvious that PV panel with PCM can produce higher output power than the PV panel without PCM. Using a PV panel with PCM results in a 22.4% increase in output power per unit of electricity.

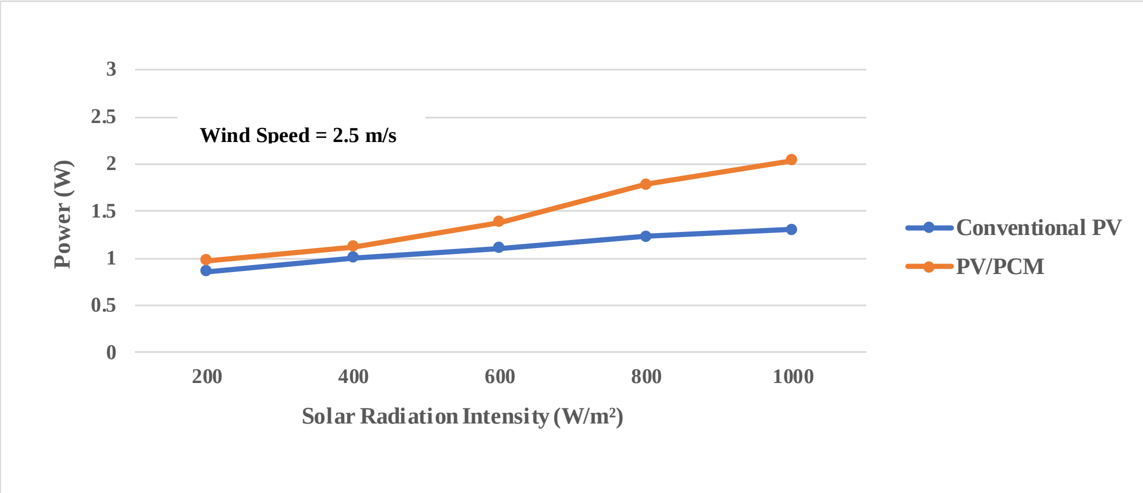

Fig. 4.25. Solar irradiance versus output power for PV panels without and with organic PCM(Wind speed = 2.5 m/s)

When the wind speed reaches 1.5 m/s, the output power produced by the two PV panels is compared in Fig. 4.26. PV panels without PCM have a minimum output power of 0.864 W and a maximum output power of 1.309 W. However, the PV panel with PCM has a minimum output power of 0.975 W and a maximum output power of 1.785 W. PV panels with PCM and those without PCM have respective average output powers of 1.309 W and 1.095 W. It is obvious that PV panel with PCM can produce higher output power than the PV panel without PCM. Using PV panels with PCM results in a 16.3% increase in output power per unit of electricity.

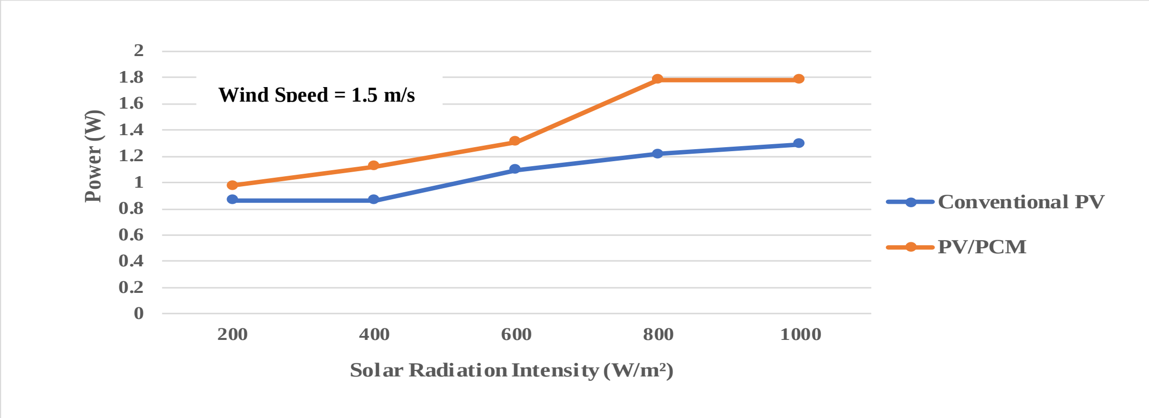

Fig. 4.26. Solar irradiance versus output power for PV panels without and with organic PCM (Wind speed = 1.5 m/s)

When the wind speed reaches 0.5 m/s, the output power produced by the two PV panels is compared in Fig 4.27. The maximum output power of a PV panel without PCM is 1.216 W. whereas 0.864 W is the minimum output power. However, the PV panel with PCM has a minimum output power of 0.975 W and a maximum output power of 1.785 W. PV panels with PCM and those without PCM have respective average output powers of 1.309 W and 1.095 W. It is obvious that PV panel with PCM can produce higher output power than the PV panel without PCM. Using PV panels with PCM results in a 16.3% increase in output power per unit of electricity.

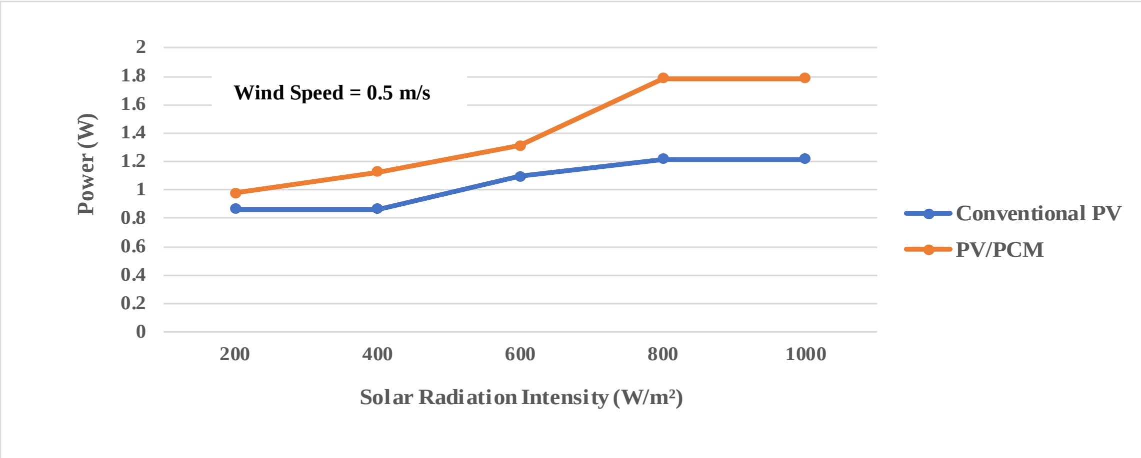

Fig. 4.27. Solar irradiance versus output power for PV panels without and with organic PCM (Wind speed = 0.5 m/s)

4.2.2 Effect of wind speed on on the enhancement of thermal and electrical performance of PV module by using organic PCM

4.2.2.1 Effect of wind speed on PV cell temperature

Figure 4.28 shows the evolution of solar cell temperatures for PV and PV-PCM designs with solar irradiation = 1000 W/m². Due to the combined effects of high wind speed and PCM's ability to dissipate heat, the surface temperature variation between conventional PV and PV-PCM systems at a wind speed of 5.5 m/s remained 54.5% greater than that between conventional PV and PV-PCM systems at a wind speed of 0.5 m/s.

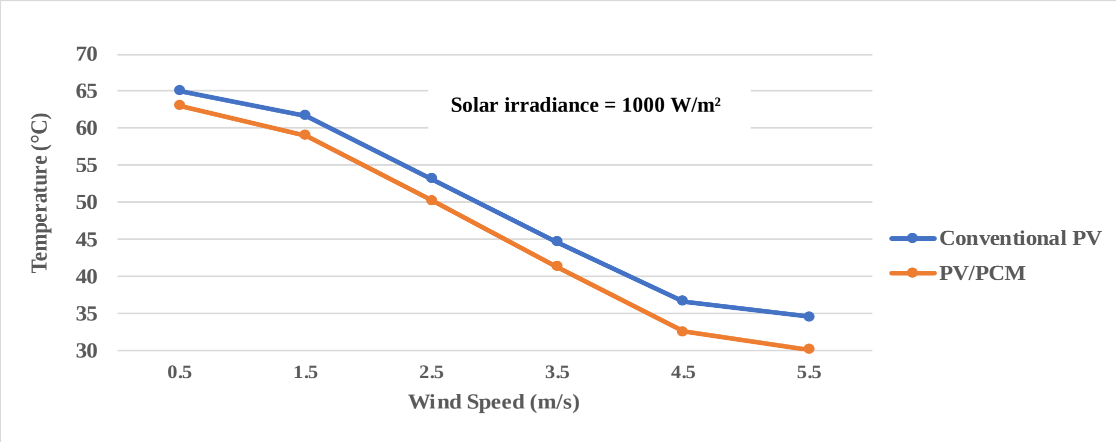

Fig. 4.28. Wind speed versus operating temperature for PV panels without and with organic PCM (Solar irradiance = 1000 W/m²)

Figure 4.29 shows the evolution of solar cell temperatures for PV and PV-PCM designs with solar irradiance = 800 W/m². Due to the combined effects of high wind speed and PCM's ability to dissipate heat, the surface temperature variation between conventional PV and PV-PCM systems at a wind speed of 5.5 m/s remained 62.8% higher than that between conventional PV and PV-PCM systems at a wind speed of 0.5 m/s.

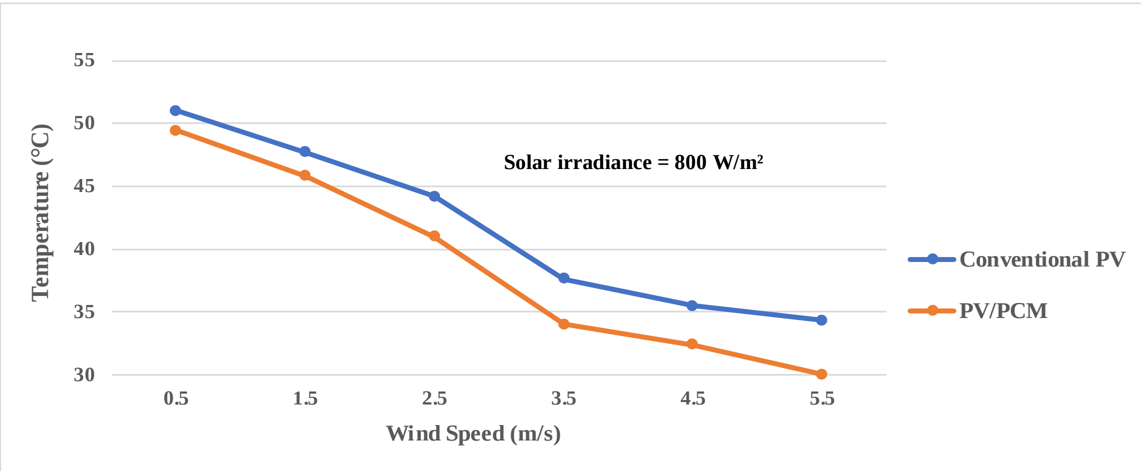

Fig. 4.29. Wind speed versus operating temperature for PV panels without and with organic PCM (Solar irradiance = 800 W/m²)

Figure 4.30 shows the evolution of solar cell temperatures for PV and PV-PCM configurations with solar irradiance = 600 W/m². Due to the combined effects of high wind speed and PCM's ability to dissipate heat, the surface temperature variation between conventional PV and PV-PCM systems at a wind speed of 5.5 m/s remained 50% greater than that between conventional PV and PV-PCM systems at a wind speed of 0.5 m/s.

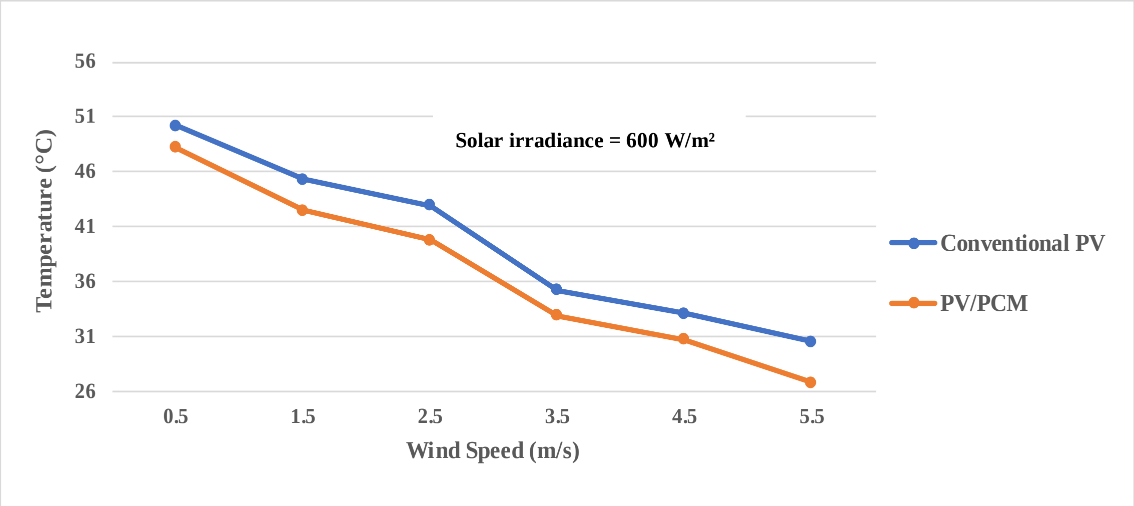

Fig. 4.30. Wind speed versus operating temperature for PV panels without and with organic PCM (Solar irradiance = 600 W/m²)

Figure 4.31 shows the evolution of solar cell temperatures for PV and PV-PCM designs with solar irradiance = 400 W/m². Due to the combined effects of high wind speed and PCM's ability to dissipate heat, the surface temperature variation between conventional PV and PV-PCM systems at a wind speed of 5.5 m/s remained 46% greater than that between conventional PV and PV-PCM systems at a wind speed of 0.5 m/s.

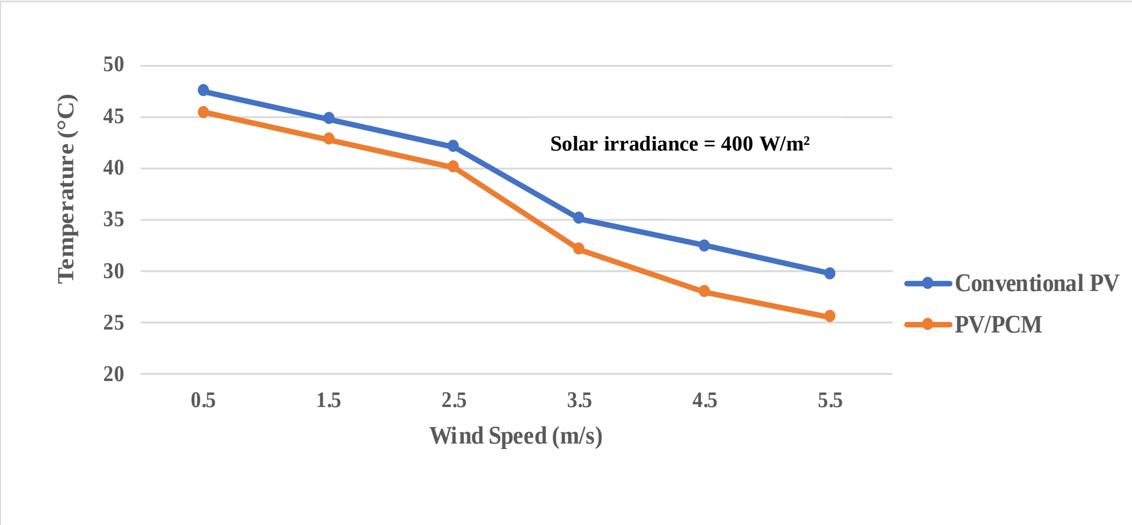

Fig. 4.31. Wind speed versus operating temperature for PV panels without and with organic PCM (Solar irradiance = 400 W/m²)

Figure 4.32 shows the evolution of solar cell temperatures for PV and PV-PCM designs with solar irradiance = 200 W/m². Due to the combined effects of high wind speed and PCM's ability to dissipate heat, the surface temperature variation between conventional PV and PV-PCM systems at a wind speed of 5.5 m/s remained 13.73% higher than that between conventional PV and PV-PCM systems at a wind speed of 0.5 m/s.

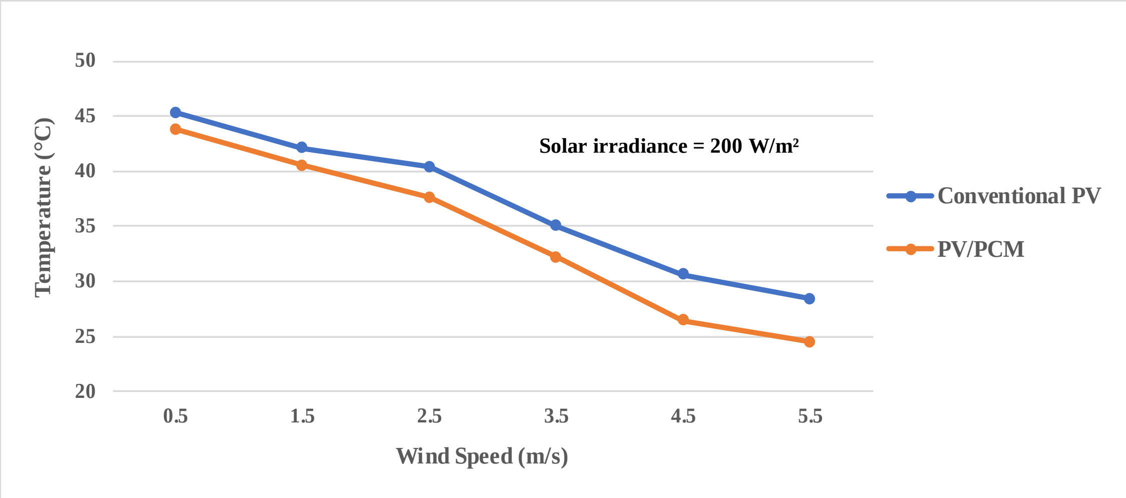

Fig. 4.32. Wind speed versus operating temperature for PV panels without and with organic PCM (Solar irradiance = 200 W/m²)

4.2.2.2 Effect of wind speed on output current

Figure 4.33 shows the output current evolutions for PV and PV-PCM systems with solar irradiation = 1000 W/m². Due to the combined effects of high wind speed and PCM's ability to dissipate heat, the output current variation between conventional PV and PV-PCM systems at a wind speed of 5.5 m/s remained 66.7% higher than that between conventional PV and PV-PCM systems at a wind speed of 0.5 m/s.

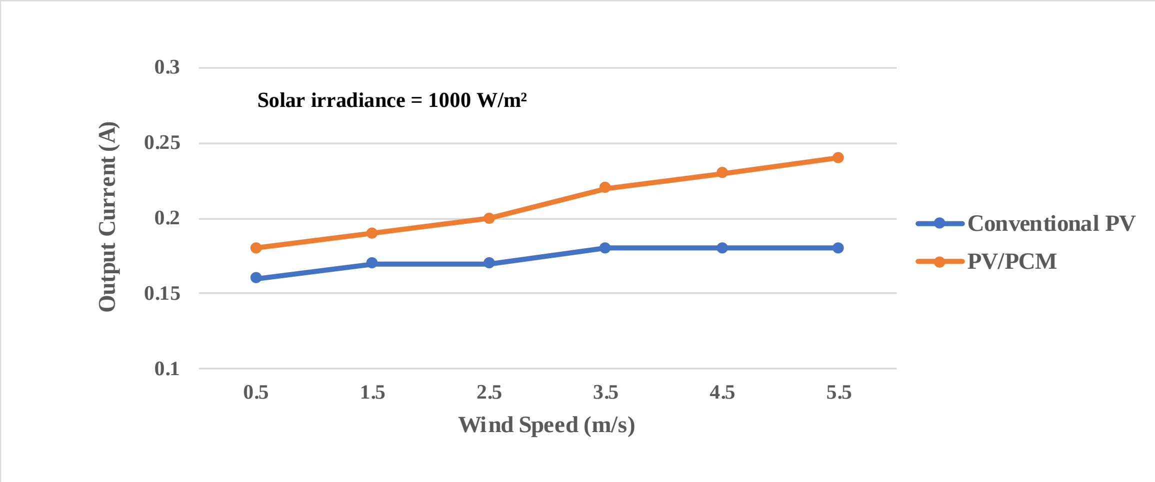

Fig. 4.33. Wind speed versus output current for PV panels without and with organic PCM (Solar irradiance = 1000 W/m²)

Figure 4.34 shows the output current evolutions for PV and PV-PCM systems with solar irradiation = 800 W/m². Due to the combined effects of high wind speed and PCM's ability to dissipate heat, the output current variation between conventional PV and PV-PCM systems at a wind speed of 5.5 m/s remained 66.7% higher than that between conventional PV and PV-PCM systems at a wind speed of 0.5 m/s.

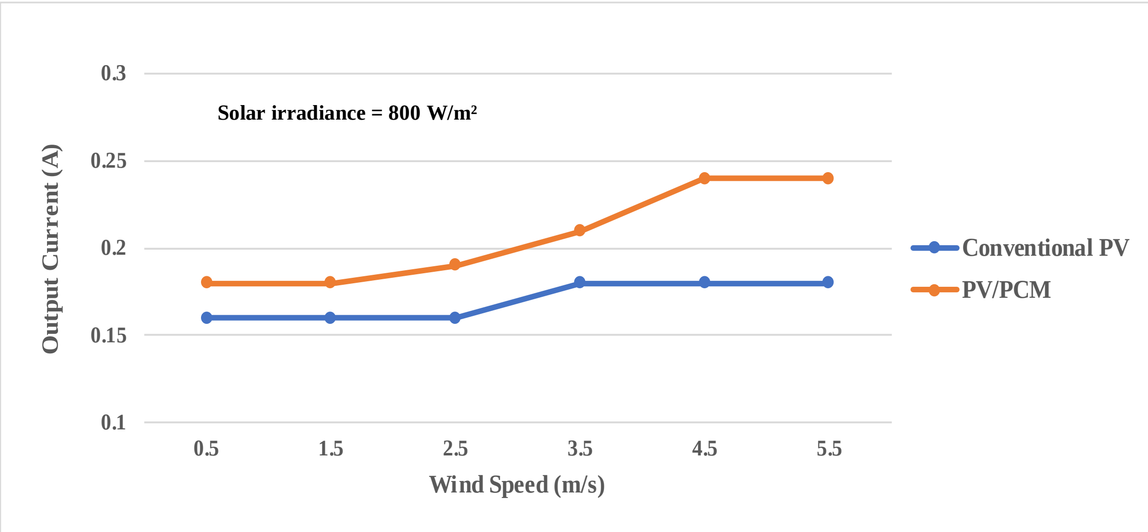

Fig. 4.34. Wind speed versus output current for PV panels without and with organic PCM (Solar irradiance = 800 W/m²)

Figure 4.35 shows the output current evolutions for PV and PV-PCM systems with solar irradiation = 600 W/m². Due to the combined effects of high wind speed and PCM's ability to dissipate heat, the output current variation between conventional PV and PV-PCM systems at a wind speed of 5.5 m/s remained 50% greater than that between conventional PV and PV-PCM systems at a wind speed of 0.5 m/s.

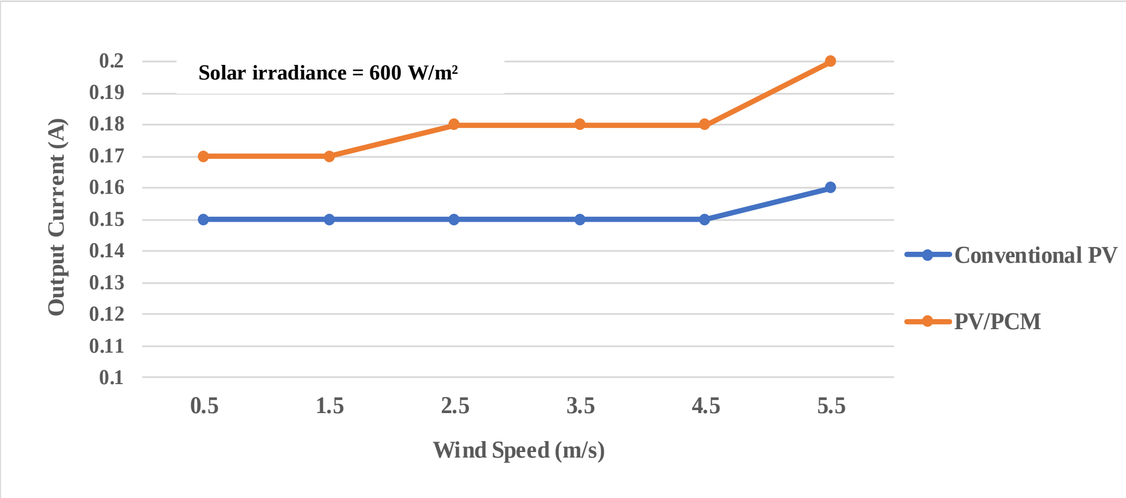

Fig. 4.35. Wind speed versus output current for PV panels without and with organic PCM (Solar irradiance = 600 W/m²)

Figure 4.36 shows the output current evolutions for PV and PV-PCM systems with solar irradiation = 400 W/m². Due to the combined effects of high wind speed and PCM's ability to dissipate heat, the output current variation between conventional PV and PV-PCM systems at a wind speed of 5.5 m/s remained 50% greater than that between conventional PV and PV-PCM systems at a wind speed of 0.5 m/s.

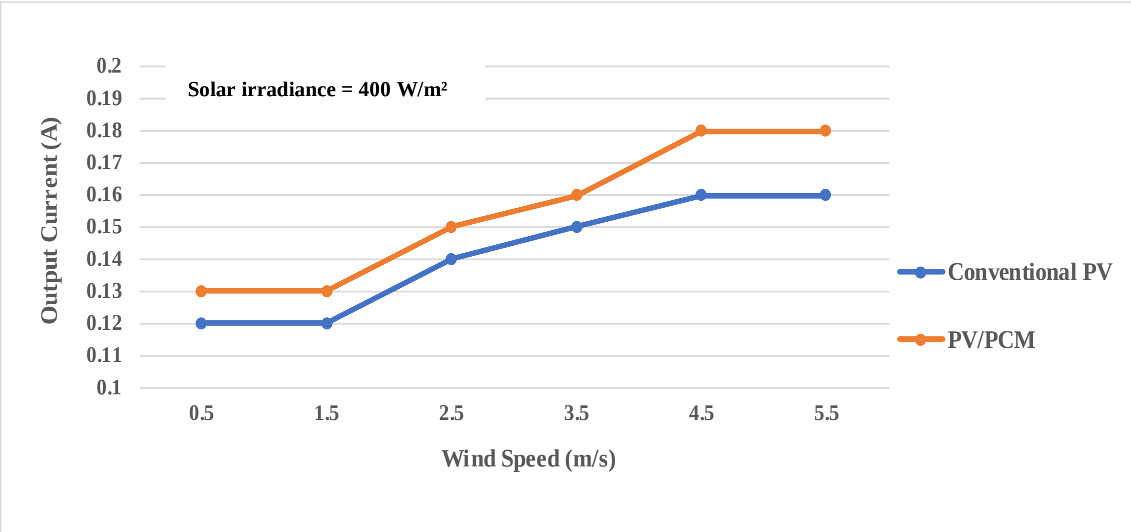

Fig. 4.36. Wind speed versus output current for PV panels without and with organic PCM (Solar irradiance = 400 W/m²)

Figure 4.37 shows the output current evolutions for PV and PV-PCM systems with solar irradiation = 200 W/m². Due to the combined effects of high wind speed and PCM's ability to dissipate heat, the output current variation between conventional PV and PV-PCM systems at a wind speed of 5.5 m/s remained 50% greater than that between conventional PV and PV-PCM systems at a wind speed of 0.5 m/s.

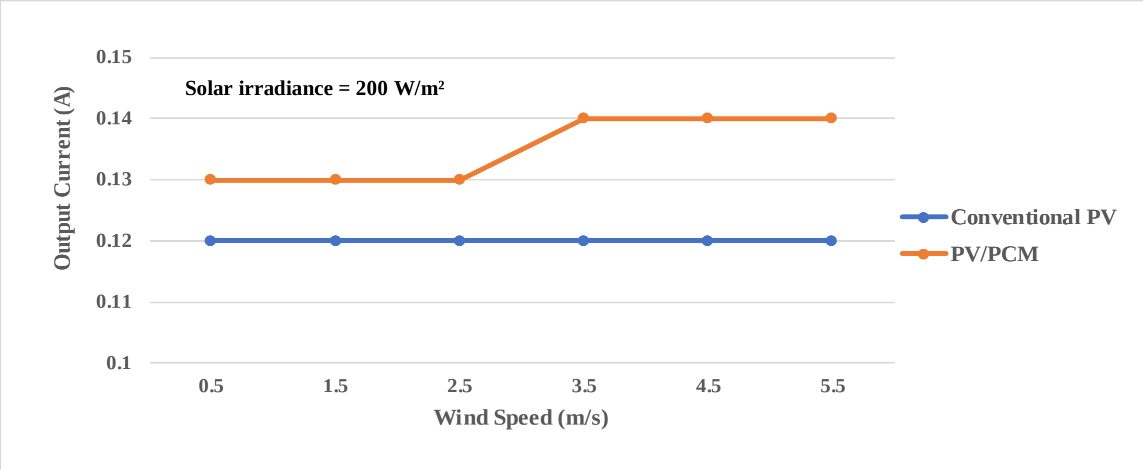

Fig. 4.37. Wind speed versus output current for PV panels without and with organic PCM (Solar irradiance = 200 W/m²)

4.2.2.3 Effect of wind speed on voltage

Figure 4.38 shows the output voltage evolutions for PV and PV-PCM systems with solar irradiation = 1000 W/m². Due to the combined effects of high wind speed and PCM's ability to dissipate heat, the output voltage variation between the conventional PV and PV-PCM systems at a wind speed of 5.5 m/s remained 37.5% higher than that between the conventional PV and PV-PCM systems at a wind speed of 0.5 m/s.

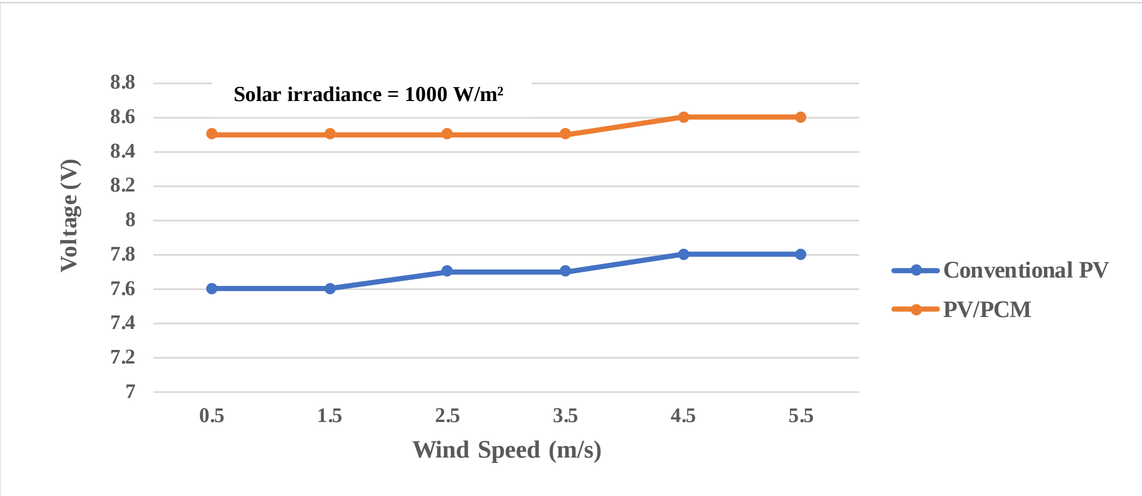

Fig. 4.38. Wind speed versus output voltage for PV panels without and with organic PCM (Solar irradiance = 1000W/m²)

Fig. 4.39 shows the output voltage evolutions for PV and PV-PCM systems with solar irradiation = 800 W/m². Due to the combined effects of high wind speed and PCM's ability to dissipate heat, the output voltage variation between the conventional PV and PV-PCM systems at a wind speed of 5.5 m/s remained 37.5% higher than that between the conventional PV and PV-PCM systems at a wind speed of 0.5 m/s.

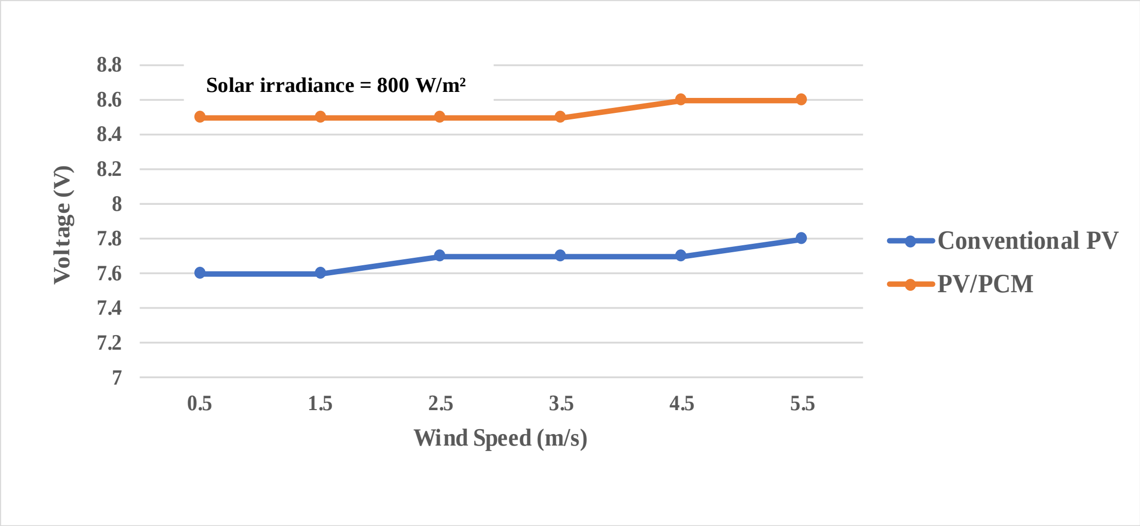

Fig. 4.39. Wind speed versus output voltage for PV panels without and with organic PCM (Solar irradiance = 800 W/m²)

Figure 4.40 shows the output voltage evolutions for PV and PV-PCM systems with solar irradiation = 600 W/m². Due to the combined effects of high wind speed and PCM's ability to dissipate heat, the output voltage variation between the conventional PV and PV-PCM systems at a wind speed of 5.5 m/s remained 33.3% higher than that between the conventional PV and PV-PCM systems at a wind speed of 0.5 m/s.

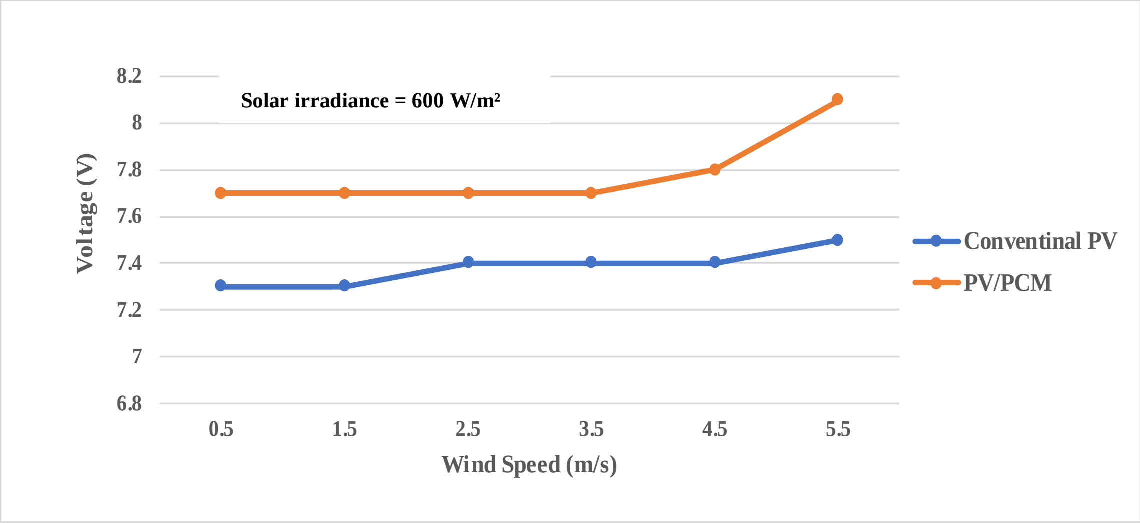

Fig. 4.40. Wind speed versus output voltage for PV panels without and with organic PCM (Solar irradiance = 600 W/m²)

Figure 4.41 shows the output voltage evolutions for PV and PV-PCM systems with solar irradiation = 400 W/m². Due to the combined effects of high wind speed and PCM's ability to dissipate heat, the output voltage variation between the conventional PV and PV-PCM systems at a wind speed of 5.5 m/s remained 33.3% higher than that between the conventional PV and PV-PCM systems at a wind speed of 0.5 m/s.

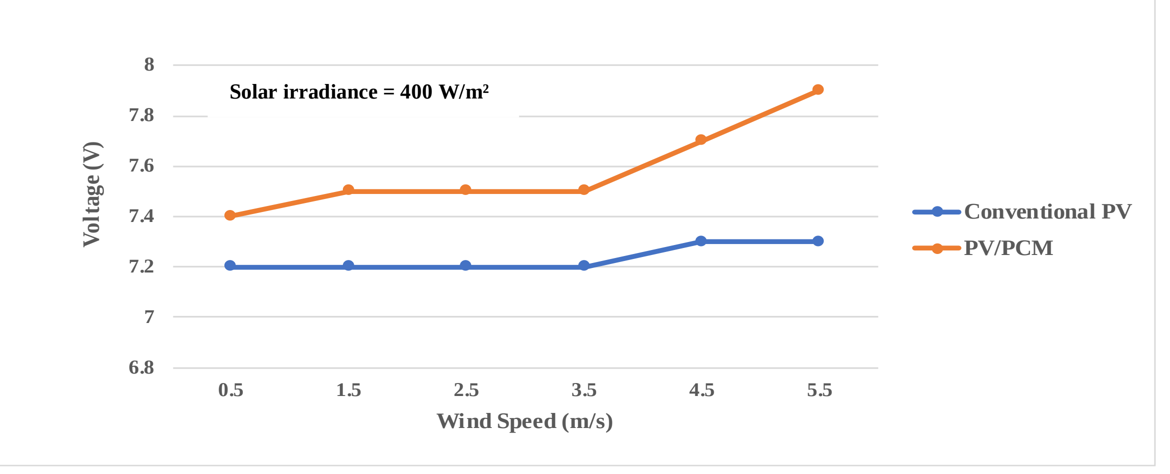

Fig. 4.41. Wind speed versus output voltage for PV panels without and with organic PCM (Solar irradiance = 400 W/m²)

Figure 4.42 shows the output voltage evolutions for PV and PV-PCM systems with solar irradiation = 200 W/m². Due to the combined effects of high wind speed and PCM's ability to dissipate heat, the output voltage variation between the conventional PV and PV-PCM systems at a wind speed of 5.5 m/s remained 13.73% higher than that between the conventional PV and PV-PCM systems at a wind speed of 0.5 m/s.

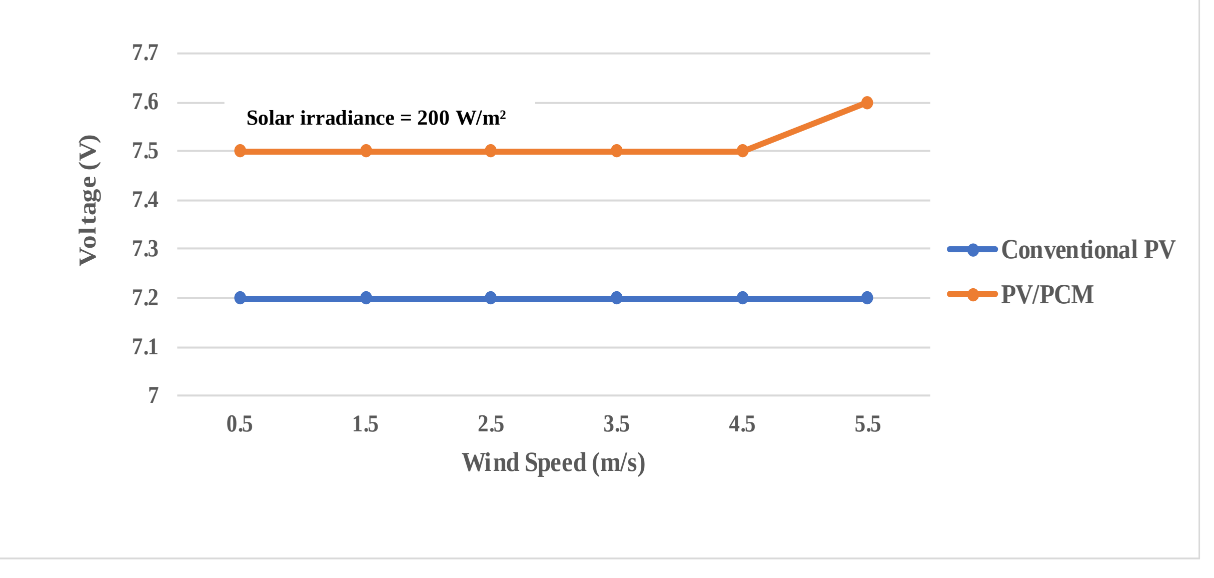

Fig. 4.42. Wind speed versus output voltage for PV panels without and with organic PCM (Solar irradiance = 200 W/m²)

4.2.2.4 Effect of wind speed on power

The output power evolutions for PV and PV-PCM systems are shown in Fig. 4.43 for solar irradiance = 1000 W/m². Due to the combined effects of high wind speed and PCM's ability to dissipate heat, the output power variation between conventional PV and PV-PCM systems at a wind speed of 5.5 m/s remained 52.4% higher than that between conventional PV and PV-PCM systems at a wind speed of 0.5 m/s.

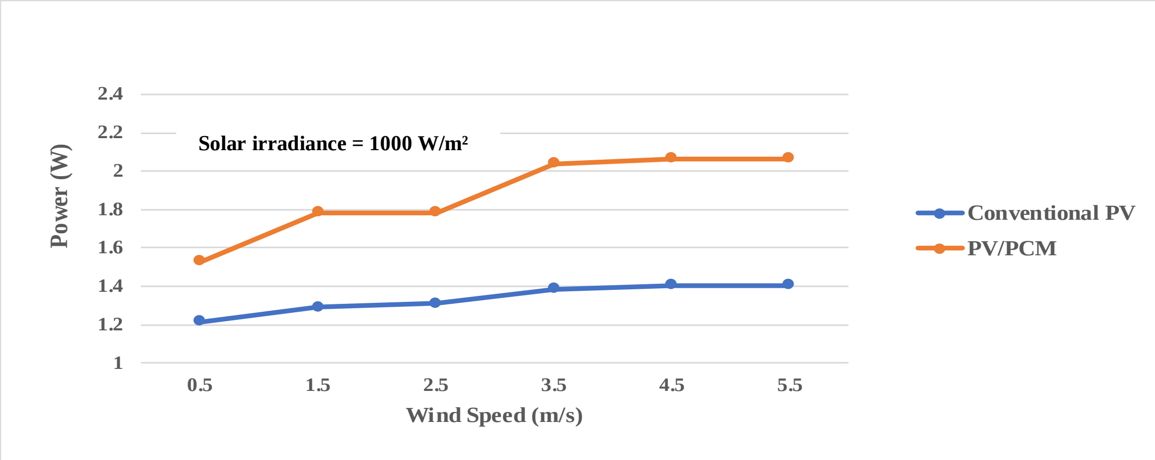

Fig. 4.43. Wind speed versus output power for PV panels without and with organic PCM (Solar irradiance = 1000 W/m²)

The output power evolutions for PV and PV-PCM systems are shown in Fig. 4.44 for solar irradiance = 800 W/m². Due to the combined effects of high wind speed and PCM's ability to dissipate heat, the output power variation between conventional PV and PV-PCM systems at a wind speed of 5.5 m/s remained 52.4% higher than that between conventional PV and PV-PCM systems at a wind speed of 0.5 m/s.

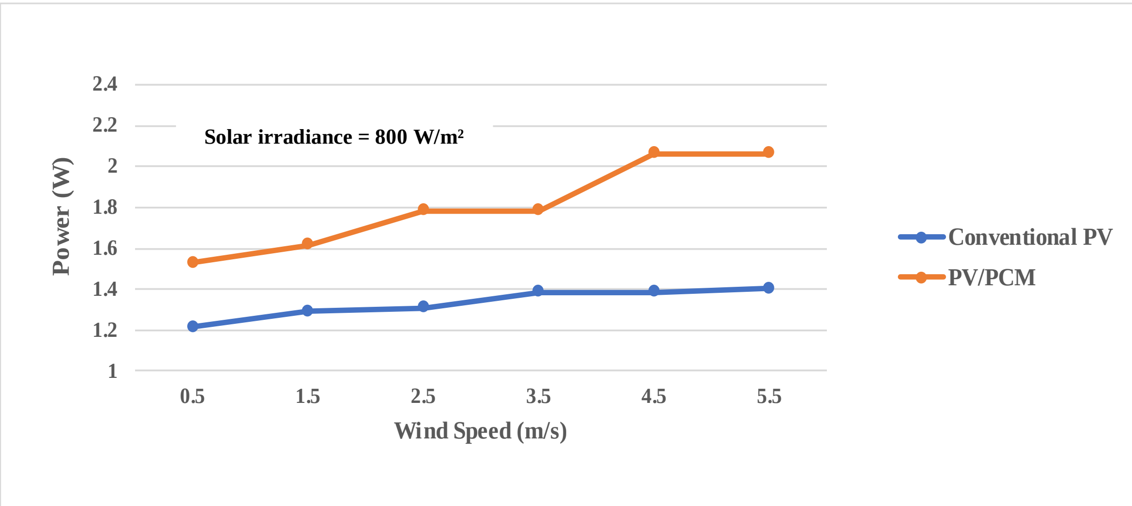

Fig. 4.44. Wind speed versus output power for PV panels without and with organic PCM (Solar irradiance = 800 W/m²)

The output power evolutions for PV and PV-PCM configurations are shown in Fig. 4.45 for solar irradiance = 600 W/m². Due to the combined effects of high wind speed and PCM's ability to dissipate heat, the output power variation between conventional PV and PV-PCM systems at a wind speed of 5.5 m/s remained 40% greater than that between conventional PV and PV-PCM systems at a wind speed of 0.5 m/s.

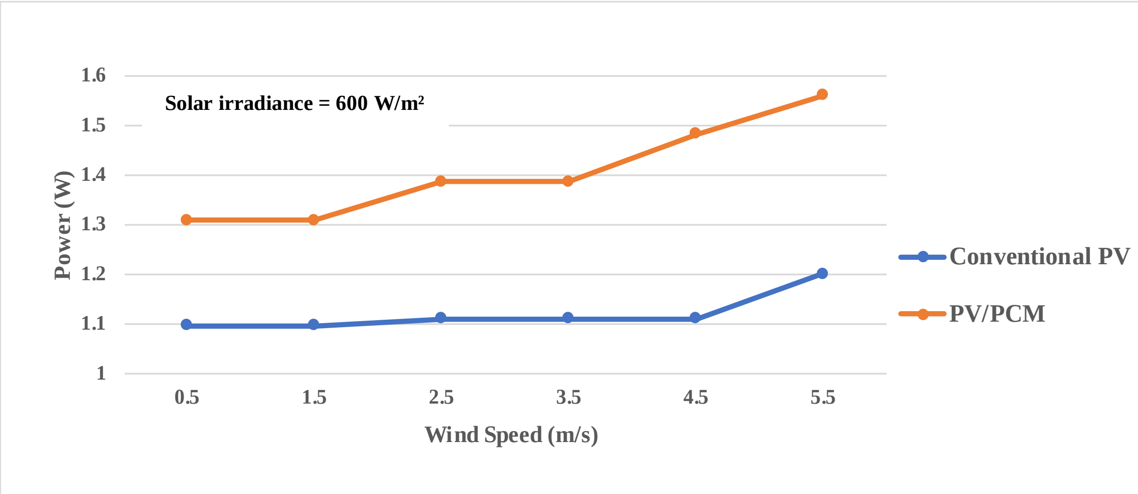

Fig. 4.45. Wind speed versus output power for PV panels without and with organic PCM (Solar irradiance = 600 W/m²)

The output power evolutions for PV and PV-PCM configurations are shown in Fig. 4.46 for solar irradiance = 400 W/m². Due to the combined effects of high wind speed and PCM's ability to dissipate heat, the output power variation between conventional PV and PV-PCM systems at a wind speed of 5.5 m/s remained 31% higher than that between conventional PV and PV-PCM systems at a wind speed of 0.5 m/s.

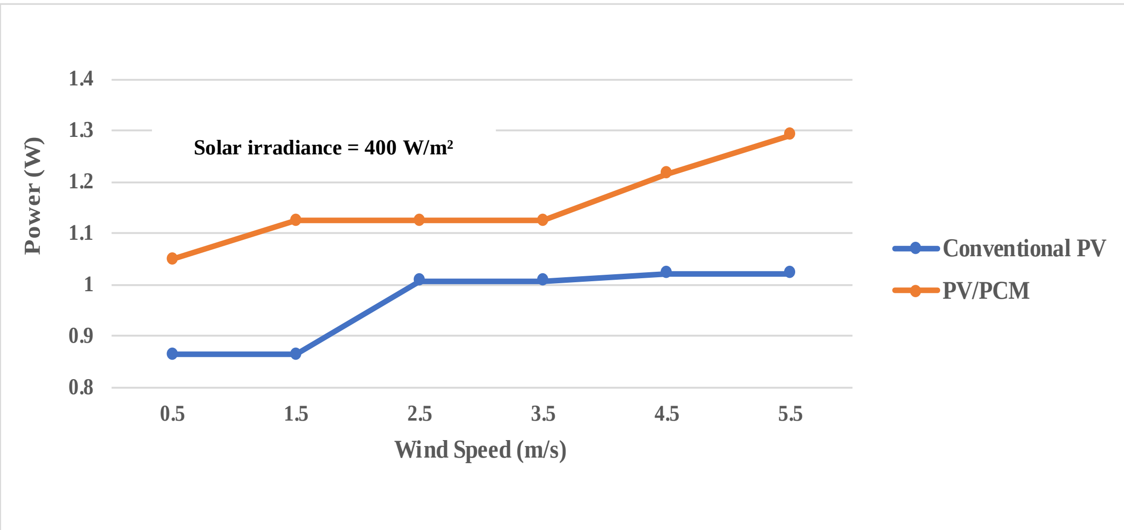

Fig. 4.46. Wind speed versus output power for PV panels without and with organic PCM (Solar irradiance = 400 W/m²)

The output power evolutions for PV and PV-PCM configurations are shown in Fig. 4.47 for solar irradiance = 200 W/m². Due to the combined effects of high wind speed and PCM's ability to dissipate heat, the output power variation between conventional PV and PV-PCM systems at a wind speed of 5.5 m/s remained 10.5% higher than that between conventional PV and PV-PCM systems at a wind speed of 0.5 m/s.

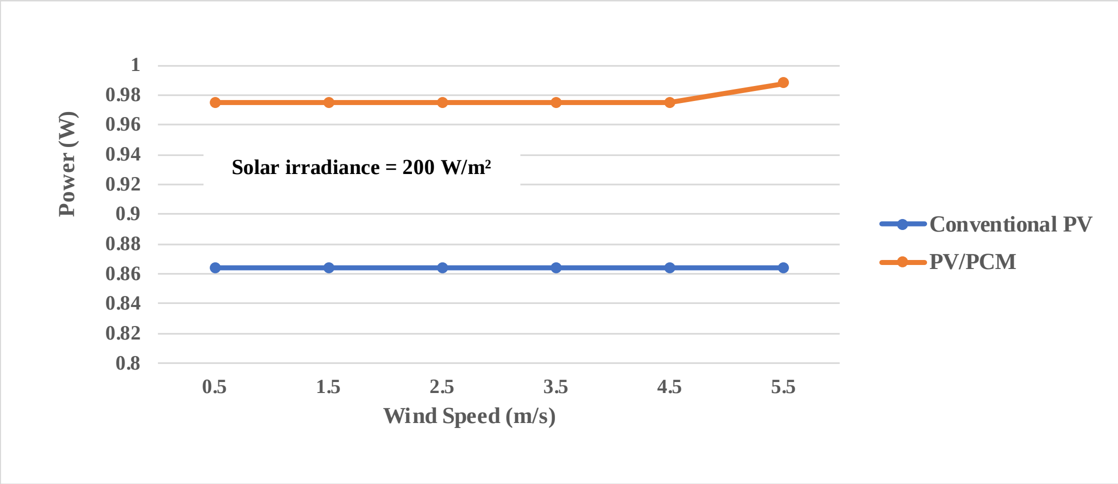

Fig. 4.47. Wind speed versus output power for PV panels without and with organic PCM (Solar irradiance = 200 W/m²)

4.2.3 Effect of solar radiation intensity on thermal and electrical performance of PV module by using inorganic PCM

4.2.3.1 Effect of solar radiation intensity on PV cell temperature

The solar cell temperature evolutions for PV and PV-PCM setups are shown in Fig. 4.48 for wind speed = 5.5 m/s. Because PCM functions as a thermal dissipation system, the surface temperature of the PV-PCM system stayed lower than that of the conventional PV, and this tendency has persisted for all solar irradiance values. The PV panel without PCM has a maximum working temperature of 35.4°C and a minimum operating temperature of 26.9°C. In addition, the PV panel without PCM operates at an average temperature of 30.6°C. However, the PV panel with PCM appears to have a maximum working temperature of 30.4°C and a minimum operating temperature of 23.3°C. Furthermore, PV panels with PCM operate at an average temperature of 25.5°C. The PV panel with PCM can be 5.1°C cooler than the PV panel without PCM when the two panels are compared. It has been demonstrated that the performance of PV panels can be impacted by the use of PCM.

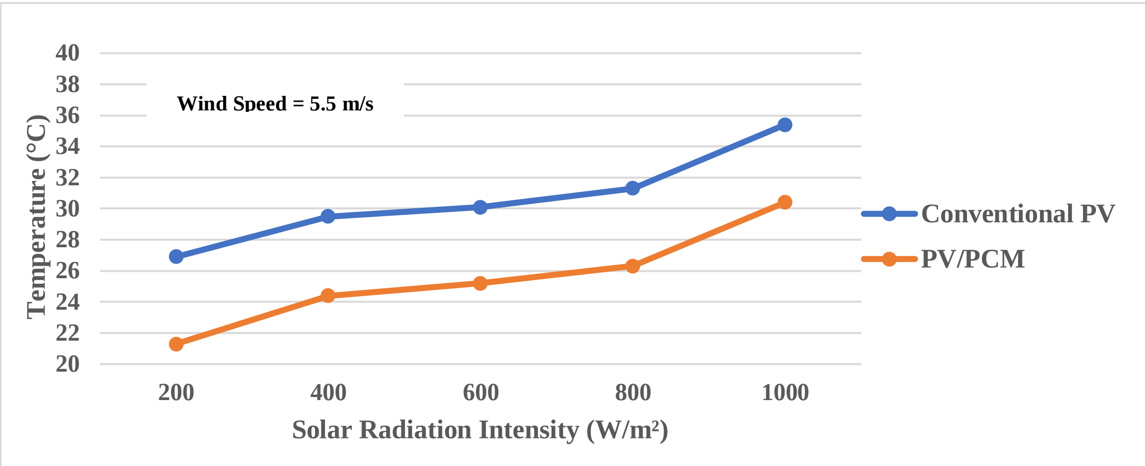

Fig. 4.48. Solar irradiance versus operating temperature for PV panels without and with inorganic PCM (Wind speed = 5.5 m/s)

The solar cell temperature evolutions for PV and PV-PCM setups are shown in Fig. 4.49 for wind speed = 4.5 m/s. Because PCM functions as a thermal dissipation system, the surface temperature of the PV-PCM system stayed lower than that of the conventional PV, and this tendency has persisted for all solar irradiance values. The PV panel without PCM has a maximum working temperature of 37.1°C and a minimum operating temperature of 29.1°C. In addition, the PV panel without PCM operates at an average temperature of 32.6°C. However, the PV panel with PCM appears to have a maximum operating temperature of 32.2°C and a minimum operating temperature of 24.1°C. Furthermore, a PV panel with PCM operates at an average temperature of 27.6°C. The PV panel with PCM can be 5°C cooler than the PV panel without PCM when the two panels are compared. It has been demonstrated that the performance of PV panels can be impacted by the use of PCM.

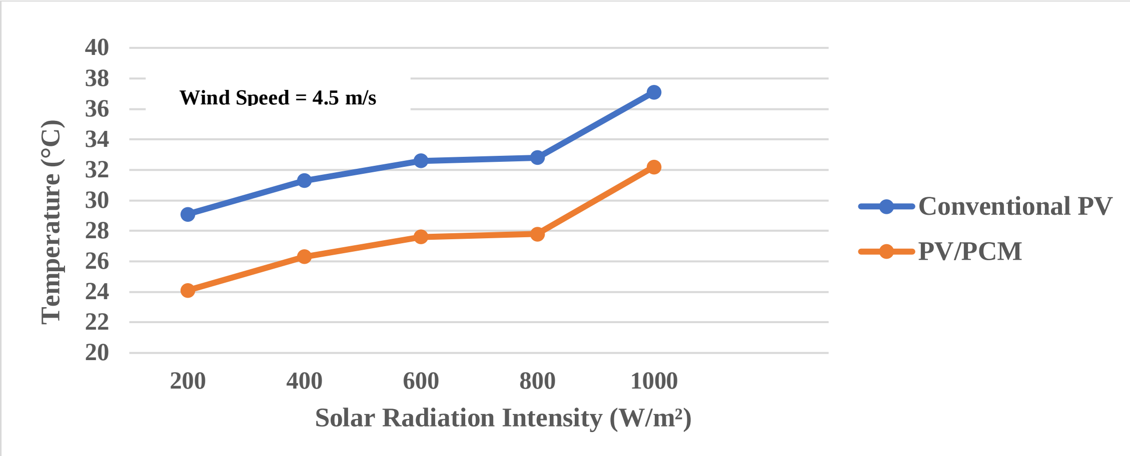

Fig. 4.49. Solar irradiance versus operating temperature for PV panels without and with inorganic PCM (Wind speed = 4.5 m/s)

The solar cell temperature evolutions for PV and PV-PCM setups are shown in Fig. 4.50 for wind speed = 3.5 m/s. Because PCM functions as a thermal dissipation system, the surface temperature of the PV-PCM system stayed lower than that of the conventional PV, and this tendency has persisted for all solar irradiance values. The PV panel without PCM may attain its maximum working temperature of 45.2°C and its minimum operating temperature of 33.2°C. In addition, the PV panel without PCM operates at an average temperature of 37.08°C. However, the PV panel with PCM appears to have a maximum operating temperature of 41.2°C and a minimum operating temperature of 28.5°C. Furthermore, PV panels with PCM have an average operating temperature of 32.98°C. When comparing the two PV panels, the PCM-equipped panel may lower its temperature by 4.1°C. It has been demonstrated that the performance of PV panels can be impacted by the use of PCM.

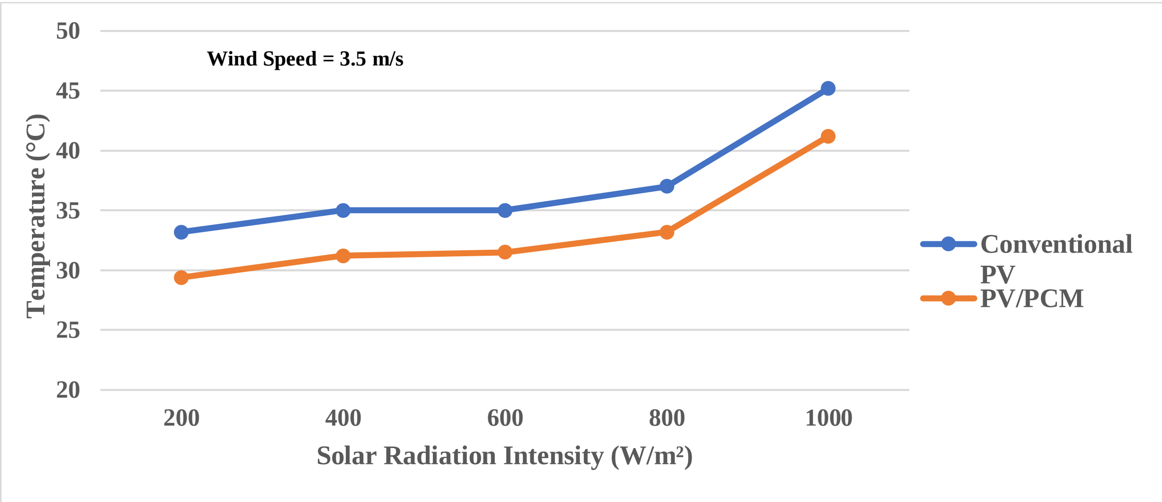

Fig. 4.50. Solar irradiance versus operating temperature for PV panels without and with inorganic PCM (Wind speed = 3.5 m/s)

The solar cell temperature evolutions for PV and PV-PCM setups are shown in Fig. 4.51 with wind speed = 2.5 m/s. Because PCM functions as a thermal dissipation system, the surface temperature of the PV-PCM system stayed lower than that of the conventional PV, and this tendency has persisted for all solar irradiance values. The PV panel without PCM operates at a maximum temperature of 54.7°C and a minimum temperature of 35.2°C. In addition, the PV panel without PCM operates at an average temperature of 43.6°C. However, the PV panel with PCM appears to have a maximum working temperature of 50.7°C and a minimum operating temperature of 31.2°C. Furthermore, PV panels with PCM have an average operating temperature of 39.6°C. The PV panel with PCM can be 4°C cooler than the PV panel without PCM when the two panels are compared. It has been demonstrated that the performance of PV panels can be impacted by the use of PCM.

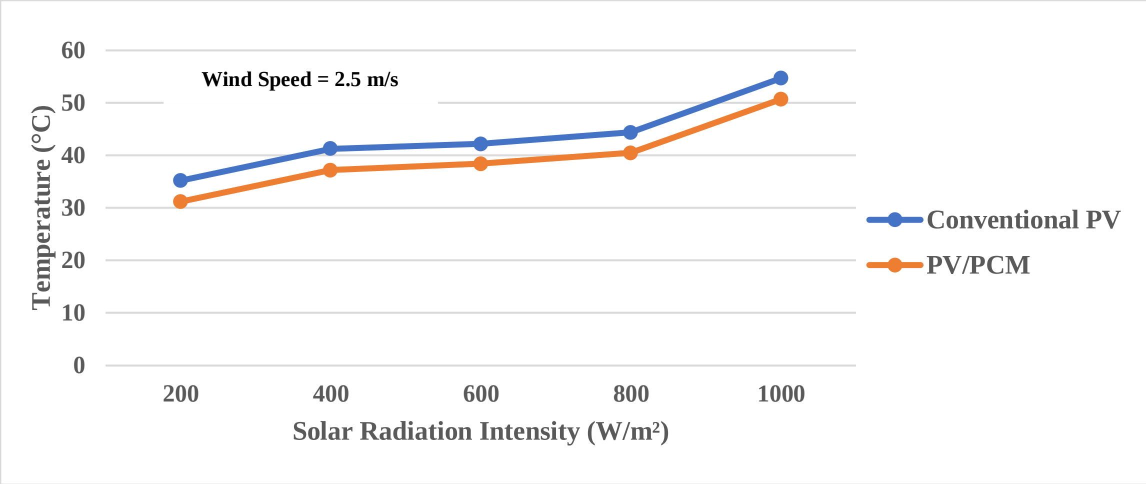

Fig. 4.51. Solar irradiance versus operating temperature for PV panels without and with inorganic PCM (Wind speed = 2.5 m/s)

The solar cell temperature evolutions for PV and PV-PCM setups are shown in Fig. 4.52 with wind speed = 1.5 m/s. Because PCM functions as a thermal dissipation system, the surface temperature of the PV-PCM system stayed lower than that of the conventional PV, and this tendency has persisted for all solar irradiance values. The PV panel without PCM has a maximum working temperature of 62°C and a minimum operating temperature of 39.6°C. In addition, the PV panel without PCM operates at an average temperature of 48.4°C. However, the PV panel with PCM appears to have a maximum working temperature of 59°C and a minimum operating temperature of 35.7°C. Furthermore, a PV panel with PCM operates at an average temperature of 45.5°C. The PV panel with PCM can be 3°C cooler than the PV panel without PCM when the two panels are compared. It has been demonstrated that the performance of PV panels can be impacted by the use of PCM.

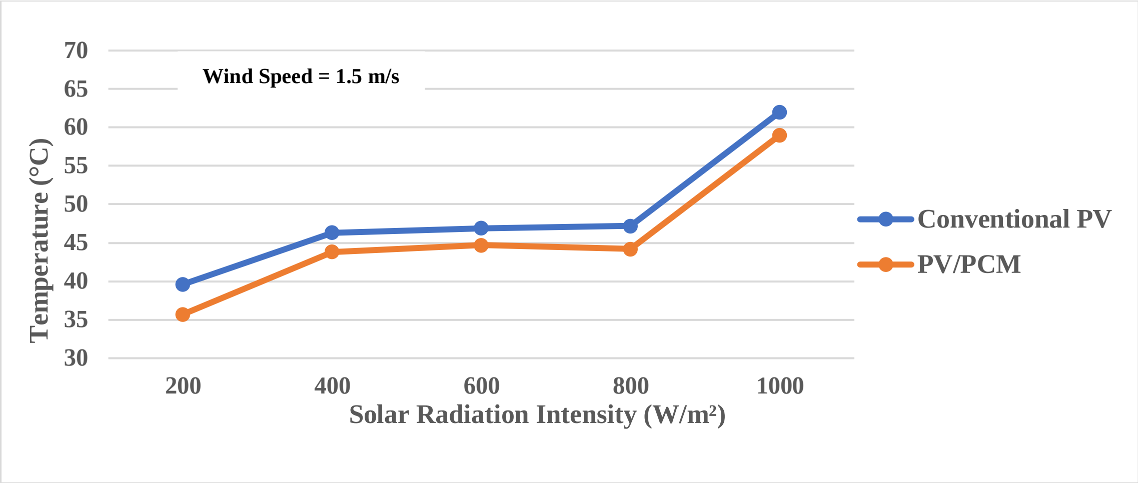

Fig. 4.52. Solar irradiance versus operating temperature for PV panels without and with inorganic PCM (Wind speed = 1.5 m/s)

The solar cell temperature evolutions for PV and PV-PCM setups are shown in Fig. 4.53 with wind speed = 0.5 m/s. Because PCM functions as a thermal dissipation system, the surface temperature of the PV-PCM system stayed lower than that of the conventional PV, and this tendency has persisted for all solar irradiance values. The PV panel without PCM may operate at a maximum temperature of 66.7°C and a minimum temperature of 42°C. In addition, the PV panel without PCM operates at an average temperature of 52°C. However, the PV panel with PCM appears to have a maximum working temperature of 64.2°C and a minimum operating temperature of 39.8°C. Furthermore, PV panels with PCM have an average working temperature of 49.8°C. The PV panel with PCM can be 2.2°C cooler than the PV panel without PCM when the two panels are compared. It has been demonstrated that the performance of PV panels can be impacted by the use of PCM.

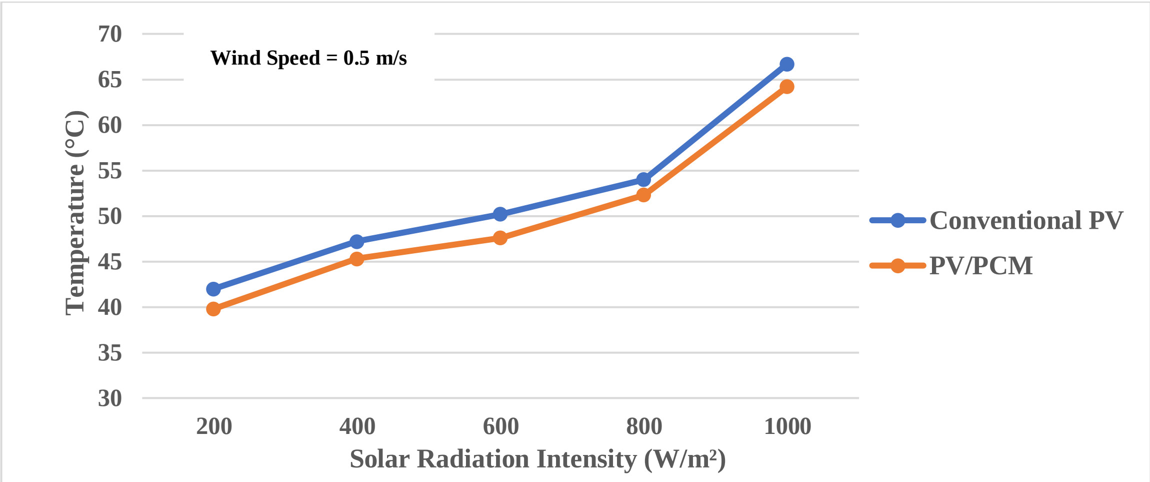

Fig. 4.53. Solar irradiance versus operating temperature for PV panels without and with inorganic PCM (Wind speed = 0.5 m/s)

4.2.3.2 Effect of solar radiation intensity on output current

Figure 4.54 shows the output current comparison between PV panels with and without PCM for wind speed = 5.5 m/s. When compared to a PV panel without PCM, the PV panel with PCM may deliver the maximum output current. The PV panel without PCM has a minimum output current of 0.12 A and a maximum output current of 0.18 A. Furthermore, the average output current of the PV panel without PCM was 0.16 A. At the same time, the PV panel with PCM produces an average output current of 0.22 A, with maximum and minimum output currents of 0.26 A and 0.18 A, respectively. The output current of the PV panel with PCM is 27.3% higher than that of the PV panel without PCM when compared to these two PV panels.

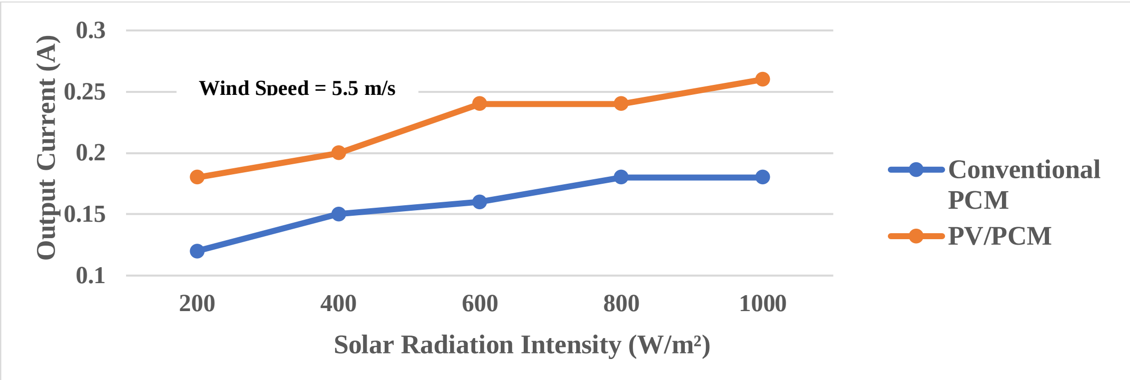

Fig. 4.54. Solar irradiance versus output current for PV panels without and with inorganic PCM (Wind speed = 5.5 m/s)

Figure 4.55 shows the output current comparison between PV panels with and without PCM for wind speed = 4.5 m/s. When compared to a PV panel without PCM, the PV panel with PCM may deliver the maximum output current. The PV panel without PCM has a minimum output current of 0.12 A and a maximum output current of 0.18 A. Furthermore, the average output current of the PV panel without PCM was 0.16 A. At the same time, the PV panel with PCM produces an average output current of 0.22 A, with maximum and minimum output currents of 0.26 A and 0.18 A, respectively. The output current of the PV panel with PCM is 27.3% higher than that of the PV panel without PCM when compared to these two PV panels.

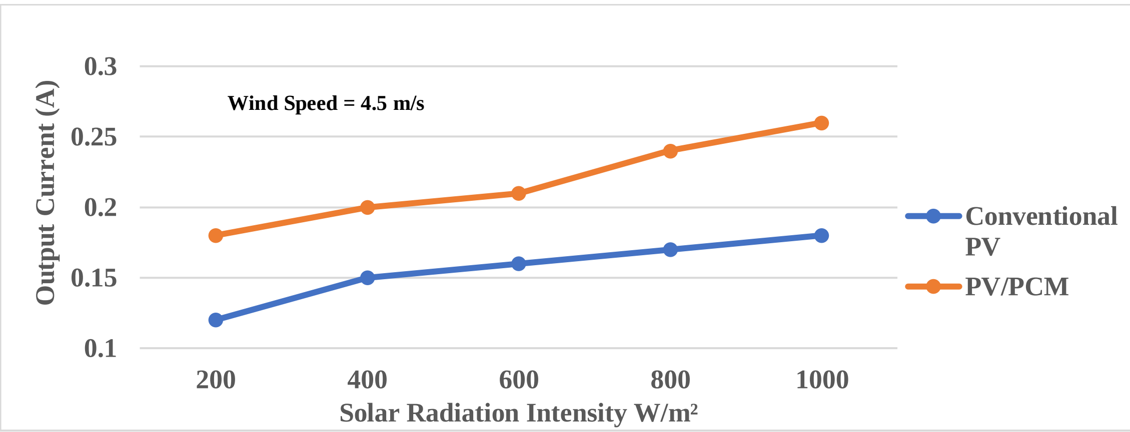

Fig. 4.55. Solar irradiance versus output current for PV panels without and with inorganic PCM (Wind speed = 4.5 m/s)

Figure 4.56 shows the output current comparison between PV panels with and without PCM for wind speed = 3.5 m/s. When compared to a PV panel without PCM, the PV panel with PCM may deliver the maximum output current. The PV panel without PCM has a minimum output current of 0.12 A and a maximum output current of 0.18 A. Furthermore, the average output current of the PV panel without PCM was 0.15 A. At the same time, the PV panel with PCM produces an average output current of 0.20 A, with maximum and minimum output currents of 0.26 A and 0.14 A, respectively. The PV panel with PCM has a 25% higher output current than the PV panel without PCM when compared to these two PV panels.

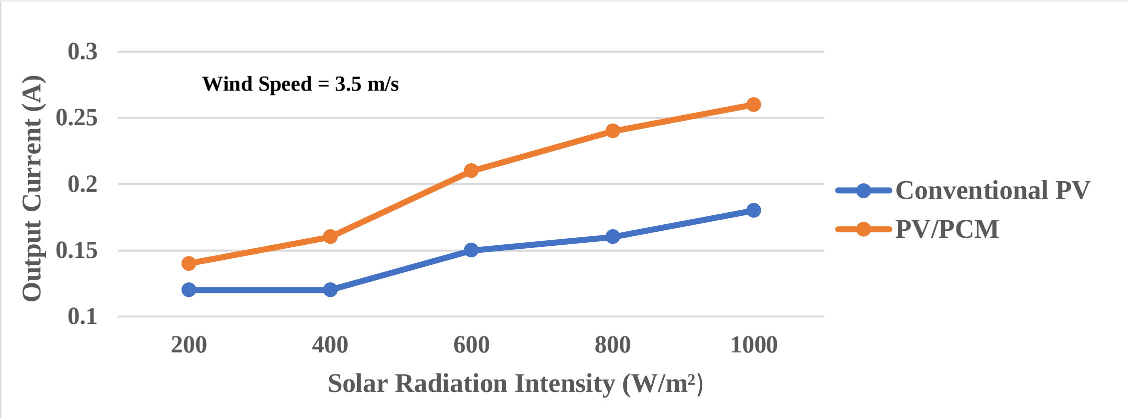

Fig. 4.56. Solar irradiance versus output current for PV panels without and with inorganic PCM (Wind speed = 3.5 m/s)

Figure 4.57 shows the output current comparison between PV panels with and without PCM for wind speed = 2.5 m/s. When compared to a PV panel without PCM, the PV panel with PCM may deliver the maximum output current. The PV panel without PCM has a minimum output current of 0.12 A and a maximum output current of 0.17 A. Furthermore, the average output current of the PV panel without PCM was 0.15 A. At the same time, the PV panel with PCM produces an average output current of 0.19 A, with maximum and minimum output currents of 0.24 A and 0.13 A, respectively. The PV panel with PCM has a 21.1% higher output current than the PV panel without PCM when compared to these two PV panels.

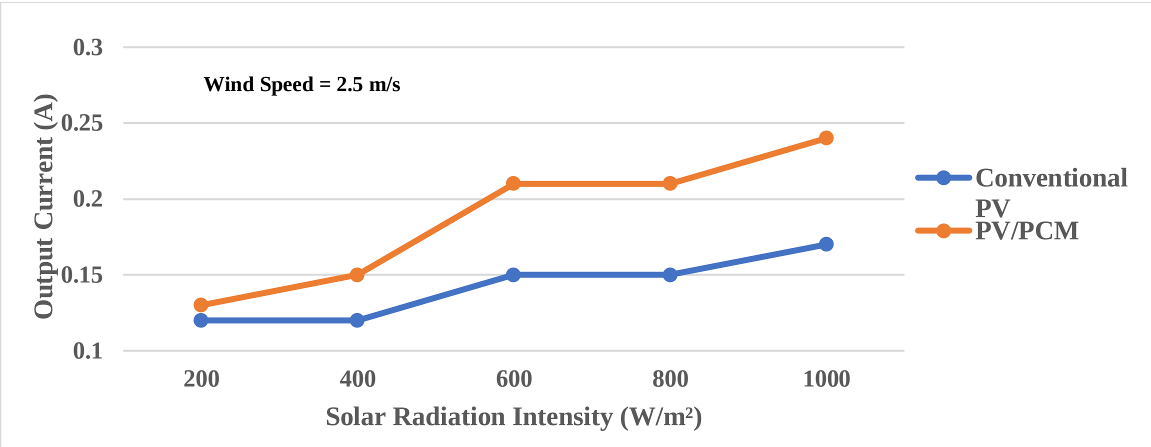

Fig. 4.57. Solar irradiance versus output current for PV panels without and with inorganic PCM (Wind speed = 2.5 m/s)

Figure 4.58 shows the output current of PV panels with and without PCM at a wind speed of 1.5 m/s. When compared to a PV panel without PCM, the PV panel with PCM may deliver the maximum output current. The PV panel without PCM has a minimum output current of 0.11 A and a maximum output current of 0.15 A. Furthermore, the average output current of the PV panel without PCM was 0.13 A. At the same time, the PV panel with PCM produces an average output current of 0.17 A, with maximum and minimum output currents of 0.21 A and 0.13 A, respectively. The PV panel with PCM has a 21.1% higher output current than the PV panel without PCM when compared to these two PV panels.

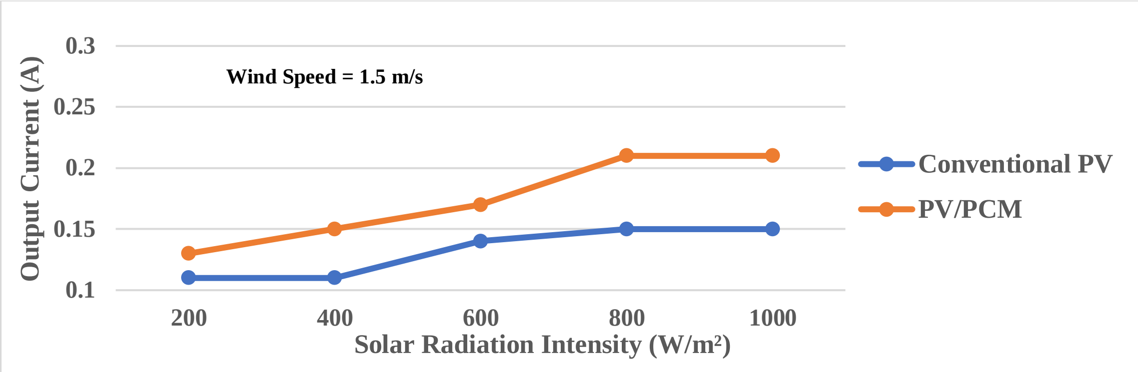

Fig. 4.58. Solar irradiance versus output current for PV panels without and with inorganic PCM (Wind speed = 1.5 m/s)

Figure 4.59 shows the output current comparison between PV panels with and without PCM for wind speed = 0.5 m/s. When compared to a PV panel without PCM, the PV panel with PCM may deliver the maximum output current. The PV panel without PCM has a minimum output current of 0.11 A and a maximum output current of 0.15 A. Furthermore, the average output current of the PV panel without PCM was 0.13 A. At the same time, the PV panel with PCM produces an average output current of 0.16 A, with maximum and minimum output currents of 0.21 A and 0.13 A, respectively. The output current of the PV panel with PCM is 18.75% higher than that of the PV panel without PCM when compared to these two PV panels.

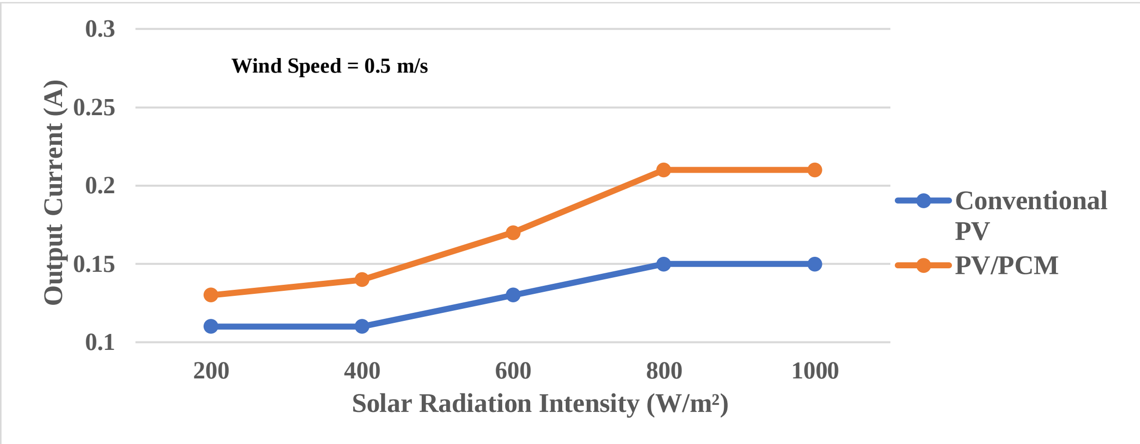

Fig. 4.59. Solar irradiance versus output current for PV panels without and with inorganic PCM (Wind speed = 0.5 m/s)

4.2.3.3 Effect of solar radiation intensity on voltage

The output voltage fluctuation produced by PV panels with and without PCM when the wind speed reaches 5.5 m/s is depicted in Fig. 4.60. It is evident that compared to a PV panel without PCM, one with PCM can yield a higher output voltage. PV panels without PCM have a maximum output voltage of 7.8 V and a minimum output voltage of 7.1 V. Meanwhile, a PV panel without PCM achieves an average output voltage of 7.4 V. Conversely, a PV panel with PCM can provide a maximum output voltage of 8.8 V and a minimum output voltage of 8.2 V. Additionally, the average output voltage of the PV panel with PCM is 8.4 V. The PV panel with PCM can create 11.9% more output voltage than the PV panel without PCM when these two panels are compared. It is evident that a PV panel with a low operating temperature can produce a higher output voltage.

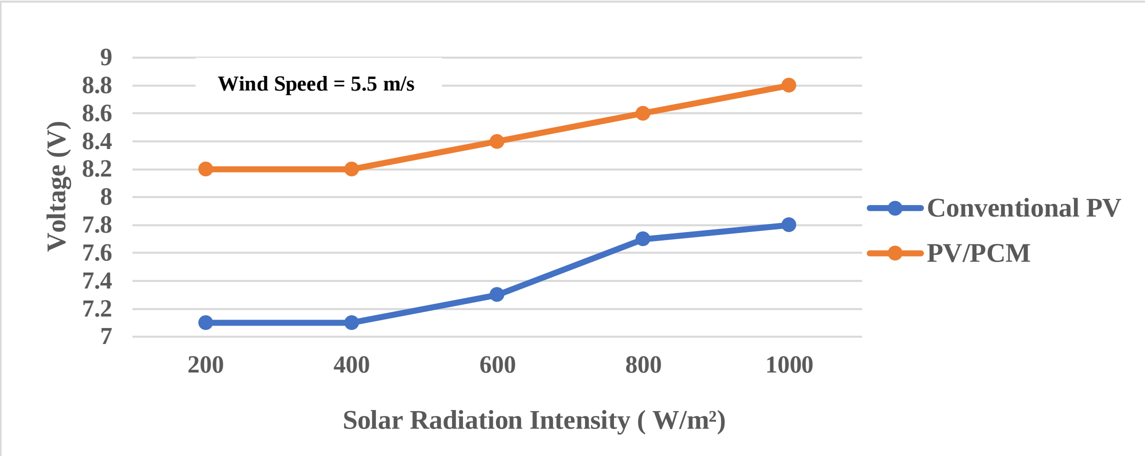

Fig. 4.60. Solar irradiance versus output voltage for PV panels without and with inorganic PCM (Wind speed = 5.5 m/s)

The output voltage fluctuation produced by PV panels with and without PCM when the wind speed reaches 4.5 m/s is depicted in Fig. 4.61. The ability of the PV panel with PCM to provide higher output voltage than the PV panel without PCM is evident. PV panels without PCM have a maximum output voltage of 7.7 V and a minimum output voltage of 7.1 V. Meanwhile, a PV panel without PCM achieves an average output voltage of 7.4 V. Conversely, a PV panel with PCM can provide a maximum output voltage of 8.8 V and a minimum output voltage of 8.2 V. Additionally, the average output voltage of the PV panel with PCM is 8.4 V. The PV panel with PCM can create 11.9% more output voltage than the PV panel without PCM when these two panels are compared. It is evident that a PV panel with a low operating temperature can produce a higher output voltage.

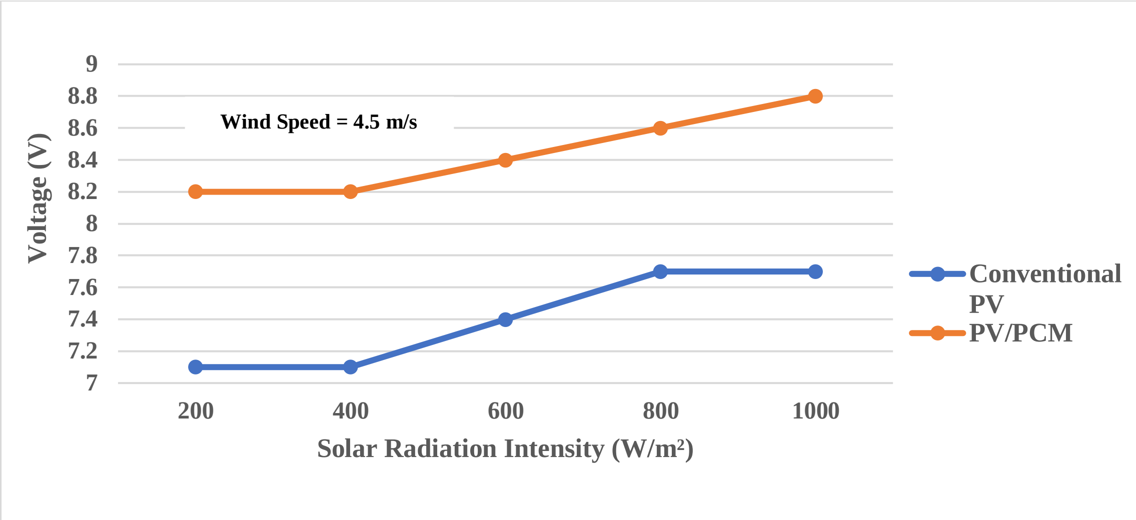

Fig. 4.61. Solar irradiance versus output voltage for PV panels without and with inorganic PCM (Wind speed = 4.5 m/s)

When the wind speed reaches 3.5 m/s, Figure 4.62 illustrates the difference in output voltage produced by PV panels with and without PCM. It is evident that compared to a PV panel without PCM, one with PCM can yield a higher output voltage. PV panels without PCM have a maximum output voltage of 7.8 V and a minimum output voltage of 7.1 V. Meanwhile, a PV panel without PCM achieves an average output voltage of 7.4 V. Conversely, a PV panel with PCM can generate a minimum output voltage of 8 V and a maximum output voltage of 8.4 V. Additionally, the average output voltage of the PV panel with PCM is 8.2 V. The PV panel with PCM can create 9.76% more output voltage than the PV panel without PCM when these two panels are compared. It is evident that a PV panel with a low operating temperature can produce a higher output voltage.

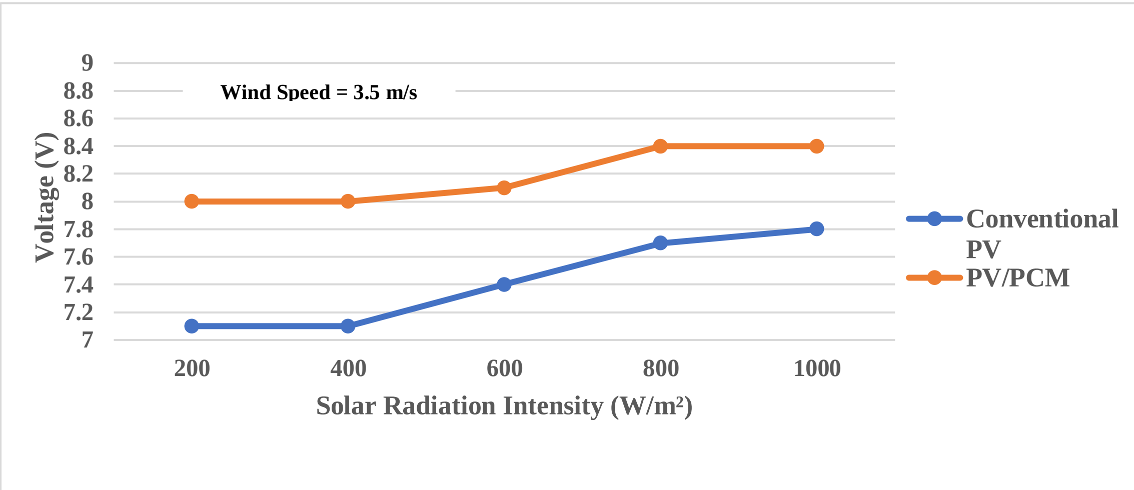

Fig. 4.62. Solar irradiance versus output voltage for PV panels without and with inorganic PCM (Wind speed = 3.5 m/s)

The output voltage fluctuation produced by PV panels with and without PCM when the wind speed reaches 2.5 m/s is depicted in Fig. 4.63. It is evident that compared to a PV panel without PCM, one with PCM can yield a higher output voltage. PV panels without PCM have a maximum output voltage of 7.8 V and a minimum output voltage of 7.1 V. Meanwhile, a PV panel without PCM achieves an average output voltage of 7.4 V. Conversely, a PV panel with PCM can generate a minimum output voltage of 8 V and a maximum output voltage of 8.4 V. Additionally, the average output voltage of the PV panel with PCM is 8.2 V. The PV panel with PCM can create 9.76% more output voltage than the PV panel without PCM when these two panels are compared. It is evident that a PV panel with a low operating temperature can produce a higher output voltage.

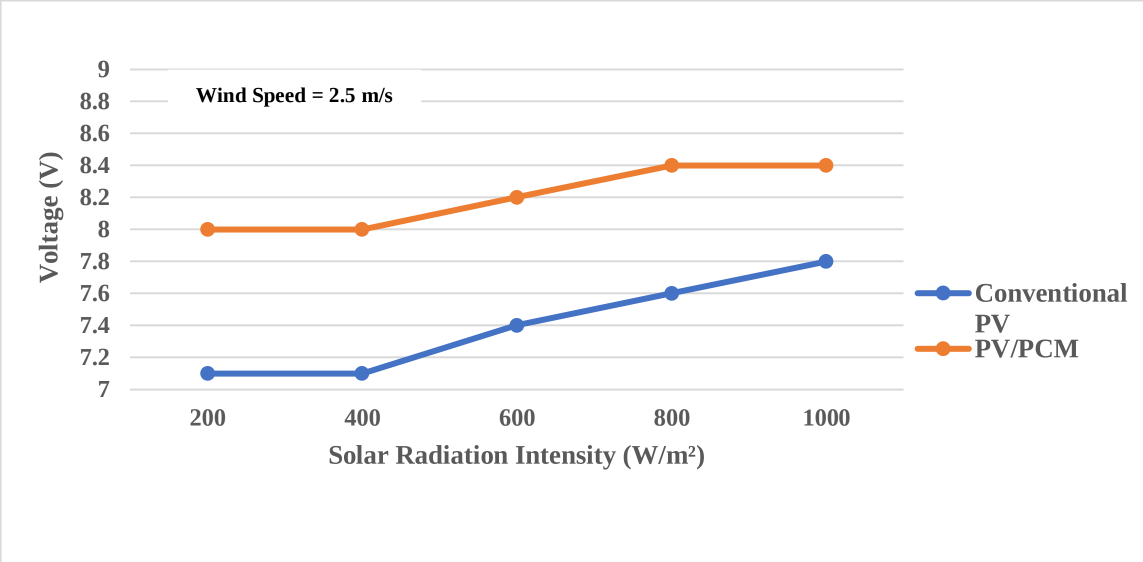

Fig. 4.63. Solar irradiance versus output voltage for PV panels without and with inorganic PCM (Wind speed = 2.5 m/s)

When the wind speed reaches 1.5 m/s, Figure 4.64 illustrates the difference in output voltage produced by PV panels with and without PCM. It is evident that compared to a PV panel without PCM, one with PCM can yield a higher output voltage. PV panels without PCM have a maximum output voltage of 7.7 V and a minimum output voltage of 7 V. Meanwhile, a PV panel without PCM achieves an average output voltage of 7.3 V. However, a PV panel with PCM can provide a minimum output voltage of 7.5 V and a maximum output voltage of 8.5 V. In addition, the average output voltage of the PV panel with PCM is 7.8 V. The PV panel with PCM can create 6.4% more output voltage than the PV panel without PCM when these two panels are compared. It is evident that a PV panel with a low operating temperature can produce a higher output voltage.

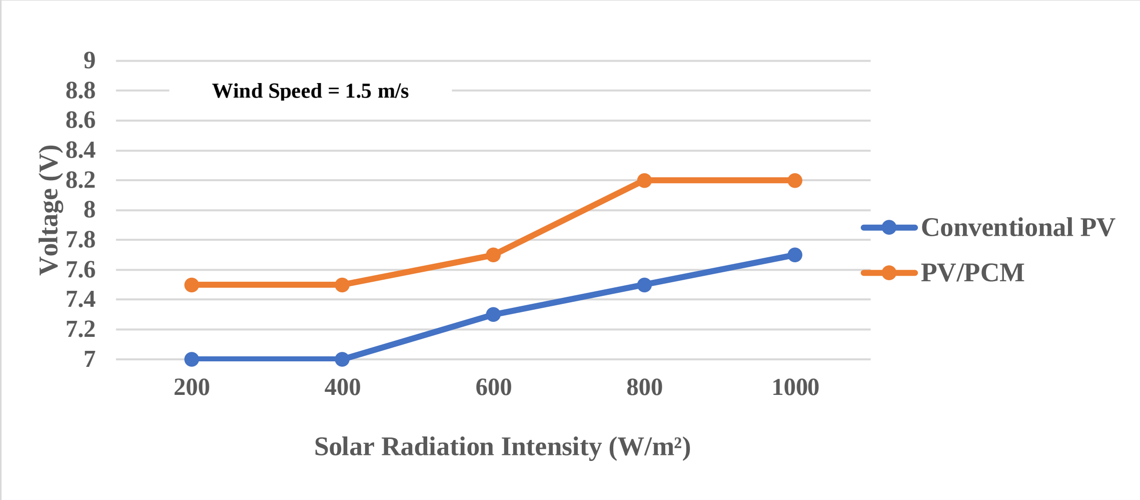

Fig. 4.64. Solar irradiance versus output voltage for PV panels without and with inorganic PCM (Wind speed = 1.5 m/s)

When the wind speed reaches 0.5 m/s, Figure 4.65 illustrates the difference in output voltage produced by PV panels with and without PCM. The ability of the PV panel with PCM to provide higher output voltage than the PV panel without PCM is evident. PV panels without PCM have a maximum output voltage of 7.7 V and a minimum output voltage of 7 V. Meanwhile, a PV panel without PCM achieves an average output voltage of 7.3 V. Conversely, a PV panel with PCM can provide a maximum output voltage of 8.2 V and a minimum output voltage of 7.2 V. Additionally, the average output voltage of the PV panel with PCM is 7.7 V. The PV panel with PCM can create 6.4% more output voltage than the PV panel without PCM when these two panels are compared. It is evident that a PV panel with a low operating temperature can produce a higher output voltage.

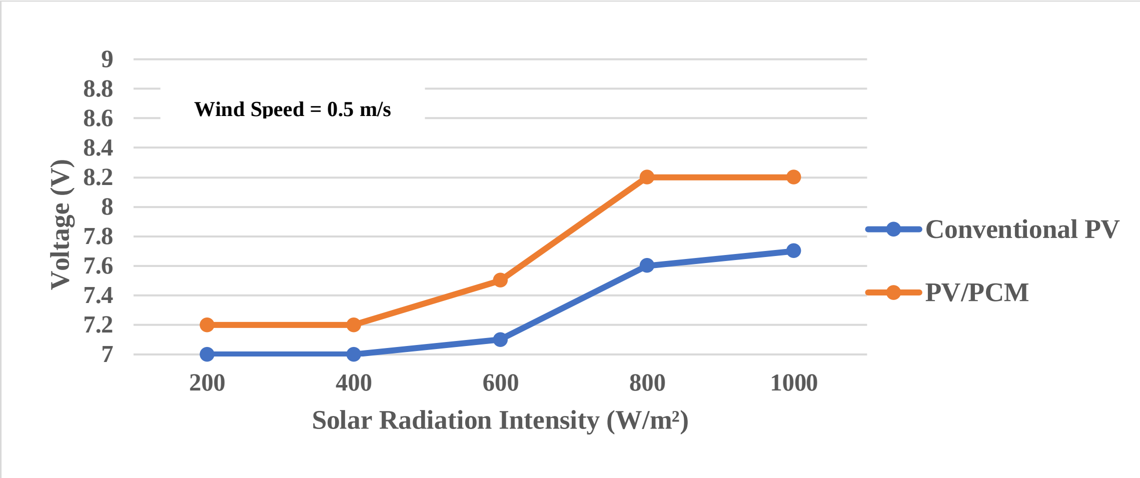

Fig. 4.65. Solar irradiance versus output voltage for PV panels without and with inorganic PCM (Wind speed = 0.5 m/s)

4.2.3.4 Effect of solar radiation intensity on power

The output power produced by the two PV panels is compared in Fig. 4.66 when the wind speed reaches 5.5 m/s. The maximum output power of a PV panel without PCM is 1.404 W. However, 0.852 W is the minimal output power. However, the PV panel with PCM has a minimum output power of 1.476 W and a maximum output power of 2.288 W. PV panels with PCM and those without PCM have respective average output powers of 1.897 W and 1.175 W. It is obvious that PV panel with PCM can be produced higher output power than the PV panel without PCM. The use of PV panels with PCM results in a 38.06% increase in output power per unit of electricity.

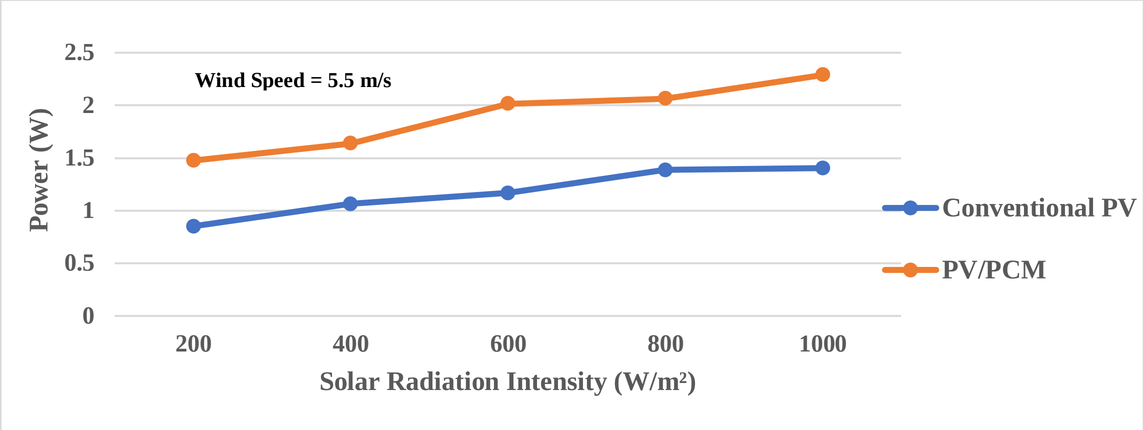

Fig. 4.66. Solar irradiance versus output power for PV panels without and with inorganic PCM (Wind speed = 5.5 m/s)

When the wind speed reaches 4.5 m/s, the output power produced by the two PV panels is compared in Fig. 4.67. The maximum output power of a PV panel without PCM is 1.386 W. whereas 0.852 W is the lowest output power. However, the PV panel with PCM has a minimum output power of 1.476 W and a maximum output power of 2.288 W. PV panels with PCM and those without PCM had respective average output powers of 1.846 W and 1.16 W. It is obvious that PV panel with PCM can be produced higher output power than the PV panel without PCM. The use of PV panels with PCM results in a 37.16% increase in output power per unit of electricity.

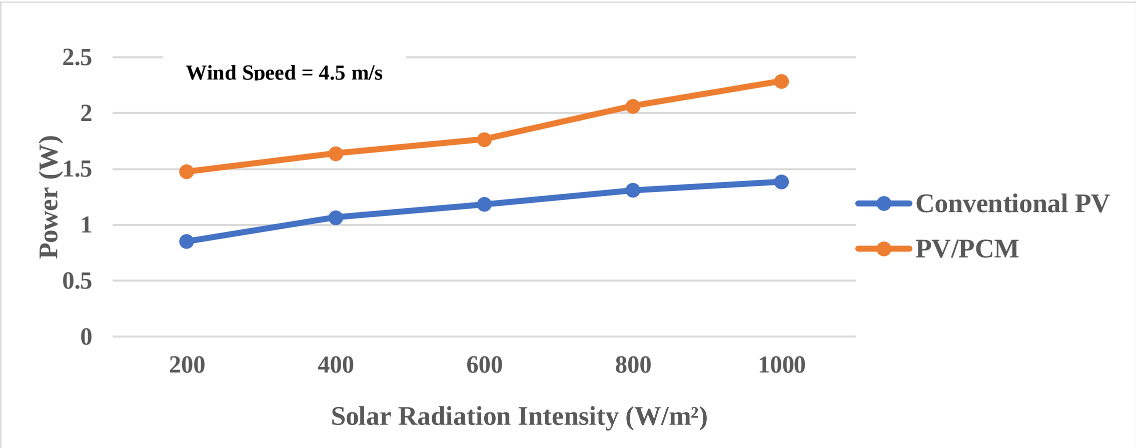

Fig. 4.67. Solar irradiance versus output power for PV panels without and with inorganic PCM (Wind speed = 4.5 m/s)

When the wind speed reaches 3.5 m/s, the output power produced by the two PV panels is compared in Fig. 4.68. The maximum output power of a PV panel without PCM is 1.404 W. However, 0.852 W is the minimal output power. However, the PV panel with PCM has a minimum output power of 1.12 W and a maximum output power of 2.184 W. PV panels with PCM and those without PCM have respective average output powers of 1.66 W and 1.09 W. It is obvious that PV panel with PCM can be produced higher output power than the PV panel without PCM. Using a PV panel with PCM results in a 34.3% increase in output power per unit of electricity.

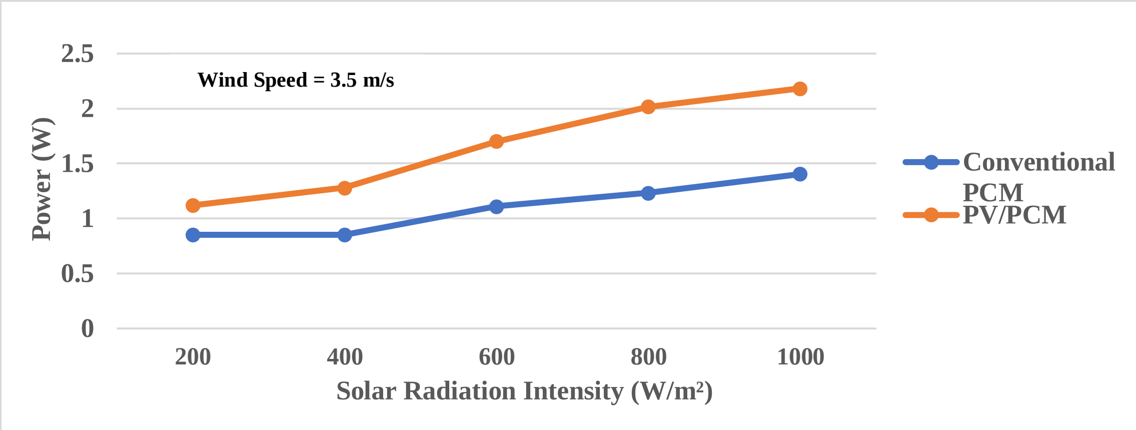

Fig. 4.68. Solar irradiance versus output power for PV panels without and with inorganic PCM (Wind speed = 3.5 m/s)

When the wind speed reaches 2.5 m/s, the output power produced by the two PV panels is compared in Fig. 4.69. The greatest output power of a PV panel without PCM is 1.306 W, and the lowest output power is 0.852 W. However, the PV panel with PCM has a maximum output power of 2.02 W and a minimum output power of 1.04 W. PV panels with PCM and those without PCM have respective average output powers of 1.548 W and 1.056 W. It is obvious that PV panel with PCM can be produced higher output power than the PV panel without PCM. Using a PV panel with PCM results in a 31.7% increase in output power per unit of electricity.

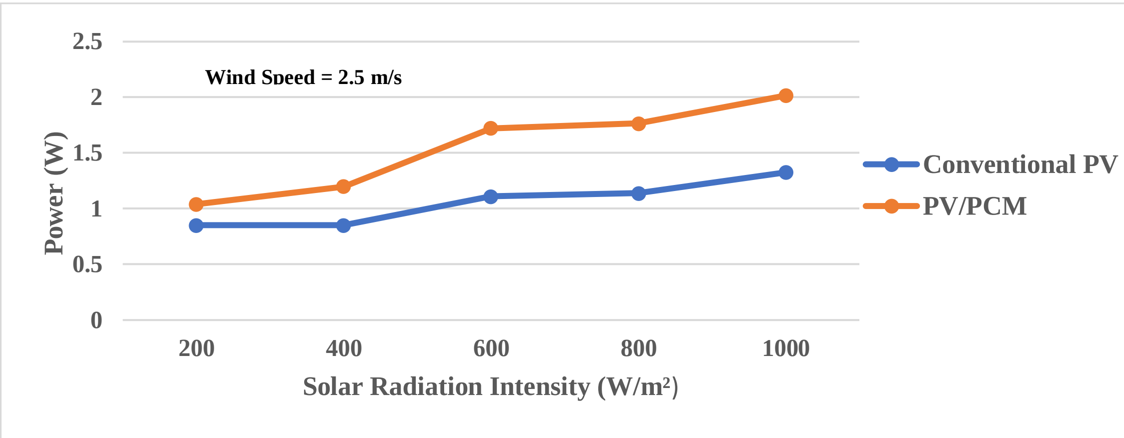

Fig. 4.69. Solar irradiance versus output power for PV panels without and with inorganic PCM (Wind speed = 2.5 m/s)

When the wind speed reaches 1.5 m/s, the output power produced by the two PV panels is compared in Fig. 4.70. The maximum output power of a PV panel without PCM is 1.155 W. However, 0.77 W is the minimal output power. However, the PV panel with PCM has a minimum output power of 0.975 W and a maximum output power of 1.722 W. PV panels with PCM and those without PCM have respective average output powers of 1.371 W and 0.968 W. It is obvious that PV panel with PCM can be produced higher output power than the PV panel without PCM. Using a PV panel with PCM results in a 29.4% increase in output power per unit of electricity.

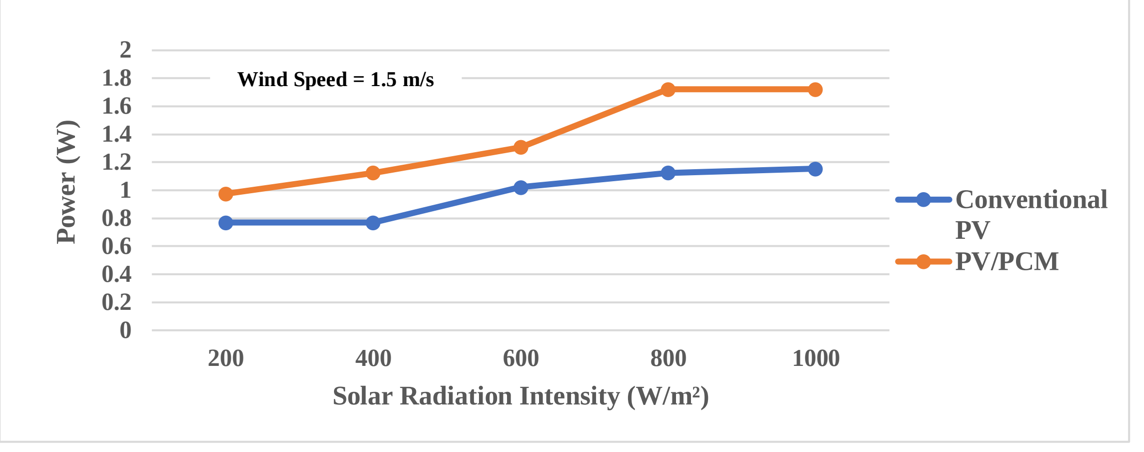

Fig. 4.70. Solar irradiance versus output power for PV panels without and with inorganic PCM (Wind speed = 1.5 m/s)

When the wind speed reaches 0.5 m/s, the output power produced by the two PV panels is compared in Fig. 4.71. The maximum output power of a PV panel without PCM is 1.155 W. However, 0.77 W is the minimal output power. However, the PV panel with PCM has a minimum output power of 0.936 W and a maximum output power of 1.722 W. PV panels with PCM and those without PCM have respective average output powers of 1.333 W and 0.952 W. It is obvious that PV panel with PCM can be produced higher output power than the PV panel without PCM. Using a PV panel with PCM results in a 28.6% increase in output power per unit of electricity.

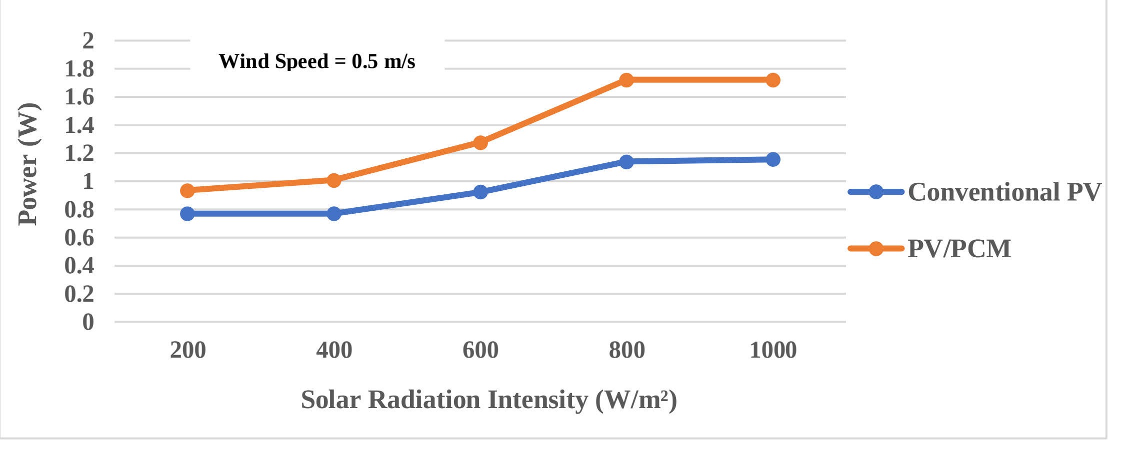

Fig. 4.71. Solar irradiance versus output power for PV panels without and with inorganic PCM (Wind speed = 0.5 m/s)

4.2.4 Effect of wind speed on thermal and electrical performance of PV module by using inorganic PCM

4.2.4.1 Effect of wind speed on PV cell temperature

Figure 4.72 shows the evolution of solar cell temperatures for PV and PV-PCM configurations with solar irradiance = 1000 W/m². Due to the combined effects of high wind speed and PCM's ability to dissipate heat, the surface temperature variation between conventional PV and PV-PCM systems at a wind speed of 5.5 m/s remained 76.9% higher than that between conventional PV and PV-PCM systems at a wind speed of 0.5 m/s.

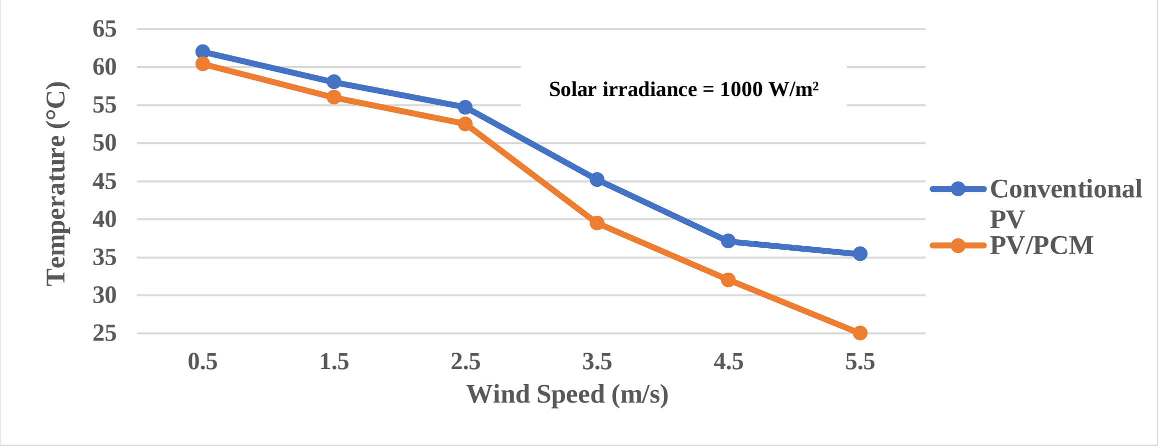

Fig. 4.72. Wind speed versus operating temperature for PV panels without and with organic PCM (Solar irradiance = 1000 W/m²)

Figure 4.73 shows the evolution of solar cell temperatures for PV and PV-PCM configurations with solar irradiance = 800 W/m². Due to the combined effects of high wind speed and PCM's ability to dissipate heat, the surface temperature variation between conventional PV and PV-PCM systems at a wind speed of 5.5 m/s remained 75% greater than that between conventional PV and PV-PCM systems at a wind speed of 0.5 m/s.

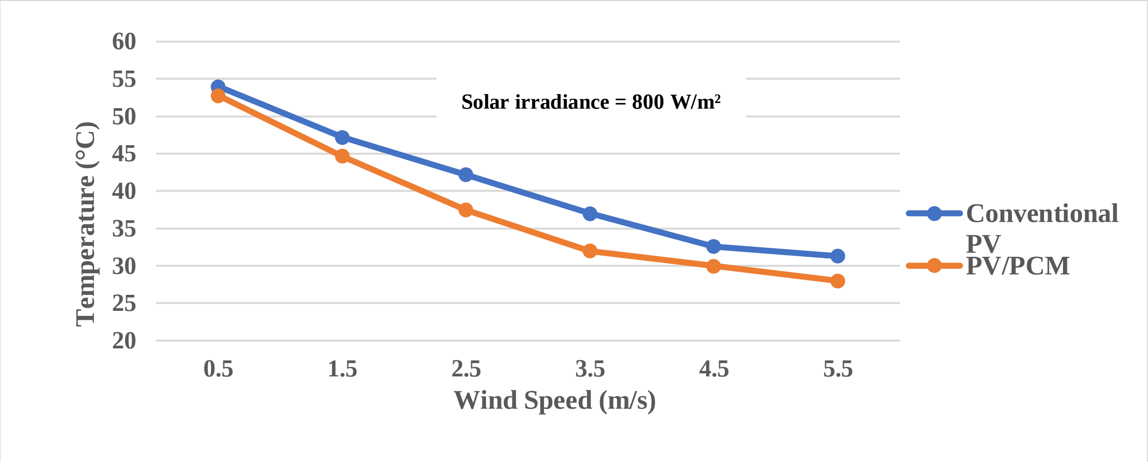

Fig. 4.73. Wind speed versus operating temperature for PV panels without and with inorganic PCM (Solar irradiance = 800 W/m²)

Figure 4.74 shows the evolution of solar cell temperatures for PV and PV-PCM configurations with solar irradiance = 600W/m². Due to the combined effects of high wind speed and PCM's ability to dissipate heat, the surface temperature variation between conventional PV and PV-PCM systems at a wind speed of 5.5 m/s remained 64.2% higher than that between conventional PV and PV-PCM systems at a wind speed of 0.5 m/s.

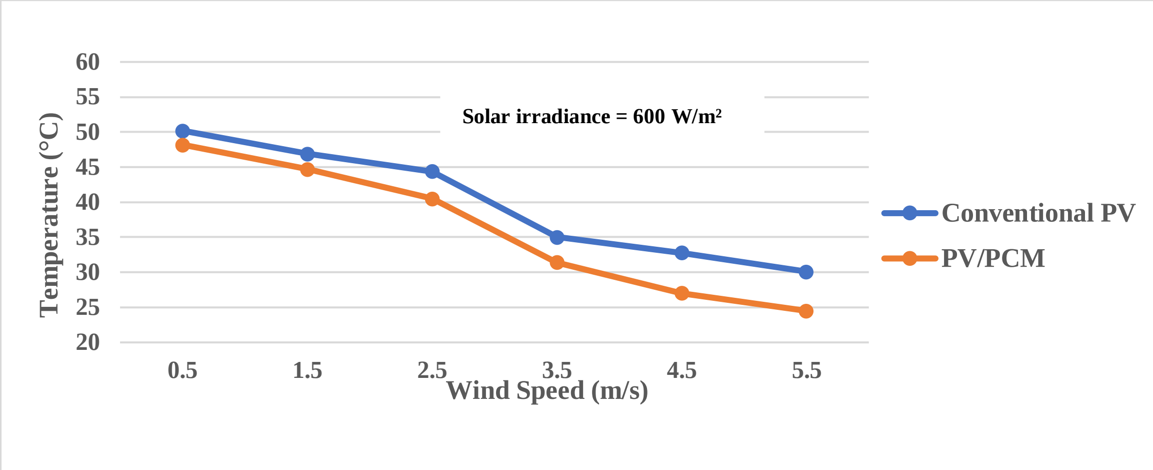

Fig. 4.74. Wind speed versus operating temperature for PV panels without and with inorganic PCM (Solar irradiance = 600 W/m²)

Figure 4.75 shows the evolution of solar cell temperatures for PV and PV-PCM configurations with solar irradiation = 400 W/m². Due to the combined effects of high wind speed and PCM's ability to dissipate heat, the surface temperature variation between conventional PV and PV-PCM systems at a wind speed of 5.5 m/s remained 55.8% greater than that between conventional PV and PV-PCM systems at a wind speed of 0.5 m/s.

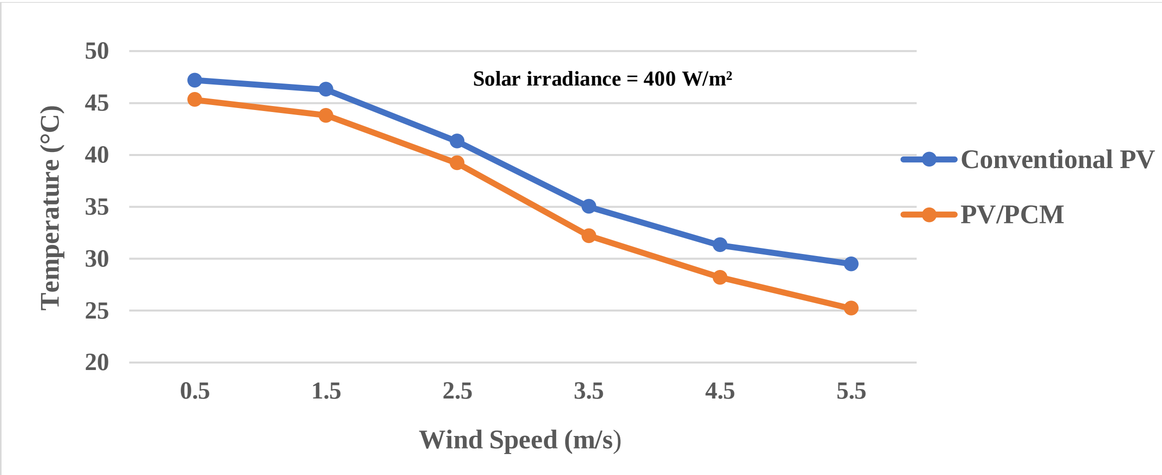

Fig. 4.75. Wind speed versus operating temperature for PV panels without and with inorganic PCM (Solar irradiance = 400 W/m²)

Figure 4.76 shows the evolution of solar cell temperatures for PV and PV-PCM designs with solar irradiation = 200 W/m². Due to the combined effects of high wind speed and PCM's ability to dissipate heat, the surface temperature variation between conventional PV and PV-PCM systems at a wind speed of 5.5 m/s remained 47.8% higher than that between conventional PV and PV-PCM systems at a wind speed of 0.5 m/s.

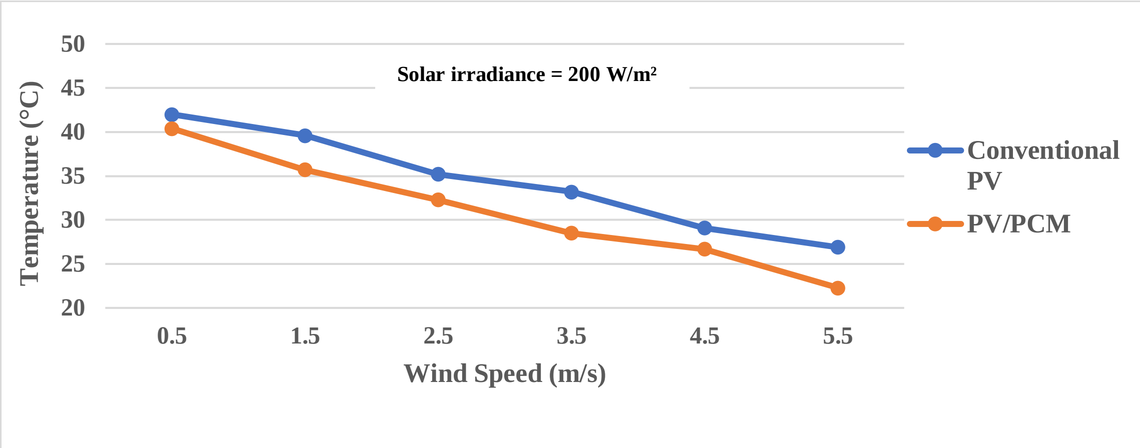

Fig. 4.76. Wind speed versus operating temperature for PV panels without and with inorganic PCM (Solar irradiance = 200 W/m²)

4.2.4.2 Effect of wind speed on output current

Figure 4.77 shows the output current evolutions for PV and PV-PCM systems with solar irradiation = 1000W/m². Due to the combined effects of high wind speed and PCM's ability to dissipate heat, the output current variation between conventional PV and PV-PCM systems at a wind speed of 5.5 m/s remained 75% higher than that between conventional PV and PV-PCM systems at a wind speed of 0.5 m/s.

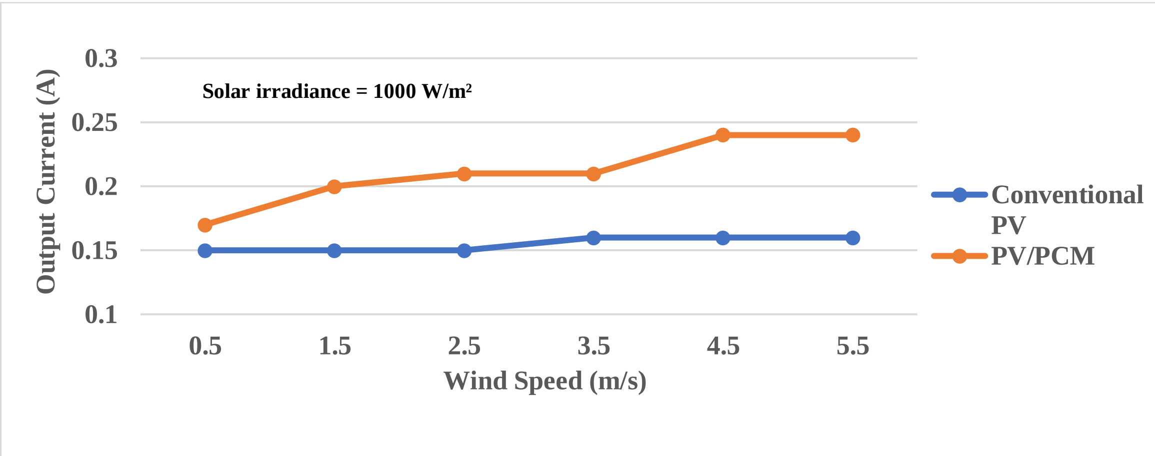

Fig. 4.77. Wind speed versus output current for PV panels without and with inorganic PCM (Solar irradiance = 1000 W/m²)

Figure 4.78 shows the output current evolutions for PV and PV-PCM systems with solar irradiation = 800 W/m². Due to the combined effects of high wind speed and PCM's ability to dissipate heat, the output current variation between conventional PV and PV-PCM systems at a wind speed of 5.5 m/s remained 75% higher than that between conventional PV and PV-PCM systems at a wind speed of 0.5 m/s.

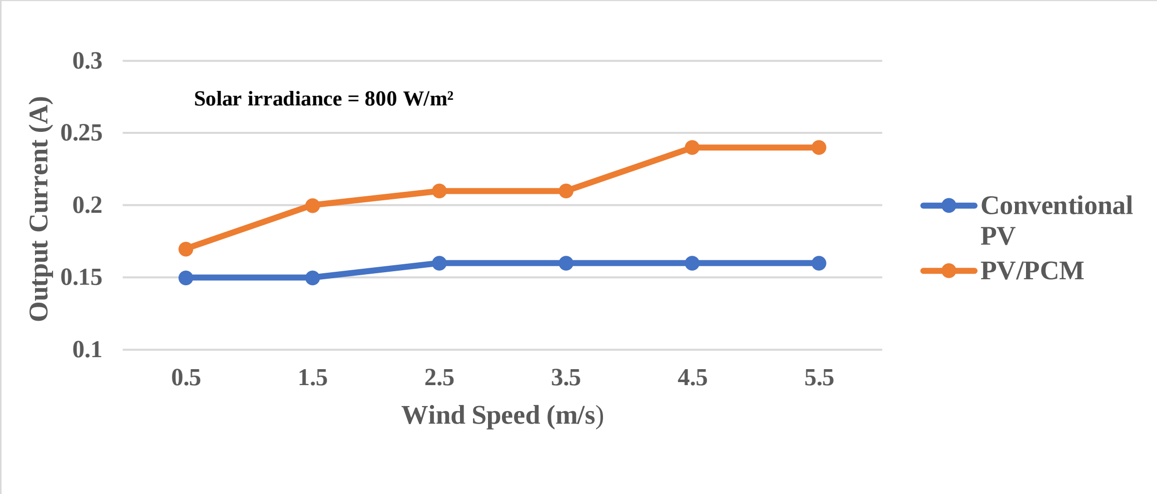

Fig. 4.78. Wind speed versus output current for PV panels without and with inorganic PCM (Solar irradiance = 800 W/m²)

Figure 4.79 shows the output current evolutions for PV and PV-PCM systems with solar irradiation = 600 W/m². Due to the combined effects of high wind speed and PCM's ability to dissipate heat, the output current variation between conventional PV and PV-PCM systems at a wind speed of 5.5 m/s remained 66.7% higher than that between conventional PV and PV-PCM systems at a wind speed of 0.5 m/s.

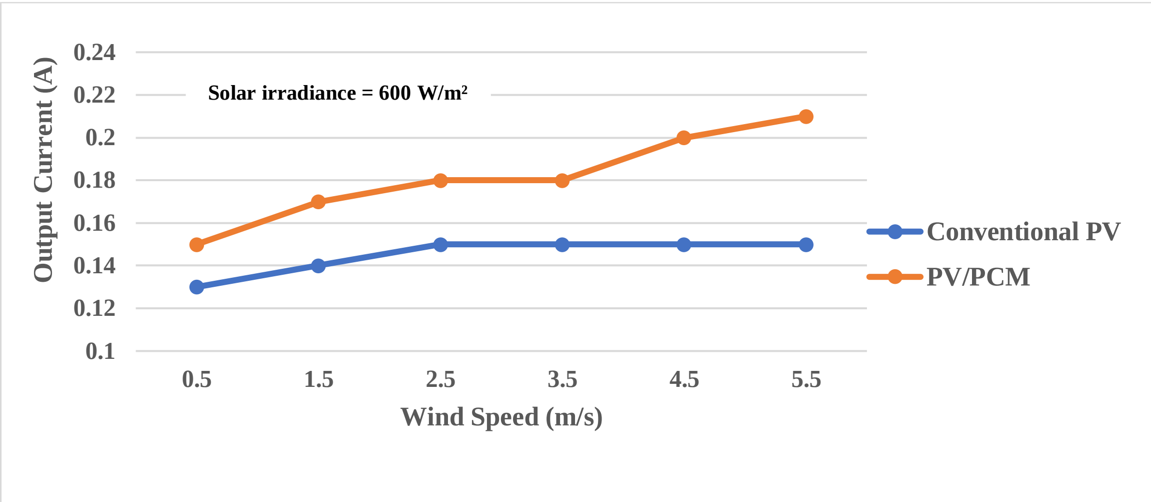

Fig. 4.79. Wind speed versus output current for PV panels without and with inorganic PCM (Solar irradiance = 600 W/m²)

Figure 4.80 shows the output current evolutions for PV and PV-PCM systems with solar irradiation = 400 W/m². Due to the combined effects of high wind speed and PCM's ability to dissipate heat, the output current variation between conventional PV and PV-PCM systems at a wind speed of 5.5 m/s remained 62.5% higher than that between conventional PV and PV-PCM systems at a wind speed of 0.5 m/s.

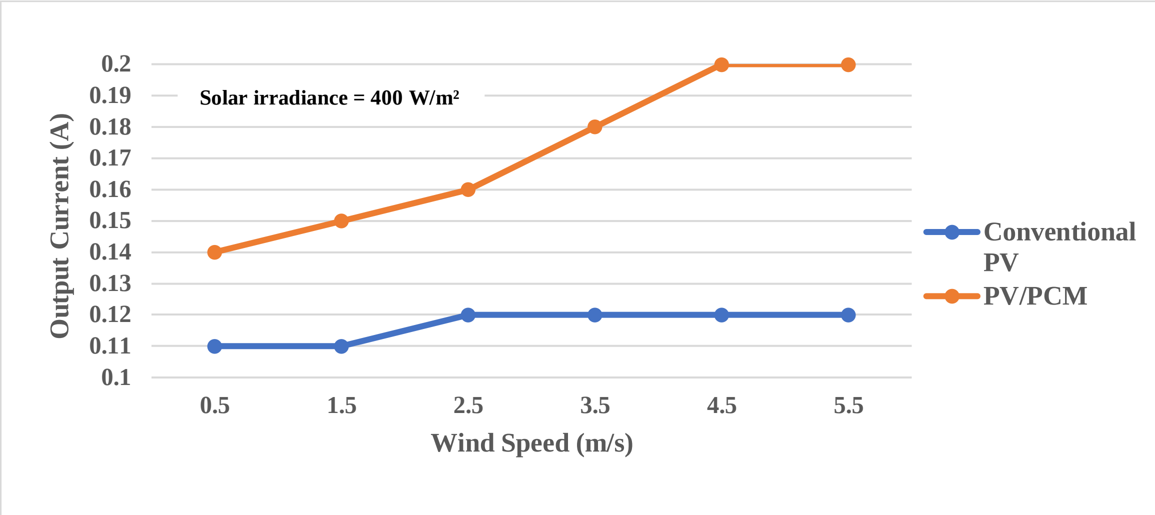

Fig. 4.80. Wind speed versus output current for PV panels without and with inorganic PCM (Solar irradiance = 400 W/m²)

Figure 4.81 shows the output current evolutions for PV and PV-PCM systems with solar irradiation = 200 W/m². Due to the combined effects of high wind speed and PCM's ability to dissipate heat, the output current variation between conventional PV and PV-PCM systems at a wind speed of 5.5 m/s remained 60% greater than that between conventional PV and PV-PCM systems at a wind speed of 0.5 m/s.

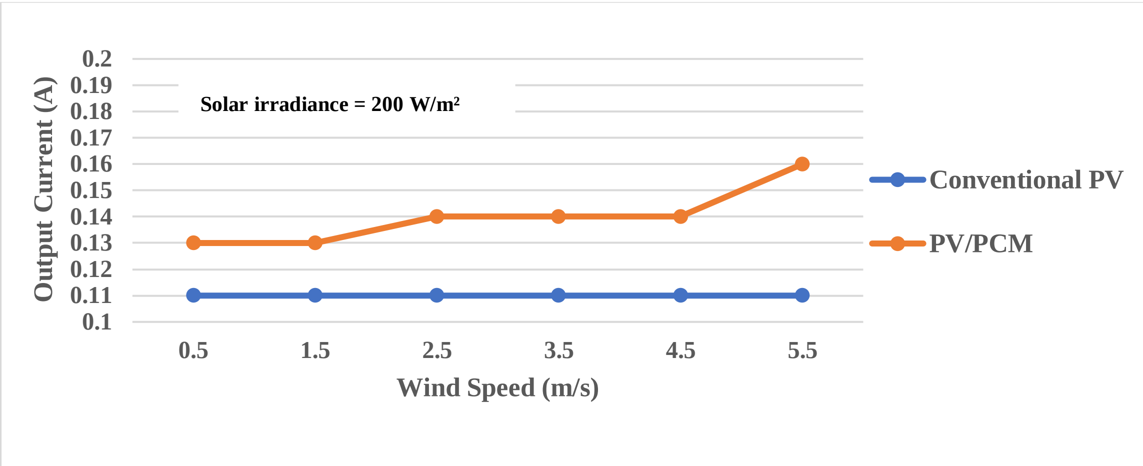

Fig. 4.81. Wind speed versus output current for PV panels without and with inorganic PCM (Solar irradiance = 200 W/m²)

4.2.4.3 Effect of wind speed on voltage

Figure 4.82 shows the output voltage evolutions for PV and PV-PCM systems with solar irradiation = 1000 W/m². Due to the combined effects of high wind speed and PCM's ability to dissipate heat, the output voltage variation between the conventional PV and PV-PCM systems at a wind speed of 5.5 m/s remained 50% greater than that between the conventional PV and PV-PCM systems at a wind speed of 0.5 m/s.

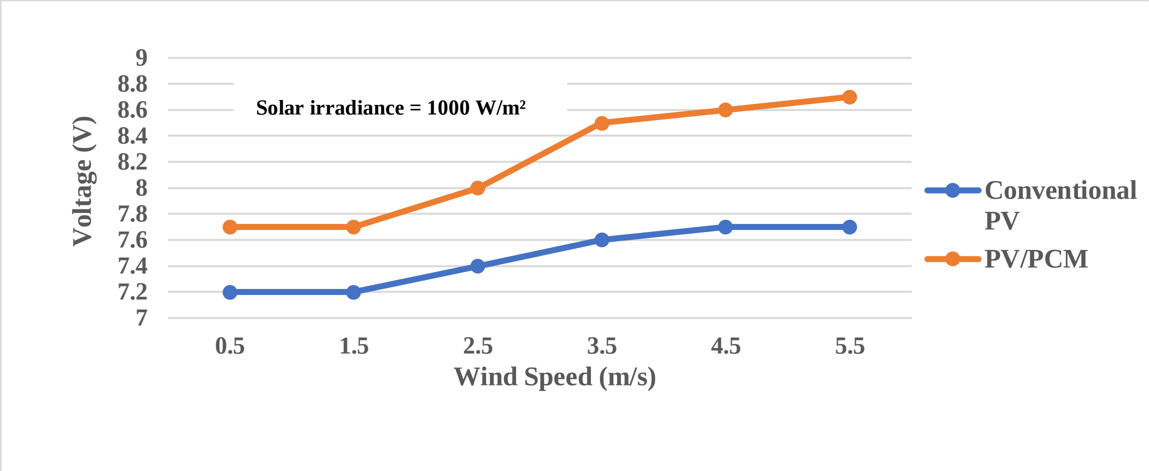

Fig. 4.82. Wind speed versus output voltage for PV panels without and with inorganic PCM (Solar irradiance = 1000 W/m²)

Figure 4.83 shows the output voltage evolutions for PV and PV-PCM systems with solar irradiance = 800 W/m². Due to the combined effects of high wind speed and PCM's ability to dissipate heat, the output voltage variation between the conventional PV and PV-PCM systems at a wind speed of 5.5 m/s remained 50% greater than that between the conventional PV and PV-PCM systems at a wind speed of 0.5 m/s.

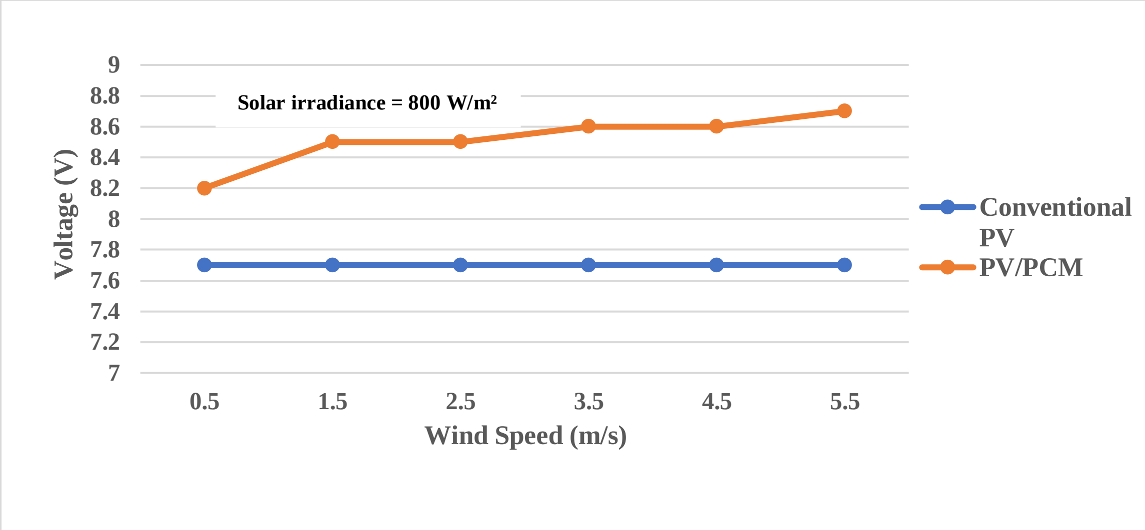

Fig. 4.83. Wind speed versus output voltage for PV panels without and with inorganic PCM (Solar irradiance = 800 W/m²)

Figure 4.84 shows the output voltage evolutions for PV and PV-PCM systems with solar irradiation = 600 W/m². Due to the combined effects of high wind speed and PCM's ability to dissipate heat, the output voltage variation between the conventional PV and PV-PCM systems at a wind speed of 5.5 m/s remained 44.4% higher than that between the conventional PV and PV-PCM systems at a wind speed of 0.5 m/s.

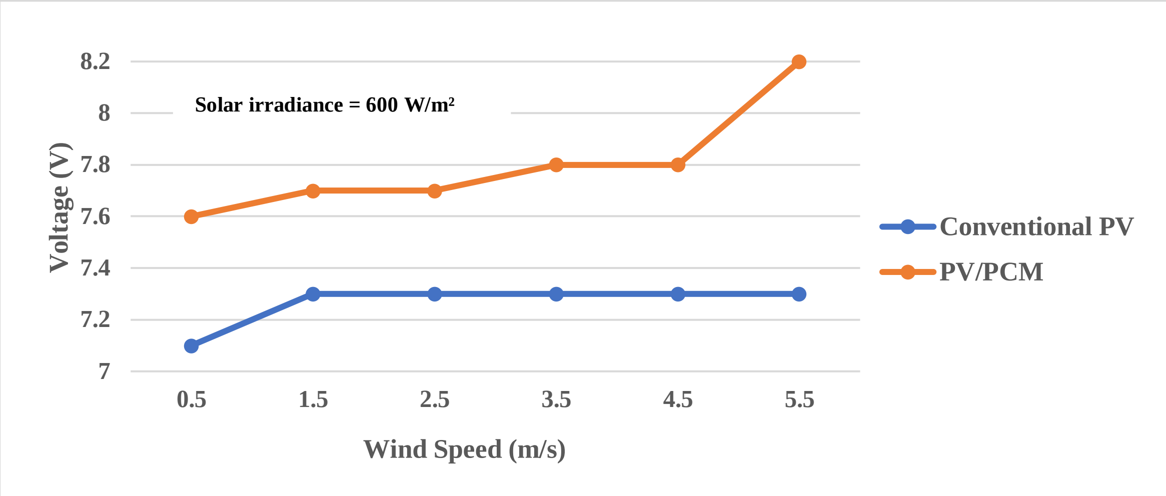

Fig. 4.84. Wind speed versus output voltage for PV panels without and with inorganic PCM (Solar irradiance = 600 W/m²)

Figure 4.85 shows the output voltage evolutions for PV and PV-PCM systems with solar irradiation = 400 W/m². Due to the combined effects of high wind speed and PCM's ability to dissipate heat, the output voltage variation between the conventional PV and PV-PCM systems at a wind speed of 5.5 m/s remained 44.4% higher than that between the conventional PV and PV-PCM systems at a wind speed of 0.5 m/s.

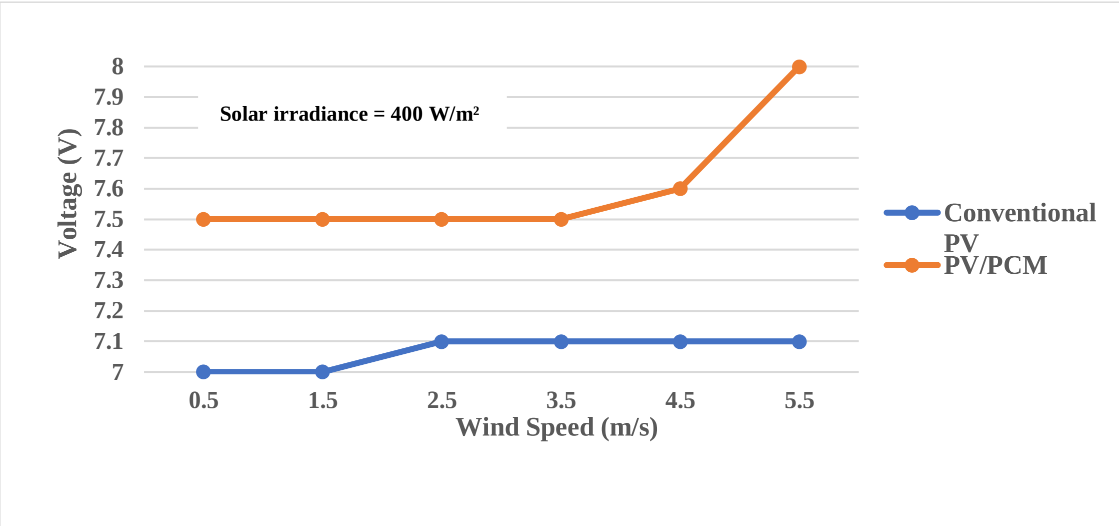

Fig. 4.85. Wind speed versus output voltage for PV panels without and with inorganic PCM (Solar irradiance = 400 W/m²)

Figure 4.86 shows the output voltage evolutions for PV and PV-PCM systems with solar irradiation = 200 W/m². Due to the combined effects of high wind speed and PCM's ability to dissipate heat, the output voltage variation between the conventional PV and PV-PCM systems at a wind speed of 5.5 m/s remained 37.5% higher than that between the conventional PV and PV-PCM systems at a wind speed of 0.5 m/s.

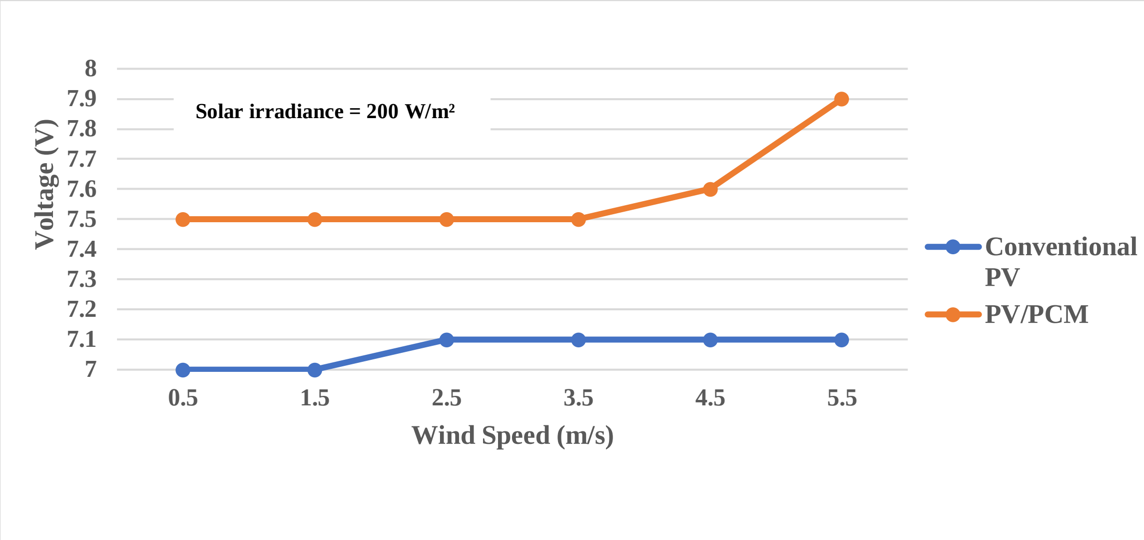

Fig. 4.86. Wind speed versus output voltage for PV panels without and with inorganic PCM (Solar irradiance = 200 W/m²)

4.2.4.4 Effect of wind speed on power

The output power evolutions for PV and PV-PCM configurations are shown in Fig. 4.87 for solar irradiance = 1000 W/m². Due to the combined effects of high wind speed and PCM's ability to dissipate heat, the output power variation between conventional PV and PV-PCM systems at a wind speed of 5.5 m/s remained 60% greater than that between conventional PV and PV-PCM systems at a wind speed of 0.5 m/s.

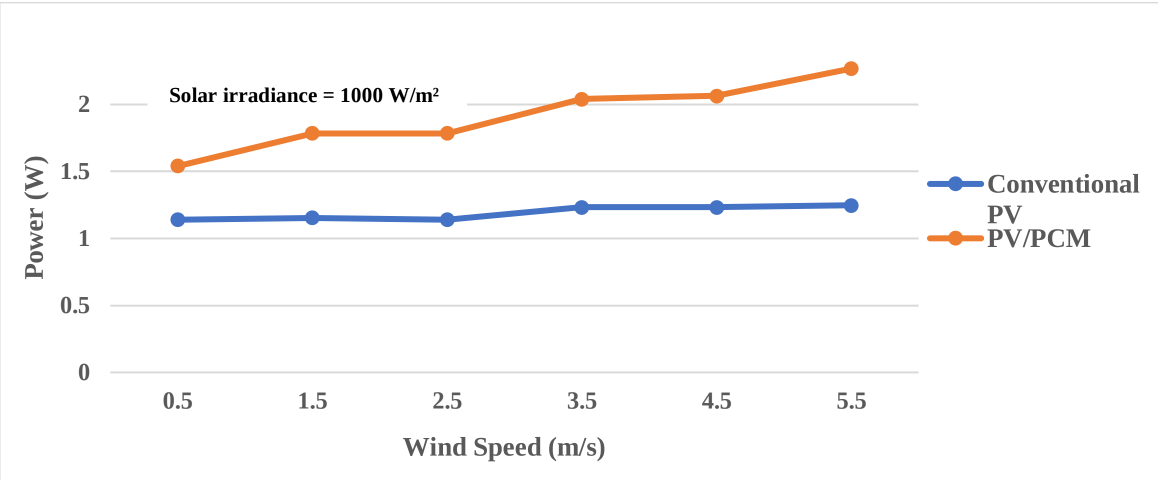

Fig. 4.87. Wind speed versus output power for PV panels without and with inorganic PCM (Solar irradiance = 1000 W/m²)

The output power evolutions for PV and PV-PCM configurations are shown in Fig. 4.88 for solar irradiance = 800 W/m². Due to the combined effects of high wind speed and PCM's ability to dissipate heat, the output power variation between conventional PV and PV-PCM systems at a wind speed of 5.5 m/s remained 60% greater than that between conventional PV and PV-PCM systems at a wind speed of 0.5 m/s.

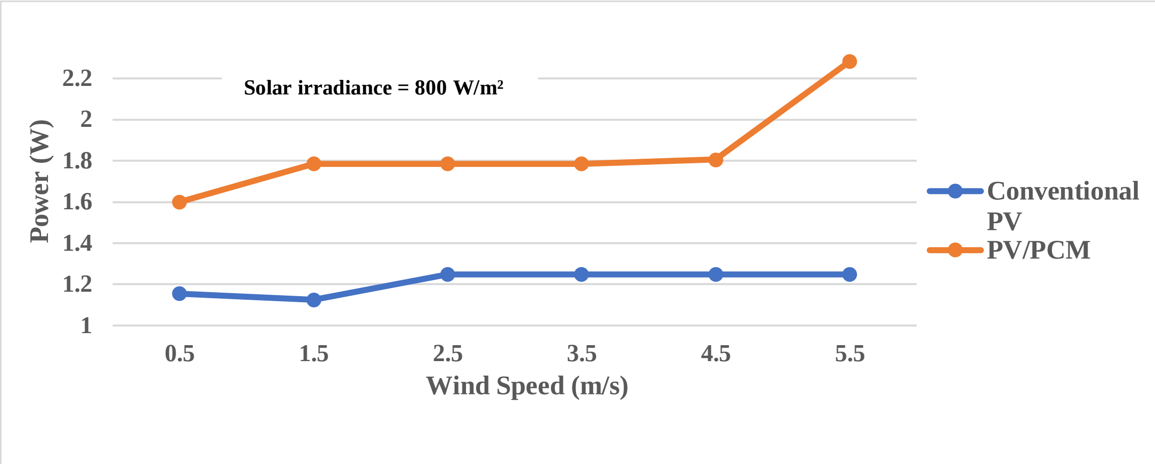

Fig. 4.88. Wind speed versus output power for PV panels without and with inorganic PCM (Solar irradiance = 800 W/m²)

The output power evolutions for PV and PV-PCM combinations are shown in Fig. 4.89 for solar irradiance = 600W/m². Due to the combined effects of high wind speed and PCM's ability to dissipate heat, the output power variation between conventional PV and PV-PCM systems at a wind speed of 5.5 m/s remained 50.3% higher than that between conventional PV and PV-PCM systems at a wind speed of 0.5 m/s.

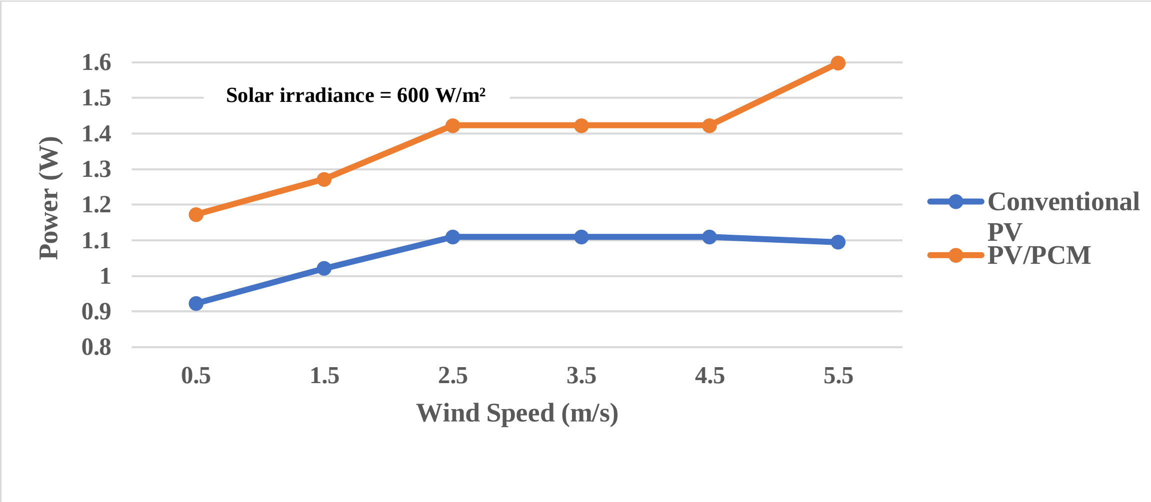

Fig. 4.89. Wind speed versus output power for PV panels without and with inorganic PCM (Solar irradiance = 600 W/m²)

The output power evolutions for PV and PV-PCM configurations are shown in Fig. 4.90 for solar irradiance = 400 W/m². Due to the combined effects of high wind speed and PCM's ability to dissipate heat, the output power variation between conventional PV and PV-PCM systems at a wind speed of 5.5 m/s remained 50.3% higher than that between conventional PV and PV-PCM systems at a wind speed of 0.5 m/s.

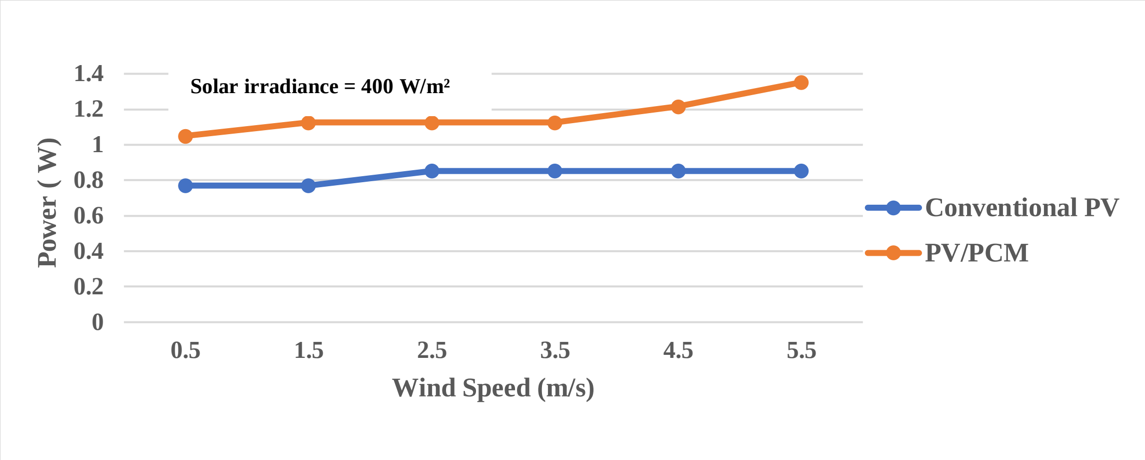

Fig. 4.90. Wind speed versus output power for PV panels without and with inorganic PCM (Solar irradiance = 400 W/m²)

The output power evolutions for PV and PV-PCM systems are shown in Fig. 4.91 with solar irradiance = 200 W/m². Due to the combined effects of high wind speed and PCM's ability to dissipate heat, the output power variation between conventional PV and PV-PCM systems at a wind speed of 5.5 m/s remained 27.6% higher than that between conventional PV and PV-PCM systems at a wind speed of 0.5 m/s.

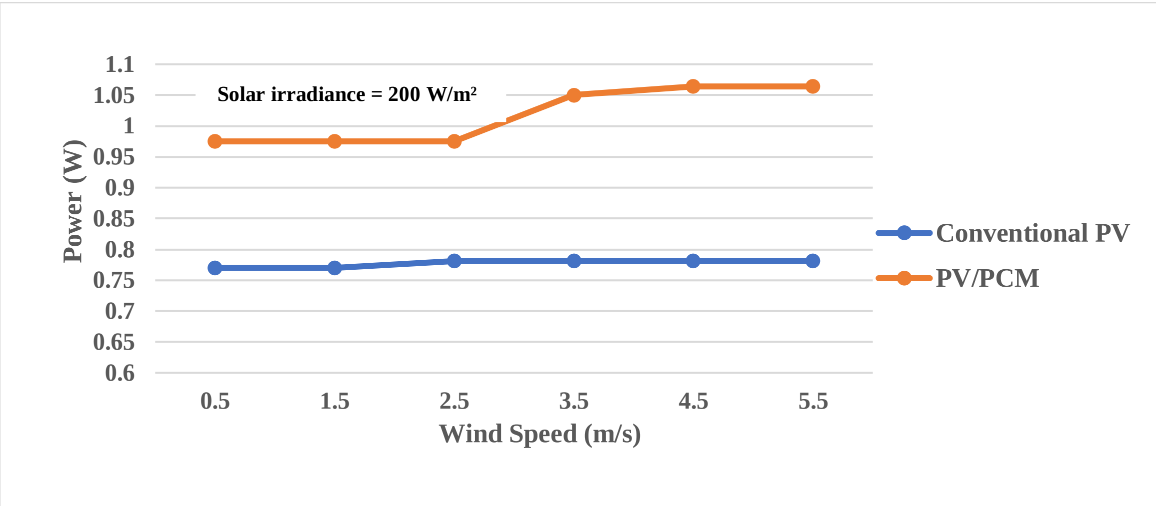

Fig. 4.91. Wind speed versus output power for PV panels without and with inorganic PCM (Solar irradiance = 200 W/m²)

4.3. PV Cell Efficiency

The efficiency is the most commonly used parameter to compare the performance of one solar cell to another. Efficiency is defined as the ratio of energy output from the solar cell to input energy from the sun. In addition to reflecting the performance of the solar cell itself, the efficiency depends on the spectrum and intensity of the incident sunlight and the temperature of the solar cell. Therefore, conditions under which efficiency is measured must be carefully controlled in order to compare the performance of one device to another.

The short-circuit current and the open-circuit voltage are the maximum current and voltage respectively from a solar cell. However, at both of these operating points, the power from the solar cell is zero. The "fill factor", more commonly known by its abbreviation "FF", is a parameter which, in conjunction with V_{oc} and I_{sc}, determines the maximum power from a solar cell. The FF is defined as the ratio of the maximum power from the solar cell to the product of V_{oc} and I_{sc}

The efficiency of a solar cell is determined as the fraction of incident power which is converted to electricity and is defined as:

$$P_{max} = V_{oc} I_{sc} FF$$

$$\eta = \frac{V_{oc} I_{sc} FF}{P_{in}}$$

Where:

V_{oc} is the open-circuit voltage;

I_{sc} is the short-circuit current;

FF is the fill factor = $P_{max} / (V_{oc} \times I_{sc})$ and

η is the efficiency.

4.3.1. Effect of organic PCM on PV cell efficiency

Table 4.1: Comparison of PV cell efficiency for the effect of organic PCM

Conventional PV	**PV-PCM**
From experimental data For solar radiation intensity = 1000 W/m², P_{max} =1.404W V_{oc} =21.65 V I_{sc}=1.15 A *Solar panel area, A=0.18 m²* P_{in} =180W $FF=1.404/(21.65\times1.15)$ $=0.06$ $\eta= \{(21.65\times1.15\times0.06)/180\}\times100\%$ $=0.83\%$	From experimental data For solar radiation intensity = 1000 W/m², P_{max} =2.064W V_{oc} =21.65 V I_{sc}=1.15 A *Solar panel area, A=0.18 m²* P_{in} =180W $FF=2.064/(21.65\times1.15)$ $=0.08$ $\eta = \{(21.65\ V\times1.15\ A\times0.08/180)\ \times100\%$ $=1.11\ \%$

4.3.2. Effect of inorganic PCM on PV cell efficiency

Table 4.2: Comparison of PV cell efficiency for the effect of inorganic PCM

Conventional PV	PV-PCM
From experimental data	From experimental data
For solar radiation intensity =1000 W/m²,	For solar radiation intensity = 1000 W/m²,
P_{max} =1.404W	P_{max} =2.288W
Voc =21.65 V	*Voc =21.65 V*
Isc=1.15 A	*Isc=1.15 A*
Solar panel area, A=0.18 m²	*Solar panel area, A=0.18 m²*
P_{in} =180W	P_{in} =180W
$FF=1.404/(21.65\times1.15)$ $=0.06$	$FF=2.288/(21.65\times1.15)$ $=0.09$
$\eta=\{(21.65\times1.15\times0.06)/180\}\times100\%$ $=0.83\%$	$\eta = \{(21.65\ V\times1.15\ A\times0.09/180)\ \times100\%$ $=1.25\%$

CHAPTER-V

CONCLUSIONS AND RECOMMENDATIONS

The result of study and research on the PV- PCM system has been explained, and future research directions are also presented in this chapter:

- For photovoltaic cell, passive cooling method like PV-PCM system gives good result compared to the conventional cooling system.
- PV – PCM system gives efficient result and a measurable temperature drop of PV panel. PV-PCM configurations for both organic and inorganic PCM give an effective temperature drop of PV panel. But from analysis, it is clear that PV-PCM configuration with inorganic PCM give more efficient result for cooling purpose than PV-PCM configuration with organic PCM because inorganic PCM has high heat conductivty and organic PCM has very low heat conductivity. Combined effect of high wind speed and PCM as a thermal dissipating system give good result.
- PV-PCM configurations for both organic and in-organic PCM give a significant increase in electrical efficiency. It is clear from analysis that PV-PCM configuration with inorganic PCM give more efficiency gain % than PV-PCM configuration with organic PCM because of high thermal conductivity of inorganic PCM and as shown in Table 5.1.

Table 5.1: PV cell efficiency gain %

	Conventional PV	PV-PCM	Efficiency gain %
Organic	0.83%	1.11%	0.28%
Inorganic	0.83%	1.25%	0.42%

5.1. Recommendation for future research

PV – PCM system along with different configuration like PV-PCM-TE, PV-PCM-Nanofluid, and PV-PCM – CPV, etc. also will give efficient result and a measurable temperature drop of PV panel.

APPENDICES

APPENDIX-A

Table-1: Data for solar radiation intensity = 1000 W/m² with and without organic PCM

Wind Speed (m/s)	PV Cell Temperature (ºC)		Current (A)		Voltage (V)	
	Conventional PV	PV/PCM	Conventional PV	PV/PCM	Conventional PV	PV/PCM
0.5	65	63	0.16	0.18	7.6	8.5
1.5	61.7	59	0.17	0.19	7.6	8.5
2.5	53.2	50.2	0.17	0.2	7.7	8.5
3.5	44.6	41.3	0.18	0.22	7.7	8.5
4.5	36.6	32.5	0.18	0.23	7.8	8.6
5.5	34.5	30.1	0.18	0.24	7.8	8.6

Table-2: Data for solar radiation intensity = 800 W/m² with and without organic PCM

Wind Speed (m/s)	PV Cell Temperature (ºC)		Current (A)		Voltage (V)	
	Conventional PV	PV/PCM	Conventional PV	PV/PCM	Conventional PV	PV/PCM
0.5	51	49.4	0.16	0.18	7.6	8.5
1.5	47.7	45.8	0.16	0.18	7.6	8.5
2.5	44.2	41	0.16	0.19	7.7	8.5
3.5	37.6	34	0.18	0.21	7.7	8.5
4.5	35.5	32.4	0.18	0.24	7.7	8.6
5.5	34.3	30	0.18	0.24	7.8	8.6

Table-3: Data for solar radiation intensity = 600 W/m² with and without organic PCM

Wind Speed (m/s)	PV Cell Temperature (ºC)		Current (A)		Voltage (V)	
	Conventional PV	PV/PCM	Conventional PV	PV/PCM	Conventional PV	PV/PCM
0.5	50.2	48.2	0.16	0.18	0.15	0.17
1.5	45.3	42.5	0.17	0.19	0.15	0.17
2.5	42.9	39.8	0.17	0.2	0.15	0.18
3.5	35.2	32.9	0.18	0.22	0.15	0.18
4.5	33.1	30.7	0.18	0.23	0.15	0.18
5.5	30.5	26.8	0.18	0.24	0.16	0.2

Table-4: Data for solar radiation intensity = 400 W/m² with and without organic PCM

Wind Speed (m/s)	PV Cell Temperature (ºC)		Current (A)		Voltage (V)	
	Conventional PV	PV/PCM	Conventional PV	PV/PCM	Conventional PV	PV/PCM
0.5	47.5	45.4	0.12	0.13	7.2	7.4
1.5	44.8	42.8	0.12	0.13	7.2	7.5
2.5	42.1	40.1	0.14	0.15	7.2	7.5
3.5	35.1	32.1	0.15	0.16	7.2	7.5
4.5	32.5	28	0.16	0.18	7.3	7.7
5.5	29.8	25.6	0.16	0.18	7.3	7.9

Table-5: Data for solar radiation intensity = 200 W/m² with and without organic PCM

Wind Speed (m/s)	PV Cell Temperature (ºC)		Current (A)		Voltage (V)	
	Conventional PV	PV/PCM	Conventional PV	PV/PCM	Conventional PV	PV/PCM
0.5	45.3	43.8	0.12	0.13	7.2	7.5
1.5	42.1	40.5	0.12	0.13	7.2	7.5
2.5	40.4	37.6	0.12	0.13	7.2	7.5
3.5	35	32.2	0.12	0.14	7.2	7.5
4.5	30.6	26.4	0.12	0.14	7.2	7.5
5.5	24.5	24.5	0.12	0.14	7.2	7.6

APPENDIX-B

Table-1: Data for solar radiation intensity = 1000 W/m² with and without inorganic PCM.

Wind Speed (m/s)	PV Cell Temperature (ºC)		Current (A)		Voltage (V)	
	Conventional PV	PV/PCM	Conventional PV	PV/PCM	Conventional PV	PV/PCM
0.5	62	60.4	0.15	0.17	7.2	7.7
1.5	58	56	0.15	0.2	7.2	7.7
2.5	54.7	52.5	0.15	0.21	7.4	8
3.5	45.2	39.5	0.16	0.21	7.6	8.5
4.5	37.1	32	0.16	0.24	7.7	8.6
5.5	35.4	25	0.16	0.24	7.7	8.7

Table-2: Data for solar radiation intensity = 800 W/m² with and without inorganic PCM

Wind Speed (m/s)	PV Cell Temperature (ºC)		Current (A)		Voltage (V)	
	Conventional PV	PV/PCM	Conventional PV	PV/PCM	Conventional PV	PV/PCM
0.5	54	50.8	0.15	0.17	7.7	8.2
1.5	47.2	44.7	0.15	0.2	7.7	8.5
2.5	42.2	40.5	0.16	0.21	7.7	8.5
3.5	37	36.4	0.16	0.21	7.7	8.6
4.5	32.6	31.8	0.16	0.24	7.7	8.6
5.5	31.3	30.2	0.16	0.24	7.7	8.7

Table-3: Data for solar radiation intensity = 600 W/m² with and without inorganic PCM

Wind Speed (m/s)	PV Cell Temperature (ºC)		Current (A)		Voltage (V)	
	Conventional PV	PV/PCM	Conventional PV	PV/PCM	Conventional PV	PV/PCM
0.5	50.2	48.2	0.13	0.15	7.1	7.6
1.5	46.9	44.7	0.14	0.17	7.3	7.7
2.5	44.4	40.5	0.15	0.18	7.3	7.7
3.5	35	31.4	0.15	0.18	7.3	7.8
4.5	32.8	27	0.15	0.2	7.3	7.8
5.5	30.1	24.5	0.15	0.21	7.3	8.2

Table-4: Data for solar radiation intensity = 400 W/m² with and without inorganic PCM

Wind Speed (m/s)	PV Cell Temperature (ºC)		Current (A)		Voltage (V)	
	Conventional PV	PV/PCM	Conventional PV	PV/PCM	Conventional PV	PV/PCM
0.5	47.2	45.3	0.11	0.14	7	7.5
1.5	46.3	43.8	0.11	0.15	7	7.5
2.5	41.3	39.2	0.12	0.16	7.1	7.5
3.5	35	32.2	0.12	0.18	7.1	7.5
4.5	31.3	28.2	0.12	0.2	7.1	7.6
5.5	29.5	25.2	0.12	0.2	7.1	8

Table-5: Data for solar radiation intensity = 200 W/m² with and without inorganic PCM

Wind Speed (m/s)	PV Cell Temperature (ºC)		Current (A)		Voltage (V)	
	Conventional PV	PV/PCM	Conventional PV	PV/PCM	Conventional PV	PV/PCM
0.5	42	40.4	0.11	0.13	7	7.5
1.5	39.6	35.7	0.11	0.13	7	7.5
2.5	35.2	32.3	0.11	0.14	7.1	7.5
3.5	33.2	28.5	0.11	0.14	7.1	7.5
4.5	29.1	26.7	0.11	0.14	7.1	7.6
5.5	26.9	22.3	0.11	0.16	7.1	7.9

REFERENCE

1. H.M. Teamah, Comprehensive review of the application of phase change materials in residential heating applications,*Alexandria Eng.J. 2021, 60(4): 3829–3843, https://doi.org/ 10.1016/j.aej.2021.02.053.*
2. M.S. Yousef, A.K. Abdel Rahman, S. Ookawara, Performance investigation of low Concentration photovoltaic systems under hot and arid conditions: Experimental and numerical results, *Energy Convers. Manag. 2016, 128: 82–94, https://doi.org/ 10.1016/j.enconman.2016.09.061*.
3. K. Emery, J. Burdick, Y. Caiyem, D. Dunlavy, H. Field, B. Kroposki, T. Moriatry, Temperature dependence of photovoltaic cells, modules and systems, *Proceedings of the 25th IEEE PV Specialists Conference, Washington DC, USA, May 13–19, 1996, pp. 1275–1278.*
4. A. Hasan, S.J. McCormack, M.J. Huang, B.Norton, Evaluation of phase change materials for thermal regulation enhancement of building integrated photovoltaics, *Sol. Energy. 2010, 84 (9): 1601–1612, https://doi.org/10.1016/ j.solener.2010.06.010*.
5. M. Sandberg, Cooling of Building Integrated Photovoltaics by Ventilation Air, *First Int, One Day Forum Nat. Hybrid Vent. 1999.01.10.*
6. E. Skoplaki, J.A. Palyvos, On the temperature dependence of photovoltaic module electrical performance: A review of efficiency/power correlations, *Sol. Energy. 2009, 83 (5): 614–624, https://doi.org/10.1016/j.solener.2008.10.008*.
7. M.M. Rahman, M. Hasanuzzaman, N.A. Rahim, Effects of various parameters on PV-module power and efficiency, *Energy Convers. Manag. 2015, 103: 348–358, https://doi.org/10.1016/j. enconman.2015.06.067*.
8. A.R. Amelia, Y.M. Irwan, M. Irwanto, W.Z. Leow, N. Gomesh, I. Safwati, M.A.M. Anuar, Cooling on photovoltaic panel using forced air convection induced by DC fan,*Int.J.Electr.Comput.Eng.2016,6,526–534, https://doi.org/10.11591/ijece.v6i1.9118.*
9. S. Krauter, Increased electrical yield via water flow over the front of photovoltaic panels,*Sol.EnergyMater.Sol.Cells.2004,82 (1-2),131– 137,https://doi.org/10.1016/ j.solmat.2004.01.011*.
10. M. Ozgoren, M.H. Aksoy, C. Bakir, S. Dogan, P. Dancŏva, P. Novonty, Experimental performance investigation of photovoltaic/thermal (PV-T) system, *EPJ Web Conf. 2013 45: 01-106, https://doi.org/10.1051/epjconf/20134501106*.

11. H.G. Teo, P.S. Lee, M.N.A. Hawlader, An active cooling system for photovoltaic modules,*Appl.Energy.2012,90,309–315,https://doi.org/10.1016/j.apenergy.2011.01.017*.

12. E. Wilson, Theoretical and operational thermal performance of a "wet" crystalline silicon PV module under Jamaican conditions, *Renew. Energy. 2009, 34 (6), 1655– 1660, https:// doi.org/10.1016/j.renene.2008.10.024.*

13. S.Mehrotra et al, Performance of a solar panel with water immersion cooling technique*, Int. J. Sci., Environ. Technol. 2014, 3 (3), 1161–1172.*

14. F. Bayrak, H.F. Oztop, F. Selimefendigil, Effects of different fin parameters on temperature and efficiency for cooling of photovoltaic panels under natural convection,*Sol.Energy.2019,188,484–494,https://doi.org/10.1016/j.solener.2019.06.036*.

15. M.S. Yousef, H. Hassan, Energetic and exergetic performance assessment of the inclusion of phase change materials (PCM) in a solar distillation system, *Energy Convers.Manag.2019,179,349–361, https://doi.org/10.1016/j.enconman.2018.10.078*.

16. M.S.Yousef, H.Hassan, Energy payback time, exergoeconomic and enviroeconomic analyses of using thermal energy storage system with a solar desalination system*: An experimental study,J. Clean. Prod. 2020, 270, 122082,https://doi.org/10.1016/j. jclepro.2020.122082*.

17. A. Abhat, Low temperature latent heat thermal energy storage: *Heat storage materials, Sol. Energy. 1983, 30 (4), 313–332, https://doi.org/10.1016/0038-092X(83)90186-X.*

18. R. Stropnik, U. Stritih, Increasing the efficiency of PV panel with the use of PCM, *Renew.Energy. 2016, 97, 671–679, https://doi.org/10.1016/j.renene.2016.06.011*.

19. F. Hachem, B. Abdulhay, M. Ramadan, H. El, M. Gad, E. Rab, M. Khaled, Improving the performance of photovoltaic cells using pure and combined phase change materials, Experiments and transient energy balance, *Renew. Energy. 2017, 107, 567–575,https://doi.org/10.1016/j.renene.2017.02.032*.

20. A. Waqas, J. Ji, Thermal management of conventional PV panel using PCM with movable shutters–A numerical study, *Sol.Energy. 2017, 158, 797–807, https://doi.org/10.1016/ j.solener.2017.10.050.*

21. H. Fayaz, N.A. Rahim, M. Hasanuzzaman, R. Nasrin, A. Rivai, Numerical and experimental investigation of the effect of operating conditions on performance of

PVT and PVT-PCM, *Renew.Energy. 2019, 143, 827–841, https://doi.org/10.1016/j. renene.2019.05.041*.

22. A. Gaur, C. Ménézo, S. Giroux-Julien, Numerical studies on thermal and electrical performance of a fully wetted absorber PVT collector with PCM as a storage medium,*Renew.Energy.2017,109,168–187, https://doi.org/10.1016/j.renene.2017.01.062.*

23. A. Hassan, A. Wahab, M.A. Qasim, M.M. Janjua, M.A. Ali, H.M. Ali, T.R. Jadoon, E. Ali, A. Raza, N. Javaid, (2020), Thermal management and uniform temperature regulation of photovoltaic modules using hybrid phase change materials-nanofluids system,*Renew.Energy 2020, 145, 282–293,https://doi.org/10.1016/j.renene.2019.05.130.*

24. M.S. Hossain, A.K. Pandey, J. Selvaraj, N.A. Rahim, M.M. Islam, V.V. Tyagi, Two side serpentine flow based photovoltaic-thermal-phase change materials (PVT-PCM) system: *Energy, exergy and economic analysis, Renew. Energy. 2019, 136, 1320–1336, https://doi.org/10.1016/j.renene.2018.10.097.*

25. A. Hasan, J. Sarwar, H. Alnoman, S. Abdelbaqi, Yearly energy performance of a photovoltaic-phase change material (PV-PCM) system in hot climate, *Sol. Energy. 2017, 146, 417–429, https://doi.org/10.1016/j.solener.2017.01.070*.

26. T. Wongwuttanasatian, T. Sarikarin, A. Suksri, Performance enhancement of a photovoltaic module by passive cooling using phase change material in a finned container heat sink, *Sol.Energy. 2020, 195, 47–53, https://doi.org/10.1016/ j.solener.2019.11.053*.

27. H.M. Teamah, M.F. Lightstone, Numerical study of the electrical load shift capability of a ground source heat pump system with phase change thermal storage, *Energy.Build. 2019,199, 235–246, https://doi.org/10.1016/j.enbuild.2019.06.056*.

28. H.A.M. Teamah, M.F. Lightstone, J.S. Cotton, Numerical investigation and nondimensional analysis of the dynamic performance of a thermal energy storage system containing phase change materials and liquid water, *J. Sol. Energy Eng.Trans. ASME. 2017, 139, 1–14, https://doi.org/10.1115/1.4034642.*

29. M.J. Huang, P.C. Eames, B. Norton, Phase change materials for limiting temperature rise in building integrated photovoltaics, *Sol. Energy. 2006, 80 (9): 1121–1130, https://doi.org/10.1016/ j.solener.2005.10.006*.

30. M. Rajvikram, S. Leoponraj, S. Ramkumar, H. Akshaya, A. Dheeraj, Experimental investigation on the abasement of operating temperature in solar photovoltaic panel using PCM and aluminium, *Sol. Energy. 2019, 188, 327–338, https:// doi.org/10.1016/j.solener.2019.05.067*.

31. S. Mousavi, A. Kasaeian, M. Behshad, Numerical investigation of the effects of a copper foam filled with phase change materials in a water-cooled photovoltaic/thermal system, *2018, 116, 387-195.https://doi.org/10.1016/j. enconman.2018.02.039.*

32. A.R. Abdulmunem, P.M. Samin, H.A. Rahman, H.A. Hussien, I.I. Mazali, Enhancing PV Cell electrical efficiency using phase change material with copper foam matrix and multi-walled carbon nanotubes as passive cooling method, *Renew. Energy. 2020, 160, 663–675,https://doi.org/10.1016/j. renene.2020.07.037.*

33. S.A. Nada, D.H. El-Nagar, H.M.S. Hussein, Improving the thermal regulation and efficiency enhancement of PCM-Integrated PV modules using nano particles, *Energy Convers.Manag.2018,166,735–743,https://doi.org/10.1016/j.enconman.2018.04.035.*

34. A.H.A. Al-Waeli, K. Sopian, H.A. Kazem, J.H. Yousif, M.T. Chaichan, A. Ibrahim, S. Mat, M.H. Ruslan, Comparison of prediction methods of PV/T nanofluid and nano-PCM system using a measured dataset and artificial neural network, *Sol. Energy. 2018, 162, 378–396, https://doi.org/10.1016/ j.solener.2018.01.026.*

35. L. Siahkamari, M. Rahimi, N. Azimi, M. Banibayat, Experimental investigation on using a novel phase change material (PCM) in micro structure photovoltaic cooling system,*Int.Commun.HeatMassTransf.2019,100,60–66, https://doi.org/10.1016/j.icheatmasstransfer.2018.12.020.*

36. www.solarpowernotes.com Md. Zunaid Baten, Emran Md. Amin, Anika Sharin, Raisul Islam, Shahriar A. Chowdhury, Renewable Energy Scenario of Bangladesh: Physical Perspective, *International Conference on the Developments in Renewable Energy Technology (ICDRT) 2009,Dhaka,Bangladesh.http://bangladesheconomy.wordpress.com http://www.ecoticias.com.*

37. V.V. Tyagi, S.C. Kaushik, S.K. Tyagi, T. Akiyama, Development of phase change materials basedmicroencapsulated technology for buildings: *A review. Renew. Sustain. Energy Rev. 2011, 15, 1373–1391.*

38. P. Verma, Varun, S.K. Singal, Review of mathematical modeling on latent heat thermal energy storage systems using phase-change material. *Renew. Sustain. Energy Rev. 2008, 12, 999–1031.*

39. B. Zalba, B. J.M. Marín, L.F. Cabeza, H. Mehling, Review on thermal energy storage with phase change: Materials, heat transfer analysis and applications. *Appl. Therm. Eng. 2003, 23, 251–283.*

40. C.Y. Zhao, G.H. Zhang, Review on microencapsulated phase change materials (MEPCMs): Fabrication, characterization and applications. *Renew. Sustain. Energy Rev. 2011, 15, 3813–3832.*

41. D. Zhou, C.Y. Zhao, Y. Tian, Review on thermal energy storage with phase change materials (PCMs) in building applications. *Appl. Energy 2012, 92, 593–605.*
42. N. Zhu, Z. Ma, S. Wang, Dynamic characteristics and energy performance of buildings using phase change materials: *A review. Energy Convers. Manag. 2009, 50, 3169–3181.*
43. L. Aditya, T.M.I. Mahlia, B. Rismanchi, H.M. Ng, M.H Hasan, H.S.C. Metselaar, O. Muraza, H.B. Aditiya, A review on insulation materials for energy conservation in buildings. *Renew. Sustain. Energy Rev.2017, 73, 1352–1365.*
44. M. Mehrali, S.T. Latibari, M. Mehrali, T.M.I. Mahlia, H.S.C. Metselaar, Effect of carbon nanospheres on shape stabilization and thermal behavi of phase change materials for thermal energy storage. *Energy Convers. Manag. 2014, 88, 206–213.*
45. M. Silakhori, H.S.C. Metselaar, T.M.I. Mahlia, H. Fauzi, S. Baradaran, M.S. Naghavi, Palmitic acid/polypyrrole composites as form-stable phase change materials for thermal energy storage. *Energy Convers. Manag. 2014, 80, 491–497.*
46. M. Amin, N. Putra, E.A. Kosasih, E. Prawiro, R.A. Luanto, T.M.I. Mahlia, Thermal properties of beeswax/graphene phase change material as energy storage for building applications. *Appl. Therm. Eng. 2017, 112, 273–280.*
47. A. Abhat, Low temperature latent heat thermal energy storage: Heat storage materials. *Sol. Energy 1983, 30, 313–332.*
48. A. Fallahi, G. Guldentops, M. Tao, S. Granados-Focil, S. Van Dessel, Review on solid-solid phase change materials for thermal energy storage: Molecular structure and thermal properties. *Appl. Therm. Eng. 2017, 127, 1427–1441.*
49. A. Sharma, V.V. Tyagi, C.R. Chen, D. Buddhi, Review on thermal energy storage with phase change materials and applications. *Renew. Sustain. Energy Rev. 2009, 13, 318–345.*
50. U. Hamdani, R. Thaib, I. Irwansyah, T.M.I. Mahlia, Experimental investigation on melting heat transfer of paraffin wax-Al_2O_3 storage system. *Int. J. Appl. Eng. Res. 2014, 9, 17903–17910.*
51. M. Silakhori, H.S.C. Metselaar, T.M.I. Mahlia, H. Fauzi, Preparation and characterisation of microencapsulated paraffin wax with polyaniline-based polymer shells for thermal energy storage. *Mater.Res. Innov.* 2014, *18*, S6–S480.
52. M. Silakhori, M.S. Naghavi, H.S.C. Metselaar, T.M.I. Mahlia, H. Fauzi, M. Mehrali, Accelerated thermal cycling test of microencapsulated paraffin wax/polyaniline made by simple preparation method for solar thermal energy storage. *Materials 2013, 6, 1608–1620.*
53. M.M. Yasin, T. Yusaf, R. Mamat, A.F. Yusop, Characterization of a diesel engine operating with a small proportion of methanol as a fuel additive in biodiesel blend. *Appl. Energy 2014, 114, 865–873.*

54. Y.-H. Huang, J.-H. Wu, Analysis of biodiesel promotion in Taiwan. *Renew. Sustain. Energy Rev. 2008, 12, 1176–1186.*

55. N. Xie, Z. Huang, Z. Luo, X. Gao, Y. Fang, Z. Zhang, Inorganic salt hydrate for thermal energy storage. *Appl. Sci. 2017, 7, 1317.*

56. E. Oró, A. de Gracia, A. Castell, M.M. Farid, L.F. Cabeza, Review on phase change materials (PCMs) forcold thermal energy storage applications. *Appl. Energy 2012, 99, 513–533.*

57. A. Bland, M. Khzouz, T. Statheros, E. Gkanas, PCMs for residential building applications: A short review focused on disadvantages and proposals for future development. *Buildings 2017, 7, 78.*

58. Y. Fan, X. Zhang, X. Wang, J. Li, Q. Zhu, Super-cooling prevention of microencapsulated phase change material. *Thermochim. Acta 2004, 413, 1–6.*

59. Y. Yamagishi, T. Sugeno, T. Ishige, H. Takeuchi, A.T. Pyatenko, An evaluation of microencapsulated PCM for use in cold energy transportation medium. *In Proceedings of the 31st Intersociety Energy Conversion Engineering Conference; Washington, DC, USA, 11–16 August 1996, pp. 2077–2083.*

60. Y. Jin, Q. Wan, Y. Ding, PCMs heat transfer performance enhancement with expanded graphite and its thermal stability. *Proc. Eng. 2015, 102, 1877–1884.*

61. T.M. Letcher, R. Law, D. Reay, Storing Energy: With Special Reference to Renewable Energy Sources; *Elsevier: Oxford, UK, 2016.*

62. P. Sittisart, M.M. Farid, Fire retardants for phase change materials. *Appl. Energy 2011, 88, 3140–3145.*

63. G. Song, S. Ma, G. Tang, Z. Yin, X. Wang, Preparation and characterization of flame retardant form-stable phase change materials composed by EPDM, paraffin and nano magnesium hydroxide. *Energy 2010, 35, 2179–2183.*

64. Y. Lin, G. Alva, G. Fang, Review on thermal performances and applications of thermal energy storage systems with inorganic phase change materials. *Energy 2018, 165, 685–708.*

65. S.A. Mohamed, F.A. Al-Sulaiman, N.I. Ibrahim, M.H. Zahir, A. Al-Ahmed, R. Saidur, B.S. Yılbaş, A.Z. Sahin, A review on current status and challenges of inorganic phase change materials for thermal energy storage systems. *Renew. Sustain. Energy Rev. 2017, 70, 1072–1089.*

66. M.J. Montes, A. Abanades, J.M. Martinez-Val, Performance of a direct steam generation solar thermal power plant for electricity production as a function of the solar multiple. *Sol. Energy 2009, 83, 679–689.*

67. X.D. Wang, L. Zhao, Analysis of zeotropic mixtures used in low-temperature solar Rankine

cycles for power generation. *Sol. Energy 2009, 83, 605–613.*

68. W.T. Chong, M.S. Naghavi, S.C. Poh, T.M.I. Mahlia, K.C. Pan, Techno-economic analysis of a wind-solar hybrid renewable energy system with rainwater collection feature for urban high-rise application. *Appl. Energy 2011, 88, 4067–4077.*

69. M.S. Ismail, M. Moghavvemi, T.M.I. Mahlia, Techno-economic analysis of an optimized photovoltaic anddiesel generator hybrid power system for remote houses in a tropical climate. *Energy Convers. Manag. 2013, 69, 163–173.*

70. A. Gil, M. Medrano, I. Martorell, A. Lazaro, P. Dolado, B. Zalba, L.F. Cabeza, State of the art on high temperature thermal energy storage for power generation. Part 1—Concepts, materials and modellization. *Renew. Sustain. Energy Rev. 2010, 14, 31–55.*

71. B. Stutz, N. Le Pierres, F. Kuznik, K. Johannes, E. Palomo Del Barrio, J.-P. Bédécarrats, S. Gibout, P. Marty, L. Zalewski, J. Soto, Storage of thermal solar energy. *Comptes Rendus Phys. 2017, 18, 401–414.*

72. H. Michels, R. Pitz-Paal, Cascaded latent heat storage for parabolic trough solar power plants. *Sol. Energy 2007, 81, 829–837.*

73. D. Hunold, Zur Auslegung und Konstruktion von Thermischen Energiespeichern Mit Einem Fest/Flüssig Phasenwechsel des Speichermaterials für Parabolrinnen-Solarkraftwerke; *VDI-Verl: Dusseldorf, Germany, 1994.*

74. D. Hunold, R. Ratzesberger, R. Tamme, Heat Transfer mechanism in latent-heat thermal energy storage for medium temperature application. *In Proceedings of the 6th International Symposium on Solar Thermal Concentrating Technologies, Mojacar, Spain, 28 September–2 October 1992.*

75. D. Hunold, R. Tamme, Thermal energy storage at medium and high temperatures for solar power plants, Forschungsverbund Sonnenenergie. *Sol. Therm. Power. Therm. Use Sol. Energy 1994, 93, 94.*

76. E.E. SunShot, US Department of Energy, 2012; SunShot Vision Study: Washington, DC, USA, 2012. *NREL Report No. BK5200-47927. DOE/GO–102012-3037.*

77. C.S. Turchi, Z. Ma, T.W. Neises, M.J. Wagner, Thermodynamic study of advanced supercritical carbondioxide power cycles for concentrating solar power systems. *J. Sol. Energy Eng. 2013, 135, 041007.*

78. A.F. Regin, S. Solanki, J. Saini, Heat transfer characteristics of thermal energy storage system using PCMcapsules*: A review. Renew. Sustain. Energy Rev. 2008, 12, 2438–2458.*

79. F. Agyenim, P. Eames, M. Smyth, Heat transfer enhancement in medium temperature thermal energy storage system using a multitube heat transfer array. *Renew. Energy 2010, 35, 198–207.*

80. T. Pirasaci, D.Y. Goswami, Influence of design on performance of a latent heat storage system for a directsteam generation power plant. *Appl. Energy 2016, 162, 644–652.*

81. L. Valenzuela, Thermal energy storage concepts for direct steam generation (DSG) solar plants. In Advances in Concentrating Solar Thermal Research and Technology; *Elsevier: Amsterdam, The Netherlands, 2017; pp. 269–289.*

82. F. Dinter, M. Geyer, R. Tamme, Thermal Energy Storage for Commercial Application (TESCA), a Feasibility Study on Economic Storage Systems; *Springer: Berlin/Heidelberg, Germany, 1991.*

83. R. Ratzesberger, B. Beine, E. Hahne, Regeneratoren mit Beton und Phasenwechselmaterial als Speichermasse. *VDI Berichte-Verein Deutscher Ingenieure 1994, 1168, 467.*

84. A.K. Pandey, M.S. Hossain, V.V. Tyagi, N. Abd Rahim, J.A.L. Selvaraj, A. Sari, Novel approaches and recent developments on potential applications of phase change materials in solar energy. *Renew. Sustain. Energy Rev. 2018, 82, 281–323.*

85. C. Zauner, F. Hengstberger, B. Mörzinger, R. Hofmann, H. Walter, Experimental characterization and simulation of a hybrid sensible-latent heat storage. *Appl. Energy 2017, 189, 506–519.*

86. G. Zanganeh, M. Commerford, A. Haselbacher, A. Pedretti, A. Steinfeld, Stabilization of the outflow temperature of a packed-bed thermal energy storage by combining rocks with phase change materials. *Appl. Therm. Eng. 2014, 70, 316–320.*

87. U. Pelay, L. Luo, Y. Fan, D. Stitou, M. Rood, Thermal energy storage systems for concentrated solar power plants. *Renew. Sustain. Energy Rev. 2017, 79, 82–100.*

88. S. Jaisankar, J. Ananth, S. Thulasi, S.T. Jayasuthakar, K.N. Sheeba, A comprehensive review on solar water heaters. *Renew. Sustain. Energy Rev. 2011, 15, 3045–3050.*

89. M. Mehrali, M.K. Ghatkesar, R. Pecnik, Full-spectrum volumetric solar thermal conversion via graphene/silver hybrid plasmonic nanofluids. *Appl. Energy 2018, 224, 103–115.*

90. A. Shukla, D. Buddhi, R.L. Sawhney, Solar water heaters with phase change material thermal energy storage medium: *A review. Renew. Sustain. Energy Rev. 2009, 13, 2119–2125.*

91. S.C. Bhatia, 4—Solar thermal energy. In Advanced Renewable Energy Systems; *Bhatia, S.C., Ed.; Woodhead Publishing India: Delhi, India, 2014; pp. 94–143, doi:10.1016/B978-1-78242-269-3.50004-8.*

92. M. Chaabane, H. Mhiri, P. Bournot, Thermal performance of an integrated collector storage solar water heater (ICSSWH) with phase change materials (PCM). *Energy Convers. Manag. 2014, 78, 897–903.*

93. J. Prakash, H. Garg, G. Datta, A solar water heater with a built-in latent heat storage. *Energy Convers. Manag. 1985, 25, 51–56.*

94. N. Bansal, D. Buddhi, An analytical study of a latent heat storage system in a cylinder. *Energy Convers. Manag. 1992, 33, 235–242.*

95. J. Porteiro, J.L. Míguez, B. Crespo, J. De Lara, J.M. Pousada, On the behavior of different PCMs in a hot water storage tank against thermal demands. *Materials 2016, 9, 213.*

96. F. Benmoussa, A. Benzaoui, H. Benmoussa, Thermal behavior of latent thermal energy storage unit using two phase change materials: Effects of HTF inlet temperature. *Case Stud. Therm. Eng. 2017, 10, 475–483.*

97. K. Kaygusuz, Experimental and theoretical investigation of latent heat storage for water based solar heating systems. *Energy Convers. Manag. 1995, 36, 315–323.*

98. Y. Rabin, I. Bar-Niv, E. Korin, B. Mikic, Integrated solar collector storage system based on a salt-hydrate phase-change material. *Sol. Energy 1995, 55, 435–444.*

99. A. Sharma, N. Pradhan, B. Kumar, Performance evaluation of a solar water heater having built in latent heat storage unit, IEA, ECESIA Annex 17. Advanced thermal energy storage through phase change materials and chemical reactions—feasibility studies and demonstration projects. *In Proceedings of the 4th workshop, Indore, India, 21–24 March 2003; pp. 109–115*

100. E.B.S. Mettawee, G.M.R. Assassa, Experimental study of a compact PCM solar collector. *Energy 2006, 31, 2958–268.*

101. L.F. Cabeza, M. Ibanez, C. Sole, J. Roca, M. Nogués, Experimentation with a water tank including a PCM module. *Sol. Energy Mater. Sol. Cells 2006, 90, 1273–1282.*

102. B. Kumar. Design, Development and Performance Evaluation of a Latent Heat Storage Unit for Evening and Morning Hot Water Using a Box Type Solar Collector. *Project Report, M. Tech. (Energy Management); School of Energy and Environmental Studies, Devi Ahilya University: Indore, India, 2001.*

103. A. Shukla, Heat transfer studies on phase change materials and their utilization in solar water heaters. *Ph.D. Thesis, School of Energy and Environmental Studies, Devi Ahilya University, Indore, India, 2006.*

104. A. Hasan, Phase change material energy storage system employing palmitic acid. *Sol. Energy 1994, 52, 143– 154.*

105. A. Hasan, Thermal energy storage system with stearic acid as phase change material. Energy Convers. *Manag. 1994, 35, 843–856.*

106. A. Hasan, A. Sayigh, Some fatty acids as phase-change thermal energy storage materials. *Renew. Energy 1994, 4, 69–76.*

107. G. Tiwari, S. Rai, S. Ram, M. Singh, Performance prediction of PCCM collection-cum-storage

water heater: Quasi-steady state solution. *Energy Convers. Manag. 1988, 28, 219–223.*

108. D. Ling, G. Mo, Q. Jiao, J. Wei, X. Wang, Research on solar heating system with phase change thermal energy storage. *Energy Procedia 2016, 91, 415–420.*
109. E. Boy, R. Boss, M. Lutz, A collector storage module withy integrated phase change material. *Proc. ISES Pergamon Press Hambg. 1987, 3672–3680, doi:10.1115/POWER-ICOPE2017-3520.*
110. A.M. Tayeb, A simulation model for a phase-change energy storage system: Experimental and verification. *Energy Convers. Manag. 1993, 34, 243–250.*
111. J. Font, J. Muntasell, F. Cardoner, Preliminary study of a heat storage unit using a solid-solid transition. *Sol. Energy Mater. Sol. Cells 1994, 33, 169–176.*
112. A.K. Bhargava, A solar water heater based on phase-changing material. *Appl. Energy 1983, 14, 197–209. 115.*
113. S. Canbazoglu, A. Sahinaslan, A. Ekmekyapar, Y.G. Aksoy, F. Akarsu, Enhancement of solar thermal energy storage performance using sodium thiosulfate pentahydrate of a conventional solar water-heating system. *Energy Build. 2005, 37, 235–242.*
114. M.H. Mahfuz, M.R. Anisur, M.A. Kibria, R. Saidur, I.H.S.C. Metselaar, Performance investigation of thermal energy storage system with phase change material (PCM) for solar water heating application. *Int. Commun. Heat Mass Transf. 2014, 57, 132–139.*
115. H. Hussein, H. El-Ghetany, S. Nada, Experimental investigation of novel indirect solar cooker with indoor PCM thermal storage and cooking unit. *Energy Convers. Manag. 2008, 49, 2237–2246.*
116. E. Cuce, P.M. Cuce, A comprehensive review on solar cookers. *Appl. Energy 2013, 102, 1399–1421.*
117. C.G. Ozoegwu, C.A. Mgbemene, P.A. Ozor, The status of solar energy integration and policy in Nigeria. *Renew. Sustain. Energy Rev. 2017, 70, 457–471.*
118. F. Yettou, B. Azoui, A. Malek, A. Gama, N.L. Panwar, Solar cooker realizations in actual use*: An overview. Renew. Sustain. Energy Rev. 2014, 37, 288–306.*
119. P.P. Otte, Solar cooking in Mozambique—An investigation of end-user's needs for the design of solar cookers. *Energy Policy 2014, 74, 366–375.*
120. G. Kumaresan, R. Santosh, G. Raju, R. Velraj, Experimental and numerical investigation of solar flat plate cooking unit for domestic applications. *Energy 2018, 157, 436–447.*
121. D. Buddhi, L. Sahoo, Solar cooker with latent heat storage: Design and experimental testing. *Energy Convers. Manag. 1997, 38, 493–498.*
122. J. Zhao, Y. Ji, Y. Yuan, Z. Zhang, J. Lu, Energy-saving analysis of solar heating system with PCM storage tank. *Energies 2018, 11, 237.*
123. R. Domanski, A. El-Sebaii, M. Jaworski, Cooking during off-sunshine hours using PCMs as storage media. *Energy 1995, 20, 607–616.*

124. S. Sharma, D. Buddhi, R. Sawhney, A. Sharma, Design, development and performance evaluation of a latent heat storage unit for evening cooking in a solar cooker. *Energy Convers. Manag. 2000, 41, 1497–1508.*
125. S.D. Sharma, T. Iwata, H. Kitano, K. Sagara, Thermal performance of a solar cooker based on an evacuated tube solar collector with a PCM storage unit. *Sol. Energy 2005, 78, 416–426.*
126. M. Kenisarin, K. Mahkamov, Solar energy storage using phase change materials. *Renew. Sustain. Energy Rev. 2007, 11, 1913–1965.*
127. R.M. Muthusivagami, R. Velraj, R. Sethumadhavan, Solar cookers with and without thermal storage—A review. *Renew. Sustain. Energy Rev. 2010, 14, 691–701.*
128. S. Indora, T.C. Kandpal, Institutional cooking with solar energy: A review. *Renew. Sustain. Energy Rev. 2018, 84, 131–154.*
129. A. Munir, O. Hensel, W. Scheffler, Design principle and calculations of a Scheffler fixed focus concentrator for medium temperature applications. *Sol. Energy 2010, 84, 1490–1502.*
130. A. Saxena, S.P. Pandey, G. Srivastav, A thermodynamic review on solar box type cookers. *Renew. Sustain. Energy Rev. 2011, 15, 3301–3318. Energies 2019, 12, 3167 20 of 20.*
131. L. Nkhonjera, T.Bello-Ochende, G. John, C.K. King'ondu, A review of thermal energy storage designs, heat storage materials and cooking performance of solar cookers with heat storage. *Renew. Sustain. Energy Rev. 2017, 75, 157–167.*
132. M.A. Leon, S. Kumar, S. Bhattacharya, A comprehensive procedure for performance evaluation of solar food dryers. *Renew. Sustain. Energy Rev. 2002, 6, 367–393.*
133. K. Kant, A. Shukla, A. Sharma, A. Kumar, A. Jain, Thermal energy storage based solar drying systems: A review. *Innov. Food Sci. Emerg. Technol. 2016, 34, 86–99.*
134. F. Raponi, R. Moscetti, D. Monarca, A. Colantoni, R. Massantini, Monitoring and optimization of the process of drying fruits and vegetables using computer vision: A Review. *Sustainability 2017, 9, 2009.*
135. V.K. Sharma, A. Colangelo, G. Spagna, Experimental investigation of different solar dryers suitable for fruit and vegetable drying. *Renew. Energy 1995, 6, 413–424.*
136. S.M. Shalaby, M.A. Bek, A.A. El-Sebaii, Solar dryers with PCM as energy storage medium: A review. *Renew. Sustain. Energy Rev. 2014, 33, 110–116.*
137. S. Devahastin, S. Pitaksuriyarat, Use of latent heat storage to conserve energy during drying and its effect on drying kinetics of a food product. *Appl. Therm. Eng. 2006, 26, 1705–1713.*
138. L.M. Bal, S. Satya, S.N. Naik, Solar dryer with thermal energy storage systems for drying agricultural food products: A review. *Renew. Sustain. Energy Rev. 2010, 14, 2298–2314.*
139. R.O. Lamidi, L. Jiang, P.B. Pathare, Y.D. Wang, A.P. Roskilly, Recent advances in sustainable drying of agricultural produce: A review. *Appl. Energy 2019, 233, 367–385.*
140. G. Alva, Y. Lin, G. Fang, An overview of thermal energy storage systems. *Energy 2018, 144, 341–378.*

141. V. Shanmugam, E. Natarajan, Experimental study of regenerative desiccant integrated solar dryer with and without reflective mirror. *Appl. Therm. Eng. 2007, 27, 1543–1551.*
142. V. Shringi, S. Kothari, N.L. Panwar, Experimental investigation of drying of garlic clove in solar dryer using phase change material as energy storage. *J. Therm. Anal. Calorim. 2014, 118, 533–539.*
143. D. Jain, P. Tewari, Performance of indirect through pass natural convective solar crop dryer with phase change thermal energy storage. *Renew. Energy, 2015, 80, 244–250.*
144. P. Sain, V. Songara, R. Karir, N. Balan, Natural convection type solar dryer with latent heat storage. *In Proceedings of 2013 International Conference on Renewable Energy and Sustainable Energy (ICRESE), Coimbatore, India, 5–6 December 2013; pp. 9–14.*
145. H. Dina, H. Ambarita, F.H. Napitupulu, H. Kawai, Study on effectiveness of continuous solar dryer integrated with desiccant thermal storage for drying cocoa beans. *Case Stud. Therm. Eng., 2015, 5, 32–40.*
146. A. Reyes, A. Mahn, F. Vásquez, Mushrooms dehydration in a hybrid-solar dryer, using a phase change material. *Energy Convers. Manag., 2014, 83, 241–248.*
147. I. Sarbu, C. Sebarchievici, Solar heating and cooling systems: fundamentals, experiments and applications. *1st Ed. Elsevier; 2016.*
148. A. Sharma, VV. Tyagi, CR. Chen, D. Buddhi, Review on thermal energy storage with phase change materials and applications. *Renew Sustain Energy Rev, 2009, 13, 318–45.*
149. SC. Costa, M. Kenisarin, A review of metallic materials for latent heat thermal energy storage: thermophysical properties, applications, and challenges. *Renew Sustain Energy Rev 2022, 154, 111812.*
150. P. Talebizadehsardari, JM. Mahdi, HI. Mohammed, M. Moghimi, AH. Eisapour, M. Ghalambaz, Consecutive charging and discharging of a PCM-based plate heat exchanger with zigzag configuration. *Appl Therm Eng 2021, 193, 116970.*
151. P. Talebizadeh Sardari, HI. Mohammed, JM. Mahdi, M. Ghalambaz, M. Gillott, GS. Walker, et al. Localized heating element distribution in composite metal foamphase change material: fourier's law and creeping flow effects. *Int J Energy Res 2021, 45, 13380–96.*
152. H. Zhang, L. Ren, Y. Gao, B. Jin, A comprehensive study of energy conservation in electric-hydraulic injection-molding equipment. *Energies 2017, 10, 1768.*
153. JN. Chiu, V. Martin, Multistage latent heat cold thermal energy storage design analysis. *Appl Energy 2013, 112, 1438–45.*
154. Z. Yuan, A. Horibe, K. Liang, Y. Yamada, K. Isobe, Y. Xue, Experimental evaluation of latent heat use of a microencapsulated phase change material slurry in spraying. *Int J Heat Mass Tran 2023, 201, 123573.*
155. J. Zheng, Y. Deng, Y. Liu, F. Wu, W. Wang, H. Wang, et al. Paraffin/polyvinyl alcohol/MXene flexible phase change composite films for thermal management applications.

Chem Eng J 2023, 453, 139727.

156. R. Dinesh, SI. Hussain, AA. Roseline, S. Kalaiselvam, Experimental investigation on heat transfer behavior of the novel ternary eutectic PCM embedded with MWCNT for thermal energy storage systems. *J Therm Anal Calorim 2021, 145, 2935–49.*
157. SI. Hussain, R. Dinesh, AA. Roseline, S. Dhivya, S. Kalaiselvam, Enhanced thermal performance and study the influence of sub cooling on activated carbon dispersed eutectic PCM for cold storage applications. *Energy Build 2017, 143, 17–24.*
158. D. Su, Y. Jia, G. Alva, L. Liu, G. Fang, Comparative analyses on dynamic performances of photovoltaic–thermal solar collectors integrated with phase change materials. *Energy Convers. Manag., 2017, 131, 79–89.*
159. M.M. Rahman, Md. Hasanuzzaman, N.A. Rahim, Effects of various parameters on PV-module power and efficiency. *Energy Convers. Manag., 2015, 103, 348–358.*
160. Y. Baghzouz, *"Photovoltaic Devices III." Retrieved March 6 (2017).*
161. Van Helden, G.J. Wim, J. Ronald, van Zolingen, Ch, Zondag, A. Herbert. PV thermal systems: PV panels supplying renewable electricity and heat. *Prog. Photovoltaics Res. Appl., 2004, 12 (6), 415–426.*
162. M. Muneeshwaran, 2020. U. Sajjad, T. Ahmed, Md. Amer, H.M. Ali, and C. Wang. Performance improvement of photovoltaic modules via temperature homogeneity improvement. *Energy, 203, 117816.*
163. M. Gharzi, A. Akbar, Z. Gholami, M.H. Rahmati. Progressive cooling technologies of photovoltaic and concentrated photovoltaic modules: *a review of fundamentals, thermal aspects, nanotechnology utilization and enhancing performance. Sol. Energy, 2020, 211, 117–146.*
164. K.A Moharram, M.S. Abd-Elhady, H.A. Kandil, H. El-Sherif. Enhancing the performance of photovoltaic panels by water cooling. *Ain Shams Eng. J., 2013, 4 (4), 869–877.*
165. W. Pang, Y. Cui, Q. Zhang, G.J Wilson, H. Yan. A comparative analysis on performances of flat plate photovoltaic/thermal collectors in view of operating media, structural designs, and climate conditions. *Renew. Sustain. Energy Rev. 2020, 119, 109599.*
166. S.M. Parsa, A. Yazdani, H. Aberoumand, Y. Farhadi, A. Ansari, S. Aberoumand, N. Karimi, M. Afrand, G. Cheraghian, H.M. Ali, A critical analysis on the energy and exergy performance of photovoltaic/thermal (PV/T) system: the role of nanofluids stability and synthesizing method. *Sustain. Energy Technol. Assessments*, 2022, *51, 101887.*
167. B. Ramkiran, C.K. Sundarabalan, K. Sudhakar. Sustainable passive cooling strategy for PV module: a comparative analysis. *Case Stud. Therm. Eng., 2021,*

27, 101317.

168. T. Ma, Z. Li, J. Zhao, Photovoltaic panel integrated with phase change materials (PV-PCM): technology overview and materials selection. Renew. *Sustain. Energy Rev., 2019, 116, 109406.*
169. A.M. Elbreki, M.A. Alghoul, K. Sopian, T. Hussein. Towards adopting passive heat dissipation approaches for temperature regulation of PV module as a sustainable solution. *Renew. Sustain. Energy Rev., 2017, 69, 961–1017.*
170. D. Vittorini, R. Cipollone, Fin-cooled photovoltaic module modeling–Performances mapping and electric efficiency assessment under real operating conditions. *Energy, 2019, 167, 159–167.*
171. F. Rosa, Building-Integrated Photovoltaics (BIPV) in historical buildings: opportunities and constraints. *Energies, 2020, 13 (14), 3628.*
172. B.J. Brinkworth, B.M. Cross, R.H. Marshall, Yang, Hongxing. Thermal regulation of photovoltaic cladding. *Sol. Energ, 1997, 61 (3), 169–178.*
173. A. EL Mays, R. Ammar, M. Hawa, M.A. Akroush, F. Hachem, M. Khaled, M. Ramadan, Improving photovoltaic panel using finned plate of aluminum. *Energy Proc., 2017, 119, 812–817.*
174. Grubiˇsi´c-Cˇabo, Filip, Niˇzeti´c, Sandro, Cˇoko, Duje, Kragi´c, Ivo Marini´c, Papadopoulos, Agis. Experimental investigation of the passive cooled free-standing photovoltaic panel with fixed aluminum fins on the backside surface. *J. Clean. Prod., 2018, 176, 119–129.*
175. F. Bayrak, H.F Oztop, and F. Selimefendigil. "Effects of different fin parameters on temperature and efficiency for cooling of photovoltaic panels under natural convection. *Sol. Energy, 2019, 188, 484–494.*
176. J.A. Duffy, W.A. Beckman. *Solar Engineering of Thermal Processes. John Willey & Sons, NY., 2013.*
177. A.M Elbreki, A.F. Muftah, K. Sopian, H. Jarimi, A. Fazlizan, A. Ibrahim. Experimental and economic analysis of passive cooling PV module using fins and planar reflector. *Case Stud. Therm. Eng., 2021, 23, 100801.*
178. E.Z. Ahmad, A. Fazlizan, H. Jarimi, K. Sopian, A. Ibrahim. Enhanced heat dissipation of truncated multi-level fin heat sink (MLFHS) in case of natural convection for photovoltaic cooling. *Case Stud. Therm. Eng., 2021, 28, 101578.*
179. M. Kragi´c, Ivo, Niˇzeti´c, Sandro, Grubiˇsi´c-Cˇabo, Filip, Cˇoko, Duje. Analysis and optimization of passive cooling approach for free-standing photovoltaic panel: introduction of slits. *Energy Convers. Manag., 2020, 204, 112277.*
180. A. Glick, S.E. Smith, N. Ali, J. Bossuyt, G. Recktenwald, M. Calaf, and R. Bayo´an

Cal. "Influence of flow direction and turbulence intensity on heat transfer of utility-scale photovoltaic solar farms. *Sol. Energy, 2020, 207, 173–182.*

181. D. Eryener, H. Kuscu, Hybrid transpired solar collector updraft tower. *Sol. Energy, 2018, 159, 561–571.*
182. O.K. Ahmed, A.S. Hussein, New design of solar chimney (case study). *Case Stud. Therm. Eng., 2018, 11, 105–112.*
183. M.J. Huang, P.C. Eames, Brian, Norton. Comparison of predictions made using a new 3D phase change material thermal control model with experimental measurements and predictions made using a validated 2D model. *Heat Tran. Eng., 2007, 28 (1), 31–37.*
184. M.J. Huang, P.C. Eames, B. Norton. Thermal regulation of building-integrated photovoltaics using phase change materials. *Int. J. Heat Mass Tran., 2004, 47 (12–13), 2715–2733.*
185. M.J. Huang, P.C. Eames, Norton, Brian, N.J. Hewitt. Natural convection in an internally finned phase change material heat sink for the thermal management of photovoltaics. *Sol. Energy Mater. Sol. Cell., 2011, 95 (7), 1598–1603.*
186. M. Huang, L. Chen, L. Lei, P. He, J.J. Cao, Y.L. He, Z.P. Feng, W.Q. Tao, Experimental and numerical studies for applying hybrid solar chimney and photovoltaic system to the solar-assisted air cleaning system. *Appl. Energy, 2020, 269, 115150.*
187. G. Huang, K. Wang, N.C. Markides, Efficiency limits of concentrating spectral-splitting hybrid photovoltaic-thermal (PV-T) solar collectors and systems. *Light Sci. Appl., 2021, 10 (1), 1–14.*
188. Y. Wang, Z. Fang, L. Zhu, Q. Huang, Y. Zhang, Z. Zhang, The performance of silicon solar cells operated in liquids. *Appl. Energy, 2009, 86, 1037–1042, 7-8.*
189. G.M. Tina, M. Rosa-Clot, P. Rosa-Clot, P.F. Scandura. Optical and thermal behavior of submerged photovoltaic solar panel: *SP2. Energy, 2012, 39 (1), 17–26.*
190. R. Lanzafame, S. Nachtmann, M. Rosa-Clot, P. Rosa-Clot, P.F. Scandura, S. Taddei, G.M. Tina, Field experience with performances evaluation of a single-crystalline photovoltaic panel in an underwater environment. *IEEE Trans. Ind. Electron.*, 2009, *57 (7), 2492–2498.*
191. M. Rosa-Clot, P. Rosa-Clot, G.M. Tina, Submerged PV solar panel for swimming pools: *SP3. Energy Proc., 2017, 134, 567–576.*
192. S. Mehrotra, P. Rawat, M. Debbarma, K. Sudhakar. Performance of a solar panel with water immersion cooling technique. *Int. J. Sci. Environ. Technol., 2014, 3 (3), 1161–1172.*
193. F. Al-Amri, TS. Maatallah, O.F Al-Amri, S. Ali, S. Ali, I.S. Ateeq, R. Zachariah, T.S. Kayed, Innovative technique for achieving uniform temperatures across solar panels using heat pipes and liquid immersion cooling in the harsh climate in the Kingdom of Saudi Arabia. *Alex. Eng. J. 2021, 61, 1413–1424.*
194. J.D. Stachiw. Performance of Photovoltaic Cells in Undersea Environment, *pp., 1980, 51–59.*

195. L.M. Stagno, Floating Photovoltaics–Technological Issues, Cost and Practical Implications., *2014*.

196. S.P.D. Sujay, M.M. Wagh, N.N. Shinde. A review on floating solar photovoltaic power plants. *Int. J. Sci. Eng. Res., 2017, 8 (6), 789.*

197. M. Barbuscia, Economic viability assessment of floating photovoltaic energy. *Work. Pap., 2018, 1, 1–11.*

198. P. Ranjbaran, H. Yousefi, G.B. Gharehpetian, F.R Astaraei, A review on floating photovoltaic (FPV) power generation units. Renew. *Sustain. Energy Rev., 2019, 110, 332–347.*

199. H.D.M.R. Perera. Designing of 3MW floating photovoltaic power system and its benefits over other PV technologies. *Int. J. Adv. Sci. Res. Eng, 2020, 6, 37–48.*

200. P Sharma, B Muni, D. Sen, Design parameters of 10 KW floating solar power plant. *In: Proceedings of the International Advanced Research Journal in Science, Engineering and Technology (IARJSET), National Conference on Renewable Energy and Environment (NCREE-2015), Ghaziabad, India, vol. 2., 2015.*

201. T. Kjeldstad, D. Lindholm, E. Marstein, J. Selj, Cooling of floating photovoltaics and the importance of water temperature. *Sol. Energy, 2021, 218, 544–551.*

202. N. Lee, U. Grunwald, E. Rosenlieb, H. Mirletz, A. Aznar, R. Spencer, S. Cox. Hybrid floating solar photovoltaics-hydropower systems: benefits and global assessment of technical potential. *Renew. Energy, 2020, 162, 1415–1427.*

203. T. Brahim, M.H. Dhaou, A. Jemni, Theoretical and experimental investigation of plate screen mesh heat pipe solar collector. *Energy Convers. Manag., 2014, 87, 428–438.*

204. X. Han, X. Zhao, X. Chen, Design and analysis of a concentrating PV/T system with nanofluid based spectral beam splitter and heat pipe cooling. *Renew. Energy, 2020, 162, 55–70.*

205. M. Hu, R. Zheng, G. Pei, P. Renchun, Y. Wang, J. Li, J. Ji, Experimental study of the effect of inclination angle on the thermal performance of heat pipe photovoltaic/thermal (PV/T) systems with wickless heat pipe and wire- meshed heat pipe. *Appl. Therm. Eng., 2016, 106, 651–660.*

206. T. Zhang, Z.W. Yan, L. Xiao, H.D. Fu, G. Pei, J. Ji. Experimental, study and design sensitivity analysis of a heat pipe photovoltaic/thermal system. *Appl. Therm. Eng., 2019, 162, 114318.*

207. M. Modjinou, J. Ji, W. Yuan, Z. Fan, S. Holliday, A. Waqas, X. Zhao, Performance comparison of encapsulated PCM PV/T, microchannel heat pipe PV/T and conventional PV/T systems. *Energy, 2019, 166, 1249–1266.*

208. M. Moradgholi, S.M Nowee, I. Abrishamchi, Application of heat pipe in an experimental investigation on a novel photovoltaic/thermal (PV/T) system. *Sol. Energy, 2014, 107, 82–88.*

209. S. Koundinya, N. Vigneshkumar, A.S. Krishnan. Experimental study and comparison with the

computational study on cooling of PV solar panel using finned heat pipe technology. *Mater. Today Proc., 2017, 4 (2), 2693–2700.*

210. H. Alizadeh, R. Ghasempour, M.B. Shafii, M.H. Ahmadi, W.M Yan, M.A. Nazari, Numerical simulation of PV cooling by using single turn pulsating heat pipe. *Int. J. Heat Mass Tran., 2018, 127, 203–208.*

211. S.Y. Wu, Y.C. Zhang, L. Xiao, Z.G. Shen, Performance comparison investigation on solar photovoltaic-thermoelectric generation and solar photovoltaic-thermoelectric cooling hybrid systems under different conditions. *Int. J. Sustain. Energy, 2018, 37 (6), 533–548.*

212. C. Babu, P. Ponnambalam. The theoretical performance evaluation of hybrid PV-TEG system. *Energy Convers. Manag., 2018, 173, 450–460.*

213. G. Kidegho, F. Njoka, C. Muriithi, R. Kinyua, Evaluation of thermal interface materials in mediating PV cell temperature mismatch in PV–TEG power generation. *Energy Rep., 2021, 7, 1636–1650.*

214. A. Makki, S. Omer, Y. Su, H. Sabir, Numerical investigation of heat pipe-based photovoltaic–thermoelectric generator (HP-PV/ TEG) hybrid system. *Energy Convers. Manag., 2016, 112, 274–287.*

215. A. Mahdavi, M.A.E. Moghaddam, D.D. Ganji, Hierarchical implementation of hybrid heat promoters fixated on operational conditions to accelerate the melting phenomenon of a triplex tube heat exchanger. *Therm. Sci. Eng. Prog., 2021a, 25, 101008.*

216. P. Dwivedi, K. Sudhakar, A. Soni, E. Solomin, I. Kirpichnikova. Advanced cooling techniques of PV modules: a state of art. *Case Stud. Therm. Eng., 2020, 21, 100674.*

217. T. Klemm, A. Hassabou, A. Abdallah, O. Andersen, Thermal energy storage with phase change materials to increase the efficiency of solar photovoltaic modules. *Energy Proc., 2017, 135, 193–202.*

218. O. Mahian, S. Ghafarian, S. Hamid, A. Kasaeian, H. Yousefi, W.M. Yan, Phase change materials in solar photovoltaics applied in buildings: *an overview. Sol. Energy, 2021, 224, 569–592.*

219. H.M. Ali, Recent advancements in PV cooling and efficiency enhancement integrating phase change materials based systems–A comprehensive review. *Sol. Energy, 2020, 197, 163–198.*

220. S.S. Chandel, T. Agarwal, Review of cooling techniques using phase change materials for enhancing efficiency of photovoltaic power systems. Renew. *Sustain. Energy Rev., 2017, 73, 1342–1351.*

221. M.A. Ezan, C. yuksel, C. kalkan, M. aydin, and G. nergiz. "Passive thermal management of a photovoltaic panel: influence of fin arrangements. *In: Exergetic, Energetic and Environmental*

Dimensions. Academic Press, 2018, pp. 341–352.

222. S. Maiti, S. Banerjee, K. Vyas, P. Patel, P.K. Ghosh. Self regulation of photovoltaic module temperature in V-trough using a metal–wax composite phase change matrix. *Sol. Energy, 2011, 85 (9), 1805–1816.*

223. N. Savvakis, T. Tsoutsos, Phase change materials in photovoltaic's: the assessment of system performance in the present mediterranean climate conditions. *Power Systems, Energy Markets and Renewable Energy Sources in South-Eastern Europe. Trivent Publishing, 2016.*

224. J.H.C. Hendricks, W.G.J.H.M. Van Sark. Annual performance enhancement of building integrated photovoltaic modules by applying phase change materials. *Prog. Photovoltaics Res. Appl., 2013, 21 (4), 620–630.*

225. S. Khanna, K.S. Reddy, T.K. Mallick, Optimization of finned solar photovoltaic phase change material (finned pv pcm) system. *Int. J. Therm. Sci., 2018, 130, 313–322.*

226. V. Sun, A. Asanakham, T. Deethayat, T. Kiatsiriroat, Study on phase change material and its appropriate thickness for controlling solar cell module temperature. *Int. J. Ambient Energy, 2020, 41 (1), 64–73.*

227. M. Rajvikram, S. Leoponraj, S. Ramkumar, H. Akshaya, A. Dheeraj. Experimental investigation on the abasement of operating temperature in solar photovoltaic panel using PCM and aluminium. *Sol. Energy, 2019, 188, 327–338.*

228. J. Darkwa, J. Calautit, D. Du, G. Kokogianakis, A numerical and experimental analysis of an integrated TEG-PCM power enhancement system for photovoltaic cells. *Appl. Energy, 2019, 248, 688–701.*

229. F. Bayrak, F.H. Oztop, and F. Selimefendigil. "Effects of different fin parameters on temperature and efficiency for cooling of photovoltaic panels under natural convection. *Sol. Energy, 2019, 188, 484–494.*

230. A. Kumar, A.P. Singh, O.P. Singh. Effect of novel PCM encapsulation designs on electrical and thermal performance of a hybrid photovoltaic solar panel. *Sol. Energy, 2020b, 205, 320–333.*

231. A. Mahdavi, M.A.E. Moghaddam, A. Mahmoudi, Simultaneous charging and discharging of multi-tube heat storage systems using copper fins and Cu nanoparticles. *Case Stud. Therm. Eng., 2021b, 27, 101343.*

232. R. Kumar, P. Praveen, S. Gupta, J. Saikiran, R.S. Bharj, Performance evaluation of photovoltaic module integrated with phase change material-filled container with external fins for extremely hot climates. *J. Energy Storage, 2020c, 32, 101876.*

233. J.M. Mahdi, R.P. Singh, H.M.T. Al-Najjar, S. Singh, C.E. Nsofor, Efficient thermal

management of the photovoltaic/ phase change material system with innovative exterior metal-foam layer. *Sol. Energy, 2021, 216, 411–427.*

234. J. Duan, A novel heat sink for cooling concentrator photovoltaic system using PCM-porous system. *Appl. Therm. Eng., 2021, 186, 116522.*

235. I. Zarma, M. Ahmed, S. Ookawara, Enhancing the performance of concentrator photovoltaic systems using Nanoparticle-phase change material heat sinks. *Energy Convers. Manag., 2019, 179, 229–242.*

236. M. Emam, M. Ahmed, Cooling concentrator photovoltaic systems using various configurations of phase-change material heat sinks. *Energy Convers. Manag., 2018, 158, 298–314.*

237. M.B Elsheniti, M.A. Hemedah, M.M. Sorour, W.M. El-Maghlany, Novel enhanced conduction model for predicting performance of a PV panel cooled by PCM. *Energy Convers. Manag., 2020, 205, 112456.*

238. R. Ahmadi, F. Monadinia, M. Maleki, Passive/active photovoltaic-thermal (PVT) system implementing infiltrated phase change material (PCM) in PS-CNT foam. *Sol. Energy Mater. Sol. Cell., 2021, 222, 110942.*

239. N. Sandro, M. Jurˇcevi´c, D. Cˇoko, M. Arıcı, A novel and effective passive cooling strategy for photovoltaic panel. *Renew. Sustain. Energy Rev., 2021, 145, 111164.*

240. S. Zhang, D. Feng, L. Shi, L. Wang, Y. Jin, L. Tian, Z. Li, G. Wang, L. Zhao, Y. Yan, A review of phase change heat transfer in shape-stabilized phase change materials (ss-PCMs) based on porous supports for thermal energy storage. *Renew. Sustain. Energy Rev., 2021, 135, 110127.*

241. M. Ostrý, S. Bantov´a, K. Struhala, Compatibility of phase change materials and metals: experimental evaluation based on the corrosion rate. *Molecules, 2020, 25 (12), 2823.*

242. T. Xiong, L. Zheng, K.W. Shah, Nano-enhanced phase change materials (NePCMs): a review of numerical simulations. *Appl. Therm. Eng., 2020, 178, 115492.*

243. L. Siahkamari, M. Rahimi, N. Azimi, M. Banibayat, Experimental investigation on using a novel phase change material (PCM) in micro structure photovoltaic cooling system. *Int. Commun. Heat Mass Tran., 2019, 100, 60–66.*

244. A.S. Abdelrazik, F.A. Al-Sulaiman, R. Saidur. Numerical investigation of the effects of the nano-enhanced phase change materials on the thermal and electrical performance of hybrid PV/thermal systems. *Energy Convers. Manag., 2020a, 205, 112449.*

245. A.S. Abdelrazik, F.A. Al-Sulaiman, R. Saidur. Thermal regulation and performance assessment of a hybrid photovoltaic/thermal system using different combinations of nano-

enhanced phase change materials. *Sol. Energy Mater. Sol. Cell., 2020b, 215, 110645.*

246. M.A.V. Rad, A. Kasaeian, S. Mousavi, F. Rajaee, A. Kouravand, Empirical investigation of a photovoltaic-thermal system with phase change materials and aluminum shavings porous media. *Renew. Energy, 2021, 167, 662–675.*

247. D.M.C. Shastry, U.C. Arunachala. Thermal management of photovoltaic module with metal matrix embedded PCM. *J. Energy Storage, 2020, 28, 101312.*

248. S.S. Chandel, T. Agarwal, Review of cooling techniques using phase change materials for enhancing efficiency of photovoltaic power systems. *Renew. Sustain. Energy Rev., 2017, 73, 1342–1351.*

249. R. Kumar, V. Deshmukh, R.S. Bharj, Performance enhancement of photovoltaic modules by nanofluid cooling*: a comprehensive review. Int. J. Energy Res., 2020a, 44 (8), 6149–6169.*

250. H. Liang, F. Wang, C. Xu, G. Li, Y. Shuai, Full-spectrum solar energy utilization and enhanced solar energy harvesting via photon anti- reflection and scattering performance using biomimetic nanophotonic structure. *ES Energy Environ., 2020, 8 (2), 29–41.*

251. H. Liang, F. Wang, L. Yang, Z. Cheng, Y. Shuai, H. Tan, Progress in full spectrum solar energy utilization by spectral beam splitting hybrid PV/T system. *Renew. Sustain. Energy Rev., 2021a, 141, 110785.*

252. H. Liang, R. Su, W. Huang, Z. Cheng, F. Wang, G. Huang, D. Yang, A Novel Spectral Beam Splitting Photovoltaic/ thermal Hybrid System Based on Semi-transparent Solar Cell with Serrated Groove Structure for Co-generation of Electricity and High-Grade Thermal Energy. *Energy Conversion and Management, 2021b, 115049.*

253. H. Abou-Ziyan, M. Ibrahim, H. Abdel-Hameed, Characteristics enhancement of one-section and two-stepwise microchannels for cooling high- concentration multi-junction photovoltaic cells. *Energy Convers. Manag., 2020, 206, 112488.*

254. N. Xu, P. Zhu, Y. Sheng, L. Zhou, X. Li, H. Tan, S. Zhu, Z. Jia, Synergistic tandem solar electricity-water generators. *Joule, 2020, 4 (2), 347–358.*

255. N. JY. Liew, Z. Yu, Z. Holman, H. Lee, Application of spectral beam splitting using Wavelength-Selective filters for Photovoltaic/Concentrated solar power hybrid plants. *Appl. Therm. Eng., 2022, 201, 117823.*

256. S. Jamali, M. Yari, S.M.S. Mahmoudi, Enhanced power generation through cooling a semi-transparent PV power plant with a solar chimney. *Energy Convers. Manag., 2018, 175, 227–235.*

257. S. Jamali, A. Nemati, F. Mohammadkhani, M. Yari, Thermal and economic assessment of a solar chimney cooled semi-transparent photovoltaic (STPV) power plant in different climates.

Sol. Energy, 2019, 185, 480–493.

258. D.H.W. Li et al. Analysis of the operational performance and efficiency characteristic for photovoltaic system *in Hong Kong Energy Convers Manag, 2005.*

259. A.R. Gxasheka et al. Evaluation of performance parameters of PV modules deployed outdoors *Renew Energy, 2005.*

260. B. Parida et al. A review of solar photovoltaic technologies *Renew Sustain Energy Rev, 2011.*

261. X. Dong et al. Time-resolved spectra of solar simulators employing metal halide and xenon arc lamps *Solar Energy, 2015.*

262. S. Kohraku et al. A fundamental experiment for discrete-wavelength LED solar simulator *Sol Energy Mater Sol Cells (2006).*

263. D. Bickler. The simulation of solar radiation *Sol Energy, 1962.*

264. J. Sarwar et al. Description and characterization of an adjustable flux solar simulator for solar thermal, thermochemical and photovoltaic applications *Sol Energy, 2014.*

265. D. Bari et al. Reliability study of dye-sensitized solar cells by means of solar simulator and white LED Microelectron *Reliab, 2012.*

266. Q. Meng et al. Irradiance characteristics and optimization design of a large- scale solar simulator *Sol Energy, 2011.*

267. B.M. Ekman et al. Development of high flux solar simulators for solar thermal research *Sol Energy Mater Sol Cells, 2015.*

268. P. Krusi et al. The csi 1000W lamp as source for solar radiation simulation *Sol Energy, 1983.*

269. R. Shankar et al. A practical review on photooxidation of crude oil: Laboratory lamp setup and factors affecting it *Water Res, 2015.*

270. M.O. Reese et al. Consensus stability testing protocols for organic photovoltaic materials and devices *Sol Energy Mater Sol Cells, 2011.*

271. D. Kockott et al. To what extent does the radiation of a solar simulator meet a “reference sun”? *A quantitative approach Polym Test, 2012.*

272. Y. Li et al. Experimental analysis on use of thermal conductivity enhancers (TCEs) for solar chimney applications with energy storage layer *Energy Build, 2016.*

273. B. Muthuraaman et al. Increased charge transfer of Poly (ethylene oxide) base electrolyte by addition of small molecule and its application in dye- sensitized solar cells Electrochim *Acta, 2013.*

274. H. Brandhorst, J. Hickey, H. Curtis, E. Ralph, Interim solar cell testing procedures for

terrestrial applications. *NASA TM...*

275. *ERDA/NASA. Terrestrial photovoltaic measurement procedures. NASA...*
276. M.G. Villalva et al. Comprehensive approach to modeling and simulation of photovoltaic arrays *IEEE Trans Power Electron, 2009.*
277. M. Haifeng et al. Uncertainty analysis of solar simulator's spectral irradiance measurement *Proc SPIE, 2012.*
278. M. Yamamoto, O. Ikki. National survey report of PV power applications in Japan. *International Energy Agency Co-operative...*
279. *20110504-RD-LSC-0621 - Flickr - USDAgov by U.S. Department of Agriculture. Licensed under CC BY 2.0 via Wikimedia Commons http://commons.wikimedia.org/wiki/File:20110504-RD-LSC-0621_-_Flickr__USDAgov.jpg#/media/File:20110504-RD-LSC-0621_-_Flickr_-_USDAgov.jpg.*
280. C. Julian Chen. *Physics of Solar Energy, 1st ed. Hoboken, NJ, USA: John Wiley & Sons Inc., 2011.*
281. Wikimedia Commons [Online], Available: *http://upload.wikimedia.org/wikipedia/commons/7/7d/Operation_of_a_basic_photovoltaic_cell.gif.*
282. Created internally by a member of the Energy Education team. Adapted from: *Ecogreen Electrical. (August 14, 2015). Solar PV Systems [Online]. Available: http://www.ecogreenelectrical.com/solar.htm*
283. G. Boyle. Renewable Energy: Power for a Sustainable Future, *2nd ed. Oxford, UK: Oxford University Press, 2004.*
284. R. Wolfson, "Photovoltaic Solar Energy" in Energy, Environment, and Climate, *2nd ed., New York, NY: W.W. Norton & Company, 2012, ch. 9, sec. 5, pp. 244-252.*
285. D. C. Jordan and S. R. Kurtz. Photovoltaic Degradation Rates — An Analytical Review, *National Renewable Energy Laboratory, USA, 2012. Accessed April 24, 2018. [Online] Available at https://www.nrel.gov/docs/fy12osti/51664.pdf.*
286. *Wikimedia Commons.(August 18, 2015). Comparison of Solar Cells[Online]. Available:https://upload.wikimedia.org/wikipedia/commons/7/71/Comparison_solar_cell_poly-Si vs_mono-Si.png.*
287. *https://www.climatestotravel.com/temperatures/bangladesh.*
288. *Bangladesh - Solar Radiation Measurement Data - Dataset - ENERGYDATA.INFO.*
289. *https://www.weather-atlas.com/en/bangladesh/dhaka-climate.*